Table of Contents

List of Figures

CHAPTER 1: LITERATURE REVIEW

CHAPTER 3: METHODS

CHAPTER 4: RESULTS

APPENDICES

List of Tables

CHAPTER 1: LITERATURE REVIEW

CHAPTER 3: METHODS

CHAPTER 4: RESULTS

APPENDICES

Abbreviations

Abbreviation	Full Name
$A_{2A}R$	Adenosine A_{2A} Receptor
$A_{2A}RKO^{-/-}$	Adenosine A_{2A} Receptor Homozygous Recessive Knockout
ABC	Avidin:Biotinylated Horseradish Peroxidase Complex
ABR	Auditory Brainstem Response
ADAC	Adenosine Amine Congener
ADP	Adenosine Diphosphate
AMP	Adenosine Monophosphate
ANOVA	Analysis of Variance
ATP	Adenosine Triphosphate
BMDC	Bone Marrow-Derived Cell
BrdU	Bromodeoxyuridine
cAMP	Cyclic Adenosine Monophosphate
CCL2	Chemokine (C-C motif) Ligand 2
cDNA	Complementary DNA
COX-2	Cyclooxygenase-2
CREB	cAMP Response Element-Binding Protein
CV	Collecting Venule
DAB	3,3'-Diaminobenzine
DAPI	4',6-Diamidino-2-Phenylindole
DEPC	Diethylpyrocarbonate
DMSO	Dimethyl Sulfoxide
dNTPs	Deoxynucleotide Triphosphates
E-NTPDase	Ectonucleoside Triphosphate Diphosphohydrolase
EDTA	Ethylenediaminetetraacetate
ERK	Extracellular Signal-Regulated Kinase
FDA	Food and Drug Administration
GGA	Geranylgeranylacetone
GPCR	G Protein-Coupled Receptor
H_2O_2	Hydrogen Peroxidase
HSF1	Heat Shock Transcription Factor 1

HSP	Heat Shock Protein
ICAM-1	Intercellular Adhesion Molecule-1
IgG	Immunoglobulin G
IL-1β	Interleukin-1Beta
IL-1RI	IL-1 Receptor Type I
IL-1RII	IL-1 Receptor Type II
IL-6	Interleukin-6
iNOS	Inducible Nitric Oxide Synthase
i.p.	Intraperitoneal
JAK	Janus Kinase
JNK	c-Jun N-Terminal Kinase
KC	Keratinocyte-Derived Chemokine
KLH	Keyhole Limpet Hemocyanin
LFA-1	Leukocyte Function Associated Antigen-1
LPS	Lipopolysaccharide
M	Modiolus
MAPK	Mitogen-Activated Protein Kinase
MAC-1	Macrophage Adhesion Ligand-1
MCP-1	Monocyte Chemoattractant Protein-1
MCP-5	Monocyte Chemoattractant Protein-5
MET	Mechanoelectical Transduction
MIP-1β	Macrophage Inflammatory Protein-1β
MIP-2	Macrophage Inflammatory Protein-2
mRNA	Messenger RNA
NaCl	Sodium Chloride
NADPH	Nicotinamide Adenine Dinucleotide Phosphate
$NaNO_2$	Sodium Nitrite
NF-κB	Nuclear Factor Kappa-Light-Chain-Enhancer of Activated B Cells
NPP	Nucleotide Pyrophosphatase/Phosphodiesterase
NTC	No Template Control
OC	Organ of Corti
OCT	Optimal Cutting Temperature
PARP-1	Poly(ADP-Ribose) Polymerase-1

PB	Phosphate Buffer
PBS	Phosphate-Buffered Saline
PECAM-1	Platelet Endothelial Cell Adhesion Molecule-1
PFA	Paraformaldehyde
PKA	Protein Kinase A
PVM	Perivascular Resident Macrophage
RNase	Ribonuclease
ROI	Region of Interest
RNS	Reactive Nitrogen Species
ROS	Reactive Oxygen Species
+RT	Positive Reverse Transcriptase Control
-RT	Negative Reverse Transcriptase Control
RT-PCR	Reverse Transcription-Polymerase Chain Reaction
SDF-1α	Stromal Cell-Derived Factor-1α
SEM	Standard Error of the Mean
SG	Spiral Ganglion
siRNA	Short Interfering RNA
SL	Spiral Ligament
SLm	Spiral Limbus
SM	Scala Media
SOM	Suppurative Otitis Media
SPL	Sound Pressure Level
ST	Scala Tympani
STAT1	Signal Transducer and Activator of Transcription-1
SV	Stria Vascularis
SVb	Scala Vestibuli
TNF-α	Tumour Necrosis Factor-Alpha
VCAM-1	Vascular Cell Adhesion Molecule-1
TRAF	TNF-Receptor Associated Factor
VJU	Vernon Jansen Unit
WHO	World Health Organisation

Introduction to Thesis

Located within the inner ear is the cochlea, the specialised peripheral end organ of the auditory system which mediates the transduction of sound waves into electrical nerve impulses that travel to the brain for central processing of auditory information. The cochlea is an exquisitely sensitive organ, allowing us to perceive and distinguish among the myriad sounds around us. Unfortunately, this extreme sensitivity of the cochlea comes at a cost as it makes it highly susceptible to injury when exposed to loud sound. The injury inflicted on the cochlea affects almost all cell types, particularly the sensory hair cells, and since sensory cells in the mammalian cochlea are incapable of regeneration, this damage is irreversible, leading to cochlear dysfunction and permanent hearing loss. According to recent global estimates released by the World Health Organisation (WHO, 2012), there are 360 million people worldwide (5.3% of the world's population) with disabling hearing loss. A significant proportion (16%) of the disabling hearing loss in the adult population is attributed to occupational noise exposure (WHO, 2002).

There is a growing body of evidence that oxidative stress in the cochlea is a key mechanism of noise-induced cochlear injury. However, emerging evidence suggests that cochlear inflammation may also be a major contributor. Several studies have demonstrated an inflammatory response in the cochlea following noise exposure involving an upregulation of proinflammatory mediators by various resident cochlear cells, followed by the rapid recruitment and infiltration of inflammatory cells from the systemic circulation which may cause bystander tissue injury to the delicate structures in the cochlea. Cochlear inflammation has also been implicated as a major etiologic factor in a range of other conditions that cause hearing loss, such as otitis media, meningitis, ototoxicity, and autoimmune inner ear disease. The cochlea thus responds to trauma and infection like organs elsewhere in the body. Although a great deal has been learned over the years of the noise-induced inflammatory response in the cochlea from animal models, the precise molecular mechanisms underlying the response and its role in the development of cochlear injury remain to be elucidated. This thesis thus aims to improve our understanding of the underlying mechanisms and time course of the noise-induced cochlear inflammatory response.

Hearing loss can be caused not only by an acute exposure to loud sound but also from repeated exposure to noise over an extended period of time. Previous research has

demonstrated the inflammatory response following acute noise exposure, however studies focussing on cochlear inflammation associated with chronic noise exposure, which leads to slowly developing hearing loss, are lacking. There is a strong possibility that chronic environmental noise exposure at moderate noise levels, such as the workplace noise, could be linked to the development of an inflammatory response in the cochlea, which can contribute to cochlear injury in the long run. The second study of the thesis thus investigates the cochlear inflammatory response induced by chronic exposure to moderate noise levels.

At present, there is no cure for noise-induced hearing loss, or any other type of sensorineural hearing loss. Steroid-based drugs (corticosteroids) have long been used in the management of sensorineural hearing loss of various causes, including noise-induced hearing loss, and have been able to suppress excessive inflammation at appropriate doses, but are unable to recover the associated hearing loss. Higher doses, on the other hand, can be deleterious to cochlear function in the long term and are often accompanied by a wide range of adverse side effects. There is therefore a need to develop more effective pharmacological therapies for cochlear inflammation and the associated hearing loss. Extensive evidence has demonstrated the strong anti-inflammatory potential of adenosine, a ubiquitous signalling and cytoprotective molecule, in a range of tissues, suggesting that adenosine may also confer a similar effect in the cochlea. Adenosine mediates anti-inflammatory effects primarily via the adenosine A_{2A} receptor, one of the four adenosine receptor subtypes. The final study of this thesis investigates the role of adenosine A_{2A} receptor signalling in the regulation of noise-induced cochlear inflammation and explores the therapeutic potential of the selective adenosine A_{2A} receptor agonist, regadenoson, in mitigating noise-induced cochlear inflammation.

CHAPTER 1: LITERATURE REVIEW

1.1. Introduction

This introductory chapter presents a comprehensive review of the existing literature related to noise-induced cochlear inflammation. It commences with a general outline of the anatomy and physiology of the cochlea, followed by a detailed overview of the current knowledge regarding cochlear inflammation and its various aetiologies, with particular emphasis on noise-induced cochlear inflammation. The review concludes with a summary of the adenosine signalling system (including the anti-inflammatory role of adenosine) and a discussion of adenosine-based therapeutic approaches.

1.2. Cochlear Anatomy and Physiology

1.2.1. General Organisation of the Cochlea

The ear is divided into three main anatomical compartments, the outer, the middle, and the inner ear (**Figure 1.1**). The outer or external ear consists of the pinna or auricle and the external auditory meatus (ear canal). The pinna collects and funnels sound to the ear canal, a long tube connecting the pinna to the tympanic membrane. The tympanic membrane, commonly known as the eardrum, is a thin and delicate semi-transparent membrane that separates the outer ear from the middle ear and transmits sound vibrations to the three ossicles (Latin for "tiny bones"; malleus, incus and stapes) in the middle ear, a small air-filled cavity. Located within the inner ear are the organs for the sense of hearing (the cochlea) and balance (the semi-circular canals, saccule and utricle). The cochlea spirals around the modiolus, a conical bony structure. The total uncoiled length of the human cochlea is approximately 35 mm, which coils into 2 ½ to 2 ¾ turns (Tabuchi & Hara, 2012). The cochlea has three fluid-filled compartments known as the scala vestibuli, scala media (or cochlear duct) and scala tympani (Dallos *et al.*, 1996; Raphael & Altschuler, 2003) (**Figure 1.2**). The scala vestibuli and scala media are separated by Reissner's membrane, a two cell layered membrane, whereas the scala media and the scala tympani are separated by the organ

of Corti sitting on the basilar membrane. At the apex of the cochlea is a narrow opening called the helicotrema, through which the scala vestibuli communicates with the scala tympani. At the base of the scala vestibuli and the scala tympani there are two membrane-covered holes, the oval window and the round window respectively (Dallos *et al.*, 1996; Raphael & Altschuler, 2003). The fluid within the scala media, known as endolymph, has an ionic composition similar to intracellular fluid, with high K^+ (157 mM) and low Na^+ (1.3 mM), whereas the scala vestibuli and scala tympani are filled with perilymph, an extracellular-like fluid with high Na^+ (141 mM in scala vestibuli, 148 mM in scala tympani) and low K^+ (6.0 mM in scala vestibuli, 4.2 mM in scala tympani), which communicates with the cerebrospinal fluid via the cochlear aqueduct (Wangemann, 2006). The endolymph is also unusual for its low Ca^{2+} concentration (0.023 mM), which is critical for sensory transduction in the cochlea (Wangemann, 2006).

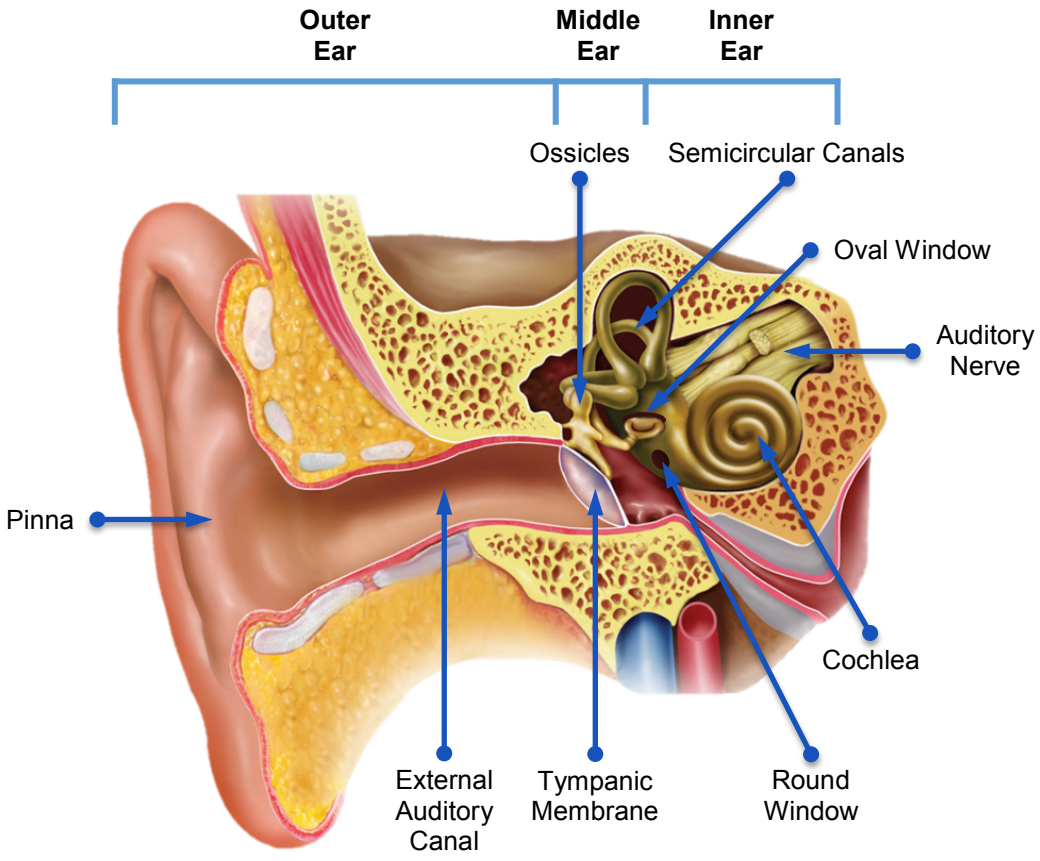

Figure 1.1: Structure of the ear. The ear is divided into three main anatomical compartments: the outer ear consisting of the pinna, the external auditory canal (ear canal) and the outer part of the tympanic membrane; the middle ear, an air-filled cavity containing the three ossicles (malleus, incus and stapes); and the inner ear comprising the cochlea and the peripheral end-organs of the vestibular system.

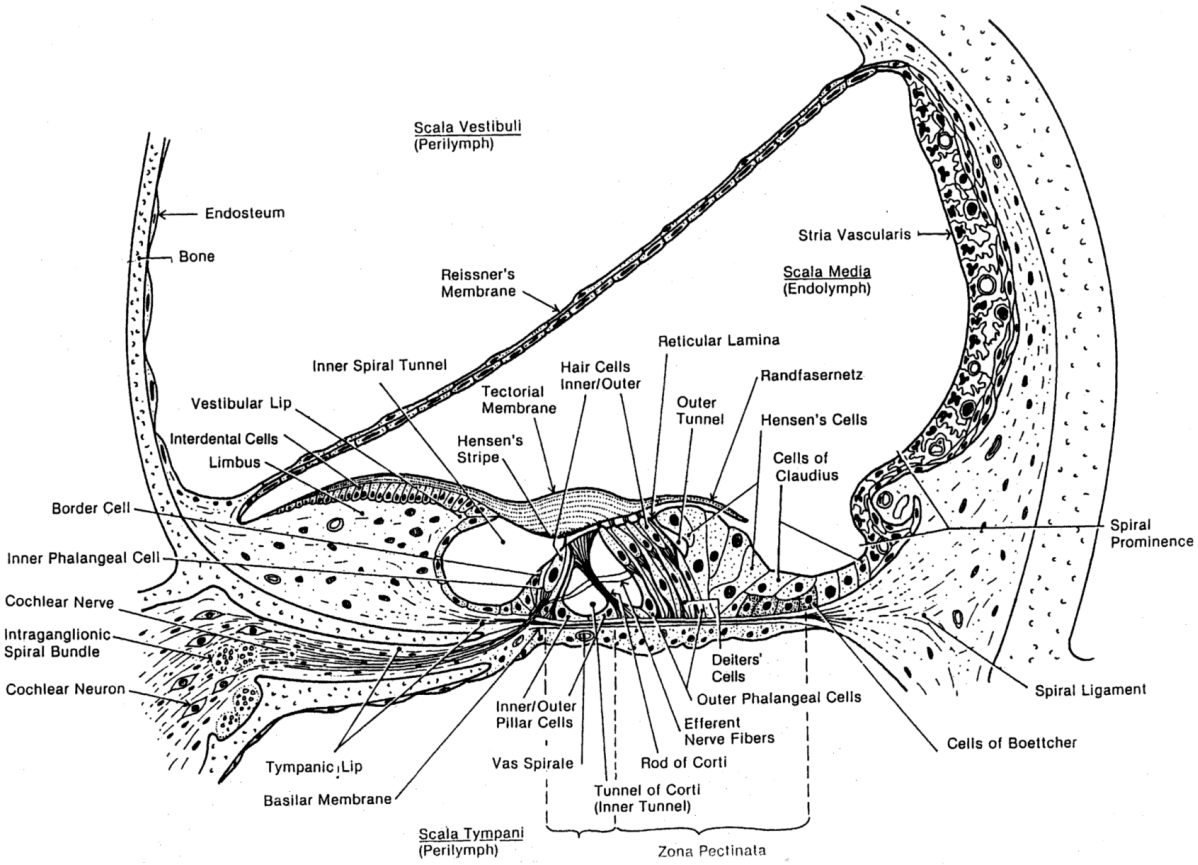

Figure 1.2: Schematic diagram of a cross-section of the cochlea. The organ of Corti, the sensory organ of hearing, resides on the basilar membrane, and is made up of sensory hair cells (inner and outer hair cells) interdigitating with various supporting cells. The lateral wall of the cochlea, with an important role in K^+ secretion and cycling, is composed of the spiral ligament fibrocytes and secretory epithelial cells of the stria vascularis, whilst the spiral ganglion, which provides afferent and efferent innervation to the sensory hair cells, is located in the modiolus, a conical shaped central axis of the cochlea. (Figure reproduced from Davis (1953), with permission from Acoustical Society of America).

1.2.2. Organ of Corti

Attached to the basilar membrane is the organ of Corti, the sensory organ of hearing (**Figure 1.2**). The organ of Corti is a highly differentiated sensory epithelium, consisting of specialised hair cells interdigitating with various types of supporting cells in an orderly pattern (Dallos *et al.*, 1996; Raphael & Altschuler, 2003). The basilar membrane, on which the organ of Corti sits, is a complex structure of connective tissue composed mainly of extracellular matrix components. The apical surfaces of the sensory and supporting cells are joined together by an elaborate network of tight junctions and adherens junctions to form the

reticular lamina which acts as a barrier between the endolymph of the scala media and the perilymph-like fluid bathing the cells of the organ of Corti (Dallos *et al.*, 1996; Raphael & Altschuler, 2003).

1.2.2.1. Hair Cells

Two types of hair cells exist – the inner hair cells, which are the primary sensory cells, forming a single row medially, and the outer hair cells, which enhance the sensitivity and frequency selectivity of hearing (often referred to as the "cochlear amplifier"), forming three rows laterally (Housley *et al.*, 2006). Occupying the apical surfaces of the sensory cells are cellular projections known as stereocilia (or sensory hairs and hence the name "hair" cell), interconnected by tip links and side links (Pickles *et al.*, 1984; Furness & Hackney, 1985). The tips of stereocilia contain mechanoelectrical transduction (MET) channels that mediate the electrical responses of the hair cells (Fettiplace & Hackney, 2006). The basilar membrane is a hydromechanical frequency analyser that encodes high frequency sound at the base and low frequency sound at the apex in response to sound (Dallos, 1992). Movement of the basilar membrane results in displacement of hair cell stereocilia and opening of the mechanically-gated transduction ion channels (Raphael & Altschuler, 2003). Influx of K^+ from the endolymph in the scala media occurs through these transduction channels, depolarising the inner hair cells, which in turn activate voltage-gated calcium channels. Ca^{2+} entry triggers the release of glutamate, which generates nerve impulses postsynaptically in the primary auditory neurons, whose cell bodies cluster together to form the spiral ganglion located within the modiolus. These nerve impulses are conducted along the brainstem auditory pathways all the way to the primary auditory cortex located in the temporal lobe for complex processing of sound information.

1.2.2.2. Supporting Cells

The supporting cells of the organ of Corti are highly differentiated epithelial cells that surround the sensory hair cells, providing them with structural stability and metabolic support (Dallos *et al.*, 1996; Raphael & Altschuler, 2003). There is evidence that supporting cells have a role in regulating the ionic environment within and around the organ of Corti (Kikuchi *et al.*, 2000). Most of these cells span the distance between the basilar membrane and the reticular lamina and numerous microvilli cover their apical surfaces which protrude into the endolymph of the scala media. The supporting cells include the inner sulcus cells, inner border cells, inner phalangeal cells, inner and outer pillar cells, Deiters' cells (outer

phalangeal cells), Hensen's cells, Claudius' cells, Boettcher's cells, and outer sulcus cells (Dallos *et al.*, 1996; Raphael & Altschuler, 2003). The inner sulcus cells form an epithelial layer joining with the connective tissue of the spiral limbus and terminate laterally with the inner border cells, which are located on the modiolar side of the inner hair cells. The inner hair cells are surrounded by inner phalangeal cells and inner pillar cells. The basal parts of the inner and outer pillar cells slant in opposite directions creating the tunnel of Corti, which provides a triangular basis of support and separate the inner hair cells from the outer hair cells. Deiters' cells run from the basilar membrane to the reticular lamina, with the middle portion providing a "seat" for the outer hair cells. Each Deiters' cell makes contact with five different outer hair cells. Hensen's cells form the lateral border of the organ of Corti, directly adjacent to the third row of Deiters' cells. Extending from the organ of Corti laterally, the Claudius' cells rest on the basilar membrane (those in the basal turn of the cochlea lie on top of Boettcher's cells), filling the distance between the Hensen's cells and the lateral wall. At the lateral extremity are the outer sulcus cells (or root cells), which are situated at the junction of the basilar membrane with the lateral wall, and are either exposed to endolymph (apical turn) or completely covered by Claudius' cells (basal turn) (Jagger & Forge, 2013). Finger-like basolateral projections extend from their cell bodies to the spiral ligament and interdigitate with the fibrocytes.

1.2.3. Lateral Wall

Cochlear fluid homeostasis and generation of the endocochlear potential (the main driving force for sensory transduction) strongly depend on normal functioning of cochlear lateral wall tissues (Wangemann, 2006). The spiral ligament and the stria vascularis, which comprise the lateral wall of the cochlea, play an integral role in the maintenance of electrochemical homeostasis (Raphael & Altschuler, 2003; Wangemann, 2006).

1.2.3.1. Spiral Ligament

The spiral ligament forms the lateral part of the cochlear lateral wall, situated between the otic capsule (part of the temporal bone) and the stria vascularis. The spiral ligament comprises connective tissues (fibrocytes), epithelial cells, extracellular matrix material, and blood vessels. The fibrocytes of the spiral ligament have been classified into four different classes (type I – IV) based on their morphology, location and function (Dallos *et al.*, 1996; Spicer & Schulte, 1996; Hirose & Liberman, 2003) (**Figure 1.3**). Type I fibrocytes are

located in the area between the stria vascularis and otic capsule and are connected to the basal cells of the stria vascularis via gap junctions (Forge *et al.*, 2007). Type II fibrocytes occupy the area below the spiral prominence close to root processes of the outer sulcus cells. They have a distinct appearance, characterised by numerous cytoplasmic extensions, and are also in gap junction continuity with type I fibrocytes and strial basal cells. Fibrocytes of similar characteristics are also found in the suprastrial region near the insertion of Reissner's membrane (sometimes referred to as type V fibrocytes). Type III fibrocytes border the bony otic capsule and consist of irregular extensions and branches. Type IV fibrocytes are spindle-shaped and are located in the inferior region of the spiral ligament. Fibrocytes in the upper and lower regions of the spiral ligament are in direct contact with the perilymph from the scala vestibuli and scala tympani respectively. Tight junctions between epithelial cells lining the spiral prominence (a highly vascularised region that bulges into the scala media) and the outer sulcus cells form a barrier preventing the perilymph in the spiral ligament and scala tympani from mixing with the endolymph in the scala media.

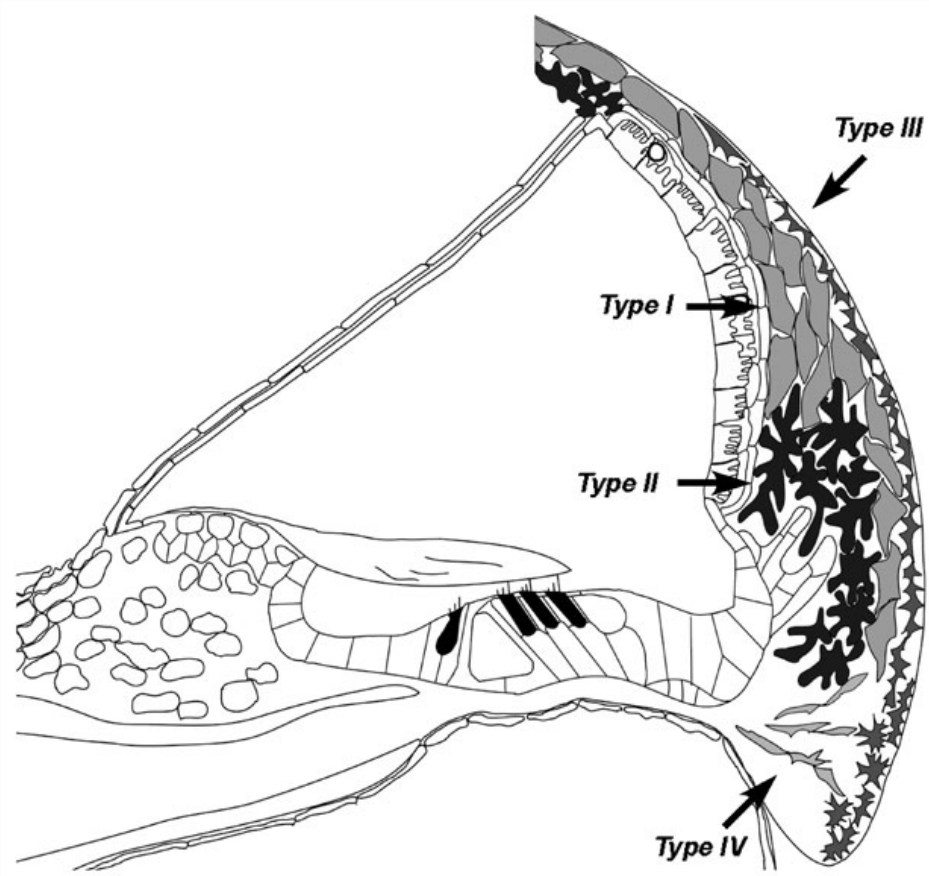

Figure 1.3: Schematic diagram of the cochlear duct illustrating the spatial organisation of the fibrocytes (type I – IV) in the spiral ligament. (Figure reproduced from Hirose and Liberman (2003), with permission from Springer).

1.2.3.2. Stria Vascularis

The stria vascularis, representing the medial part of the lateral wall, is a highly vascularised epithelium comprising three main cell types – marginal, intermediate and basal cells (Dallos *et al.*, 1996; Raphael & Altschuler, 2003). The marginal cells form a single layer of epithelial cells that line the endolymphatic space of the scala media. Their apical luminal surface contains an abundance of microvilli, indicative of their role in absorption and secretion. The basal cell layer faces the spiral ligament, and the intermediate cells, as their name indicates, are situated between the marginal and basal cells. Tight junctions between the marginal cells of the stria vascularis help protect the intrastrial space from the endolymph in the scala media, while the tight junctions of the basal cells protect the intrastrial space from perilymph. Both marginal and intermediate cells abundantly express Na^+/K^+-ATPases and play an important role in the generation of the endocochlear potential. The intermediate cells are melanocytes capable of synthesising melanin and are presumably derived from the neural crest (Hilding & Ginzberg, 1977; Steel & Barkway, 1989). The basal cells communicate with type I and II fibrocytes of the spiral ligament via gap junctions (Forge *et al.*, 2007).

1.2.4. Spiral Ganglion

The spiral ganglion, located within the modiolus, is made up of the cell bodies of the spiral ganglion neurons, satellite glial cells and blood vessels. There are two classes of spiral ganglion neurons – type I spiral ganglion neurons, which comprise 90-95% of the neurons, innervate the inner hair cells; and type II spiral ganglion neurons, which innervate the outer hair cells (Rosenbluth, 1962; Thomsen, 1967). The type I neurons are large, bipolar and myelinated, while the type II neurons are smaller, pseudounipolar and unmyelinated. The axons of the spiral ganglion neurons enter the auditory nerve, a branch of the vestibulocochlear nerve (cranial nerve VIII), which projects to the cochlear nuclei (dorsal cochlear nucleus and ventral cochlear nucleus) in the brainstem (Bear *et al.*, 2007).

1.2.5. Spiral Limbus

The spiral limbus (limbus laminae spiralis) is a structure located medial to the organ of Corti, consisting of epithelial cells, fibrocytes, extracellular matrix and blood vessels (Van De Water & Staecker, 2011). The epithelial cells, which are known as interdental cells, form well-arranged rows on the top surface of the spiral limbus. The tectorial membrane, an

acellular connective tissue overlying the organ of Corti, is anchored medially to the interdental cells, which secrete components of the tectorial membrane during foetal and postnatal life (Dallos *et al.*, 1996; Raphael & Altschuler, 2003). Occupying the main stroma of the spiral limbus beneath the interdental cells are fibrocytes, of which four types have been identified (stellate, mesothelial, osmiophilic, and light cells) (Kimura *et al.*, 1990). The fibrocytes of the spiral limbus are thought to play a significant role in maintaining cochlear fluid homeostasis. Below the spiral limbus is the osseous spiral lamina, which consist of two plates of bone, with the afferent and efferent nerve fibres innervating the sensory hair cells running between them.

1.2.6. Cochlear Vasculature

Adequate blood supply to the cochlea is critical to the normal functioning of the cochlea. The vascular anatomy of the cochlea shows widespread similarity among most mammalian species, including humans (Axelsson, 1988). The cochlear vasculature is segmentally arranged, with the capillary beds in the modiolus completely separated from those in the lateral wall by avascular structures such as Reissner's membrane, tectorial membrane and the peripheral part of the basilar membrane. No other organ in the body has such a number of distinct, specialised, microvascular networks as does the cochlea.

The inner ear is supplied by the internal auditory artery (also known as the auditory artery or labyrinthine artery), which arises from either the anterior inferior cerebellar artery or the basilar artery (Mom *et al.*, 2005). The internal auditory artery gives rise to the common cochlear artery near the site where the cochlear nerve enters the modiolus, and this in turn gives rise to the spiral modiolar artery in the modiolus. Radiating arterioles which branch off the spiral modiolar artery pass through the bone over the scala vestibuli into the lateral wall. In the lateral wall, the arterioles branch further to form distinct capillary beds in the suprastrial region of the spiral ligament, the stria vascularis, the peripheral region of the spiral ligament, and the inferior region of the spiral ligament (spiral prominence) (Hawkins, 1976; Dallos *et al.*, 1996). These capillary networks are arranged in parallel with no cross-connections between them. The walls of the capillaries form a continuous layer, with tight junctions between adjacent endothelial cells and a lack of fenestrations, thereby preventing free diffusion of solutes from the blood into the tissue spaces (blood-labyrinth barrier). The capillaries are also surrounded by a prominent basement membrane and pericytes. All of

these capillaries are drained by collecting venules, which leave the lateral wall through the bone under the scala tympani and empty into the spiral modiolar vein within the modiolus. Radiating arterioles arising from the spiral modiolar artery also branch to form capillary beds within the modiolus, spiral ganglion, spiral limbus, tympanic lip, and basilar membrane (Hawkins, 1976; Dallos *et al.*, 1996). The modiolar capillaries are fenestrated, which allows for rapid transfer of fluids and solutes. At the tympanic lip portion of the spiral limbus near the basilar membrane, the capillaries loop to form a network, which in most species is the nearest blood supply to the sensory hair cells of the organ of Corti. An additional blood vessel runs underneath the basilar membrane in a few species (Dallos *et al.*, 1996).

1.3. Inflammation

1.3.1. Introduction

Inflammation underlies a wide range of physiological and pathological processes. It is an immediate response by the body to infection, tissue injury, or noxious stimuli (Han & Ulevitch, 2005; Medzhitov, 2008). In general, an inflammatory reaction, if controlled properly, is beneficial. However, if unregulated, inflammation becomes detrimental. This forms the basis of the two general types of inflammation: acute and chronic. Acute inflammation is a short-term and well-controlled response that usually results in healing. In contrast, chronic inflammation is a long-term, dysregulated and maladaptive response that usually involves tissue destruction, and is associated with a wide variety of chronic conditions and diseases such as cardiovascular disease, arthritis, type 2 diabetes, cancer, allergy and autoimmune diseases.

The inflammatory pathway consists of inducers, sensors, mediators and effectors, with the type of inflammatory response determined by each component (Medzhitov, 2008) (**Figure 1.4a**). Inducers of inflammation are the signals that initiate the response, and can be divided into two main classes: exogenous or endogenous (**Figure 1.4b**). Exogenous inducers are external signals that are either microbial or non-microbial in nature. Endogenous inducers are signals produced by tissues that are stressed, damaged or malfunctioning. Sensors of inflammation sense the signal, become activated, and then elicit the production of specific sets of inflammatory mediators. These in turn alter the functional state of the downstream

effectors of inflammation – different types of cells and organs. There are in general seven groups of mediators in relation to their biochemical properties: vasoactive amines, vasoactive peptides, complement fragments, lipid mediators, inflammatory cytokines (discussed later), chemokines and proteolytic enzymes. Most inflammatory mediators have similar effects on the vasculature and on the recruitment of leukocytes.

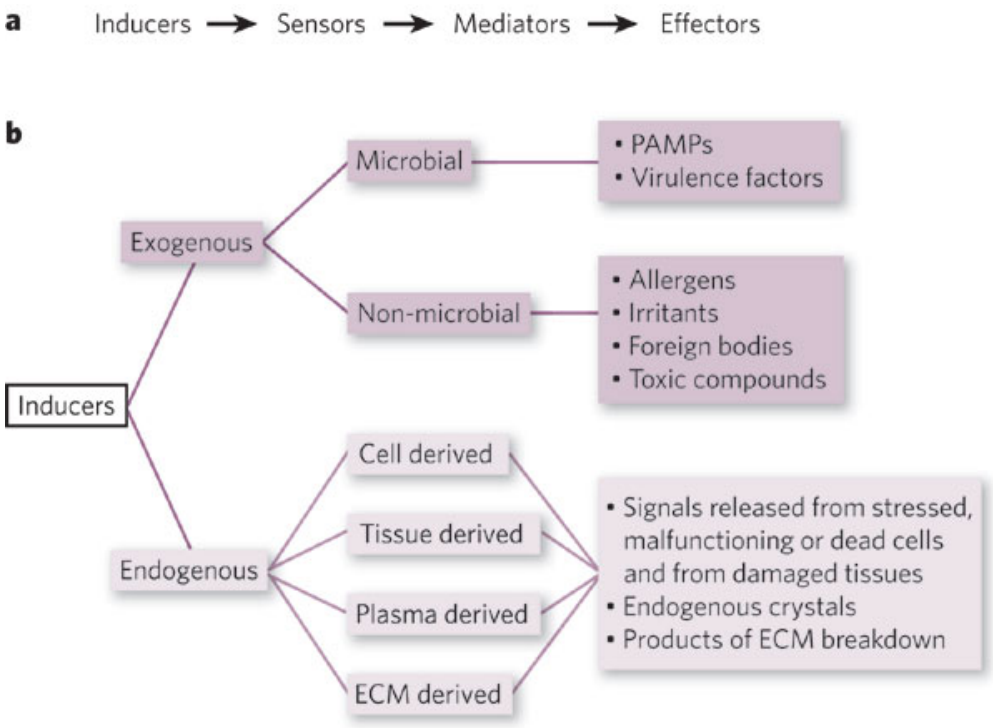

Figure 1.4: The general inflammatory pathway. (**a**) The general inflammatory pathway consists of inducers, sensors, mediators and effectors; (**b**) Inducers of inflammation can be classified as either exogenous or endogenous, which can be further subdivided as shown above. Abbreviations: PAMP, pathogen-associated molecular pattern; ECM, extracellular matrix. (Figure reproduced from Medzhitov (2008), with permission form Nature Publishing Group).

1.3.2. Proinflammatory Cytokines

Proinflammatory cytokines, which are small soluble secretory proteins that are normally produced by leukocytes but also by a range of other cell types, play a key role in promoting and modulating inflammation (Dinarello, 2000; Adams, 2002; Khan *et al.*, 2010). They mediate their effects by binding to their distinct receptors on the surface of cells, activating intracellular signalling cascades. Cytokines can act in either an autocrine or paracrine

manner, and consequently, cells that express them also have corresponding surface receptors. The cytokines most traditionally associated with inflammation include tumour necrosis factor-alpha (TNF-α), interlukin-1beta (IL-1β) and interleukin-6 (IL-6). These proinflammatory cytokines are together actively involved in the initiation and regulation of the inflammatory response. They have pleiotropic roles, but TNF-α, IL-1β and IL-6 are chiefly involved in the recruitment of inflammatory cells, the activation of T and B lymphocytes, and promoting the differentiation of proliferating B cells into plasma cells and the secretion of antibodies respectively (Yoshida *et al.*, 1999; Dinarello, 2000; Khan *et al.*, 2010). Cytokines such as these also participate in a variety of other important roles, such as development, tissue remodelling, apoptosis and cellular stress response (Adams, 2002; Khan *et al.*, 2010). Because of their important physiological roles, the actions of cytokines are regulated by numerous exquisite molecular mechanisms (e.g. cytokine networks). When such cytokine regulating mechanisms become disrupted, a range of inflammatory and autoimmune disorders may develop (Nishimoto, 2010).

1.3.2.1. Tumour Necrosis Factor-Alpha (TNF-α)

TNF-α is a potent proinflammatory cytokine produced by a vast array of cell types, including macrophages, monocytes, T and B lymphocytes, fibroblasts and keratinocytes (Tracey & Cerami, 1993; Baud & Karin, 2001; Khan *et al.*, 2010; Park & Bowers, 2010). It is considered one of the primary mediators of the inflammatory response, inducing the production of several other cytokines and activating and recruiting leukocytes and lymphocytes. Additionally, it plays a central role in apoptosis, cell proliferation and differentiation. TNF-α is 212-amino acid protein that exist and is active in both cell-associated (as a type-II transmembrane protein) and soluble forms. It elicits its effects via two distinct cell surface receptors, TNFR1 and TNFR2 (Baud & Karin, 2001; Park & Bowers, 2010). Binding to either receptor triggers the activation of one of three major signalling cascades: apoptotic signalling cascade, nuclear factor-kappa B (NF-κB) signalling pathway, or the c-Jun N-terminal kinase (JNK) signalling pathway (Baud & Karin, 2001; Park & Bowers, 2010).

1.3.2.2. Interleukin-1Beta (IL-1β)

IL-1β, which is part of the IL-1 family, is another proinflammatory cytokine playing an important role in immune and inflammatory responses (Dinarello, 2002; Fogal & Hewett, 2008; Dinarello, 2009; Khan *et al.*, 2010). It is produced as a proprotein (precursor) that

requires cleavage by a specific intracellular cysteine protease called IL-1β converting enzyme (also known as caspase-1) to become biologically active. IL-1β is released by many cell types, including monocytes, macrophages, dendritic cells, and B lymphocytes, and binds to IL-1 receptor type I (IL-1RI) or IL-1 receptor type II (IL-1RII) (Dinarello, 2002; Dinarello, 2009). IL-1β shares several biological properties with TNF-α, but does not induce apoptosis in contrast to TNF-α. Some of the fundamental properties of IL-1β include the activation of T and B lymphocytes, and the induction proinflammatory cytokines, extracellular proteases, cyclooxygenase-2 (COX-2), type 2 phospholipase A_2, and inducible nitric oxide synthase (iNOS) (Dinarello, 2002; Fogal & Hewett, 2008; Dinarello, 2009).

1.3.2.3. Interleukin-6 (IL-6)

IL-6 is a pleiotropic cytokine that has important functions in the immune response, inflammation, and haematopoiesis (Nishimoto & Kishimoto, 2006; Khan *et al.*, 2010; Nishimoto, 2010; Wakabayashi *et al.*, 2010). It is produced and secreted by various types of cells, including T lymphocytes, B lymphocytes, monocytes, endothelial cells, astrocytes, microglia, neurons, fibroblasts and keratinocytes. Some of its biological activities include inducing the differentiation of activated B cells into antibody-producing plasma cells, the proliferation of T cells, the differentiation of cytotoxic T cells, and the infiltration of macrophages to local damaged areas via upregulation of cell adhesion molecules. IL-6 protects from oxidative stress by upregulating anti-apoptotic genes (Fujioka *et al.*, 2006). IL-6 exerts its effects through a unique cell-surface receptor system consisting of a ligand-binding component (IL-6R) together with a signal-transducing chain (gp130) (Nishimoto & Kishimoto, 2006). Binding of IL-6 to IL-6R activates the receptor complex and initiates a signal transduction cascade involving Janus kinases (JAKs) and Signal Transducer and Activator of Transcription (STAT) proteins.

1.3.3. Chemokines

Chemokines are chemotactic cytokines that mediate the directional migration of immune cells (chemotaxis) to sites of injury and inflammation, and are also involved in routine immunosurveillance, lymphocyte development, central nervous system development, haematopoiesis, angiogenesis, cardiogenesis, metastasis, tumorigenesis, and HIV infection (Le *et al.*, 2004; Allen *et al.*, 2007; Mélik-Parsadaniantz & Rostène, 2008; Griffith *et al.*, 2014). Produced by a variety of cell types, chemokines constitutes the largest family of

cytokines, with approximately 50 endogenous chemokines identified to date. They exert their effects by binding to G protein-coupled receptors, which are differentially expressed on all leukocytes. They have been classified into four subfamilies on the basis of the arrangement of N-terminal cysteine residues: C, CC, CXC, and CX3C (C represents cysteine; X/X3 represents one or three non-cysteine amino acids). These chemokine subfamilies attract distinct classes of leukocytes. For example, the chemokines of the CC subfamily are primarily chemotactic for monocytes and macrophages, and include chemokine (C-C motif) ligand 2 (CCL2), which was previously known as monocyte chemoattractant protein-1 (MCP-1). CCL2 binds to the chemokine receptors CCR2 and CCR4.

1.3.4. Cell Adhesion Molecules

During an inflammatory response, circulating leukocytes adhere to and transmigrate across the vascular endothelium to the site of tissue damage or infection. This process, known as extravasation (or diapedesis), is predominantly orchestrated by various vascular cell adhesion molecules including E-selectin, P-selectin, ICAM-1, VCAM-1 and PECAM-1 (Crawford & Watanabe, 1994; Shi & Nuttall, 2007). These cell adhesion molecules are constitutively expressed at low levels on the luminal surface of vascular endothelial cells, but can become significantly increased under inflammatory conditions. They are also present on the surface of some circulating leukocytes. E-selectin and P-selectin are involved in the initial step in the extravasation process, mediating the deceleration and rolling of leukocytes along the luminal surface of activated endothelial cells by forming loose connections with the circulating leukocytes. Intercellular adhesion molecule-1 (ICAM-1), also known as Cluster of Differentiation 54 (CD54), is essential for the temporary adherence of leukocytes to the vasculature prior to their transendothelial migration into tissue. They are ligands for leukocyte function associated antigen-1 (LFA-1) and macrophage adhesion ligand-1 (MAC-1), which are β2 integrin molecules present on leukocytes (Hubbard & Rothlein, 2000; Lawson & Wolf, 2009). Firm connections are formed between leukocytes and endothelial cells via interactions between β2 integrins and ICAM-1. Vascular cell adhesion molecule-1 (VCAM-1; CD106) plays a similar role to ICAM-1, facilitating the temporary immobilisation of leukocytes to the endothelium (Zhang, 2000). The final phase of leukocyte emigration involves platelet-endothelial cell-adhesion molecule-1 (PECAM-1; CD31), and like ICAM-1 and VCAM-1, is a membrane protein of the immunoglobulin (Ig) superfamily. PECAM-1 is constitutively expressed in the intercellular junctions of vascular endothelial

cells and mediates the transmigration of leukocytes across the endothelium (Muller *et al.*, 1993; Woodfin *et al.*, 2007). The entire extravasation process thus consists of three successive stages: 1) rolling, mediated by E-selectin and P-selectin; 2) firm adhesion, mediated by ICAM-1 and VCAM-1; and 3) transendothelial migration, mediated by PECAM-1.

1.3.5. Macrophages

Macrophages are a class of white blood cells or leukocytes that serve as effector cells of the immune system. They are generally considered to be derived from circulating monocytes via the process of differentiation, and are classified into two broad categories: 1) infiltrating macrophages, which transmigrate from the circulation into tissues (a process referred to as extravasation, mediated by cell adhesion molecules) in response to specific inflammatory signals, and 2) resident tissue macrophages, which reside in specific tissues during steady-state conditions, and are present in almost all tissues of the body (Luster *et al.*, 2005; Okano *et al.*, 2008). Resident tissue macrophages are versatile cells, having multiple key roles such as recognising and phagocytosing foreign bodies (e.g. pathogens) or dying (senescent) cells, producing and secreting various cytokines that influence cell function, and regulating specific immune and inflammatory responses (Warchol, 1997; Okano *et al.*, 2008). Macrophages are also recruited to sites of tissue injury and have been reported to be involved in initiating the process of wound healing (Warchol, 1997).

1.3.6. Resolution of Inflammation

A prerequisite for successful resolution of the inflammatory response is effective elimination of granulocytes and the return of the macrophage and lymphocyte population to normal baseline numbers. Emerging evidence suggests that inflammation is resolved by an active, coordinated program that is engaged early in the inflammatory response (Serhan & Savill, 2005). This so called “resolution program” involves the production of specific chemical mediators, programmed leukocyte death by apoptosis and subsequent clearance of the dead cells by the phagocytic action of macrophages. The usual fate of these inflammatory macrophages is departure from the inflamed tissue site through nearby lymphatics.

1.4. Cochlear Inflammation

Cochlear inflammation has been implicated as a major etiologic factor in a range of conditions that cause hearing loss. These include acoustic trauma (noise-induced cochlear damage), otitis media (middle ear infection), meningitis, autoimmune inner ear disease, and ototoxicity (drug-induced inner ear damage, e.g. by aminoglycoside antibiotics, platinum-based chemotherapeutic agents) (Kawauchi *et al.*, 1988; Gloddek *et al.*, 1999; Hirose *et al.*, 2005; Trinidad *et al.*, 2005; Tornabene *et al.*, 2006; So *et al.*, 2007; So *et al.*, 2008; Cayé-Thomasen *et al.*, 2009). Inflammation can also be evoked by cochlear surgery and the insertion of cochlear implants (Backhouse *et al.*, 2008; Okano *et al.*, 2008). Pathogen-induced labyrinthitis as a consequence of otitis media or meningitis is usually associated with bacterial and viral infections. Labyrinthitis secondary to otitis media (tympanogenic labyrinthitis) primarily occurs by the spread of the infection from the middle ear into the inner ear through the three-layered round window membrane (Kawauchi *et al.*, 1988; Cureoglu *et al.*, 2005; Trinidad *et al.*, 2005; MacArthur & Trune, 2006). Meningogenic labyrinthitis most likely occurs by the spread of infection from the meninges into the perilymphatic space of the cochlea through the cochlear aqueduct (Merchant & Gopen, 1996; Klein *et al.*, 2008; Cayé-Thomasen *et al.*, 2009). Mycotic (fungal) labyrinthitis is rare, and is usually associated with systemic debilitating diseases and occurs by either the tympanogenic, meningogenic or hematogenic route (Cureoglu *et al.*, 2005).

Labyrinthitis usually affects the cochlea more severely than the vestibular system, resulting in adverse effects on cochlear function (Cureoglu *et al.*, 2005). A well-documented complication of cochlear inflammation is partial or complete sensorineural hearing loss. Pathological consequences that have been observed in animal models of cochlear inflammation include degeneration of hair cells of the organ of Corti, disruption of fibrocytes in the spiral ligament, loss of interdental cells of the spiral limbus, swelling of the stria vascularis, and vascular damage (Ichimiya *et al.*, 2000; Barkdull *et al.*, 2005; Cureoglu *et al.*, 2005; Moon *et al.*, 2006). The disruption of the spiral ligament fibrocytes has been suggested as a major contributor to the inflammation-induced cochlear dysfunction (Ichimiya *et al.*, 2000, 2004). Decreased immunostaining for gap junction protein connexin 26 in type I and type II fibrocytes and decreased Na^+-K^+-ATPase staining in type II fibrocytes, both of which are critical in the maintenance of cochlear homeostasis, were observed in a guinea pig model of labyrinthitis induced by inoculation of the protein antigen keyhole limpet hemocyanin

(KLH) into the scala tympani (Ichimiya *et al.*, 1998). In addition, reduced connexin 26 immunostaining in the spiral ligament was also demonstrated in a mouse model of otitis media induced by the transtympanic inoculation of viable *Streptococcus pneumonia* (Ichimiya *et al.*, 1999).

Analogous to the central nervous system and the retina of the eye, the cochlea is separated from the systemic circulation by a blood-labyrinth barrier, which has similar physiological characteristics as the blood-brain barrier and the blood-retinal barrier. This barrier is important in maintaining the ionic composition of the cochlear fluid compartments, and is essential for the functional integrity of the cochlea (Harris & Ryan, 1995). Because of the existence of this blood-labyrinth barrier and the relative absence of resident tissue macrophages, the inner ear was originally considered an immunologically privileged organ, isolated from the immune system and protected from immune surveillance. However, this hypothesis has been refuted by research demonstrating that the inner ear is capable of rapidly generating an active inflammatory/immune response in the presence of antigens or pathogens (Harris, 1983; Harris, 1984; Harris *et al.*, 1990; Fukuda *et al.*, 1992). In addition, connections exist between the inner ear and the systemic lymphatic system through cervical lymph nodes (Yimtae *et al.*, 2001).

Although the intended purpose of the immune response in the inner ear is to defend the hearing organ against invading pathogens and to clear cellular debris, the inflammatory response can also cause significant bystander injury to the delicate structures of the cochlea (Harris & Ryan, 1995; Ma *et al.*, 2000). Because mammalian inner ear tissues have limited abilities of repair and regeneration (unlike avian auditory hair cells which have the capacity to regenerate), this damage is irreversible, leading to permanent hearing loss. Immune-related cochlear inflammation is increasingly recognised as a potential mechanism of inner ear disease and associated hearing loss. Systemic administration of immunosuppressive drugs (e.g. corticosteroids) has been shown to effectively ameliorate some cases of idiopathic, rapidly progressive bilateral sensorineural hearing loss, implicating inner ear inflammation as an underlying mechanism of the hearing loss (Ryan *et al.*, 2002). Histopathological studies of human temporal bones also support the hypothesis that a number of otological disorders are linked with inflammatory responses (Keithley *et al.*, 1998). The severity of hearing impairment and the potential for recovery correlate with the extent of inflammation-induced tissue damage. Animal studies have demonstrated that the development of inflammation and

hearing loss following an immunological challenge can be rapid, with the onset of hearing loss occurring at 12 to 15 hours, and peaking at 24 to 48 hours (Keithley *et al.*, 1989; Kesser *et al.*, 1999).

Regardless of the cause, the cochlear inflammatory response, which lasts approximately three to seven days, is characterised by the production of proinflammatory mediators such as cytokines and chemokines, an increased expression of cell adhesion molecules, the recruitment and infiltration of inflammatory cells such as polymorphonuclear leukocytes (mostly neutrophils), monocytes, macrophages and lymphocytes, and the breakdown of the blood-labyrinth barrier (Barkdull *et al.*, 2005; Schramm, 2010). In more severe forms of cochlear inflammation, this phase is followed by a chronic stage, in which a fibrotic matrix is formed in the perilymphatic spaces, which later becomes calcified (Schramm, 2010). This bony occlusion of the fluid-filled cochlear scalae, known as labyrinthitis ossificans, is most extensive in post-meningitis cases (Xu *et al.*, 2009).

The cochlea itself can mount an immune response. Resident cells in the cochlea can express a range of inflammatory mediators, which are thought to play critical roles in the inflammatory response (Yoshida *et al.*, 1999; Fujioka *et al.*, 2006; Tabuchi & Hara, 2012). The cochlea communicates with the immune system via the systemic circulation. Entry of inflammatory cells occurs primarily through the spiral modiolar vein and its tributaries (collecting venules) situated at the base of the scala tympani (Harris *et al.*, 1990; Fukuda *et al.*, 1992). Inflammatory cells accumulate in the perivascular space surrounding the spiral modiolar vein, and then stream into the scala tympani along the extravascular space of the collecting venules. Other areas where circulating inflammatory cells enter the cochlea include the blood vessels of the spiral ligament and the spiral ganglion. The lateral wall of the cochlea and the spiral ganglion represent the most permeable parts of the blood-labyrinth barrier, partly due to their high vascularisation (Sato *et al.*, 2008; Sato *et al.*, 2010).

The mammalian cochlea contains resident macrophages at normal/steady state (Hirose *et al.*, 2005; Lang *et al.*, 2006; Okano *et al.*, 2008; Sato *et al.*, 2008). These macrophages are phenotypically similar to the tissue macrophages in other organs of the body (e.g. microglia of the central nervous system) and are found in small numbers predominantly in the spiral ligament and the spiral ganglion. Moreover, it was recently reported that a large number of perivascular resident macrophages (PVMs) are present in the stria vascularis surrounding the

endothelial cells of the capillaries (Shi, 2010). Data from radiation chimeras have shown that these resident macrophages in the cochlea form an exchanging and migratory population, supplied continuously from haematopoietic precursors in the bone marrow, and exhibiting slow turnover during steady-state conditions (Okano *et al.*, 2008; Sato *et al.*, 2008; Shi, 2010) (**Figure 1.5**). These haematopoietic precursors migrate into the cochlea and differentiate into tissue macrophages. Bromodeoxyuridine (BrdU) labelling has demonstrated that the marked increase in macrophage numbers in the cochlea following an insult such as noise exposure is not due to the proliferation of these resident cochlear macrophages, but rather occurs by the migration of macrophages from the vascular system (Hirose *et al.*, 2005; Ladrech *et al.*, 2007).

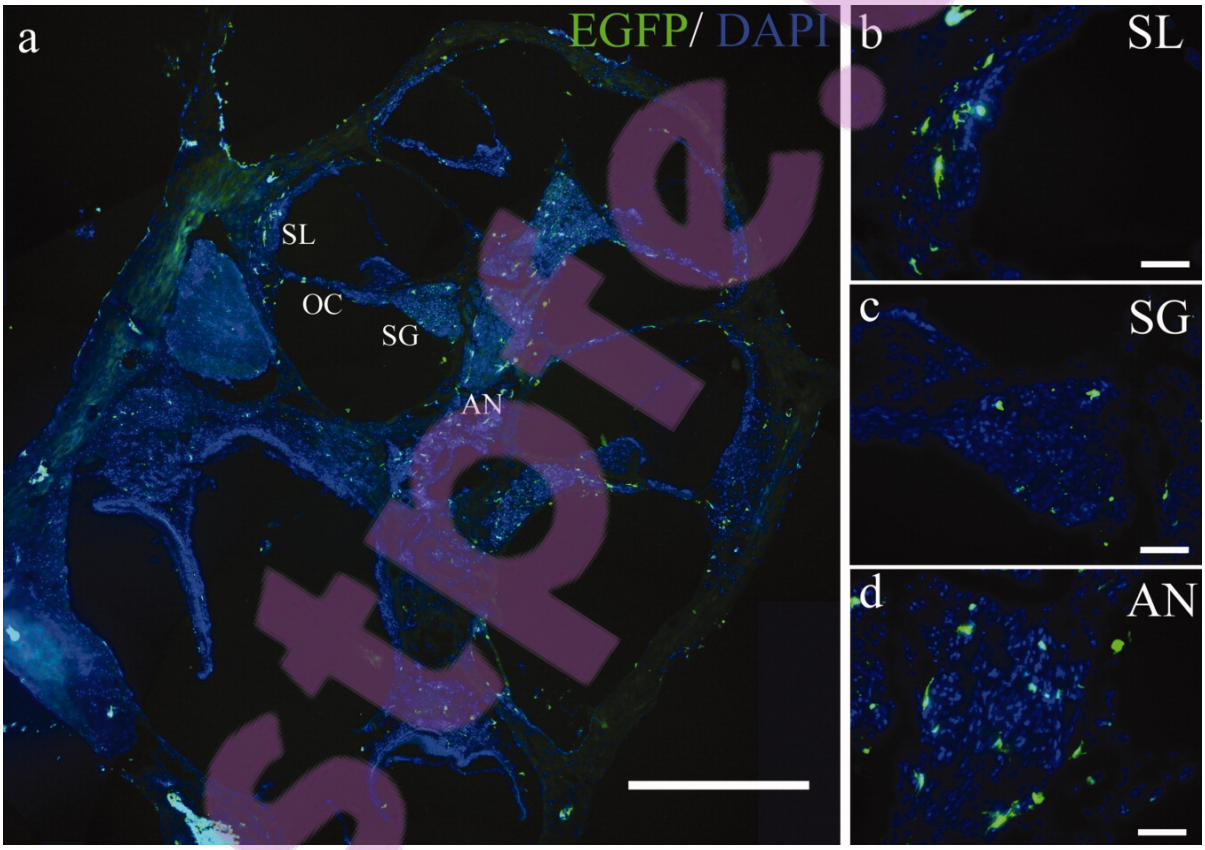

Figure 1.5: Distribution of haematopoietic cell-derived cells in the cochlea. (**a**) Distribution of haematopoietic cell-derived cells (expressing EGFP) in the cochlea of a bone marrow chimeric mouse 6 months after transplantation. Blue fluorescence shows nuclear staining with DAPI. EGFP-positive cells were observed predominantly in the lower portion of the spiral ligament among type II and IV fibrocytes (**b**) and along nerve fibers in the spiral ganglion (**c**) and auditory nerve (**d**). *Abbreviations*: SL, spiral ligament; OC, organ of Corti; SG, spiral ganglion; AN, auditory nerve. Scale bars = 500 µm (in a); 50 µm (in b-d). (Figure reproduced from Okano *et al.* (2008), with permission from John Wiley and Sons).

The signals that initiate the recruitment and infiltration of inflammatory cells into the cochlea are still under scrutiny, and a wide range of soluble mediators (e.g. cytokines, chemokines) may be involved. The sources of proinflammatory mediators in the cochlea include various resident cochlear cells types (e.g. spiral ligament fibrocytes, supporting cells) and infiltrating leukocytes migrating from the cochlear vasculature. *In vitro* studies using cultured murine spiral ligament fibrocytes have shown that upon stimulation with proinflammatory cytokines, fibrocytes secrete a variety of inflammatory mediators such as TNF-α, IL-1β, IL-6, CCL2, macrophage inflammatory protein-2 (MIP-2), keratinocyte-derived chemokine (KC), soluble intercellular adhesion molecule-1 (sICAM-1) and vascular endothelial growth factor (VEGF), which play important roles in the recruitment of inflammatory cells into the cochlea (Yoshida *et al.*, 1999; Ichimiya *et al.*, 2000; Maeda *et al.*, 2005; Moon *et al.*, 2006). The secretion of sICAM-1 is compatible with an earlier study that reported strong ICAM-1 expression in the spiral ligament and spiral modiolar vein in the early phase of labyrinthitis induced by the inoculation of KLH into the scala tympani (Suzuki & Harris, 1995). It has been speculated that these mediators produced by the fibrocytes are presented on the surface of vascular endothelial cells via the process of transcytosis, which consequently attract and activate inflammatory cells (Yoshida *et al.*, 1999). Fibrocytes, vascular endothelial cells, and inflammatory cells together may form networks interconnected by cytokines, chemokines and various other inflammatory mediators (Yoshida *et al.*, 1999; Ichimiya *et al.*, 2000).

It is well documented that inhibition of TNF-α with the soluble TNF-α receptor-FC fusion protein Etanercept, given either systemically or directly into the cochlea, significantly attenuates the cochlear inflammatory response (Satoh *et al.*, 2002; Wang *et al.*, 2003b). The reduction in inflammation by blocking TNF-α strongly suggests that TNF-α plays a critical role in the development of cochlear inflammation. Studies on organ of Corti explants have shown that TNF-α alone, in the absence of antigens or pathogens, has the ability to induce the recruitment of inflammatory cells into the cochlea from the systemic circulation (Keithley *et al.*, 2008). TNF-α is also expressed by infiltrating leukocytes, suggesting that it is likely involved in a positive feedback loop that further amplifies the recruitment of inflammatory cells. This is supported by the evidence that TNF-α inhibition can prevent the recruitment of inflammatory cells into the cochlea (Satoh *et al.*, 2002). TNF-α can also induce nitric oxide synthesis by stimulating the expression of iNOS, which can further aggravate inflammation and degeneration in the cochlea (Khan *et al.*, 2010).

The expression of many proinflammatory mediators is mostly regulated by nuclear factor-kappa-light-chain-enhancer of activated B cells (NF-κB) (So *et al.*, 2008). NF-κB comprises a family of inducible transcription factors that play a pivotal role in immune and inflammatory responses. Activation of NF-κB induces the transcription of cytokines such as TNF-α, IL-1β and IL-6, as well as iNOS, and the cell adhesion molecules, ICAM-1 and VCAM-1. NF-κB activation in the cochlea has been demonstrated following intraperitoneal injection of lipopolysaccharide (LPS) (Adams, 2002; Adams *et al.*, 2009), suggesting that the cochlea can become immunologically active even after systemic administration of bacterial toxins. Cochlear activation of NF-κB has also been reported to occur following acoustic trauma (Ramkumar *et al.*, 2004; Masuda *et al.*, 2006; Adams *et al.*, 2009; Yamamoto *et al.*, 2009) (see **Section 1.6**) and in cisplatin-induced ototoxicity (So *et al.*, 2007).

At present, it is technically impossible to positively identify inflammatory processes within the human inner ear. There are no well-defined detection methods available and diagnostic biopsy of the human cochlea is not feasible. To overcome this limitation, high field magnetic resonance imaging (MRI) techniques were recently developed by our group to quantitatively evaluate the development of cochlear inflammatory processes in a guinea pig model induced by the intratympanic injection of LPS (Le Floc'h *et al.*, 2013). For the first time, dynamic changes in cochlear vascular permeability following cochlear inflammation was quantified using dynamic contrast enhanced (DCE)-MRI and ultrasmall superparamagnetic iron oxide particles (USPIOs) were used to characterise the recruitment of macrophages into the cochlea. These methodologies therefore hold considerable potential as diagnostic tools for human inner ear diseases such as labyrinthitis and could also be used to quantitatively assess the efficacy of treatments for cochlear inflammation.

Below is a brief discussion of each of the main aetiologies of cochlear inflammation (otitis media, meningitis, autoimmune inner ear disease, ototoxicity, and cochlear surgery), including how they are suggested to induce inflammation in the cochlea and the reported inflammatory and pathological features specific to the condition. Noise-induced cochlear inflammation, which is the primary focus of this thesis, will be discussed in depth in a subsequent section (**Section 1.6**) following an overview of noise-induced cochlear injury and hearing loss (**Section 1.5**).

1.4.1. Otitis Media

Acute or chronic suppurative otitis media (SOM), a bacterial or viral infection of the middle ear, is one of the most prevalent inflammatory diseases among young children, with significant personal and societal costs (MacArthur & Trune, 2006; Ghaheri *et al.*, 2007). The middle ear disease is caused most frequently by the bacteria *Streptococcus pneumonia* and *Haemophilus influenza* (Engel et al., 1995). Partial or complete sensorineural hearing loss and vestibular dysfunction (vertigo) are well-recognised sequelae of otitis media (Trinidad *et al.*, 2005). These otitis media-induced inner ear complications are believed to be caused by immune-mediated tissue damage as a result of inner ear inflammation. Human temporal bone studies of patients who had chronic otitis media show that inner ear pathology (inflammation and damage) occurs in 20% to 67% of cases (Ghaheri *et al.*, 2007).

A long-standing debate of how SOM impacts the inner ear has led to a widely accepted opinion that the labyrinthitis secondary to SOM primarily occurs by the spread of otitis media pathogens, bacterial toxins (endotoxins and exotoxins) and other bacterial molecules, inflammatory cells or inflammatory mediators (e.g. cytokines, chemokines) from the middle ear into the inner ear through the three-layered round window membrane (Kawauchi *et al.*, 1988; Ichimiya *et al.*, 2000; Cureoglu *et al.*, 2005; Trinidad *et al.*, 2005; MacArthur & Trune, 2006). This is considered the most likely pathway between the middle and inner ear, as the round window membrane is the only true soft tissue/permeability barrier between the two compartments (Engel *et al.*, 1995; Cureoglu *et al.*, 2005). However, very recent evidence has demonstrated that there is also some permeability through the oval window (King *et al.*, 2014). Once in the cochlea, these inflammatory agents are thought to induce an inflammatory reaction.

Studies have shown that various biological substances placed in the middle ear cavity diffuse across the round window membrane or are recovered from the perilymph (Cureoglu *et al.*, 2005). These substances are usually confined to the basal turn of the cochlea (Cureoglu *et al.*, 2005), hence otitis media-induced cochlear damage is often limited to the high frequency region (Engel *et al.*, 1995). It has been suggested, based on histopathological findings, that substances can also spread from the inner ear to the middle ear (Cureoglu *et al.*, 2005). Furthermore, it has been reported that exposure of the round window membrane to endotoxins such as LPS results in structural and permeability changes to the membrane (Spandow *et al.*, 1990; Watanabe *et al.*, 2001).

The spread of middle ear disease to the cochlea has been the subject of numerous studies. SOM has been successfully modelled by intratympanic or transbullar inoculation of viable bacteria (e.g. *S. pneumonia*, *H. influenza*) or endotoxin (e.g. LPS) into the middle ear cavity (Hess *et al.*, 1999; Ichimiya *et al.*, 2000; Watanabe *et al.*, 2001; Ichimiya *et al.*, 2004; Hashimoto *et al.*, 2005; Trinidad *et al.*, 2005; Ghaheri *et al.*, 2007). The extensive middle ear inflammation that occurs in these animals is often seen to spread to the inner ear. Pathological findings in the cochlea include inflammatory cell invasion particularly in the perilymphatic spaces, disruption of the spiral ligament fibrocytes (decreased connexin 26 immunostaining in the spiral ligament), disruption of the blood-labyrinth barrier (marked fibrinogen deposition primarily in the lower region of the spiral ligment), loss of outer hair cells, and strial swelling (Ichimiya *et al.*, 2000, 2004; Trinidad *et al.*, 2005; MacArthur & Trune, 2006; Moon *et al.*, 2006; Ghaheri *et al.*, 2007). SOM-induced inner ear inflammation has also been associated with increased ABR thresholds (MacArthur *et al.*, 2006; Ghaheri *et al.*, 2007)

Cultured spiral ligament fibrocytes (type I) treated with *S. pneumonia* or *H. influenza* release various cytokines and chemokines, suggesting that they respond to otitis media pathogens and may play a role in the recruitment of inflammatory cells (Moon *et al.*, 2006). In addition, intratympanic inoculation of the middle ear with *H. influenza* significantly affects the cochlear expression of numerous genes involved in inflammation (Ghaheri *et al.*, 2007). This study provides clear evidence that cochlear inflammation induced by SOM occurs not only by inflammatory agents permeating the round window membrane into the cochlea, but also by the local production of inflammatory mediators within the cochlea.

1.4.2. Meningitis

Sensorineural hearing loss is the most frequent complication of meningitis, an inflammatory disease of the meninges, the membranous envelopes of the central nervous system (Merchant & Gopen, 1996; Kesser *et al.*, 1999; Kastenbauer *et al.*, 2001; Klein *et al.*, 2008; Cayé-Thomasen *et al.*, 2009). The hearing loss usually develops in the very early stages of the disease and the severity of it can range from mild to severe and even profound deafness. Meningogenic inflammation of the cochlea has been demonstrated to occur via one of three different routes: 1) spread of inflammatory cells from the meninges to the perilymphatic space via the cochlear aqueduct, 2) spread of inflammatory cells from the bloodstream to the endolymphatic space via capillaries within the spiral ligament, or 3) spread of inflammatory

cells from the scala tympani to Rosenthal's canal and the spiral ganglion via canaliculi of the osseous spiral lamina (Merchant & Gopen, 1996; Klein *et al.*, 2008; Cayé-Thomasen *et al.*, 2009). Cochlear injury caused by infiltration of inflammatory cells secreting cytotoxic mediators include damage to the organ of Corti, spiral ganglion, and the blood-labyrinth barrier (Klein *et al.*, 2008). With chronic meningitis-associated hearing loss, bony occlusion of the membranous labyrinth occurs in the final stage, a process known as labyrinthitis ossificans.

1.4.3. Autoimmune Inner Ear Disease

Cases of idiopathic, bilateral, rapidly progressive hearing loss are often suspected to be of autoimmune origin. This was first described by McCabe (1979) in which an improvement in auditory function was observed in patients following immunosuppressive therapy (dexamethasone with or without cyclophosphamide). Autoimmune inner ear disease is considered a rare disorder and can affect patients at any age, but is more common in adults than in children (Gopen & Harris, 2008). A number of experimental animal models of autoimmune inner ear disease have been developed using various antigens and these have demonstrated the occurrence of labyrinthitis in the cochlea, with large infiltration of inflammatory cells and damage to cochlear tissues (Harris, 1983; Yoo *et al.*, 1983; Gloddek *et al.*, 1999; Carcia-Berrocal *et al.*, 2004). An animal model of autoimmune inner ear disease mediated by the adoptive transfer of T cells specific for calcium-binding protein S-100β, an autoantigen, induces severe labyrinthitis and is associated with an impairment of hearing (Gloddek *et al.*, 1999). The inflammatory response is characterised by an infiltration of lymphocytes (mainly T-helper cells) predominantly in the scala vestibuli, and perivasculitis of the modiolar blood vessels.

1.4.4. Aminoglycoside and Cisplatin-Induced Ototoxicity

Ototoxicity refers to drug-induced damage to inner ear structures, and is typically characterised by sensorineural hearing loss and balance disorders. Drugs with ototoxic potential include aminoglycoside antibiotics (e.g. kanamycin, streptomycin, neomycin, amikacin) and platinum-based chemotherapeutic agents (e.g. cisplatin, carboplatin). Inflammatory cell infiltration into the cochlea has been documented following amikacin (Ladrech *et al.*, 2007) and kanamycin (Sato *et al.*, 2010; Hirose *et al.*, 2014) treatment. A

peak increase in macrophage density occurs during the first week post-amikacin treatment, coinciding with the massive hair cell death by apoptosis (Ladrech *et al.*, 2007). This macrophage infiltration ends by the end of the first week when all the outer hair cells and most of the inner hair cells have died, suggesting that hair cell death triggers macrophage infiltration to phagocytose cellular debris. Increase in expression of the proinflammatory cytokines IL-1β, IL-6 and TNF-α via activation of extracellular signal-regulated kinase (ERK) and NF-κB has also been observed with cisplatin administration (So *et al.*, 2007; So *et al.*, 2008), suggesting that these inflammatory mediators may contribute to tissue injury. Cisplatin also induces the activation of signal transducer and activator of transcription-1 (STAT1), a transcription factor that regulates the expression of a number inflammatory genes, such as iNOS, COX-2 and TNF-α (Kaur *et al.*, 2011). Knockdown of STAT1 by short interfering RNA (siRNA) was shown to suppress cisplatin-induced cochlear inflammation and protect against ototoxicity, implicating an essential role of STAT1 in cisplatin-mediated ototoxicity.

1.4.5. Cochlear Surgery

Cochlear surgery also evokes an inflammatory reaction due to the local exogenous stress on the cochlea (Backhouse *et al.*, 2008; Okano *et al.*, 2008). Application of physiological saline into the posterior semicircular canal, a surgical procedure which has been used for administering drugs or cells into the inner ear, has been shown to increase the number of inflammatory cells in the spiral ligament and spiral ganglion, peaking seven days post-surgery (Okano *et al.*, 2008). This increase in cochlear macrophages, which was shown to be due mainly to the migration of macrophages from the systemic circulation, was associated with a temporary increase in ABR thresholds. A recent study examining the early response of the cochlea to implantation of a cochlear electrode into the scala tympani reported an increased expression of ICAM-1 in the spiral ligament (type II and IV fibrocytes) and a large infiltration of inflammatory cells (neutrophils and macrophages) (Kel *et al.*, 2013). This response is thus similar to that observed following other types of cochlear injury such as acoustic trauma, infection, and inner ear antigen challenge.

1.5. Noise-Induced Hearing Loss

1.5.1. Introduction

The human ear is an exquisitely sensitive organ, allowing us to perceive and distinguish among the myriad sounds around us, be they pleasurable, informative or damaging. Unfortunately, this extreme sensitivity of the cochlea comes at a cost as it makes it highly susceptible to injury when exposed to loud sound. The consequence of this injury is the loss of hearing, which can be either temporary or permanent. Noise-induced hearing loss may result from either brief exposure to an intense "impulse" noise or sustained and repeated exposure to excessive sound levels (i.e. continued exposure to high levels of noise over an extended period of time). The hearing loss from noise exposure is typically binaural (symmetric), and the severity of it is related to the intensity, frequency, duration and temporal characteristics (e.g. impulse/impact, intermittent or continuous noise) of the noise exposure (Henderson *et al.*, 2008; Thorne *et al.*, 2008).

Excessive noise is the most common occupational and environmental health hazard. Dangerous levels of noise are generated in a large number of workplaces such as construction sites, mines, saw mills, military bases, and airports, among many others. Although usually associated with occupational exposure, noise-induced hearing loss is becoming increasingly prevalent in recreational settings. Many people, especially children and teenagers, voluntarily expose themselves to potentially injurious noise levels via portable music players, stereos, video games, rock concerts, and nightclubs. Other non-occupational sources of loud noise include firearms, power tools such as chain saws and drills, lawn mowers, and recreational vehicles such as motorcycles. **Table 1.1** illustrates some common sources of sounds and their associated sound intensity (dB).

Table 1.1: Common sounds and their decibel level (Table modified from Daniel (2007), with additional examples from http://www.ata.org and http://american-hearing.org).

Sound Level (dB)	Source
0	Quietest sound that can be heard (threshold of hearing)
10	Normal breathing
30	Whisper, quiet library
50-65	Normal conversation, sewing machine
70	Washing machine
80-85	Heavy traffic
90	Lawnmower
95-110	Motorcycle
100	Chainsaw, drill, hair dryer, subway train
110	Busy video arcade, screaming child
120	Nightclub
110-125	Stereo, portable music player
120	Rock concert, thunder
140-150	Gunshot, firecracker, jet plane (nearby)

Noise-induced hearing loss is the second most common sensorineural hearing deficit, after age-related hearing loss (presbyacusis), and is the leading cause of preventable sensorineural hearing loss in the industrialised world (Kopke, 2007). According to recent global estimates released by the World Health Organisation (WHO, 2012), there are 360 million people worldwide (5.3% of the world's population) with disabling hearing loss. Of these, 328 million (91%) are adults (183 million males, 145 million females) and 32 million (9%) are children. Disabling hearing loss, as defined by WHO, is "hearing loss greater than 40 dB in the better hearing ear in adults (15 years or older) and a hearing loss greater than 30 dB in the better hearing ear in children (0 to 14 years)". A significant proportion (16%) of the disabling hearing loss in the adult population worldwide is attributed to occupational noise exposure (WHO, 2002), ranging from 7% in the most developed countries to 21% in developing regions (Nelson *et al.*, 2005). In the United States, approximately 15% (26 million) of people between 20 to 69 years of age have high frequency hearing loss from overexposure to loud noise at work or during leisure activities (www.nidcd.nih.gov). It is estimated that

approximately 10% of the New Zealand population (445,000 people) suffer from hearing loss, and between 30 to 50% of the hearing loss in adults are associated with noise exposure (Thorne *et al.*, 2008). Hearing loss has considerable social and economic implications at both the individual and societal level. This devastating sensory disability and the serious communication difficulties that arise have a negative impact on the quality of life of affected individuals and can lead to feelings of loneliness, social isolation and depression.

1.5.2. Historical Perspective

The association between noise exposure and hearing loss was first recognised by the physician Sir Francis Bacon (1561 – 1626) (Hawkins, 2004). In 1890, Habermann was the first to describe the cochlear histopathological features of noise-induced hearing loss from examining the temporal bones of an elderly ex-boilermaker (Hawkins & Schacht, 2005). However, it was not until 1907 that Wittmaack conducted the first experimental research of noise-induced deafness in animals (Hawkins & Schacht, 2005; Talaska & Schacht, 2007). Substantial insights into the pathophysiology of noise-induced cochlear injury were gained by Wittmaack's experiments and that of many others that followed, including Hallowell Davis's systemic studies on guinea pigs and humans at Harvard University in 1943.

1.5.3. Preventive Measures

Noise-induced hearing loss is virtually 100 percent preventable (Rabinowitz, 2000). Obviously, the best preventive measure against noise-induced hearing loss is to completely avoid or minimise exposure to noisy environments. When this is not possible, the only preventative measure available is the consistent and proper use of hearing protection devices such as earplugs and earmuffs. When used correctly, these protective devices can provide 20 to 40 dB of attenuation. However the use of these devices is often impractical in certain industrial and military settings. In addition, they are often ineffective because of incorrect or lack of use (Verbeek *et al.*, 2012). Recreational activities and loud music from personal listening devices also contribute to the growth of hearing disability, and this type of hearing loss is highly preventable.

1.5.4. Risk Factors

Avoiding or reducing modifiable risk factors associated with noise-induced hearing loss such as voluntary exposure to loud noise, non-use of hearing protection, cigarette smoking, lack of exercise, poor diet (low dietary intake of antioxidant-rich food), and poor oral health (tooth loss) may reduce the risk or delay the onset of this debilitating condition (Daniel, 2007; Trivedi & Pingle, 2013). The presence of cardiovascular disease and diabetes are also major risk factors. In addition to these, several non-modifiable risk factors related to noise-induced hearing loss exist, particularly age and genetics (Daniel, 2007). Age plays the most significant role, with the risk typically increasing with advancing age and exposure. Furthermore, great genetic variability in the susceptibility to noise-induced hearing loss has been documented in both humans and mice (Gong & Lomax, 2012; Wong *et al.*, 2013).

1.5.5. Noise-Induced Cochlear Injury

The cochlea sustains dramatic cellular injury following noise overexposure. The pathological consequences (pattern and extent) depend on the acoustic characteristics of the noise (i.e. sound intensity, frequency and duration), and age and genetics of the individual (Talaska & Schacht, 2007). The two types of hearing loss from noise exposure - temporary and permanent hearing loss (also known as temporary and permanent threshold shift) - also vary in their mechanisms (Wang *et al.*, 2002). Noise exposure is known to produce a variety of structural changes to the various cells within the cochlea (**Figure 1.6**). The most vulnerable are the sensory hair cells, particularly the outer hair cells, which have traditionally been the focus of most hearing loss studies. A major impact is on sensory hair cell stereocilia which can undergo mechanical damage during noise exposure. Stereocilia can become broken/fractured, fused, or have broken tip links (Thorne *et al.*, 1986; Liberman, 1987; Pickles *et al.*, 1987). Other pathological changes include the loss of outer hair cells by apoptosis or necrosis, damage to the inner hair cell – auditory nerve synapse, swelling and rupturing of the dendrites of primary auditory neurones, damage to the supporting cells, acute swelling of the stria vascularis, reduced cochlear blood flow, and the loss of fibrocytes in the spiral ligament and spiral limbus (Spoendlin, 1971; Axelsson & Dengerink, 1987; Thorne & Nuttall, 1987; Fredelius, 1988; Hu *et al.*, 2002; Wang *et al.*, 2002; Henderson *et al.*, 2006; Henderson *et al.*, 2008; Hu, 2012).

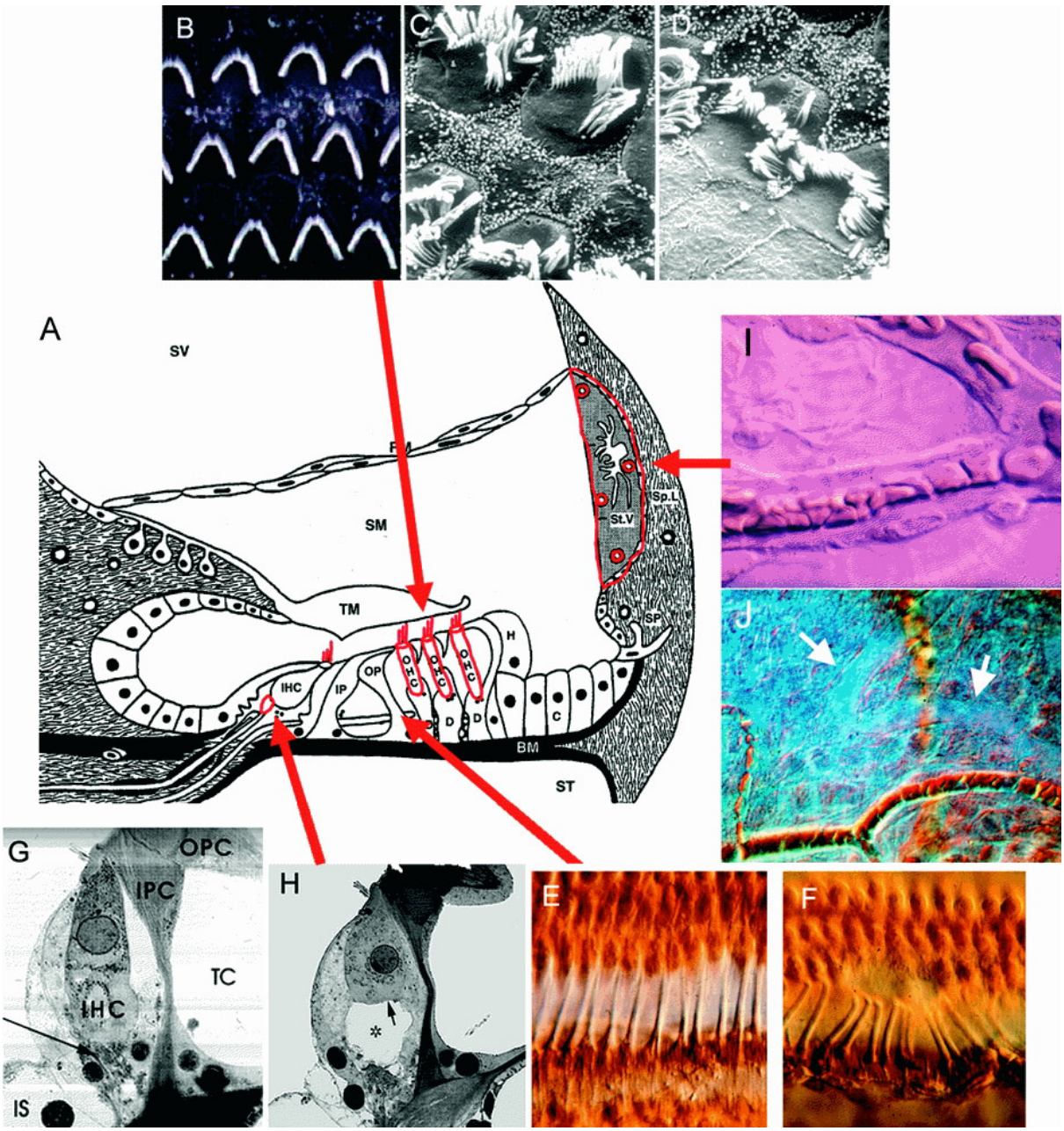

Figure 1.6: Noise-induced cochlear injury. The schematic diagram illustrates the major areas of the cochlea (**A**) that are vulnerable to loud noise: outer hair cell stereocilia (**B-D**), outer pillar cells (**E-F**), inner hair cell-auditory nerve synapse (**G-H**), strial capillaries (**I-J**). *Abbreviations*: SV, scala vestibuli; SM, scala media; ST, scala tympani; Sp.L, spiral ligament; SLV, stria vascularis; BM, basilar membrane; IHC, inner hair cell; OHC, outer hair cell; IPC, inner pillar cell; OPC, outer pillar cell; TC, tunnel of Corti; D, Deiters' cell; C, Claudius cell; H, Hensen's cell. (Figure reproduced from Henderson *et al.* (2006), with permission from Wolters Kluwer Health).

1.5.6. Mechanisms of Noise-Induced Cochlear Injury

Research over the years has advanced our understanding of the underlying cellular and molecular mechanisms of noise-induced cochlear injury. Based on observations from various animal models of noise-induced hearing loss, two main theories have been suggested: mechanical damage and metabolic damage. Direct mechanical disruption of the cochlea is usually associated with exposure to impulse noise. This includes disruption of hair cell stereocilia, direct damage to sensory and supporting cells, and rupturing of the organ of Corti and its separation from the basilar membrane (Hamernik *et al.*, 1986; Henderson & Hamernik, 1986; Henderson *et al.*, 2006).

One of the most compelling hypotheses postulates oxidative stress, the excessive formation of reactive oxygen species (ROS) or free radicals, in the cochlea as a key mechanism of noise-induced hearing loss (Ohlemiller *et al.*, 1999; Henderson *et al.*, 2006; Talaska & Schacht, 2007; Poirrier *et al.*, 2010; Wong *et al.*, 2013; Hu & Henderson, 2014). The appearance of free radicals in the cochlea following noise exposure was first observed by Yamane *et al.* (1995). Superoxide (O_2^-) was detected along the luminal surface of the marginal cells of the stria vascularis immediately after exposure. This finding was corroborated by a subsequent study by Ohlemiller *et al.* (1999) which demonstrated an early elevation of hydroxyl radicals ($^{\bullet}HO$) in the cochlea following noise exposure. In addition to superoxide and hydroxyl radicals, another common type of free radical that has been identified in noise-exposed cochlear tissues is nitric oxide (NO^-) (Shi & Nuttall, 2003). It is suggested that acoustic overstimulation causes intense metabolic activity, which overdrives the mitochondria and leads to increased formation of free radicals. Traumatic noise also reduces cochlear blood flow, resulting in ischemia and hence a shortage of oxygen for mitochondrial function, leading to further superoxide production (Le Prell *et al.*, 2007; Henderson *et al.*, 2008). The subsequent reperfusion of available oxygen can lead to even more free radicals. Oxidative stress alters the redox balance of the cells, leading to the activation of cell death pathways (apoptosis and necrosis) in the cochlea. The outer hair cells at the base of the cochlea seem to be more vulnerable to free radical damage than those at the apex, while supporting cells are considerably less susceptible to injury (i.e. more survival capacity) than sensory cells (Sha *et al.*, 2001). It is well documented that death of outer hair cells continues days after the termination of the noise exposure, from the centre of the lesion toward the base of the cochlea (Fredelius, 1988). The mechanism driving this post-exposure expansion is primarily by free radical-mediated apoptosis (Hu *et al.*, 2002). Oxidative stress

is also thought to be implicated in age-related and drug-induced hearing loss (ototoxicity) (Poirrier *et al.*, 2010; Hu & Henderson, 2014).

Another established mechanism of noise-induced cochlear damage is the excess release of the excitatory neurotransmitter glutamate at the inner hair cell / type I spiral ganglion neuron synapse due to noise-induced overstimulation of the inner hair cells (Puel *et al.*, 1998; Pujol & Puel, 1999). This results in a phenomenon known as glutamate excitotoxicity, which is characterised by swelling and disruption of the afferent dendrites of type I spiral ganglion neurons as a result of a large influx of ions such as Ca^{2+} across the post-synaptic membrane. The disruption of the afferent dendrites leads to synaptic uncoupling and a loss of function. Increased Ca^{2+} influx can also trigger a cascade of metabolic events, such as production of ROS, and activation of calcium-dependent proteases (e.g. calpains) and endonucleases, leading to the apoptotic and necrotic death of type I spiral ganglion neurons. Acoustic overstimulation also increases the entry of Ca^{2+} into outer hair cells via voltage-sensitive L-type Ca^{2+} channels, contributing to the degeneration of the hair cells (Fridberger *et al.*, 1998).

1.6. Noise-Induced Cochlear Inflammation

Several studies have implied the involvement of inflammation in the development of noise-induced cochlear injury. Early ultrastructural studies in the noise-exposed mammalian cochlea have identified macrophage-like cells in the damaged organ of Corti, mainly in the tunnel of Corti and in the outer hair cell region, appearing five days after acoustic overstimulation (Fredelius, 1988; Fredelius & Rask-Andersen, 1990). These macrophages are likely involved in clearing cellular debris. The presence of transforming monocytes in the area and mononuclear leukocytes within the spiral lamina blood vessels suggested that these dendritic macrophages originated from blood-borne monocytes (Fredelius & Rask-Andersen, 1990).

A number of studies have demonstrated that after acoustic trauma, a large influx of inflammatory cells from the vasculature can be observed in the cochlea, generally peaking between two and seven days after exposure to traumatic noise, and diminishing thereafter (Discolo *et al.*, 2004; Hirose *et al.*, 2005; Tornabene *et al.*, 2006; Tan *et al.*, 2008;

Wakabayashi *et al.*, 2010). Inflammatory cells within the cochlea were identified immunohistochemically using their cell surface markers CD45, a receptor tyrosine phosphatase present on all hematopoietic/bone marrow-derived leukocytes or F4/80, a marker of activated macrophages and monocytes. The study by Tornabene *et al.* (2006) showed that CD45-positive cells increased from an average of 0.3 cells/section in the non-exposed cochlea to a maximum of 88 cells/section at two and four days after noise exposure. These infiltrating cells were localised predominantly in the spiral ligament, particularly in the inferior region among type I and type IV fibrocytes and in the region adjacent to the bony cochlear capsule among type III fibrocytes, and in the perilymph-filled spaces of the scala tympani and scala vestibuli (Hirose *et al.*, 2005; Tornabene *et al.*, 2006; Tan *et al.*, 2008; Wakabayashi *et al.*, 2010) (**Figure 1.7** and **Figure 1.8**). Leukocytes were also observed within the spiral limbus, another region known to be susceptible to acoustic injury, and in the spiral ganglion (Hirose *et al.*, 2005; Tan *et al.*, 2008; Wakabayashi *et al.*, 2010). A few cells were also found in the stria vascularis and the perivascular spaces of the modiolus (Tornabene *et al.*, 2006; Du *et al.*, 2011). This recruitment of macrophages to the cochlea following excessive stimulation is similar to what occurs in other sensory organs, such as the retina of the eye. Thus, exposure to damaging light causes an infiltration of inflammatory cells to the light-damaged region of the retina (Rutar *et al.*, 2010).

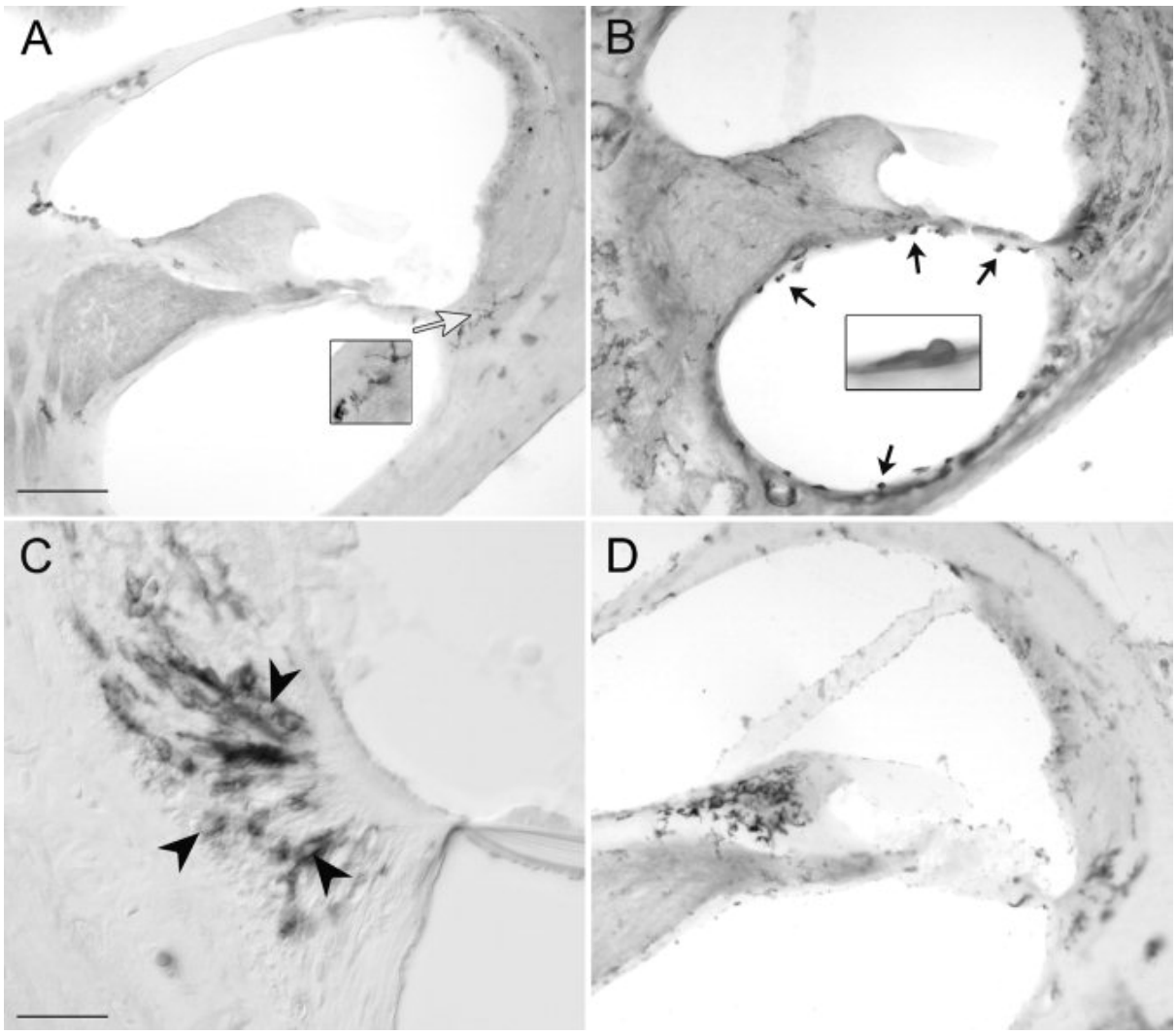

Figure 1.7: CD45$^+$ infiltrating macrophages in the cochlear upper basal turn of CBA/CaJ mice after noise exposure. (**a**) In the non-exposed control cochlea, a small resident population of CD45$^+$ cells (CD45 is a cell surface marker of hematopoietic/bone marrow-derived leukocytes) were seen in the lower region of the spiral ligament. (**b**) 7 days after noise exposure (112 dB SPL, 8-16 kHz for 2 h), CD45$^+$ cells increased greatly in number, particularly in the inferior region of the spiral ligament and in the fluid-filled space of the scala tympani (arrows). The insert shows a high magnification of a CD45$^+$ macrophage adherent to the wall of the scala tympani. (**c**) CD45$^+$ cells in the inferior region of the spiral ligament (arrowheads point to the nuclei of CD45$^+$ cells). (**d**) CD45$^+$ cells were also observed in the spiral limbus 7 days after noise exposure, but only in the lower apical turn where fibrocyte loss has previously been observed. Scale bars = 100 µm (a, b, d); 25 µm (c) (Figure reproduced from Hirose *et al.* (2005), with permission from John Wiley and Sons).

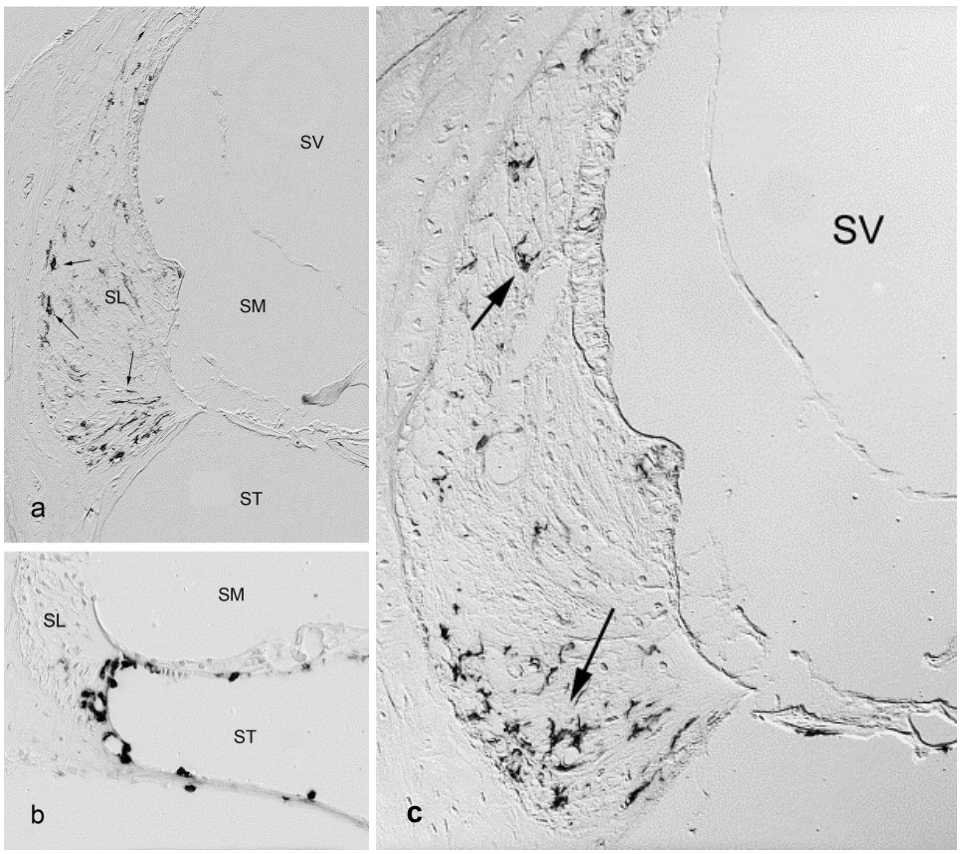

Figure 1.8: CD45$^+$ and F4/80$^+$ infiltrating macrophages in the spiral ligament from the cochlear basal turn of (NIH)-Swiss mice after noise exposure. (**a**) 7 days following noise exposure (118 dB SPL, 8-16 kHz for 2 h), CD45$^+$ inflammatory cells (CD45 is a cell surface marker of hematopoietic/bone marrow-derived leukocytes) were found throughout the spiral ligament, but mostly in the inferior region among type I and IV fibrocytes and adjacent to the junction of the spiral ligament with the otic capsule among type III fibrocytes. (**b**) CD45$^+$ cells were also seen in the perivascular space of venules and adherent to the wall of the scala tympani (24 h after noise exposure). (**c**) F4/80$^+$ cells (F4/80 is a cell surface marker of activated macrophages and monocytes) were also seen mainly in the inferior portion of the spiral ligament 7 days following noise exposure. *Abbreviations*: SL, spiral ligament; SV, scala vestibuli; SM, scala media; ST, scala tympani. (Figure reproduced from Tornabene *et al.* (2006), with permission from Elsevier).

BrdU labelling has demonstrated that these inflammatory cells migrate from the vasculature, and it appears that most of these cells enter the cochlea through the blood vessels of the lateral wall (Hirose *et al.*, 2005). The lateral wall is highly vascularised, and the spiral ligament is the site where the large majority of inflammatory cells can be found. Immunostaining with other monocyte/macrophage markers (CD68, CX3CR1, Iba-1)

demonstrated that the vast majority of these infiltrating cells are derived from the monocyte/macrophage lineage, with a small number representing other leukocytes such as T and B lymphocytes (Hirose *et al.*, 2005; Okano *et al.*, 2008). Hirose *et al.* (2005) coined the term "cochlear macrophage" for those inflammatory cells, to indicate an inducible exchanging population of phagocytic cells that respond to acoustic injury.

The recruitment and extravasation of these inflammatory cells into the cochlea is mediated by cytokines (e.g. TNF-α, IL-1β, IL-6), chemokines (e.g., MCP-1, MCP-5, MIP-1β) and cell adhesion molecules (e.g. ICAM-1, PECAM-1), which are upregulated immediately after noise exposure (Fujioka *et al.*, 2006; Tornabene *et al.*, 2006; Ohlemiller, 2008; Jo *et al.*, 2010; Nakamoto *et al.*, 2012). Fujioka *et al.* (2006) demonstrated an upregulation of the proinflammatory cytokines TNF-α, IL-1β and IL-6 in the noise-damaged cochlea as early as three hours after noise exposure. IL-6 immunoreactive cells were observed initially in the lower and lateral regions of the spiral ligament, specifically in the cytoplasm of type IV and III fibrocytes, then throughout the spiral ligament and even in the stria vascularis (Fujioka *et al.*, 2006). Double labelling with NeuN, a neuronal marker, showed IL-6 expression in the spiral ganglion neurons 12-24 h after noise exposure. IL-6 upregulation in the noise-exposed cochlea likely contributes to cochlear injury, as the inhibition of IL-6 suppressed cochlear inflammation and mitigated the hearing loss (Wakabayashi *et al.*, 2010). Chemokines that are chemotactic for macrophages such as CCL2/MCP-1, monocyte chemoattractant protein-5 (MCP-5/CCL12), and macrophage inflammatory protein-1β (MIP-1β/CCL4) are upregulated in the noise-exposed cochlea two hours following acoustic trauma (Tornabene *et al.*, 2006). The early expression of chemokines suggests that resident cochlear cells may be responsible for this upregulation.

ICAM-1 is a vascular cell adhesion molecule that plays a critical role in mediating temporary adhesion/immobilisation of leukocytes to vascular endothelial cells in preparation for extravasation. Increased expression of ICAM-1 at the protein level is seen 24 h after noise exposure, reaching a maximum at 2 and 4 days, and returning to basal levels by 14 days (Tornabene *et al.*, 2006). This elevated expression is seen chiefly in the vascular endothelial cells and fibrocytes occupying the root region of the spiral ligament, and less intensely in the region of the spiral ligament adjacent to the cochlear bony capsule (**Figure 1.9**). The endosteal cells lining the scala tympani and scala vestibuli and capillaries of the stria vascularis also show increased ICAM-1 immunolabelling. Upregulation of ICAM-1 at the

mRNA level is first observed two hours after noise exposure. The increased ICAM-1 expression in these cells regulates and directs the extravasation and cellular infiltration of inflammatory leukocytes. Other cell adhesion molecules that show increased expression following noise exposure include P-selectin, PECAM-1 and VCAM-1 (Shi & Nuttall, 2007; Yamamoto *et al.*, 2009). Shi and Nuttall (2007) demonstrated that the expression of these cell adhesion molecules is modulated by poly(ADP-ribose) polymerase-1 (PARP-1), a DNA repair enzyme. They suggested that noise activates PARP-1 in capillary endothelial cells of the spiral ligament and stria vascularis, which may act through NF-κB to regulate the expression of adhesion proteins in the lateral wall.

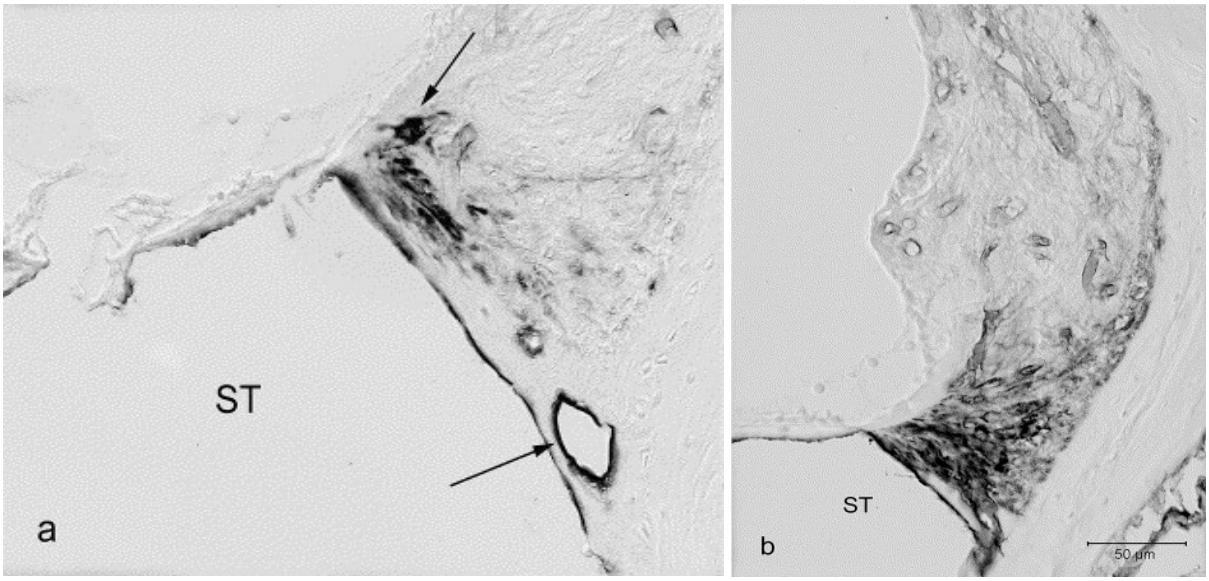

Figure 1.9: ICAM-1 immunostaining in the spiral ligament from the cochlear basal turn of (NIH)-Swiss mice after noise exposure. (**a**) In the normal non-exposed cochlea, ICAM-1 was expressed by vascular endothelial cells and type IV fibrocytes in the inferior region of the spiral ligament, as well as the endothelium of collecting venules and endosteal cells lining the scala tympani. (**b**) Four days following noise exposure (118 dB SPL, 8-16 kHz for 2 h), ICAM-1 immunostaining greatly increased to cover a much larger area of the inferior region of the spiral ligament. *Abbreviation*: ST, scala tympani. **(**Figure reproduced from Tornabene *et al.* (2006), with permission from Elsevier).

The expression of many proinflammatory mediators that participate in the acute inflammatory response is broadly regulated by the transcription factor NF-κB. Apart from its pivotal role in immune and inflammatory responses, NF-κB is also implicated in a range of processes such as cell survival, apoptosis, development, differentiation and cell growth (Denk

et al., 2000). NF-κB comprises a family of five inducible transcription factors, p50/p105 (NF-κB1), p52/p100 (NF-κB2), p65 (RelA), RelB, and c-Rel (Ghosh *et al.*, 1998). They exist as hetero- or homo-dimeric complexes, with the p50/p65 hetero-dimer being the predominant form. In quiescent cells, NF-κB is expressed in the cytoplasm in a latent form, with an inhibitory protein (IκB) bound to the dimer. Upon stimulation, the inhibitory protein is degraded, activating the NF-κB dimer, which then translocates to the nucleus where it binds to the promoters of its target genes. NF-κB activation in the cochlea has been demonstrated following noise exposure (Ramkumar *et al.*, 2004; Masuda *et al.*, 2006; Adams *et al.*, 2009; Yamamoto *et al.*, 2009). Following a 2 h exposure of mice to traumatic noise (124 dB SPL), translocation of p65 and p50 to the nucleus of fibrocytes in the lateral wall was observed, indicating NF-κB activation (Masuda *et al.*, 2006) (**Figure 1.10**). Prominent nuclear localisation of NF-κB occurred two hours after noise exposure, but the nuclear immunostaining subsided after 72 h, suggesting an early response of NF-κB to acoustic overstimulation.

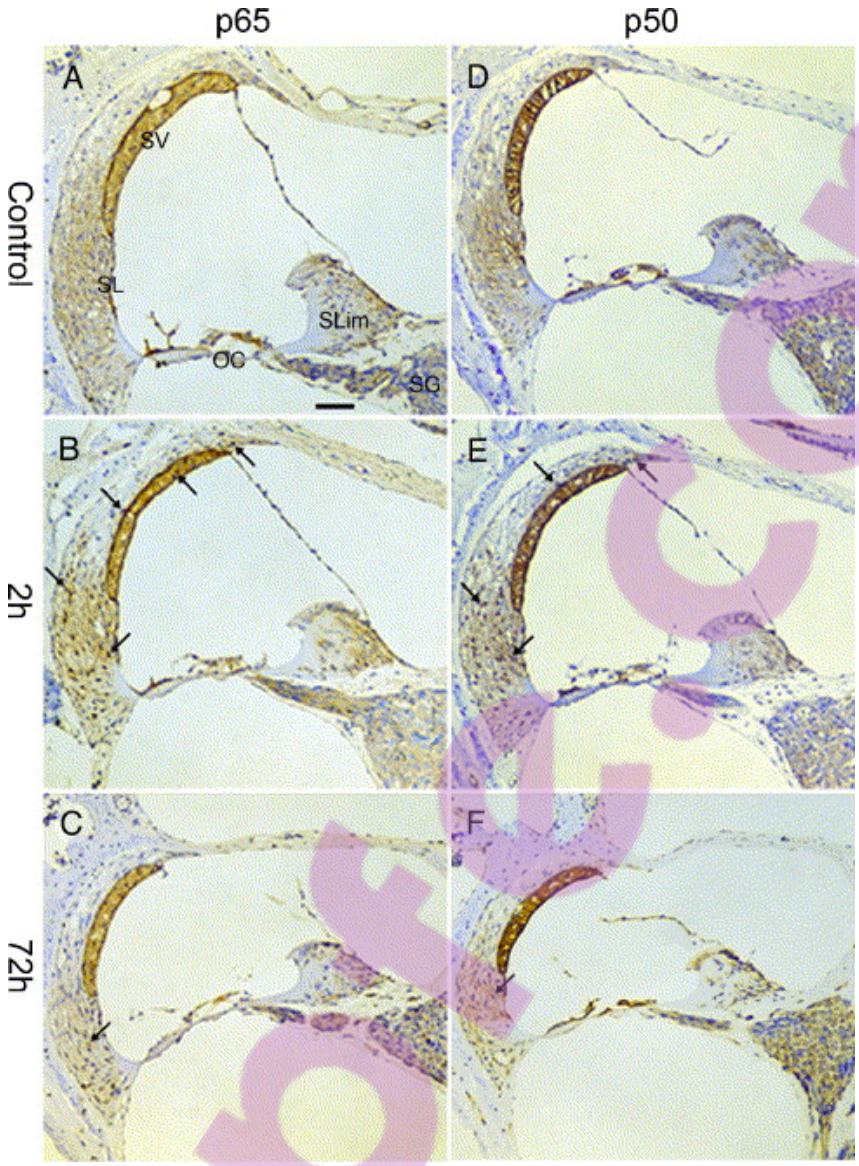

Figure 1.10: NF-κB p65 and p50 immunostaining in the noise-exposed C57BL/6 J mouse cochlea. In the non-exposed cochlea, little or no nuclear immunostaining for p65 and p50 was observed (**A**, **D**). However, prominent nuclear immunostaining of p65 and p50 (arrows) occurred in the lateral wall 2 h after noise exposure (124 dB SPL, octave band centred at 4 kHz for 2 h) (**B**, **E**), indicative of NF-κB activation, and became much less intense at 72 h post-exposure (**C**, **F**). Scale bar = 50 μm (A-F). (Figure reproduced from Masuda *et al.* (2006), with permission from Elsevier).

As mentioned earlier, a large population of PVMs exist in the stria vascularis, however, these cells are not found elsewhere in the cochlea, including the spiral ligament (Shi, 2010). The PVMs play an important role in regulating the integrity of the intrastrial fluid-blood barrier by modulating the expression of tight- and adherens-junction proteins between the endothelial cells via the secretion of pigment epithelium growth factor (PEDF) (Zhang *et al.*,

2012; Neng *et al.*, 2013). The integrity of the barrier is critical for establishing and maintaining the endocochlear potential and preventing the entry of toxic substances into the cochlea (Juhn *et al.*, 2001). Exposure to excessive noise leads to breakdown and increased permeability of the blood-labyrinth barrier by causing PVMs to change morphology and detach from strial capillaries and also by causing a significant downregulation of PEDF production and tight junction protein expression (Zhang *et al.*, 2013). Similar to the cochlea, the retina of the eye contains perivascular macrophages, which also contribute to the maintenance of the blood-retinal barrier (Mendes-Jorge *et al.*, 2009). Recent evidence has demonstrated that bone marrow-derived cells (BMDCs) are recruited to the stria vascularis during the first week after acoustic injury to repair and restore the noise-damaged blood vessels (Dai *et al.*, 2010). These cells promote angiogenesis and neovascularisation, differentiating into PVMs, pericytes and endothelial cells and integrating into the strial blood vessels by four weeks after noise exposure. This recruitment is mediated by an intrinsic (iNOS)-dependent stromal cell-derived factor-1α (SDF-1α) signalling pathway. Blocking the activity of iNOS or SDF-1α significantly reduced both the number of infiltrating BMDCs and the capillary density (vascular repair) in the stria vascularis of the noise-exposed cochlea.

Similar to noise-induced hearing loss, oxidative stress and inflammation are major contributing factors to cisplatin-induced ototoxicity. Cisplatin has been shown to increase the expression of inflammatory mediators such as iNOS, COX-2 and TNF-α, which are downstream targets of the transcription factor STAT1 (Kaur *et al.*, 2011). Cisplatin-induced activation of STAT1 is dependent on ROS generation through NOX3, a member of the NOX family of superoxide-generating nicotinamide adenine dinucleotide phosphate (NADPH) oxidases. NOX3 is expressed almost exclusively in the inner ear and serves as the primary source of ROS generation in the cochlea (Bánfi *et al.*, 2004). siRNA-mediated gene silencing of NOX3 mitigates cisplatin-induced hearing loss, demonstrating a key role of NOX3 in the development of cisplatin-mediated ototoxicity (Mukherjea *et al.*, 2010). In contrast to these findings, recent data from our group showed that exposure to noise results in a significant down-regulation of NOX3 in the cochlea (Vlajkovic *et al.*, 2013). It was proposed that the reduction in NOX3 may represent an endogenous protective mechanism to reduce oxidative stress in the noise-exposed cochlea. These studies provide evidence that NOX3 is involved in the development of noise- and cisplatin-induced cochlear injury, albeit in a different way.

The exact role inflammatory cells play once recruited to the noise-damaged cochlea remains unclear. It is possible that the inflammatory response exacerbates the cellular damage in the cochlea by causing bystander tissue injury. It has also been suggested that the recruitment of inflammatory cells following acoustic injury is part of a wound healing response, given that infiltrating cells are largely observed in the region of the spiral ligament where noise-induced fibrocyte loss is most evident (Hirose *et al.*, 2005; Tornabene *et al.*, 2006; Ohlemiller, 2008; Sato *et al.*, 2008). Leukocytes may play a critical role in promoting repair by removing cellular debris created by the primary insult. These cells may contribute to the repair process by changing the local environment via the secretion of chemical mediators such as cytokines and growth factors. Inflammatory leukocytes could function along with resident fibrocytes of the spiral ligament to regulate repair of the noise-damaged cochlear structures. It has been speculated that the fibrocytes initiate the local inflammatory process (Tan *et al.*, 2008). These cells express similar cytokines, chemokines and cell adhesion molecules, and also respond to signals used by leukocytes for cell-cell signalling. Cochlear fibrocytes can perhaps be considered facultative resident macrophages, serving some functions normally performed by circulating macrophages.

1.7. Adenosine Signalling

1.7.1. Introduction

While having positive effects in the short term, the currently used steroid-based drugs for the treatment of cochlear inflammation may have deleterious consequences to cochlear function in the long term (Barkdull *et al.*, 2005; Fujioka *et al.*, 2006). This therefore underlies the need to develop more effective therapies for cochlear inflammation that prevent (or rescue) cochlear tissue from injury and the associated hearing loss. Recent studies have demonstrated a critically important role of the signalling molecule, adenosine, in the regulation of inflammatory processes in a range of tissues, by exhibiting a strong anti-inflammatory effect (Cronstein, 1994; Sullivan & Linden, 1998; Ohta & Sitkovsky, 2001; Kirkpatrick, 2002; Haskó & Cronstein, 2004; Cunha, 2005; Bours *et al.*, 2006; Jacobson & Gao, 2006; Linden, 2006; Cronstein, 2007; Fredholm, 2007; Blackburn *et al.*, 2009; Haskó *et al.*, 2013). Hence, adenosine may have robust therapeutic potential in the treatment of cochlear inflammation. In the cochlea, adenosine is known to regulate a number of physiological processes, and also

appears to play an important role in pathological conditions, such as acoustic overstimulation, hypoxia, ischemia, and trauma, when its extracellular levels become elevated (Vlajkovic *et al.*, 2009). Previous studies by our group have demonstrated the otoprotective role of adenosine via the adenosine A_1 receptor in noise-induced cochlear injury (Vlajkovic *et al.*, 2010a; Wong *et al.*, 2010; Vlajkovic *et al.*, 2014). The following provides a detailed overview of the adenosine signalling system, including its main roles (with particular emphasis on its role in inflammation), adenosine receptors, and its metabolism. Moreover, several potential treatment strategies based on adenosine signalling are discussed.

1.7.2. Adenosine

Adenosine [(2R,3R,4R,5R)-2-(6-aminopurin-9-yl)- 5-(hydroxymethyl)oxolane-3,4-diol] is an endogenous purine nucleoside consisting of the purine base, adenine, and the pentose sugar, ribose, joined by a β-glycosidic bond (**Figure 1.11**). It is a ubiquitous signalling molecule, existing within and released by all cells of the body, and mediates a diverse range of physiological functions (Ribeiro *et al.*, 2002; Fredholm, 2007). Adenosine is also a neuromodulator, controlling neurotransmitter release and neuronal excitability (Cunha, 2001; Fredholm *et al.*, 2005a; Sebastião & Ribeiro, 2009).

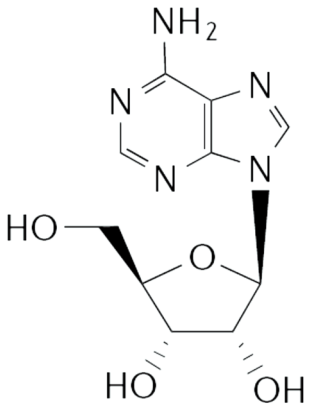

Figure 1.11: Structure of adenosine. The molecular formula of adenosine is $C_{10}H_{13}N_5O_4$ and its molecular weight is 267.241. (Figure reproduced from Jacobson and Gao (2006), with permission from Nature Publishing Group).

1.7.3. Adenosine Receptors

Extracellular adenosine mediates its diverse effects by binding to and activating specific receptors known as adenosine or P1 purinergic receptors (Fredholm *et al.*, 2000; Fredholm *et al.*, 2001; Fredholm *et al.*, 2005a; Jacobson & Gao, 2006; Jacobson, 2009; Sheth *et al.*, 2014). Adenosine receptors have been cloned and characterised from several non-mammalian and mammalian species including humans. Currently four distinct subtypes have been identified and designated as A_1, A_{2A}, A_{2B} and A_3. The adenosine A_1, A_{2A}, and A_{2B} receptors are well conserved among mammals while the adenosine A_3 receptors show considerable structural variability. All four subtypes belong to the G protein-coupled receptor (GPCR) family, possessing seven transmembrane domains, with an extracellular amino terminus and an intracellular carboxyl terminus. The adenosine-binding pocket of the receptor is thought to be formed by both transmembrane domains and extracellular regions (Fredholm *et al.*, 2001). There are consensus sites for *N*-linked glycosylation on the extracellular regions, and all but the adenosine A_{2A} receptor have palmitoylation sites near the C-terminus (Fredholm *et al.*, 2001).

From the perspective of signal transduction, adenosine A_1 and A_3 receptors preferentially couple to inhibitory G proteins (G_i or G_o) that inhibit adenylate cyclase, whereas adenosine A_{2A} and A_{2B} receptors couple primarily to stimulatory G proteins (G_s) that stimulate adenylate cyclase (Fredholm *et al.*, 2000; Fredholm *et al.*, 2001; Fredholm *et al.*, 2005a; Jacobson & Gao, 2006; Sheth *et al.*, 2014) (**Figure 1.12**). However, there is some evidence that these receptors may signal via other G proteins as well as various other signal transduction pathways in different cell types, i.e. they are pleiotropic receptors. Furthermore, they can also directly or indirectly (via second messengers) control the opening of ion channels (e.g. different types of K^+ and Ca^{2+} channels) (Ribeiro *et al.*, 2002).

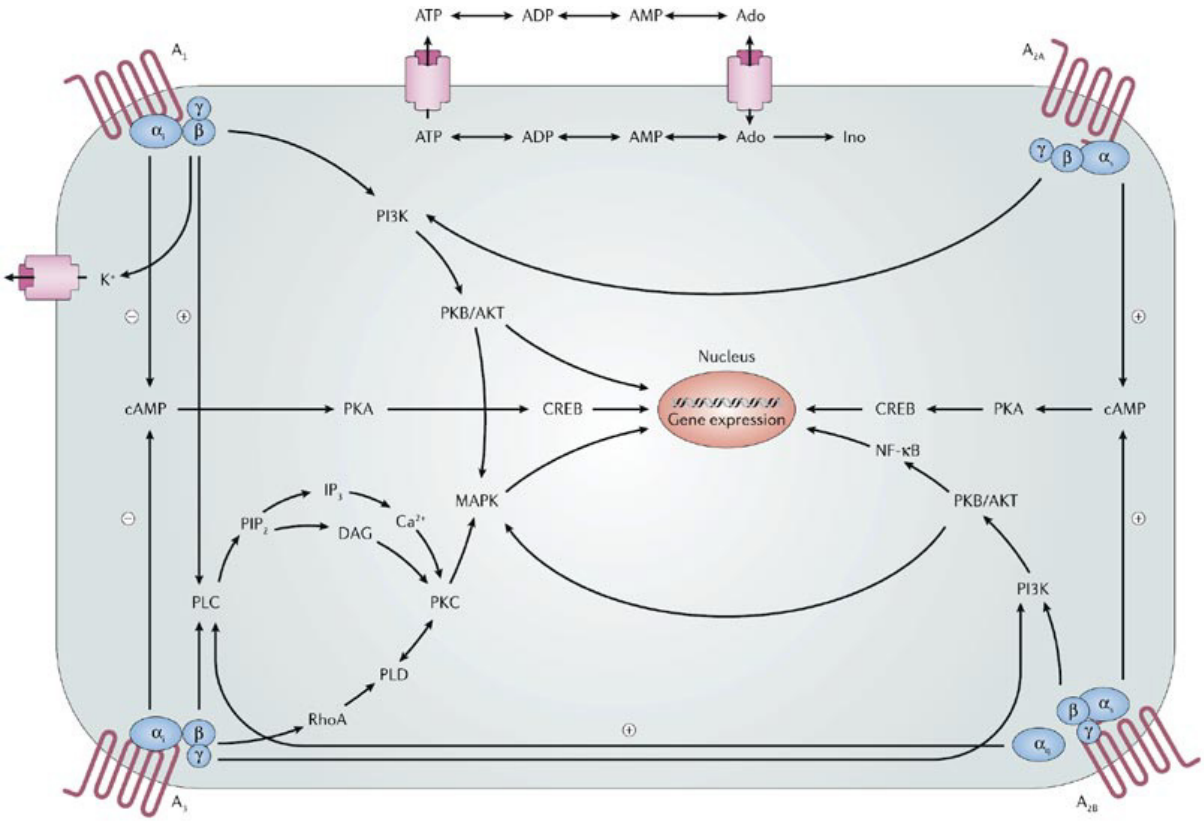

Figure 1.12: Adenosine receptor signalling pathways. Activation of the A_1 and A_3 adenosine receptors (ARs) inhibits adenylyl cyclase activity through activation of pertussis toxin-sensitive G_i proteins and results in increased activity of phospholipase C (PLC) via $G_{\beta\gamma}$ subunits. Activation of the A_{2A} and A_{2B} ARs increases adenylyl cyclase activity through activation of G_s proteins. Activation of the A_{2A}AR to induce formation of inositol phosphates can occur under certain circumstances, possibly via the pertussis toxin-insensitive $G_{\alpha}15$ and $G_{\alpha}16$ proteins. A_{2B}AR-induced activation of PLC is through G_q proteins. All four subtypes of ARs can couple to mitogen-activated protein kinase (MAPK), giving them a role in cell growth, survival, death and differentiation. *Abbreviations*: CREB, cAMP response element binding protein; DAG, diacylglycerol; IP3, inositol 1,4,5-trisphosphate; PI3K, phosphatidylinositol 3-kinase; PIP_2, phosphatidylinositol-4,5-bisphosphate; PK, protein kinase; PLD, phospholipase D; NF-kappaB, nuclear factor-kappaB. (Figure and caption reproduced from Jacobson and Gao (2006), with permission from Nature Publishing Group).

The four adenosine receptor subtypes bind extracellular adenosine with varying affinities. Basal adenosine concentrations are sufficient to activate adenosine A_1, A_{2A} and A_3 receptors because of their high affinity for adenosine (Fredholm, 2007). In contrast, the adenosine A_{2B} receptor is a low affinity receptor, requiring higher adenosine concentrations for activation. The effect of adenosine receptor-mediated signalling is partly determined by the extent of

receptor expression, and there is evidence that various forms of stress can influence the expression of adenosine receptors (Fredholm, 2007). In addition, the different subtypes exhibit different rates of desensitisation (Fredholm *et al.*, 2005a).

In the brain, the adenosine A_1 receptor is the most abundant and widespread, and has an inhibitory neuromodulatory role, inhibiting neurotransmitter release presynaptically and hyperpolarising neurons postsynaptically (Cunha, 2005; Sebastião & Ribeiro, 2009). In the rat cochlea, adenosine receptors are differentially distributed among the sensory hair cells and supporting cells of the organ of Corti, spiral ganglion neurons, lateral wall tissues and cochlear blood vessels, with the adenosine A_3 receptor having the broadest distribution (Vlajkovic *et al.*, 2007) (**Figure 1.13** and **Figure 1.14**). The localisation of adenosine receptors in these cellular regions of the cochlea implicates adenosine signalling in the modulation of sound transduction, auditory neurotransmission, cochlear micromechanics, and cochlear blood flow.

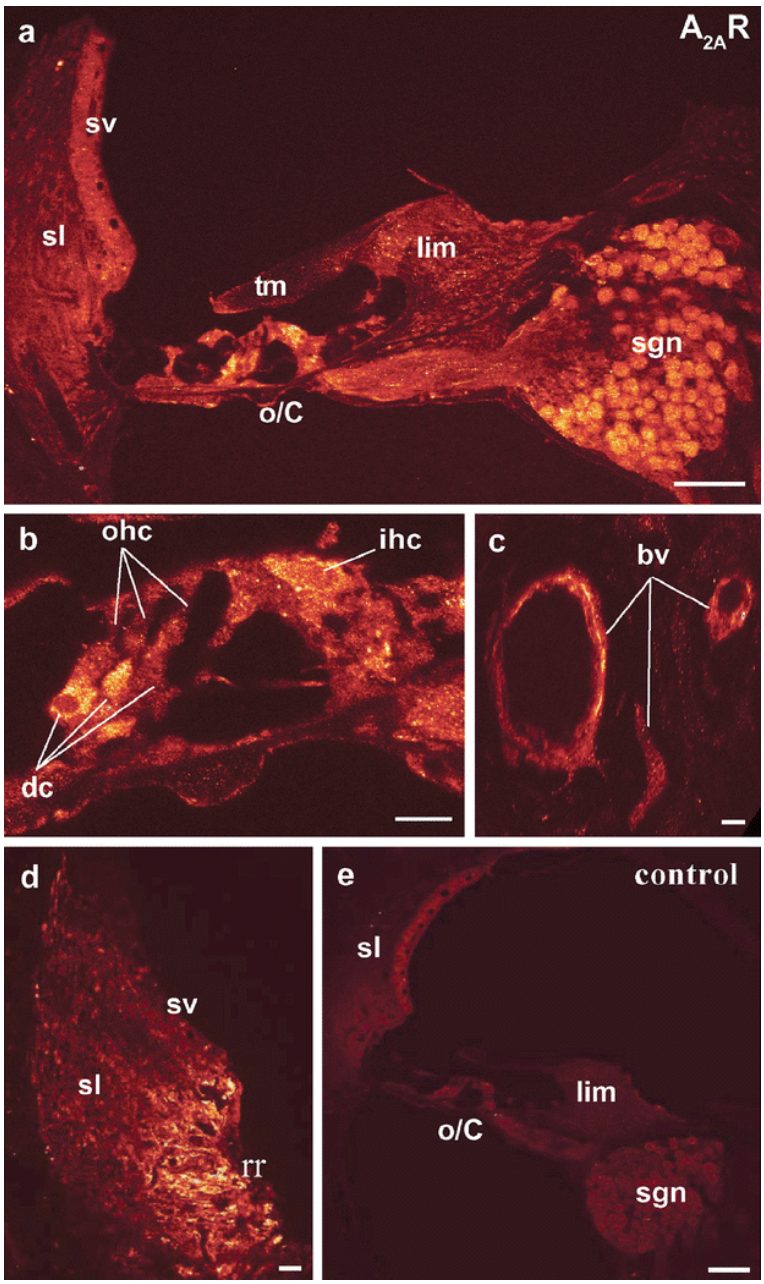

Figure 1.13: Distribution of adenosine A_{2A} receptors in the rat cochlea. (**a**) $A_{2A}R$ immunostaining was found in the organ of Corti and spiral ganglion neurons. (**b**) Detail of immunofluorescence in the organ of Corti showing immunolabelling of the inner hair cells and supporting Deiters' cells, whereas the outer hair cells had limited immunofluorescence labelling. (**c**) Immunolabelling in the cochlear vasculature was confined to the modiolar blood vessels. (**d**) Strong immunofluorescence was observed in the root region of the spiral ligament. (**e**) Minimal fluorescence signal was detected in the peptide block control. *Abbreviations*: sl, spiral ligament; SV, stria vascularis, o/C, organ of Corti, tm, tectorial membrane; lim, spiral limbus; sgn, spiral ganglion neurons; ihc, inner hair cell; ohc, outer hair cell; dc, Deiters' cell; bv, blood vessel; rr, root region. Scale bars = 50 µm (a, e); 20 µm (b–d). (Figure reproduced from Vlajkovic *et al.* (2007), with permission from Springer).

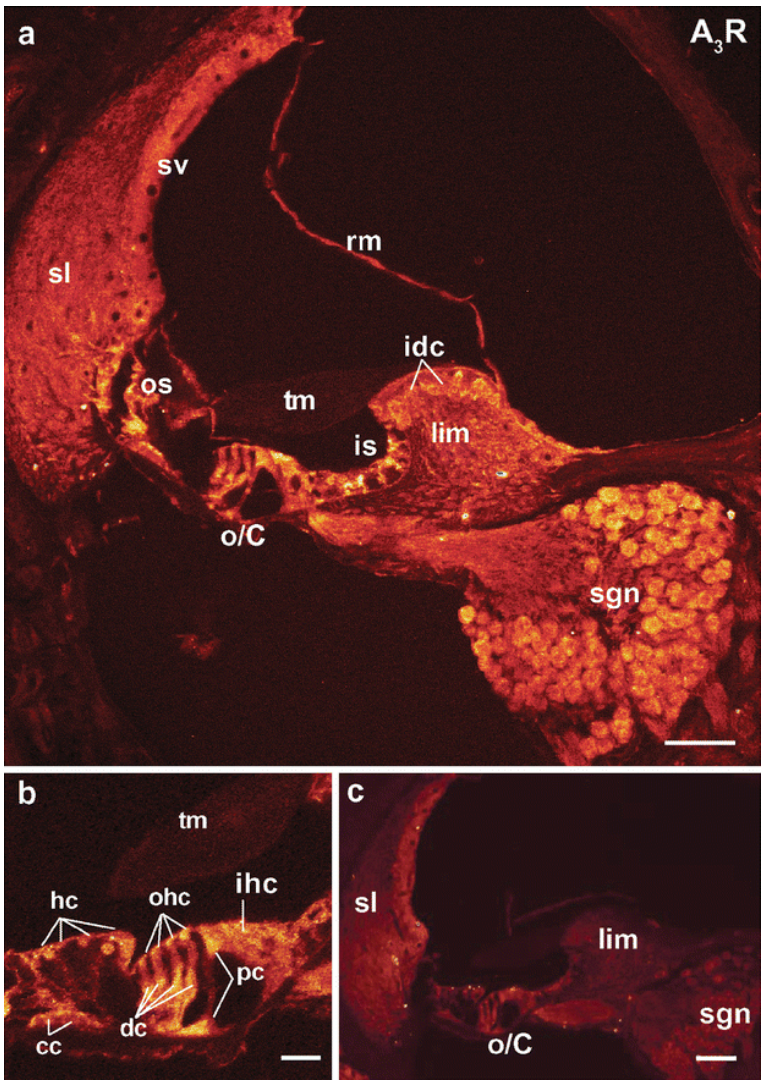

Figure 1.14: Distribution of adenosine A_3 receptors in the rat cochlea. (**a**) A_3R immunolabelling was found in the organ of Corti, inner and outer sulcus cells, interdental cells of the spiral limbus and spiral ganglion neurons. The spiral ligament was also labelled, whereas the tectorial membrane and Reissner's membrane were not stained. (**b**) In the organ of Corti, strong immunofluorescence was observed in the apical region of the outer hair cells, in Deiters' cells and in head and footplate regions of the pillar cells. Moderate immunostaining was observed in the inner hair cell region, Hensen's cells and Claudius' cells. (**c**) Peptide block control. *Abbreviations*: sl, spiral ligament; SV, stria vascularis, o/C, organ of Corti, tm, tectorial membrane; lim, spiral limbus; sgn, spiral ganglion neurons; ihc, inner hair cell; ohc, outer hair cell; dc, Deiters' cell; is, inner sulcus cell; os, outer sulcus cell; hc, Hensen's cell; cc, Claudius' cell; idc, interdental cell. Scale bars = 50 µm (a, c); 20 µm (b). (Figure reproduced from Vlajkovic *et al.* (2007), with permission from Springer).

1.7.4. Role of Adenosine in Tissue Protection and Repair

The extracellular role of adenosine was first described in a seminal study by Drury and Szent-Gyorgyi (1929), which demonstrated its potent cardiovascular effects on the heart. Adenosine extracted from heart muscle had negative inotropic and vasodilatory effects, and this has been proposed to serve a protective function against the deleterious effects of hypoxia and ischemia by reducing the metabolic demand of the myocardium and by increasing coronary blood flow and oxygen delivery respectively (Haskó & Cronstein, 2004).

Subsequent studies have provided further evidence for the protective role of extracellular adenosine in a range of cellular and organ systems. Adenosine is released locally and has protective effects under a wide range of stressful and traumatic stimuli, including inflammation, hypoxia, ischemia, seizures, pain, and sepsis (Haskó & Cronstein, 2004; Haskó *et al.*, 2013). Based on this property, adenosine has been considered a "retaliatory metabolite" or a "homeostatic" modulator of cellular function (Newby *et al.*, 1990). Extracellular adenosine protects tissues from injury and promotes tissue repair via four different receptor-mediated mechanisms: (i) increasing the oxygen supply to demand ratio, (ii) mediating ischemic preconditioning, (iii) stimulating anti-inflammatory responses, and (iv) promoting angiogenesis (Linden, 2005) (**Table 1.2**).

Table 1.2: Tissue protection and repair by adenosine receptors. Adenosine, via activation of adenosine receptors, promotes tissue protection and repair through four general modes of responses: 1) increased oxygen supply/demand ratio; 2) ischemic preconditioning; 3) anti-inflammatory effects; and 4) stimulation of angiogenesis. (Table adapted from Linden (2005), with permission from The American Society for Pharmacology and Experimental Therapeutics).

Receptor	Tissue Response
Increase in oxygen supply/demand ratio	
A_{2A}, A_{2B}	Vasodilation
A_1	Decreased heart rate Decreased neuronal activity Decreased sympathetic nerve activity
Ischemic preconditioning and postconditioning	
A_1, A_3	Preconditioning
A_{2A}?	Postconditioning
Anti-Inflammatory Responses	
A_{2A}	Heart Kidney Liver Spinal cord Skin Lung
Angiogenesis	
A_{2A}	Decreased endothelial cell thrombospondin
A_1	Chorioallantoic membrane
A_{2B}	Increase endothelial cell release of angiogenic factors
A_{2B}, A_3	Increased mast cell release of angiogenic factors

1.7.5. Anti-Inflammatory Effects of Adenosine

Extensive evidence from *in vitro* and *in vivo* studies has indicated a central role of endogenous adenosine in the regulation of inflammatory responses in a range of tissues. The functions of immune cells involved in both innate (neutrophils, monocytes, macrophages, dendritic cells, mast cells, natural killer cells) and adaptive immunity (B and T lymphocytes) are influenced by endogenous adenosine due to their abundant adenosine receptors (Sullivan & Linden, 1998; Bours *et al.*, 2006; Fredholm, 2007; Blackburn *et al.*, 2009; Haskó *et al.*, 2013). Adenosine mediates different effects in the inflammatory response depending on the cell type and the adenosine receptor subtype it binds to.

Of the four adenosine receptor subtypes, the adenosine A_{2A} receptor has been reported as the principal regulator of the inflammatory response. An adenosine A_{2A} receptor knockout study (Ohta & Sitkovsky, 2001) demonstrated the crucial role of the receptor in the suppression of inflammation and tissue damage as no other *in vivo* anti-inflammatory mechanism could fully compensate for the lack of adenosine A_{2A} receptors on immune cells. Numerous other studies have also indicated the powerful anti-inflammatory effects of adenosine A_{2A} receptor activation in a variety of tissues. The activation of adenosine A_{2A} receptors by endogenous adenosine has been referred to as a "brake for inflammation" (Kirkpatrick, 2002). The functional expression of the adenosine A_{2A} receptor, found on almost all immune cells, undergoes constant modulation during the course of an inflammatory reaction (Bours *et al.*, 2006; Haskó *et al.*, 2013). The receptor was maximally up-regulated in neutrophils in response to LPS or TNF-α stimulation (Fortin *et al.*, 2006).

The anti-inflammatory effects of adenosine A_{2A} receptor activation include: reduced recruitment of leukocytes into tissues (including adhesion to vascular endothelium, transendothelial extravasation, and migration to inflamed site), reduced production of proinflammatory cytokines, reduced formation of oxygen-centred free radicals, decreased platelet activation, inhibition of lymphocyte activation and proliferation, and enhanced production of anti-inflammatory cytokines (Cronstein, 1994; Haskó & Cronstein, 2004; Cunha, 2005; Linden, 2005; Bours *et al.*, 2006; Jacobson & Gao, 2006; Fredholm, 2007). These cellular responses are mediated predominantly by cyclic adenosine monophosphate (cAMP)-dependent pathways (Haskó & Cronstein, 2004), but some have been reported to be mediated by cAMP-independent mechanisms, e.g. inhibition of superoxide anion generation

by neutrophils occurs by the activation of a membrane-associated phosphatase and desensitisation of chemoattractant receptors (Cronstein, 1994).

1.7.6. Adenosine Metabolism

A wide range of enzymes, both intracellular and extracellular, are involved in the metabolism of adenosine (**Figure 1.15**). Extracellular adenosine levels are tightly and dynamically regulated by the interplay between the activity of these enzymes and the release and reuptake of adenosine across the cell membrane (Boison, 2006; Benarroch, 2008). The potential sources of extracellular adenosine include: (i) adenosine released from cells via facilitated diffusion through nucleoside transporters following increased intracellular adenosine levels, (ii) the extracellular catabolism of released adenine nucleotides, especially adenosine triphosphate (ATP), into adenosine by a cascade of ectonucleotidases (ectoenzymes), which include the ectonucleoside triphosphate diphosphohydrolase (E-NTPDase) family (CD39), the nucleotide pyrophosphatase/phosphodiesterase (NPP) family, the rate limiting ecto-5'-nucleotidase (CD73), and (iii) the extracellular catabolism of released cAMP into adenosine by NPP (Cunha, 2005; Fredholm *et al.*, 2005a; Bours *et al.*, 2006; Park & Gupta, 2013). In the cochlea, hydrolysis of extracellular nucleotides is mainly mediated by the E-NTPDase members, NTPDase1 and NTPDase2, which are extensively distributed in cochlear tissues and are likely involved in the regulation of P2 receptor signalling (Vlajkovic *et al.*, 1996; Vlajkovic *et al.*, 1999; Vlajkovic *et al.*, 2002a, 2002b).

Clearance of adenosine from the extracellular space is mainly driven by its intracellular phosphorylation by adenosine kinase (Fredholm *et al.*, 2005a). The decrease in intracellular adenosine promotes the rapid reuptake of adenosine into the cell. Intracellular and extracellular adenosine is also catabolised into inosine by adenosine deaminase and ecto-adenosine deaminase respectively (Fredholm *et al.*, 2005a). Enzymes involved in regulating intracellular adenosine concentrations include adenosine kinase (phosphorylates adenosine to adenosine monophosphate (AMP)), 5'-nucleotidase (dephosphorylates AMP to adenosine) and adenosine deaminase (converts adenosine to inosine) (**Figure 1.15**). Because the physiological half-life of adenosine is in the order of seconds, its actions are highly localised to its site of release (Kowaluk *et al.*, 2000).

The principal nucleoside transporter is an equilibrative (non-concentrative) bidirectional facilitated diffusion transporter, with the net direction of transport being dependent upon the concentration gradient of adenosine across the cell membrane (Griffith & Jarvis, 1996; Baldwin *et al.*, 1999; Baldwin *et al.*, 2004; Kong *et al.*, 2004). Because they equilibrate the levels of intracellular and extracellular adenosine, changes in the level on one side can alter the level on the opposite side of the membrane. There is also a group of concentrative nucleoside transporters that transport adenosine against the concentration gradient (Griffith & Jarvis, 1996; Baldwin *et al.*, 1999; Gray *et al.*, 2004; Kong *et al.*, 2004). In contrast to equilibrative nucleoside transporters, concentrative nucleoside transporters are sodium-dependant active transporters (requiring energy from Na^+-K^+-ATPase), and show higher affinity as well as selectivity for nucleoside substrates. In the rat cochlea, extracellular adenosine concentrations are regulated by two equilibrative (ENT1 and ENT2) and two concentrative (CNT1 and CNT2) nucleoside transporters (Khan *et al.*, 2007).

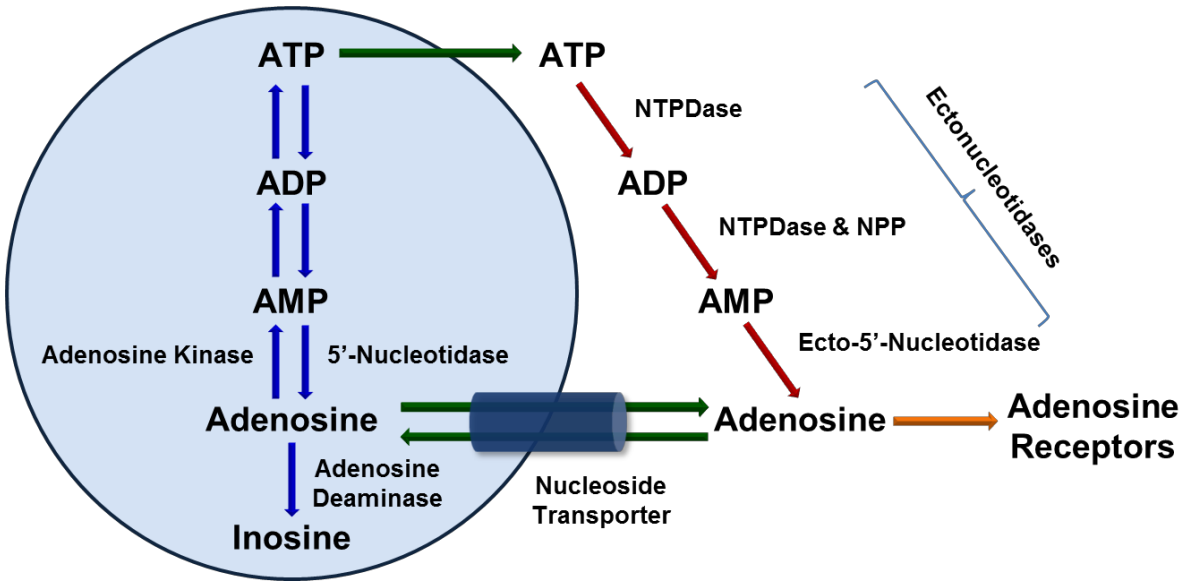

Figure 1.15: Diagram of the purinergic metabolic cascade. A wide range of enzymes, both intracellular (adenosine kinase, 5'-nucleotidase, adenosine deaminase) and extracellular (ectonucleotidases), are involved in the metabolism of adenosine. These enzymes, together with nucleoside transporters (equilibrative and concentrative) located in the cell membrane, are involved in the regulation of intracellular and extracellular adenosine levels.

Under stressful conditions, such as inflammation, hypoxia and ischemia, an imbalance between energy supply and demand occurs, leading to a net hydrolysis of intracellular ATP (Cunha, 2005; Fredholm *et al.*, 2005a). Intracellular adenosine levels rise and adenosine is

released into the extracellular space via equilibrative nucleoside transporters. Because the intracellular concentration of ATP is about 100,000 times higher than that of adenosine, slight changes in ATP concentration will result in substantial changes in adenosine levels (Cunha, 2005; Fredholm *et al.*, 2005a). The extracellular concentration of adenosine in unstressed tissues is usually below 1 µM, whereas in tissues subjected to stressful stimuli, it can reach as high as 100 µM (Haskó & Cronstein, 2004).

1.7.7. Adenosine Kinase

Adenosine kinase [ATP:adenosine 5'-phosphotransferase] is an intracellular enzyme that catalyses the phosphorylation of adenosine to AMP, using ATP as the phosphate donor. Because of its high affinity (i.e. low K_m) for adenosine, adenosine kinase is the key metabolic enzyme of adenosine under physiological conditions, and therefore an important regulator of intracellular and extracellular adenosine levels (Boison, 2006; Park & Gupta, 2008; Park & Gupta, 2013). Furthermore, it is the most abundant nucleoside kinase in mammals as indicated by tissue distribution studies (Mathews *et al.*, 1998; Park & Gupta, 2008).

In various mammalian species including humans, two isoforms of adenosine kinase exist (Park & Gupta, 2013). These isoforms show no difference in their kinetic properties, and are identical in structure except at the N-terminus, where one isoform contains extra amino acids. The structure of human adenosine kinase has been solved by X-ray crystallography and shown to be a monomer consisting of two alpha/beta domains, with the active site located between these domains (Mathews *et al.*, 1998) (**Figure 1.16**). Two adenosine binding sites exist, one being a catalytic site with high affinity for adenosine, while the other being a low affinity regulatory site that binds $MgATP^{2-}$ (McGaraughty *et al.*, 2005).

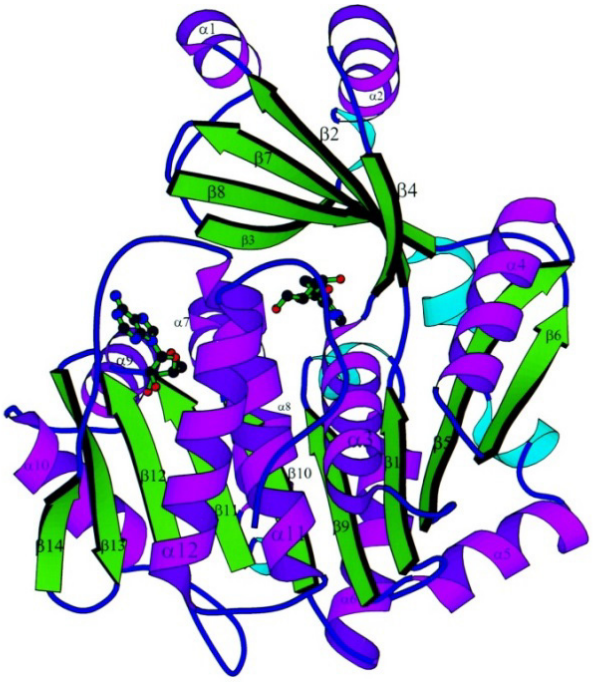

Figure 1.16: Ribbon diagram of the human adenosine kinase (with two bound adenosine molecules) as determined by X-ray crystallography. (Figure reproduced from Mathews *et al.* (1998), with permission from American Chemical Society).

A recent study conducted by our group provided the first evidence for the expression and tissue distribution of adenosine kinase in the adult mammalian (rat) cochlea (Vlajkovic *et al.*, 2010b) (**Figure 1.17**). Adenosine kinase immunofluorescence was extensively distributed in the cochlea, with nuclear or perinuclear immunostaining detected in the fibrocytes in the spiral ligament, marginal cells in the stria vascularis, spiral ganglion neurons and satellite cells in the spiral ganglion, endothelial cells of the modiolar blood vessels, and sensory outer hair cells and supporting cells (inner and outer sulcus cells) of the organ of Corti. This distribution of adenosine kinase coincides with the adenosine receptors in the adult rat cochlea, suggesting that adenosine kinase may be the principal regulator of adenosine signalling in the cochlea.

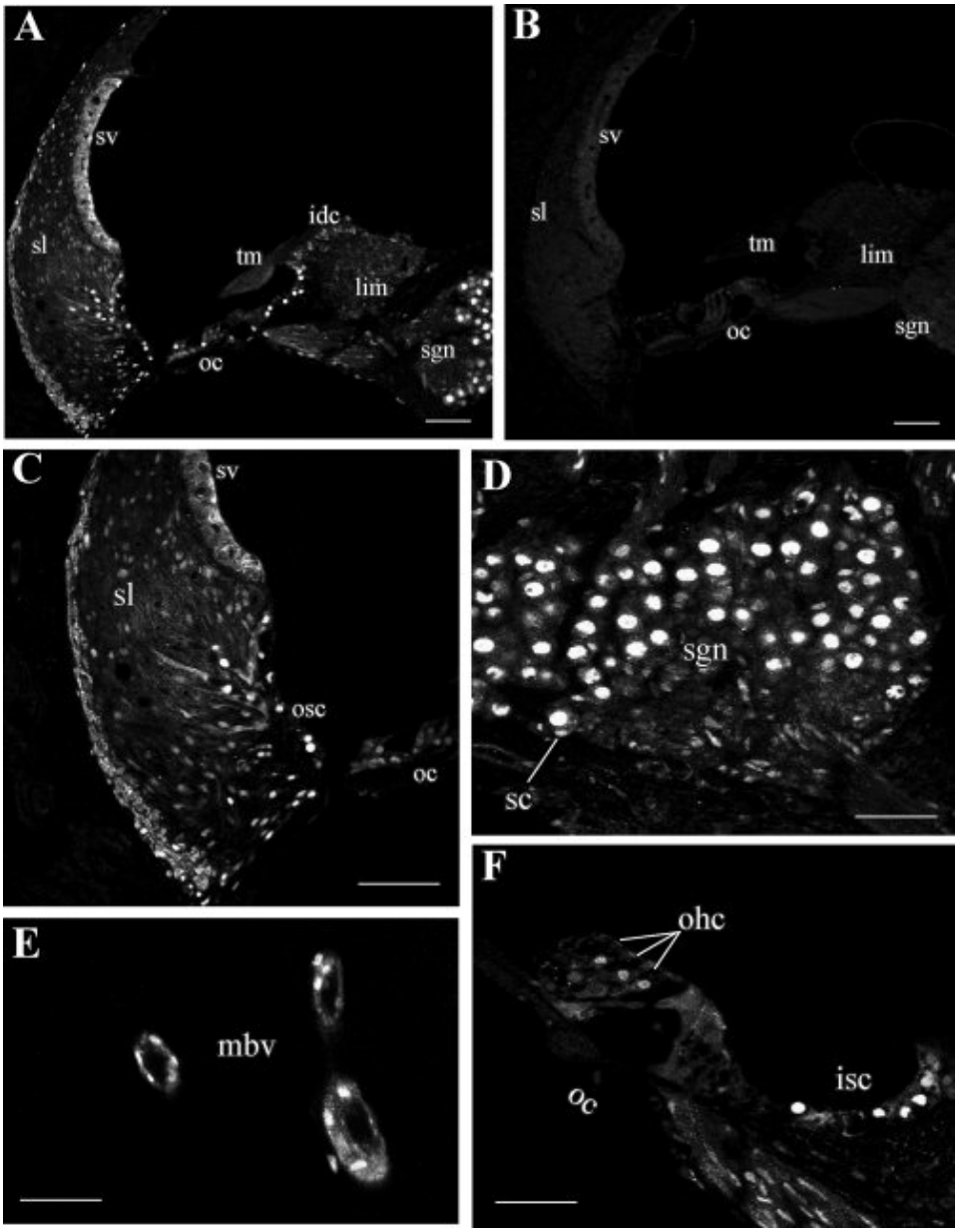

Figure 1.17: Adenosine kinase distribution in the adult rat cochlea. (**A**) Adenosine kinase immunostaining was present in the spiral ligament, stria vascularis, organ of Corti, interdental cells of the spiral limbus and spiral ganglion neurons. (**B**) No immunostaining was detected in the absence of the primary antibody for adenosine kinase. (**C**) Adenosine kinase immunolabelling of the spiral ligament and outer sulcus cells. (**D**) Strong nuclear immunolabelling in spiral ganglion neurons and weaker staining in satellite cells. (**E**) Adenosine kinase immunostaining of blood vessels in the modiolus. (**F**) Adenosine kinase immunostaining in the outer hair cells and inner sulcus cells. *Abbreviations*: sl, spiral ligament; sv, stria vascularis; oc, organ of Corti; lim, spiral limbus; idc, interdental cell; sgn, spiral ganglion neuron; tm, tectorial membrane; osc, outer sulcus cell; sc, satellite cell; mbv, modiolar blood vessel; ohc, outer hair cell; isc, inner sulcus cell. Scale bar = 50 µm. (Figure reproduced from Vlajkovic *et al.* (2010b), with permission from John Wiley and Sons).

1.7.8. Adenosine-Based Treatment Strategies

As mentioned earlier, adenosine exhibits vigorous anti-inflammatory effects in a wide range of tissues (Cronstein, 1994; Sullivan & Linden, 1998; Ohta & Sitkovsky, 2001; Kirkpatrick, 2002; Haskó & Cronstein, 2004; Cunha, 2005; Bours *et al.*, 2006; Jacobson & Gao, 2006; Linden, 2006; Cronstein, 2007; Fredholm, 2007; Blackburn *et al.*, 2009; Haskó *et al.*, 2013). This suggests that adenosine may also confer a similar effect in the cochlea. Adenosine A_{2A} receptor is therefore a highly promising target for anti-inflammatory therapies for various inflammatory conditions. The systemic administration of exogenous adenosine, however, is limited by its peripheral side effects, due to its non-selective nature and the widespread distribution of adenosine receptors (Haskó & Cronstein, 2004). Alternative adenosine receptor-based strategies have therefore been sought and have been rather promising.

1.7.8.1. Selective Activation of Adenosine A_{2A} Receptors

The adenosine A_{2A} receptor is a promising pharmacological target for the treatment of inflammatory disorders. Selective adenosine A_{2A} receptor agonists have been developed and used successfully in the therapy of sepsis, inflammatory bowel disease, skin inflammation and arthritis (Jacobson & Gao, 2006; Blackburn *et al.*, 2009).

Regadenoson, a derivative of adenosine (2-[4-[(Methylamino)carbonyl]-1H-pyrazol-1-yl]adenosine) (**Figure 1.18**), is a selective adenosine A_{2A} receptor agonist used clinically as a coronary vasodilator in radionuclide myocardial perfusion imaging, a diagnostic test for coronary artery disease (Astellas Pharma, 2008; Al Jaroudi & Iskandrian, 2009; Garnock-Jones & Curran, 2010; Chen *et al.*, 2013; Ghimire *et al.*, 2013). Regadenoson was approved for clinical use by the US Food and Drug Administration (FDA) on 10 April 2008 (the only adenosine receptor-specific drug to gain approval thus far) based on the results of two large phase III trials in patients with known or suspected coronary artery disease (Iskandrian *et al.*, 2007; Cerqueira *et al.*, 2008). Patients undergoing myocardial perfusion imaging are normally asked to exercise on a treadmill or bicycle to increase coronary blood flow (hyperaemia), but about 50% of patients are unable to exercise adequately because of medical conditions and hence need to be given a pharmacological stress agent to simulate the effects of exercise. Since its approval, regadenoson has become the most widely used pharmacological stress agent in the United States, accounting for 76% of the vasodilator market share (Ghimire *et al.*, 2013).

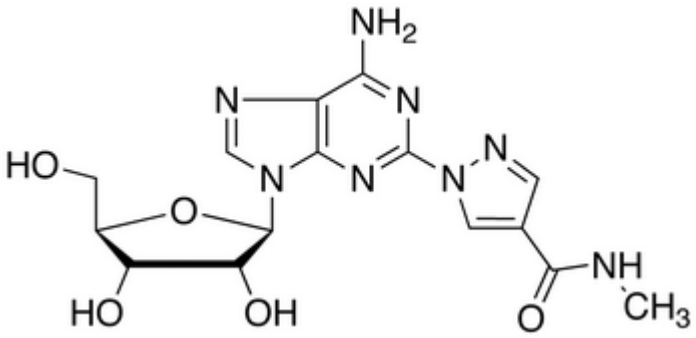

Figure 1.18: Structure of regadenoson. Regadenoson is an adenosine derivative (2-[4-[(Methylamino)carbonyl]-1H-pyrazol-1-yl]adenosine) with the molecular formula $C_{15}H_{18}N_8O_5$ and a molecular weight of 390.35. (Figure reproduced from http://www.trc-canada.com/detail.php?CatNum=R142800, Toronto Research Chemicals Inc., Toronto, Ontario, Canada).

In the United States, regadenoson is marketed by Astellas Pharma under the trade name Lexiscan®, while in the European Union, the drug is marketed by GE Healthcare under the brand name Rapiscan®. The recommended dose of Lexiscan®/Rapiscan® is 0.4 mg/5 mL. It comes in a pre-filled syringe containing 400 µg of regadenoson (**Figure 1.19**) and is administered in patients as a rapid (approximately 10 s) intravenous injection into a peripheral vein using a 22 gauge or larger catheter or needle (Astellas Pharma, 2008). The injection is immediately followed by the intravenous administration of saline flush (5 mL over 10 s) and then the radionuclide myocardial perfusion imaging agent (over 10-20 s) (Astellas Pharma, 2008). **Table 1.3** summaries the features and properties of regadenoson (Lexiscan®).

Figure 1.19: Lexiscan® prefilled syringe. Lexiscan® is supplied as a standard, IV-injection dose in a prefilled syringe containing 0.4 mg of regadenoson in a 5 mL solution. (Figure reproduced from http://www.lexiscan.com).

A recent study demonstrated that regadenoson intravenously administered in mice and rats increased the permeability of the blood-brain barrier, facilitating the entry of macromolecules into the brain (Carman *et al.*, 2011). Based on this finding, it can be speculated that regadenoson can cross the blood-brain barrier and possibly the blood-labyrinth barrier in the cochlea. This would therefore be an advantage as regadenoson could be administered systemically avoiding the inconvenience of intratympanic injections or the surgery required for direct cochlear injections.

In the clinical trials, regadenoson appeared to be well tolerated in patients, with no serious side effects such as acute myocardial infarction, congestive heart failure, or stroke (Iskandrian *et al.*, 2007; Astellas Pharma, 2008; Cerqueira *et al.*, 2008). The majority of the adverse effects were reported to be mild, and included shortness of breath (dyspnea), headache, flushing, chest discomfort or chest pain, dizziness, angina pectoris, nausea, and abdominal discomfort. Most of these effects were transient in nature, beginning soon after administration and generally resolving within approximately 15 minutes, apart from headache which lasted about 30 minutes in most patients.

Table 1.3: Features and properties of regadenoson. (Table adapted and modified from Garnock-Jones and Curran (2010), with permission from Springer).

Features and properties of regadenoson (Lexiscan®)	
Indication	
Pharmacologic stress agent (coronary vasodilator) for radionuclide myocardial perfusion imaging in patients unable to undergo adequate exercise stress	
Mechanism of action	
Selective adenosine A_{2A} receptor agonist	
Dosage and administration	
Dose	400 µg
Route of administration	Intravenous
Frequency of administration	Single bolus
Pharmacokinetic profile	
Mean maximum plasma concentration (C_{max})	13.6 ng/mL
Time to C_{max} Area under the concentration-time curve from time zero to infinity	1-4 min 11.7 ng•h/mL
Mean steady-state volume of distribution	75 L
Mean clearance Mean terminal elimination half-life	35 L/h =2 h
Most common adverse reactions	
Shortness of breath (dyspnea), headache, flushing, chest discomfort or chest pain, dizziness, angina pectoris, nausea, and abdominal discomfort	

1.7.8.2. Pharmacological Inhibition of Adenosine Kinase

An approach for augmenting the availability of extracellular adenosine, which has received increasing attention in recent years, is the inhibition of adenosine kinase (Cronstein, 1994; Rosengren *et al.*, 1995; Boyle *et al.*, 2001). Adenosine kinase inhibition decreases AMP formation from adenosine, leading to increased intracellular adenosine levels. An outward adenosine concentration gradient is created favouring adenosine release via equilibrative nucleoside transporters, and therefore resulting in a potentiated level of extracellular adenosine (**Figure 1.20**).

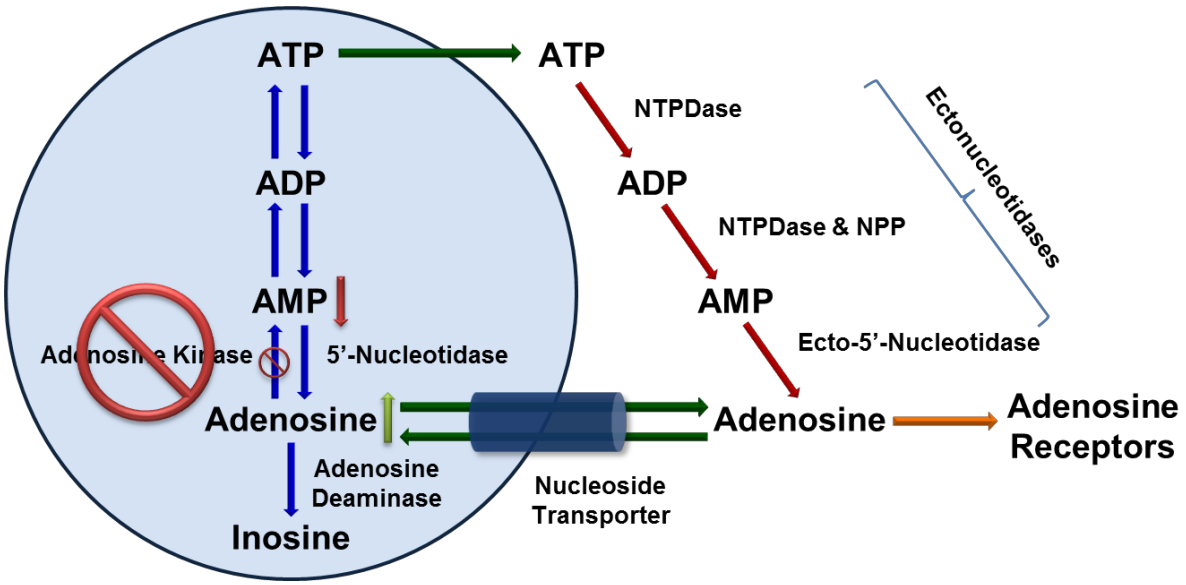

Figure 1.20: Pharmacological inhibition of adenosine kinase. Inhibition of adenosine kinase decreases the formation of AMP from adenosine, leading to an increased level of intracellular adenosine. An outward adenosine concentration gradient is created favouring the release of adenosine via equilibrative nucleoside transporters, resulting in an increased level of adenosine in the extracellular space. This is ultimately followed by the activation of adenosine receptors on neighbouring cells in a paracrine or autocrine fashion and specific adenosine receptor-mediated effects, such as suppression of inflammation.

A novel generation of adenosine kinase inhibitors have been developed that demonstrate a high degree of selectivity for adenosine kinase (Jarvis *et al.*, 2000; McGaraughty *et al.*, 2005). Adenosine kinase inhibitors inhibit the activity of adenosine kinase by binding competitively to the adenosine binding site of the enzyme (McGaraughty *et al.*, 2005). There are two general types of adenosine kinase inhibitors: nucleoside-like and non-nucleoside-like. Nucleoside-like adenosine kinase inhibitors, as their name implies, have a nucleoside-like structure, and are more water soluble than non-nucleoside adenosine kinase inhibitors (McGaraughty *et al.*, 2005). The underlying mechanism mediating the beneficial effects of adenosine kinase inhibitors is an increase in extracellular adenosine levels followed by the activation of adenosine receptors on neighbouring cells in a paracrine or autocrine fashion. Compared to adenosine receptor agonists, adenosine kinase inhibitors have reduced cardiovascular side effects as they increase endogenous adenosine levels in a site- and event-specific manner. Moreover, they have been shown to be more effective at increasing adenosine release than adenosine deaminase inhibitors (Jarvis *et al.*, 2000; McGaraughty *et al.*, 2005).

CHAPTER 2: AIMS & HYPOTHESES

2.1. Aims

The principal aim of this thesis was to improve our understanding of the underlying cellular and molecular mechanisms and dynamics of the noise-induced inflammatory response in the cochlea, and to explore the role of adenosine A_{2A} receptor signalling in noise-induced cochlear inflammation. The thesis was divided into three major studies, with the specific aims listed below.

STUDY 1: Cochlear Inflammatory Response Associated with Acute Noise Exposure

This study aimed to characterise the inflammatory response in the mouse cochlea following acute exposure to traumatic noise. The specific aims were to:

- Examine the activation of the transcription factor nuclear factor-kappa B (NF-κB) in the noise-exposed cochlea.
- Determine the changes in gene expression levels of proinflammatory cytokines (TNF-α and IL-1β), chemokines (CCL2) and cell adhesion molecules (ICAM-1) in the cochlea following acute noise exposure.
- Characterise the distribution of the cell adhesion molecules, ICAM-1 and PECAM-1, in the cochlea, and the time course of their protein expression following acute noise exposure.

STUDY 2: Cochlear Inflammatory Response Associated with Chronic Noise Exposure

This study aimed to characterise the inflammatory response in the mouse cochlea following chronic exposure to moderate noise. The specific aims were to:

- Determine the changes in gene expression levels of proinflammatory cytokines (TNF-α and IL-1β), chemokines (CCL2) and cell adhesion molecules (ICAM-1) in the cochlea following chronic noise exposure.
- Characterise the time course of ICAM-1 and PECAM-1 expression in the cochlea following chronic noise exposure.

STUDY 3: Role of Adenosine A_{2A} Receptor Signalling in Noise-Induced Cochlear Inflammation

This study aimed to ascertain the role of adenosine A_{2A} receptors in the regulation of noise-induced cochlear inflammation. The specific aims were to:

- Examine the expression and distribution of adenosine A_{2A} receptors, including $A_{2A}R^{+}$ infiltrating cells, in the noise-exposed cochlea.
- Assess the cochlear inflammatory response in adenosine A_{2A} receptor knockout ($A_{2A}RKO^{-/-}$) mice exposed to noise to determine the effect of adenosine A_{2A} receptor gene deletion in noise-induced cochlear inflammation.
- Evaluate the anti-inflammatory effect of adenosine A_{2A} receptor activation using the selective adenosine A_{2A} receptor agonist, regadenoson.

2.2. Hypotheses

- Acute exposure to traumatic noise induces an inflammatory response in the cochlea which includes excessive production of proinflammatory cytokines, chemokines, and cell adhesion molecules via the activation of the transcription factor NF-κB, followed by the recruitment of inflammatory cells and their infiltration in cochlear tissues.
- Chronic exposure to non-traumatic noise also induces an inflammatory response in the cochlea with increased expression of proinflammatory cytokines, chemokines, and cell adhesion molecules.
- Noise exposure increases the expression of adenosine A_{2A} receptors in the cochlea as an endogenous protective mechanism (adaptive response) to limit inflammation.
- Deletion of the adenosine A_{2A} receptor gene ($A_{2A}RKO^{-/-}$ mice) leads to an enhanced inflammatory response in the noise-exposed cochlea.
- Post-exposure treatment with the selective adenosine A_{2A} receptor agonist, regadenoson, suppresses inflammatory processes in the noise-exposed cochlea.

CHAPTER 3: METHODS

3.1. STUDY 1: Cochlear Inflammatory Response Associated with Acute Noise Exposure

The primary purpose of this initial study was to further our understanding of molecular mechanisms of the inflammatory response and to characterise the dynamics of the response in the C57BL/6 mouse cochlea in response to acute exposure to traumatic noise (acoustic trauma). This study also provided baseline measurements of inflammatory markers in the noise-exposed cochlea as a foundation for subsequent studies. Male C57BL/6 inbred mice (6 to 8 weeks) were exposed for 24 h to an open-field octave band noise (8-16 kHz) presented at a sound pressure level (SPL) of 100 decibels (dB). This is a traumatic noise level for mice that causes permanent hearing loss and is routinely used in our laboratory. To verify that these noise conditions produced permanent hearing loss, functional assessment of hearing acuity was performed prior to noise exposure (baseline measurements) and one month after noise exposure using auditory brainstem responses (ABRs) to acoustic clicks and tone pips (n = 4). Animals serving as controls (n = 8) for the study were exposed to ambient noise levels (55-65 dB SPL) in the animal holding facility.

Initially, the early onset phase of the noise-induced cochlear inflammatory response was studied by examining the cochlear activation of the nuclear transcription factor, nuclear factor-kappa B (NF-κB). NF-κB is activated in response to diverse stimuli such as inflammation, infections, and other stressful situations, and regulates the expression of a number of proinflammatory mediators. Specifically, the nuclear activation of the two principal subunits, p65 and p50, which normally exist together as heterodimers in the cytoplasm of quiescent (unstimulated) cells, were examined. Nuclear translocation and activation of p65 and p50 in the cochlea was examined 6 h following noise exposure using immunofluorescence.

As the next step, inflammatory influence of NF-κB signalling on the noise-induced damaged mouse cochlea was investigated by evaluating the expression of several key target genes of NF-κB, including proinflammatory cytokines (TNF-α and IL-1β), chemokines (CCL2) and

cell adhesion molecules (ICAM-1 and PECAM-1). To study the time course (dynamics) of the inflammatory events in the cochlea, outcomes were assessed at various time intervals after the cessation of noise exposure: 6 h, 1 day (24 h), 3 days (72 h), and 7 days (168 h). All animals were randomly assigned to the experimental groups (post-exposure survival times), with each group consisting of eight animals (n = 8) (see **Table 3.1**). This group size was based on our previous experience with functional and molecular studies in the cochlea. This number provides statistical power to obtain an 80% probability of detecting a 20% difference between groups ($p \leq 0.05$).

Table 3.1: Acute noise exposure groups

Group	Sound Level (dB SPL)	Sound Frequency (kHz)	Noise Duration (h)	Endpoint	Sample Size (n)
1	100	8-16	24	6 h	8
2	100	8-16	24	1 day	8
3	100	8-16	24	3 days	8
4	100	8-16	24	7 days	8

At their designated endpoint, the animals were euthanised and their cochleae collected for molecular and immunohistochemical analysis of cochlear inflammation. Of the two cochleae harvested from each noise-exposed mouse, one was analysed by quantitative real-time RT-PCR to determine noise-induced changes in the gene expression levels of TNF-α, IL-6, IL-1β, CCL2, and ICAM-1. Relative quantification of gene expression was determined using the comparative $\Delta\Delta C_T$ method. The contralateral cochlea was used to determine the distribution and protein expression levels of ICAM-1 and PECAM-1 using semi-quantitative immunohistochemistry (immunoperoxidase staining). Quantitative data obtained from the study was statistically analysed using a one-way ANOVA followed by Tukey's post-hoc multiple comparisons test (a p value of less than 0.05 was considered statistically significant).

3.2. STUDY 2: Cochlear Inflammatory Response Associated with Chronic Noise Exposure

Research on noise-induced hearing loss over the years has primarily been focused on the pathophysiological and functional outcomes of acute exposures to intense noise. The aim of this study was to examine the possible presence of cochlear inflammation following repeated exposure to moderate noise over an extended period of time (chronic noise exposures). C57BL/6 mice were exposed to 90 dB SPL octave-band noise (8-16 kHz) for 2 h per day for either 7 (1 week), 14 (2 weeks), 21 (3 weeks) or 28 (4 weeks) continuous days (**Table 3.2**). Each experimental noise group were exposed to noise at approximately the same time each day throughout their designated noise exposure period. Animals were euthanised 24 h following the completion of the final noise exposure and their cochleae extracted. As with the previous study, quantitative real-time RT-PCR analysis was carried out to assess changes in the transcriptional expression of inflammatory mediators, and immunoperoxidase staining was performed to characterise the expression and distribution of the cell adhesion molecules ICAM-1 and PECAM-1.

Table 3.2: Chronic noise exposure groups

Group	Sound Level (dB SPL)	Sound Frequency (kHz)	Noise Duration	Sample Size (*n*)
1	90	8-16	2 h/day, 1 week	8
2	90	8-16	2 h/day, 2 weeks	8
3	90	8-16	2 h/day, 3 weeks	8
4	90	8-16	2 h/day, 4 weeks	8

3.3. STUDY 3: Role of Adenosine A_{2A} Receptor Signalling in Noise-Induced Cochlear Inflammation

Adenosine has potent anti-inflammatory effects in a wide range of tissues, mediated primarily via the adenosine A_{2A} receptor. To determine its role in noise-induced cochlear inflammation, a series of interrelated studies based on adenosine A_{2A} receptor signalling were conducted as described below.

3.3.1. Adenosine A_{2A} Receptor Expression in the Noise-Exposed Cochlea

There is evidence that various forms of stress can influence the expression of adenosine receptors. In this study, the tissue distribution of the adenosine A_{2A} receptor in the mouse cochlea and the effect of excessive noise on the expression of this receptor was investigated. Mice were exposed to acute traumatic noise (100 dB SPL, 8-16 kHz for 24 h) and their cochleae collected at 6 h, 1 day, 3 days or 7 days after the cessation of noise exposure (n = 4 per time point). Immunofluorescence was carried out using a specific adenosine A_{2A} receptor antibody to localise the cochlear expression and distribution of the receptor. Protein expression levels were compared qualitatively with the normal non-noise exposed cochlea.

Because they are known to be abundantly expressed by a variety of immune cells, adenosine A_{2A} receptors were also used as a marker for inflammatory cells in the noise-exposed cochlea. The total number of adenosine A_{2A} receptor-positive infiltrating cells was counted in all cochlear turns (apical, middle and basal) of every second mid-modiolar cross-section from each noise-exposed cochlea. Labelled cells were counted under the fluorescent microscope (Nikon Eclipse 80i Microscope, Nikon Instruments Inc., Melville, NY, U.S.A.) at 40x magnification. Cochlear sections were focused throughout their entire thickness (30 µm) to ensure all infiltrating cells throughout the depth of the sections were identified. To characterise the time course of cellular infiltration, the average number of cells/section was determined in the non-exposed control cochlea and at the four time points following noise exposure.

3.3.2. Noise-Induced Cochlear Inflammatory Response in Adenosine A_{2A} Receptor Knockout Mice

For the next study, the cochlear inflammatory response in noise-exposed homozygous recessive adenosine A_{2A} receptor knockout ($A_{2A}RKO^{-/-}$) C57BL/6 mice was assessed to gain further insight into the role of adenosine A_{2A} receptor signalling in noise-induced cochlear inflammation. $A_{2A}RKO^{-/-}$ mice were exposed to acute traumatic noise (100 dB SPL, 8-16 kHz for 24 h) and euthanised at either 6 (n = 5) or 24 h (n = 5) after the cessation of the noise exposure. These time points were selected based on the results obtained from study one, in which 6 h was the initial peak time in the gene expression level of TNF-α, ICAM-1, CCL2 and IL-1β, and 24 h was the time of maximum ICAM-1 immunoexpression and cellular infiltration. The extent of cochlear inflammation was assessed by determining the protein expression level of ICAM-1 using immunoperoxidase staining and the gene expression levels of TNF-α, CCL2, ICAM-1 and IL-1β using quantitative real-time RT-PCR. It is hypothesised that a stronger cochlear inflammatory response occurs in these noise-exposed $A_{2A}RKO^{-/-}$ animals. Also included in the study was a control group of $A_{2A}RKO^{-/-}$ mice exposed to ambient sound levels (n = 5). The results obtained with the knockout mice were compared with those obtained from wild-type non-exposed and noise-exposed mice (**Study 1**). The experimental groups included in this study are shown in **Table 3.3** below.

Table 3.3: Experimental groups for $A_{2A}RKO^{-/-}$ study

Group	Genotype	Noise Exposure	Endpoint (h)	Sample size (n)
1	Wild-type	Ambient noise	-	5
2	Wild-type	100 dB, 24 h	6	5
3	Wild-type	100 dB, 24 h	24	5
4	$A_{2A}RKO^{-/-}$	Ambient noise	-	5
5	$A_{2A}RKO^{-/-}$	100 dB, 24 h	6	5
6	$A_{2A}RKO^{-/-}$	100 dB, 24 h	24	5

3.3.3. Anti-Inflammatory Effect of Regadenoson, a Selective Adenosine A_{2A} Receptor Agonist, in the Noise-Exposed Cochlea

For this final study, the therapeutic potential of adenosine signalling in attenuating inflammatory processes in the noise-exposed cochlea was explored. This intervention was based on the selective activation of adenosine A_{2A} receptors in the cochlea using the selective adenosine A_{2A} receptor agonist regadenoson. Regadenoson, a FDA approved drug, is clinically used as a coronary vasodilator (pharmacological stress agent) for radionuclide myocardial perfusion imaging in patients who are unable to undergo adequate exercise stress.

Mice in this study were randomly assigned to one of four treatment groups (n = 8 per group) as shown in **Table 3.4**. Immediately following the cessation of acute noise exposure (100 dB SPL, 8-16 kHz, 24 h), mice were lightly anaesthetised with a combination of ketamine (38 mg/kg) and domitor (0.5 mg/kg) and then intracardially injected with 0.05 mg/kg of regadenoson (dissolved in 1% dimethyl sulfoxide (DMSO) in sterile saline solution). For vehicle controls, an equivalent volume of 1% DMSO/saline was injected in a similar manner. As for the $A_{2A}RKO^{-/-}$ study, animals were euthanised at either 6 or 24 h after noise exposure. Both cochleae from each mouse were collected, one used for immunohistochemistry and the other for quantitative real-time RT-PCR.

Table 3.4: Treatment groups for regadenoson study

Group	Treatment	Endpoint (h)	Sample size (n)
1	Regadenoson	24	8
2	Vehicle	24	8
3	Regadenoson	6	8
4	Vehicle	6	8

The efficacy of this adenosine-based treatment was determined by comparing the cochlear expression of various inflammatory markers between regadenoson-treated mice and vehicle-treated control mice. This involved assessing the number of $A_{2A}R$-positive infiltrating cells by immunofluorescence, the protein expression level (intensity and area) of ICAM-1 using semi-quantitative immunoperoxidase histochemistry, and the gene expression levels of TNF-α, ICAM-1, CCL2 and IL-1β using quantitative real-time RT-PCR.

3.4. Animals

All studies conducted in this research project were carried out on male inbred C57BL/6 mice, 6 to 8 weeks old, weighing between 20 to 25 grams. Due to their fast reproductive rate, low maintenance costs, relatively short life span, and physiological and genetic similarity with humans, mice have been referred to as "biomedicine's model mammal" (Malakoff, 2000). Mice are a commonly used species in auditory research because of the anatomical and physiological similarities of their auditory system to that of humans and the existence of many genetically modified strains. C57BL/6 mice are a common inbred strain of laboratory mice and are the most widely used rodent in the laboratory. Inbred strains of mice show less inter-animal variability in noise-induced hearing loss studies compared to other animal models (Wang *et al.*, 2002). Inbred mice also often show early onset age-related hearing loss, and the C57BL/6 mouse strain is the most established experimental model of accelerated age-related hearing loss. However, the onset of hearing loss in these mice occurs at 5 months of age (Vlajkovic *et al.*, 2011), much later than the age of mice used in the present study.

C57BL/6 mice were purchased from the Vernon Jansen Unit (VJU), an animal facility based at the Faculty of Medical and Health Sciences, The University of Auckland, and were bred under specific pathogen free (SPF) conditions. The animals were housed in standard wire restraint cages (up to a maximum of either four or eight animals per cage depending on the cage size) in the main warehouse, and maintained on a 12 h light/dark cycle under controlled temperatures and relative humidity. Mice had free access to standard rodent chow and filtered water at all times. The adenosine A_{2A} receptor homozygous recessive knockout ($A_{2A}RKO^{-/-}$) C57BL/6 mice used in study three were also sourced from the VJU, after importation of the colony from the United States. These mice with a single receptor deletion are viable and have only mildly impaired function (Fredholm *et al.*, 2005b).

All animal experimental procedures carried out in these studies (as described in this chapter) were approved by The University of Auckland Animal Ethics Committee (AEC number R880) in accordance with the Animal Welfare Act 1999. The animals were cared for according to the recommendations in the "Guide for the Care and Use of Laboratory Animals" (National Institutes of Health), and all efforts were made to minimise the number of animals used in the studies as well as their suffering.

3.5. Noise Exposures

Noise exposures were carried out in a small custom-built sound exposure booth (Shelburg Acoustics Pty Ltd, Croydon North, VIC, Australia), equipped with an internal light source and ventilation system. The sound stimulus was produced by a noise generator, filtered, amplified, and delivered via two internal speakers suspended from the ceiling of the booth. The controls for sound generation and frequency selection were externally located. Animals were placed in wire mesh cages positioned in the centre of the sound chamber directly underneath the suspended speakers. Sound was gradually increased to the required decibel level so as to not startle the animals. The sound exposure levels within the chamber at the level of the animal cages were measured using a handheld calibrated sound level meter (Brüel & Kjær Precision Sound Level Meter Type 2235, Nærum, Denmark). Mice were awake (i.e. unanaesthetised), unrestrained and had free access to food and water throughout the duration of the noise exposure. When not subjected to noise exposure, mice were housed in the warehouse of the animal unit (VJU), under the care of VJU staff members, until the selected endpoint of the study.

The animals in the acute noise exposure groups were exposed to 24 h of continuous octave band (8-16 kHz) noise presented at 100 dB SPL, whereas those in the chronic noise exposure groups were exposed to octave band (8-16 kHz) noise at 90 dB SPL for 2 h per day for either one, two, three or four weeks. Mice assigned as controls were exposed to ambient noise levels (55-65 dB SPL) in the VJU prior to being euthanized for tissue collection.

These sound levels are routinely used in our laboratory for mice and rats, and our experience is that animals show limited signs of distress during noise exposure. Although we routinely carry out acute noise exposures, this was the first time exposing animals to noise for such an extended period. However, as the animals were exposed to non-traumatic sound levels (90 dB SPL), no major impact on their welfare was expected, as the animals quickly adapt to noisy environments. No animals showed signs of distress, including dehydration and weight loss.

For the noise-induced cochlear NF-κB activation experiments in study one, a few mice ($n = 4$), anaesthetised with ketamine (38 mg/kg) and domitor (0.5 mg/kg) intraperitoneally (i.p.), were exposed to 110 dB SPL closed-field noise for 2 h. This was presented to the left ear with a tube inserted into the external auditory canal and connected to the speaker.

3.6. Auditory Brainstem Responses (ABRs)

Auditory thresholds in a group of mice (n = 4) from the initial study (study one) were measured 24 h before (baseline measurements) and four weeks after acute noise exposure using auditory brainstem responses (ABRs). ABR represents the activity (sound evoked potentials) of the auditory nerve and the central auditory pathways (brainstem/mid-brain regions) in response to transient sounds (acoustic clicks or tone pips). It is a relatively simple, quick and reliable technique for assessing auditory thresholds in small rodents (Willott, 2001). The ABR measurements were carried out within a double walled sound attenuating (soundproof) booth (Shelburg Acoustics Pty Ltd, Croydon North, VIC, Australia).

The mice were firstly anaesthetised with a mixture of ketamine (38 mg/kg) and domitor (0.5 mg/kg) injected intraperitoneally, and then placed onto a heating pad, to maintain body temperature at 37 °C. ABRs were obtained by placing fine platinum electrodes subdermally at the mastoid region of the ear of interest (active electrode), scalp vertex (reference) and mastoid region of the opposite ear (ground electrode). Measurements were only performed on the left ear for all animals.

The acoustic stimuli for ABR (4-32 kHz tone pips) were produced and the responses recorded using a Tucker-Davis Technologies (TDT) ABR workstation (RZ6 Multi I/O Processor) (Tucker-Davis Technologies, Inc., Alachua, FL, U.S.A.) controlled by a computer-based digital signal processing package and software (BioSigRZ, TDT). ABRs were elicited with digitally generated (using the signal design software, SigGenRZ, TDT) acoustic clicks (10 µs square wave, alternating polarity) or pure tone pips (5 ms duration, 1.5 ms rise-fall time) presented to the external auditory canal via a tube connected to an electrostatic speaker.

The stimuli were presented in 5 dB decrements of sound intensity from 90 dB SPL and the acquired responses averaged at each sound level (1024 repeats with stimulus polarity alternated). The ABR threshold was defined as the lowest intensity (to the nearest 5 dB) capable of evoking a reproducible, visually detectable response, with a minimum amplitude of 0.25 µV for Wave 1 of the ABR complex. The magnitude of the noise-induced threshold shift was calculated as the difference between baseline and post-exposure threshold.

3.7. Cochlear Tissue Preparation

Mice were euthanised at selected time points after noise exposure and their cochleae extracted for molecular (quantitative real-time RT-PCR) and immunohistochemical analysis of cochlear inflammation. At the end of their designated survival time, the animals were deeply anaesthetised with a lethal dose of the anaesthetic sodium pentobarbitone (90 mg/kg) administered intraperitoneally. Once deep anaesthesia was attained, as indicated by the absence of withdrawal reflexes in response to firm pinching of the paws or pinna, intracardiac perfusion was performed. The mouse was placed on its dorsal side and its chest cavity opened to gain full access to the heart. With the heart held steady with forceps, a 22 gauge needle connected to a manual perfusion pump system was inserted directly into the left ventricle. The valve was released and the pressure increased using a handheld pump (80-100 mmHg) to allow slow steady perfusion of flush solution throughout the body vasculature. The right atrium was then immediately cut to bleed the animal and flush the circulation. The flush solution comprised 0.9% sodium chloride (NaCl) in Milli-Q water (saline solution), with the addition of 10% sodium nitrite ($NaNO_2$), a vasodilator, and heparin, an anticoagulant. The transcardiac perfusion was continued until the perfusate became clear.

On completion of whole-body perfusion, the mouse was decapitated and both the left and right auditory/tympanic bullae were removed from the temporal bones. The cochlea was then carefully dissected out from each bulla. From each mouse, one cochlea was immersed in 4% paraformaldehyde (PFA)/0.1 M phosphate buffer (PB) (fixative solution; pH 7.4) in a small petri dish and used for immunohistochemical staining, while the contralateral cochlea was added to ice-cold Lysis/Binding Buffer (from Dynabeads® mRNA DIRECT™ Kit, Ambion®, Life Technologies, Oslo, Norway) in a sterile microcentrifuge tube and used for quantitative real-time RT-PCR. Cochleae used for mRNA extractions were carefully trimmed to remove all non-cochlear tissue within the adjacent temporal bone which could potentially interfere with mRNA expression levels of the inflammatory markers in the cochlea.

For the cochleae collected for immunohistochemistry, the oval and round windows were opened to allow for intralabyrinthine perfusion of fixative solution (superfixation). Approximately 80 µL of 4% PFA was perfused through each cochlea via the oval and round windows. These cochleae were left immersed in the fixative solution overnight (post-fixation) at 4ºC. Decalcification of the cochleae was then carried out with 5%

ethylenediaminetetraacetate (EDTA)/0.1 M PB for 6-7 days at 4ºC, with the EDTA changed every second day. The cochleae were then cryo-protected via immersion in 30% sucrose/0.1 M PB for 24 h. Following cryo-protection, the cochleae were rinsed twice with 0.1 M phosphate-buffered saline (PBS; pH 7.4), embedded in Tissue-Tek® O.C.T. (Optimal Cutting Temperature) Compound (Sakura Finetek USA, Inc., Torrance, CA, U.S.A.) mounted on a piece of tin foil, snap-frozen in n-pentane, and stored at -80 ºC until required for cryosectioning.

3.8. Immunohistochemistry

The expression and distribution of the cell adhesion molecules ICAM-1 and PECAM-1 in the non-exposed and noise-exposed mouse cochlea was assessed by immunoperoxidase staining, an immunohistochemical method in which target proteins are visualised by a peroxidase-catalysed colour producing reaction. For the NF-κB transcription factor subunits (p50 and p65) and the adenosine A_{2A} receptor, expression was localised using immunofluorescence, which uses fluorophores to detect proteins in cells. Both methods of immunohistochemistry rely on the specificity of antibodies to the corresponding antigen. All the primary and secondary antibodies used in the present study, including their dilutions, are listed in **Table 3.5** and **Table 3.6** respectively. A titration (dilution series) for each antibody was firstly carried out in order to obtain an optimal concentration of antibody that gave a high signal to background ratio. All antibodies utilised in this study were cross-reactive with mice.

Frozen cochlear tissues were cryosectioned into either 20 µm (for immunoperoxidase staining) or 30 µm (for immunofluorescence) thick mid-modiolar sections using a cryostat (Leica CM3050 S Cryostat, Leica Microsystems, Wetzlar, Germany). The fixed cochlear cryosections were then transferred into a BD Falcon™ 24-well plate (BD Biosciences, San Jose, CA, U.S.A.) prefilled with 0.1 M PBS. Immunohistochemistry was performed using the free floating section method, and all procedures were carried out under a dissecting microscope (Olympus SZ61, Olympus Corp., Tokyo, Japan). For all solutions used, 500 µL was added to each well.

Table 3.5: List of primary antibodies used for immunohistochemistry

1° Antibody	Company	Product #	Conc.	Dilution/Conc.	Source	Specificity
ICAM-1	BD Biosciences	550287	125 µg/mL	1:1600 (0.0781 µg/mL)	Hamster	Mouse
PECAM-1	Santa Cruz	sc-18916	200 µg/mL	1:800 (0.25 µg/mL)	Rat	Mouse
NF-κB p65	Santa Cruz	sc-372	200 µg/mL	1:2500 (0.08 µg/mL)	Rabbit	Mouse, rat, human
NF-κB p50	Santa Cruz	sc-1190	200 µg/mL	1:200 (1 µg/mL)	Goat	Mouse, rat, human
$A_{2A}R$	Santa Cruz	sc-7504	200 µg/mL	1:100 (2 µg/mL)	Goat	Mouse, rat

Table 3.6: List of secondary antibodies used for immunohistochemistry

2° Antibody	Company	Product #	Conc.	Dilution/Conc.	Source	Specificity
Biotinylated goat anti-hamster	Vector Labs	BA-9100	1.5 mg/mL	1:800 (1.875 µg/mL)	Goat	Hamster
Biotinylated goat anti-rat	Vector Labs	BA-9400	1.5 mg/mL	1:1600 (0.9375 µg/mL)	Goat	Rat
Alexa Fluor 488 goat anti-rabbit	Invitrogen	A-11034	2 mg/mL	1:400 (5 µg/mL)	Goat	Rabbit
Alexa Fluor 488 donkey anti-goat	Invitrogen	A-11055	2 mg/mL	1:200 (10 µg/mL)	Donkey	Goat

3.8.1. Immunoperoxidase Staining

After being washed twice with 0.1 M PBS, the free floating cochlear sections were incubated in 0.6% hydrogen peroxidase (H_2O_2) in methanol for 20 minutes at room temperature. This allowed quenching of endogenous peroxidase activity and therefore prevention of potential non-specific background staining. Blocking solution consisting of the serum from the species in which the secondary antibody was raised (10% in 0.1 M PBS) was then added for 1 h at room temperature to block non-specific binding of secondary antibodies. For both ICAM-1 and PECAM-1, normal goat serum (Invitrogen™, Life Technologies, Frederick, MD, U.S.A.) was used. Triton X-100 (1%), a non-ionic detergent, was also included in the blocking

solution to permeabilise cell membranes, allowing intracellular access of the antibodies. Following blocking and permeabilisation, sections were incubated with the respective primary antibody overnight at 4ºC. Immunolabelling of ICAM-1 and PECAM-1 were carried out with hamster anti-mouse ICAM-1 (CD54) (BD Biosciences, San Jose, CA, U.S.A.) and rat anti-mouse PECAM-1 (Santa Cruz Biotechnology, Inc., Santa Cruz, CA, U.S.A.) respectively. The antibodies were diluted in a solution consisting of 10% normal goat serum and 0.1% Triton X-100 in 0.1 M PBS.

On the second day, after three washes with 0.1 M PBS, sections were incubated in secondary antibodies for 40 minutes at room temperature. Biotinylated goat anti-hamster IgG conjugate was used for ICAM-1, and biotinylated goat anti-rat IgG conjugate was used for PECAM-1 (both from Vector Laboratories, Inc., Burlingame, CA, U.S.A.). The secondary antibodies were diluted in a 0.1 M PBS solution containing 5% normal serum (from the same species as the secondary antibody). Following secondary antibody incubation, sections were washed three times in 0.1 M PBS and then incubated in avidin: biotinylated horseradish peroxidase complex (Vectastain® Elite ABC Kit, Vector Laboratories, Inc., Burlingame, CA, U.S.A.) for 40 minutes at room temperature. Formation of the ABC complex was achieved by mixing the ABC reagents (1:50 of Reagent A and 1:50 of Reagent B) in 0.1 M PBS and allowing it to stand for 40 minutes at room temperature prior to use. After another three washes, sections were soaked in 0.1 M PBS overnight at 4ºC.

Finally, sections were developed by the addition of 3, 3'-diaminobenzidine (DAB Peroxidase Substrate Kit; Vector Laboratories, Inc., Burlingame, CA, U.S.A.), a chromogenic peroxidase substrate that yields a brown stain/precipitate upon enzymatic reaction. The DAB working solution consisted of DAB stock solution (1:50), buffer stock solution (1:50) and H_2O_2 (1:50) in Milli-Q water. Reactions were developed at room temperature and stopped by the immediate removal of DAB and the addition of 0.1 M PBS. Development times were kept between two and ten minutes and were consistent in all experimental groups. Control sections from non-exposed cochleae were stained for the same duration as the corresponding sections from noise-exposed cochleae. All sections were then rinsed twice with 0.1 M PBS, carefully mounted on LabServ® frosted microscope glass slides (Thermo Fisher Scientific Ltd, Auckland, New Zealand) in a small amount of mounting medium (glycerol/PBS; 1:1), and covered with a coverslip (Marienfeld Laboratory Glassware, Lauda-Königshofen, Germany). To prevent possible movement of the coverslip and dehydration during storage, coverslips

were completely sealed at their edges with nail polish. Slides were stored at 4ºC until required for microscopic imaging. Immunostained cochlear sections were viewed by brightfield microscopy (Nikon Eclipse 80i Microscope, Nikon Instruments Inc., Melville, NY, U.S.A.) and images were obtained with a digital microscope camera (Nikon DS-5Mc) attached to the light microscope. Image acquisition was controlled by NIS-Elements Basic Research imaging software (version 2.30; Nikon), and images were captured using identical acquisition parameters.

3.8.2. Immunofluorescence

To localise the cochlear expression of the two NF-κB subunits and the adenosine A_{2A} receptor, immunofluorescence staining was carried out. For NF-κB, this allowed clear differentiation between nuclear and cytoplasmic immunolabelling in order to determine the activation state of NF-κB. The general protocol for immunofluorescence was similar to that of immunoperoxidase staining, but with fewer steps involved in a two-day protocol.

Frozen cochleae were cryosectioned at 30 microns and mid-modiolar cryosections were washed twice in 0.1 M PBS. A 1 h blocking and permeabilisation step was then carried out at room temperature as described above for immunoperoxidase staining followed by overnight incubation in the primary antibody at 4°C. Rabbit anti-mouse NF-κB p65 and goat anti-mouse NF-κB p50 primary antibodies (both from Santa Cruz Biotechnology, Inc., Santa Cruz, CA, U.S.A.) were used to localise the expression of the respective subunits. The A_{2A} receptor was labelled with goat anti-mouse adenosine A_{2A}R antibody (Santa Cruz Biotechnology, Inc., Santa Cruz, CA, U.S.A.). Next, sections were incubated in Alexa Fluor®-conjugated secondary antibodies (Molecular Probes®, Invitrogen™, Life Technologies, Eugene, Oregon, U.S.A.) for 2 h in the dark at room temperature. Alexa Fluor® 488 goat anti-rabbit IgG was used for p65, while Alexa Fluor® 488 donkey anti-goat IgG was used for p50 and the adenosine A_{2A} receptor. For the blocking solution, primary antibody and secondary antibody solutions, normal goat serum was used for p65, whereas normal donkey serum (Sigma-Aldrich, Inc., St. Louis, MO, U.S.A.) was used for p50 and the adenosine A_{2A} receptor. After three washes with 0.1 M PBS, the sections were mounted on microscope glass slides in Citifluor AF1 Mountant Solution (Citifluor Ltd, London, UK), an aqueous-based mounting medium composed of glycerol-PBS and an antifading reagent

(prevents photobleaching). Immunofluorescence was visualised using fluorescence microscopy (Nikon Eclipse 80i Microscope, Nikon Instruments Inc., Melville, NY, U.S.A.).

3.8.3. Negative Controls

To test for non-specific binding of secondary antibodies, negative controls were performed by omitting the primary antibodies. For ICAM-1 and PECAM-1, another set of control reactions were performed, whereby the primary antibody was replaced with an IgG antibody (IgG isotype control) of the same species and isotype as the primary antibody of interest (and at the same concentration) to test for the specificity of the primary antibody. The IgG isotype controls used for the ICAM-1 and PECAM-1 antibodies were hamster IgG1, κ chain (BD Pharmingen™, BD Biosciences, San Diego, CA, U.S.A.) and rat IgG2a, κ chain (BD Pharmingen™, BD Biosciences, San Diego, CA, U.S.A.). For the antibodies that were raised against peptide antigens (NF-κB p65/p50), an immunising peptide blocking experiment was performed to determine the specificity of the antibody. This involved incubating/pre-absorbing the antibody with a two-fold excess of the corresponding blocking peptide (both from Santa Cruz Biotechnology, Inc., Santa Cruz, CA, U.S.A.) for 3 h at room temperature using the orbital shaker incubator.

3.8.4. Quantitative Image Analysis of ICAM-1 Immunostaining

In addition to assessing ICAM-1 immunostaining qualitatively, semi-quantitative image analysis based on pixel intensity and area of staining was carried out to provide a more accurate assessment of the protein expression levels. Image analysis was performed using ImageJ (version 1.46r), an image processing and analysis software developed at the National Institutes of Health (NIH). The inferior region of the spiral ligament of the upper basal and middle cochlear turns were selected as the regions of interest for measurements as these areas showed the strongest and most consistent immunostaining. Using the freehand selection tool, the DAB stained region of interest (ROI) was selected, and intensity and area statistics were then calculated by the software. For staining intensity measurements, the mean gray value was determined by converting the RGB pixels in the image to grayscale/brightness values. The mean gray value represents the sum of the gray values of all the pixels in the selection divided by the total number of pixels. The lower the pixel value, the higher the intensity (pixel values range from 0 to 255, with 0 representing black and 255 representing white). To

present area measurements in calibrated units (μm^2), the spatial scale of the images were defined beforehand. For each cochlea, three to five mid-modiolar sections were analysed. The mean gray values and areas of the ICAM-1 immunostaining in both cochlear turns were averaged for each experimental group and presented relative to the control group.

3.9. Quantitative Real-Time RT-PCR

To quantify the mRNA expression levels of the proinflammatory cytokines TNF-α and IL-1β, the chemokine CCL2, and the cell adhesion molecule ICAM-1 in the noise-exposed mouse cochlea, a two-step quantitative real-time reverse transcription-polymerase chain reaction (real-time RT-PCR) was carried out. Real-time RT-PCR is the benchmark technology for the quantitative assessment of mRNA due to its simplicity, specificity and sensitivity (Bustin *et al.*, 2005). For each experimental group studied, cochlear mRNA samples (from a single cochlea) from eight mice were used for the real-time RT-PCR analysis (n = 8). In the adenosine A_{2A} receptor knockout study, the sample size was five (n = 5).

3.9.1. Isolation of mRNA

The first step of real-time RT-PCR involved the isolation of mRNA from the harvested cochlea tissue samples (only one cochlea per animal was used). By measuring the amount of mRNA, changes in gene expression levels in the cochlea can be determined. mRNA extraction was performed using the Dynabeads® mRNA DIRECT™ Kit (Ambion®, Life Technologies, Oslo, Norway), a simple procedure that allows rapid and direct isolation of highly purified and intact polyadenylated (polyA) mRNA from crude lysate (**Figure 3.1**). It relies on base pairing between the polyA residues at the 3' end of mRNA and the oligo$(dT)_{25}$ residues covalently coupled to the surface of the Dynabeads® (uniform, superparamagnetic beads). Other RNA species without a polyA tail (e.g. ribosomal RNA, transfer RNA, micro RNA and small nucleolar RNA) do not hybridise to the beads and are discarded.

Firstly, the extracted cochlea was homogenised in 600 µL of ice-cold Lysis/Binding Buffer (100 mM Tris-HCl pH 7.5, 500 mM LiCl, 10 mM EDTA pH 8, 1% LiDS, 5 mM dithiothreitol (DTT), RNase inhibitors) using an autoclaved Teflon mini-pestle. After being spun for one minute at high speed (13,000 rpm) in a microcentrifuge (Microcentrifuge

5415D, Eppendorf, Hamburg, Germany) to remove debris, the tissue lysate was transferred to a sterile (RNase- and DNase-free) microcentrifuge tube containing pre-conditioned (resuspended) magnetic Dynabeads® Oligo(dT)$_{25}$ (5 mg/mL). The Dynabeads® were continuously mixed with the tissue lysate for five minutes at room temperature to allow the polyA-tails of mRNA to anneal/hybridise to the oligo(dT)s on the beads. Later, the Dynabeads®/mRNA complex was magnetically separated from the mixture and washed with two different washing buffers; twice with 600 µL of Washing Buffer A (10 mM Tris-HCl pH 7.5, 0.15 M LiCl, 1 mM EDTA, 0.1% LiDS) and once with 300 µL of Washing Buffer B (10 mM Tris-HCl pH 7.5, 0.15 M LiCl, 1 mM EDTA). Following the washing steps, mRNA was eluted from the Dynabeads® by adding 10 µL of cold elution buffer (10 mM Tris-HCl, pH 7.5) and incubating the mixture at 67°C for two minutes in a PCR thermal cycler (PTC-100 Programmable Thermal Controller, MJ Research, Inc., Waltham, MA, U.S.A.). Finally, the eluate (supernatant) containing the total cochlear mRNA was transferred to an RNase-free tube and stored at -80°C until needed for reverse transcription.

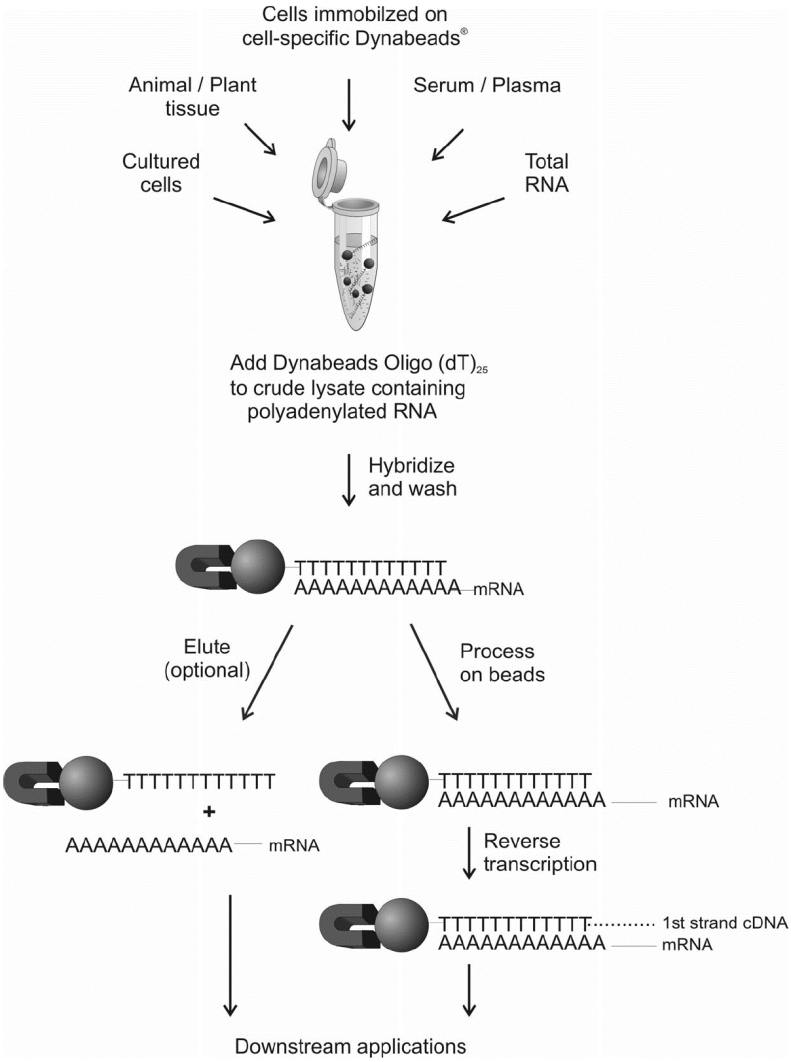

Figure 3.1: Dynabeads® mRNA Direct™ workflow. Outline of the protocol for isolating mRNA from a crude starting sample using Dynabeads Oligo(dT)25. The isolated mRNA is suitable for use in all downstream molecular biology applications. (Figure reproduced from Dynabeads® mRNA Direct™ Kit User Guide, Life Technologies, Inc. (2012)).

3.9.2. First-Strand cDNA Synthesis (Reverse Transcription)

Following the extraction of total cochlear mRNA, first-strand complementary DNA (cDNA) synthesis (reverse transcription) from the mRNA was carried out using the SuperScript® III First-Strand Synthesis SuperMix Kit (Invitrogen™, Life Technologies, Carlsbad, CA, U.S.A.). Components used for the reactions included SuperScript® III/RNaseOUT™ Enzyme Mix (contains SuperScript® III Reverse Transcriptase and RNaseOUT™ Recombinant RNase Inhibitor), 2X First-Strand Reaction Mix (contains 10 mM $MgCl_2$ and 1 mM of each dNTP), random hexamers, and annealing buffer. The RNase inhibitor included in the enzyme

mix prevents possible degradation of target RNA that could occur from contamination of the RNA preparation with ribonucleases. For each mRNA sample, a negative reverse transcriptase control (-RT) was also included, whereby diethyl pyrocarbonate (DEPC)-treated water (i.e. RNase-free water) was added in place of reverse transcriptase.

The procedure first involved combining 5 µL of each mRNA sample with 1 µL each of random hexamers, annealing buffer and DEPC-treated water. For the –RT controls, half the volume of each component was used (i.e. 2.5 µL of mRNA and 0.5 µL each of random hexamers, annealing buffer and DEPC-treated water). Next, the reaction mixtures were incubated in a thermal cycler (PTC-100 Programmable Thermal Controller, MJ Research, Inc., Waltham, MA, U.S.A.) at 65°C for 5 minutes. After collecting the contents by brief centrifugation, 10 µL of 2X First-Strand Reaction Mix and 2 µL of SuperScript® III/RNaseOUT™ Enzyme Mix were added to the +RT samples, and 5 µL of 2X First-Strand Reaction Mix and 1 µL of DEPC-treated water were added to the –RT samples. The reaction mixtures, each with a total volume of 20 µL (+RT) or 10 µL (-RT), were then vortexed and centrifuged and incubated in a PCR thermal cycler at 25°C for 10 minutes, at 50°C for 50 minutes, followed by 5 minutes at 85°C to terminate the reactions. Finally, the cDNA samples were immediately chilled on ice, and then stored at -20°C until required for real-time PCR.

3.9.3. Real-Time PCR

The synthesised first-strand cDNA templates were then amplified by real-time PCR using TaqMan® Universal PCR Master Mix (Applied Biosystems®, Life Technologies, Branchburg, NJ, U.S.A.), which contains AmpliTaq Gold® DNA polymerase and deoxynucleotide triphosphates (dNTPs), and predesigned TaqMan® Gene Expression Assays, which consist of a pair (forward and reverse) of unlabelled mouse-specific PCR primers and a TaqMan® MGB probe proprietary to Applied Biosystems® (Life Technologies, Foster City, CA, U.S.A.). The MGB probe contains a reporter dye (FAM dye) at the 5’ end, a minor groove binder (MGB) and a nonfluorescent quencher (NFQ) at the 3’ end. β-actin was also quantified for each cDNA sample as an endogenous control “housekeeping” gene to normalise the PCR results. In contrast to the target genes, the probe for β-actin was VIC dye-labelled instead of FAM dye-labelled. **Table 3.7** shows the Assay

ID, GenBank® Accession number and the dye of the TaqMan® MGB probe for each TaqMan® Gene Expression Assay.

Table 3.7: Primer/probes used for real-time PCR

Target Gene	Assay ID*	GenBank® Accession Number**	TaqMan® MGB Probe Dye
TNF-α	Mm00443258_m1	NM_013693.2	FAM
IL-1β	Mm01336189_m1	NM_008361.3	FAM
CCL2	Mm00441242_m1	NM_011333.3	FAM
ICAM-1	Mm00516023_m1	NM_010493.2	FAM
β-actin	Mm00607939_s1	NM_007393.3	VIC

*The Assay ID is a unique, alphanumeric string that identifies the TaqMan® Gene Expression Assay and encodes descriptive information. The prefix indicates the species to which the assay is designed – in this case Mm refers to *Mus musculus*. The suffix indicates the assay placement (_m identifies an assay that amplifies a region spanning an exon junction; _s identifies an assay whose primers/probes are designed within a single axon. **GenBank is the National Institutes of Health (NIH) genetic sequence database – the accession number is a unique identifier assigned to a particular genome or protein sequence.

Separate PCR master reaction mixtures were prepared for each TaqMan® Gene Expression Assay (TNF-α, IL-1β, CCL2, ICAM-1, and β-actin). The components comprising the master reaction mixes included TaqMan® Universal PCR Master Mix, the specific primers and probes, and DEPC-treated H_2O. These were all combined in a sterile (RNase- and DNase-free) microcentrifuge tube. The volume and final concentration of each component of the master mixes for the target genes and for β-actin are shown in **Table 3.8** and **Table 3.9** respectively. Because each reaction included only one pair of primers (i.e. primers amplifying target genes and those amplifying the endogenous control were in separate reactions), this method is known as a singleplex PCR.

Table 3.8: PCR master mix for target genes (TNF-α, IL-1β, CCL2 and ICAM-1)

Reaction Component	Single Reaction Volume	Final Concentration
TaqMan® Universal PCR Master Mix (2X)	6.25 µL	1X
Target Gene Primer/Probe (20X)	0.625 µL	1X
DEPC-treated H_2O	4.625 µL	-

Table 3.9: PCR master mix for β-actin

Reaction Component	Single Reaction Volume	Final Concentration
TaqMan® Universal PCR Master Mix (2X)	6.25 µL	1X
β-Actin Primer/Probe (60X)	0.21 µL	1X
DEPC-treated H_2O	5.04 µL	-

Once the master reaction mixtures were prepared, 11.5 µL was aliquoted into each assigned well of a MicroAmp® Optical 384-Well Reaction Plate (Applied Biosystems®, Life Technologies, Foster City, CA, U.S.A.), and then 1 µL of cDNA from each sample was added, making up a total reaction volume of 12.5 µL. Each sample was run in triplicates (two +RT reactions and a single –RT reaction). Two no template controls (NTCs; first-strand cDNA omitted), were also included for each TaqMan® Gene Expression Assay on the plate. This entire procedure was carried out within an Esco PCR Laminar Flow Cabinet (Esco Micro Pte. Ltd., Singapore), which provides protection against contamination from the ambient environment and cross-contamination within the chamber. The plate was then sealed with an ABI PRISM® Optical Adhesive Cover (Applied Biosystems®, Foster City, CA, U.S.A.) and spun down at 3000 rpm for 5 to 10 minutes in a centrifuge (Heraeus Multifuge X3 Centrifuge, Thermo Fisher Scientific, Langenselbold, Germany). After verifying that each mixture was positioned at the bottom of the wells and no air bubbles were present, real-time PCR was run using the 7900HT Fast Real-Time PCR System (Applied Biosystems®, Foster City, CA, U.S.A.). The thermal cycling protocol included 2 min at 50°C, 10 min at 95°C and 40 cycles of 15 s at 95°C and 1 min at 60°C. Each PCR run took approximately 1.5 h.

Raw data acquired from the real-time PCR system were analysed using the Sequence Detection System (SDS) Software v2.3 (Applied Biosystems®). Relative quantification of gene expression for each inflammatory marker was determined using the comparative C_T

method (also referred to as the $2^{(-\Delta\Delta C_T)}$ method) (Livak & Schmittgen, 2001). Fold changes, which allowed comparisons to be made between non-exposed controls and noise-exposed mice, and between vehicle controls and drug-treated mice, were determined as follows. C_T values measured from the real-time PCR experiment were used to calculate delta C_T values ($\Delta C_T = C_{T\ target} - C_{T\ \beta\text{-actin}}$). $\Delta\Delta C_T$ values per sample were then determined by subtracting the average ΔC_T of the control group from the ΔC_T of each sample of the experimental group. This was followed by averaging the $\Delta\Delta C_T$ values per sample in each group. Finally, the fold change in the target gene expression relative to the control group was calculated from the formula: $2^{(-\Delta\Delta C_T)}$ if $\Delta\Delta C_T \leq 0$ or $(-1)/2^{(-\Delta\Delta C_T)}$ if $\Delta\Delta C_T > 0$. To determine whether there were any significant differences between the groups, real-time PCR results were statistically evaluated using a one-way ANOVA followed by Tukey's post-hoc multiple comparisons test or a Student's *t*-test (two tails of unequal variances) of the $\Delta\Delta C_T$ values.

3.10. Drug (Regadenoson) Preparation and Administration

The selective adenosine A_{2A} receptor agonist, regadenoson, was administered in mice (Study 3) to activate adenosine A_{2A} receptors in the noise-exposed cochlea in an attempt to suppress the noise-induced inflammatory response. A stock solution of regadenoson (Toronto Research Chemicals Inc., Toronto, Ontario, Canada) was initially prepared by suspending 2.5 mg of the drug (an off-white to pale beige solid) in 2 mL of DMSO (Sigma-Aldrich, Inc., St. Louis, MO, USA) to give a concentration of 1.25 mg/mL. From this, a working solution (1:100 dilution) was prepared by dissolving 10 µL of the stock solution in 990 µL of sterile saline solution (0.9% NaCl) to give a final drug concentration of 12.5 µg/mL. This was a clear and colourless solution. For vehicle controls, DMSO was diluted in sterile saline solution to the same concentration (1%). The working solution of regadenoson and the vehicle solution were aliquoted and stored at -20°C for later use. When required, the aliquots were thawed at room temperature before administration.

Regadenoson was administered immediately following the cessation of acute noise exposure via a single intracardiac injection (i.e. through the left ventricle of the heart) using an insulin syringe with a 30 gauge needle. Mice received a 0.05 mg/kg dose of regadenoson; 1.25 µg per 25 g mouse, which is 100 µL of the drug working solution (12.5 µg/mL). An equivalent volume of vehicle solution (1% DMSO/saline) was given to animals serving as controls. The

animals were firstly anaesthetised with an intraperitoneal injection of ketamine (38 mg/kg) and domitor (0.5 mg/kg). When determined to be fully anaesthetised (i.e. the loss of withdrawal reflexes), the mouse was laid down in the supine position on a heating pad (~30°C) and the chest area sterilised with 70% ethanol. After ensuring the absence of air bubbles in the syringe, the needle was carefully inserted (at a 30° angle) directly into the left side of the sternum in the third intercostal space. The plunger of the syringe was pull backed slightly and the presence of blood within the syringe indicated the correct positioning of the needle in the left ventricle. The drug solution was then injected and the needle quickly removed from the chest. Upon completion of the procedure, the animal was placed back into the cage, and allowed to completely recover from anaesthesia. The animal was carefully monitored, especially during the first hour after drug injection, until it was fully awake. Body weight was measured prior to treatment and again before the animal was euthanised.

3.11. Statistical Analysis

Differences between two experimental groups were analysed using a Student's *t*-test (paired/unpaired, unequal variances) (Microsoft Excel 2013) while a one-way analysis of variance (ANOVA) followed by Tukey's post-hoc multiple comparisons test (IBM IPSS Statistics v20) was used for comparisons of three or more groups. A paired Student's *t*-test was used to compare baseline and post-exposure ABR thresholds (tone pips and auditory clicks), while an unpaired Student's *t*-test was used to compare vehicle and drug-treated mice, and wild-type and $A_{2A}RKO^{-/-}$ mice. One-way ANOVA was used to compare the gene expression levels, intensity and area of ICAM-1 immunostaining, and number of $A_{2A}R$-positive infiltrating cells at different time points. Tukey's post-hoc multiple comparisons tables for all analysis are included in **Appendix B** for reference. A p value of less than 0.05 was considered statistically significant, with ranges denoted as $*p < 0.05$; $**p < 0.01$; $***p < 0.001$. All data were presented as the mean ± standard error of the mean (SEM).

CHAPTER 4: RESULTS

4.1. General Observations

The mice in this study showed no major discernible behavioural changes, during or after noise exposure, relative to control mice exposed to ambient noise (55-65 dB SPL). The animals showed no signs of pain or distress, and appeared healthy (with normal fur and posture), active, and ate and drank normally. In addition, mice treated intracardially with the drug regadenoson or vehicle solution appeared normal, with no observable side effects.

Prior to intracardiac perfusion and cochlear tissue collection, a brief otoscopic examination was performed on each mouse while they were under general anaesthesia induced with sodium pentobarbitone (90 mg/kg, i.p.). This involved inspecting the tympanic membranes (eardrums) of both ears under a dissecting microscope for evidence of middle ear infection. The presence of signs such as milkiness/cloudiness of the tympanic membrane and dilated blood vessels would strongly indicate the occurrence of middle ear inflammation, and the mouse would be excluded from the study. None of the mice inspected displayed signs of middle ear infection.

4.2. STUDY 1: Cochlear Inflammatory Response Associated with Acute Noise Exposure

This initial study was undertaken to characterise the underlying mechanisms of the inflammatory response and its time course in the mouse cochlea following acute traumatic noise exposure. It hereby provides a foundation for the subsequent studies. To study the cochlear inflammatory response, a mouse model of noise-induced cochlear injury/permanent threshold shift was developed by exposing young adult (6 to 8 weeks old) wild-type C57BL/6 mice to continuous open-field octave band (8-16 kHz) noise presented at 100 dB SPL for 24 h.

4.2.1. Auditory Brainstem Responses (ABRs)

To verify that the noise stimulus used in the acute noise exposure studies caused permanent hearing loss (permanent threshold shift), the hearing sensitivity of a group of mice ($n = 4$) was assessed using sound-evoked ABR responses. ABR thresholds were measured 24 h prior to noise exposure (baseline measurement) and one month after noise exposure (final measurement).

Baseline ABR thresholds were consistent with our previous studies (Vlajkovic *et al.*, 2011) and comparable in all animals tested within the group. The average pre-exposure ABR thresholds to tone pips ranged from 26.3 ± 2.4 dB SPL to 37.5 ± 2.5 dB SPL over the 4-32 kHz frequency range used in the study (**Figure 4.1**). The average hearing threshold with an acoustic click stimulus in these mice was 33.8 ± 2.4 dB SPL (**Figure 4.3**).

Post-exposure ABR thresholds were significantly elevated above baseline thresholds. Threshold shifts (the difference between baseline and post-noise threshold measurements) evaluated using pure tone-evoked ABRs ranged from 7.5 ± 2.5 dB at 4 kHz to a maximum of 56.3 ± 2.4 dB at 20 kHz. These threshold shifts were statistically different from baseline ($p < 0.05$ to $p < 0.001$, paired *t*-test), apart from the threshold shift at 4 kHz ($p > 0.05$, paired *t*-test) (**Figure 4.1** and **Figure 4.2**). The average post-exposure threshold to an acoustic click stimulus was 51.3 ± 1.3 dB, a threshold shift of 17.5 ± 1.4 dB ($p < 0.01$, paired *t*-test) (**Figure 4.3**).

These results indicate that mice sustain permanent threshold shift (permanent hearing loss) following exposure to 100 dB SPL octave band (8-16 kHz) noise for 24 h, extending beyond the frequency range (8-16 kHz) of the noise.

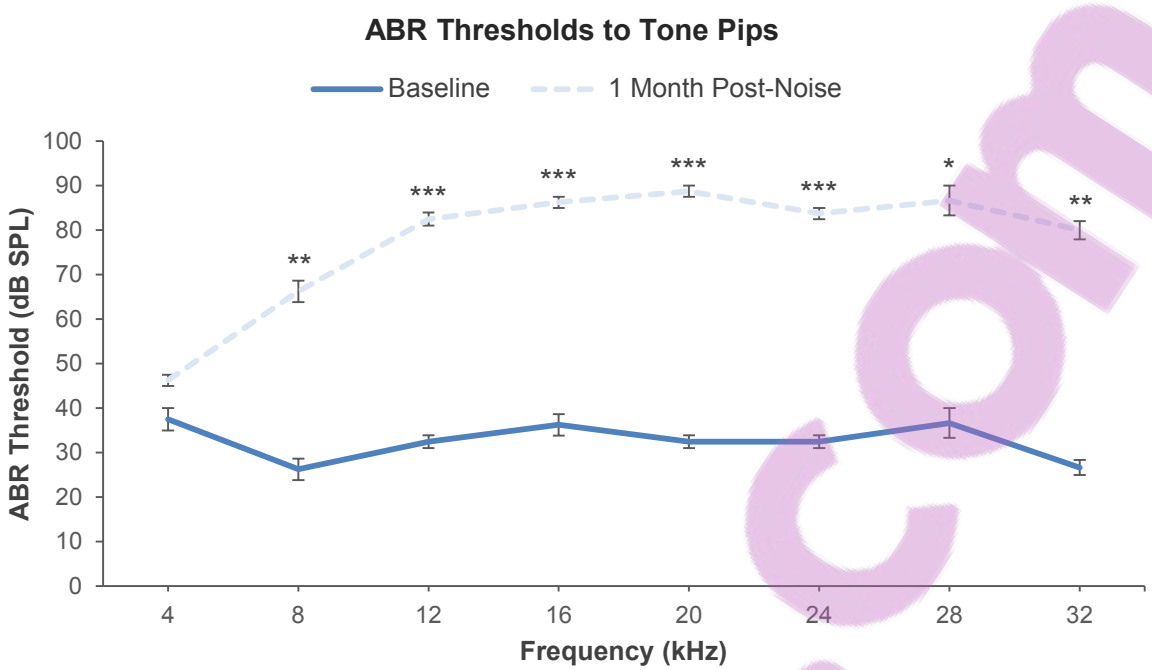

Figure 4.1: Auditory brainstem response (ABR) thresholds to tone pips prior to and one month after acute noise exposure. The graph illustrates the mean ABR threshold (dB SPL) to tone pips across the 4-32 kHz frequency range before (baseline measurement; blue line) and one month following acute exposure to traumatic noise (100 dB SPL, 8-16 kHz for 24 h; green line). The noise-exposed mice sustained permanent hearing loss (permanent threshold shift) as indicated by the large threshold shifts observed. Data presented as mean ± SEM ($n = 4$ per group). *$p < 0.05$, **$p < 0.01$, ***$p < 0.001$; paired t-test.

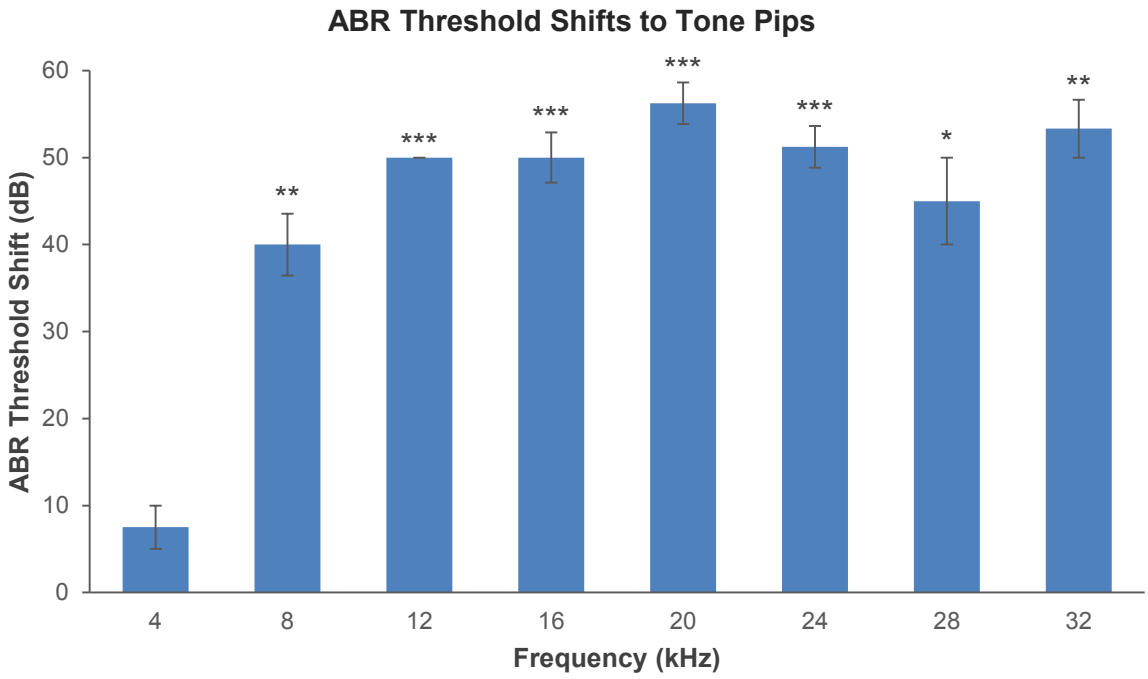

Figure 4.2: Auditory brainstem response (ABR) threshold shifts to tone pips one month after acute noise exposure. The graph illustrates the ABR threshold shifts (dB) to tone pips across the 4-32 kHz frequency range one month following acute exposure to traumatic noise (100 dB SPL, 8-16 kHz for 24 h). Threshold shifts, which were calculated as a difference between baseline and post-noise exposure thresholds, ranged from 7.5 ± 2.5 dB to 56.3 ± 2.4 dB across the frequency range. Data presented as mean ± SEM (n = 4 per group). *$p < 0.05$, **$p < 0.01$, ***$p < 0.001$; paired t-test.

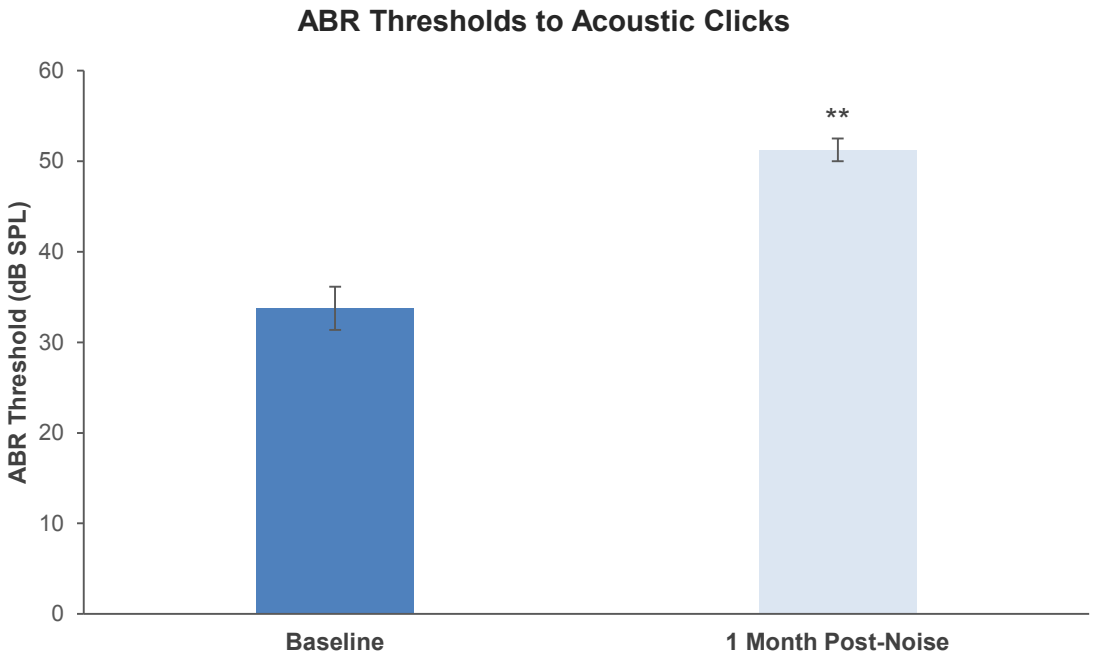

Figure 4.3: Auditory brainstem response (ABR) thresholds to acoustic clicks prior to and one month after acute noise exposure. The graph illustrates the mean ABR threshold (dB SPL) to an acoustic click stimulus before (baseline measurement) and one month following acute exposure to traumatic noise (100 dB SPL, 8-16 kHz for 24 h). The mean threshold increased from 33.8 ± 2.4 dB SPL to 51.3 ± 1.3 dB SPL, representing an average threshold shift of 17.5 ± 1.4 dB. Data presented as mean ± SEM (n = 4 per group). $^{**}p < 0.01$; paired t-test.

4.2.2. Gene Expression Levels of TNF-α, CCL2, ICAM-1 and IL-1β in the Noise-Exposed Cochlea

To identify the molecular changes associated with noise-induced cochlear inflammation, a two-step quantitative real-time RT-PCR analysis was conducted to evaluate the mRNA transcript levels of several key inflammation-related genes including the proinflammatory cytokines TNF-α and IL-1β, the chemokine CCL2, and the cell adhesion molecule ICAM-1. These inflammatory mediators have important roles in mediating the recruitment and infiltration of inflammatory cells into tissues. Cochleae were harvested at four different time intervals after noise exposure (6 h, 1 day, 3 days or 7 days) in order to assess the dynamics of gene expression (n = 8 per time point).

Using the comparative C_T ($2^{(-\Delta\Delta C_T)}$) method (Livak & Schmittgen, 2001), relative changes in mRNA expression levels between noise-exposed groups and non-exposed controls were assessed. The C_T values of each sample were normalised to the endogenous housekeeping gene, β-actin. Furthermore, a one-way ANOVA followed by Tukey's post-hoc multiple comparisons test was performed to determine the significance of the fold changes (see **Appendix B1** for the Tukey's post-hoc multiple comparisons tables).

The relative mRNA expression levels of each inflammatory mediator were analysed at the four time points following noise exposure and displayed in the graphs below (**Figure 4.4** to **Figure 4.7**). Note that the scale of the vertical bars (fold change) is different for each of the target genes. Interestingly, all genes displayed similar dynamics of expression, with an early upregulation at 6 h post-exposure followed by a subsequent peak at 7 days post-exposure. At 6 h post-exposure, TNF-α, CCL2, ICAM-1 and IL-1β increased by 4.6-fold, 22.9-fold, 3.8-fold and 1.6-fold respectively relative to non-exposed controls ($p < 0.001$ for TNF-α and CCL2, $p < 0.05$ for ICAM-1, $p > 0.05$ for IL-1β; one-way ANOVA). At 7 days post-exposure, the respective fold changes for TNF-α, CCL2, ICAM-1 and IL-1β were 5.7, 4.7, 5.1 and 1.6 ($p < 0.001$ for TNF-α and ICAM-1, $p < 0.01$ for CCL2, $p > 0.05$ for IL-1β; one-way ANOVA). The results therefore demonstrate a biphasic inflammatory response following acoustic overstimulation. No amplification was detected in the no template controls (reaction mixtures with no cDNA template) or in the –RT controls (omission of the reverse transcriptase) in all real-time PCR runs.

Of the four inflammatory genes examined, CCL2 showed the greatest increase in mRNA expression at 6 h post-exposure relative to controls, about five times higher than that for TNF-α. Furthermore, the gene expression level of CCL2 at 7 days post-exposure was significantly lower than that of the initial peak at 6 h post-exposure ($p < 0.01$, one-way ANOVA). However, for TNF-α, ICAM-1 and IL-1β, gene expression levels at the two time points were comparable ($p > 0.05$, one-way ANOVA).

In addition to these inflammatory genes, the transcriptional expression of IL-6, another key proinflammatory cytokine, was also examined in this study. However, the primer/probe combination for IL-6 (Applied Biosystems®, Life Technologies, Foster City, CA, U.S.A) did not detect IL-6 specific mRNA in any of the cochlear samples.

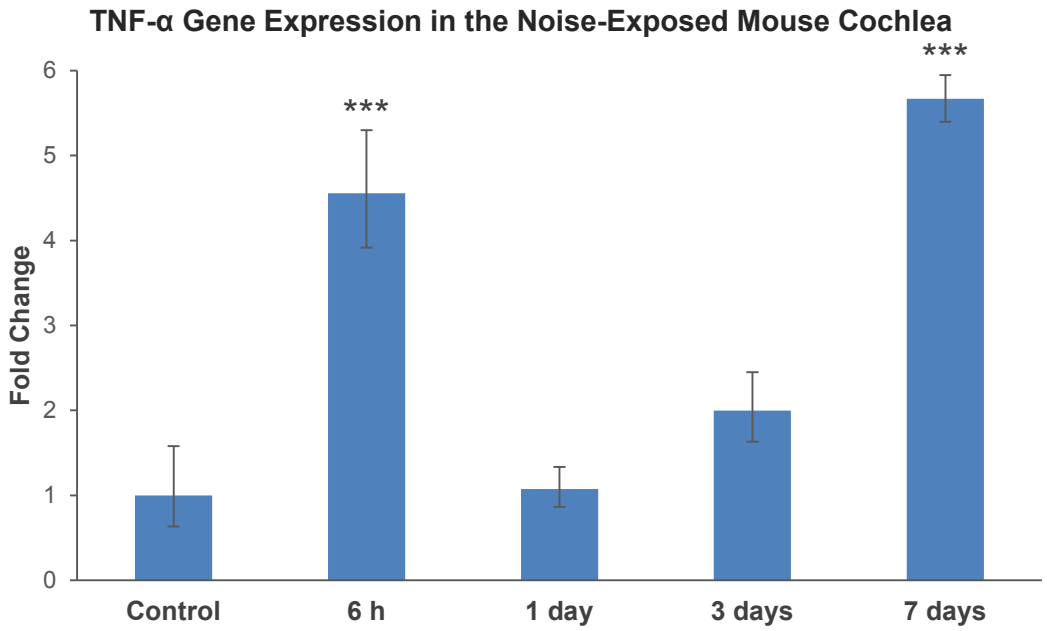

Figure 4.4: Quantitative real-time RT-PCR analysis of TNF-α gene expression in the C57BL/6 mouse cochlea following acute noise exposure. The graph illustrates the fold change in gene expression of TNF-α at 6 h, 1 day, 3 days and 7 days following acute exposure to traumatic noise (100 dB SPL, 8-16 kHz for 24 h) relative to non-noise exposed controls. Two peaks in TNF-α expression were observed; an early upregulation at 6 h (4.6-fold increase) and a later peak at 7 days post-exposure (5.7-fold increase). Data presented as mean ± SEM (n = 8 per group). ***$p < 0.001$, relative to the control group (one-way ANOVA followed by Tukey's post-hoc test).

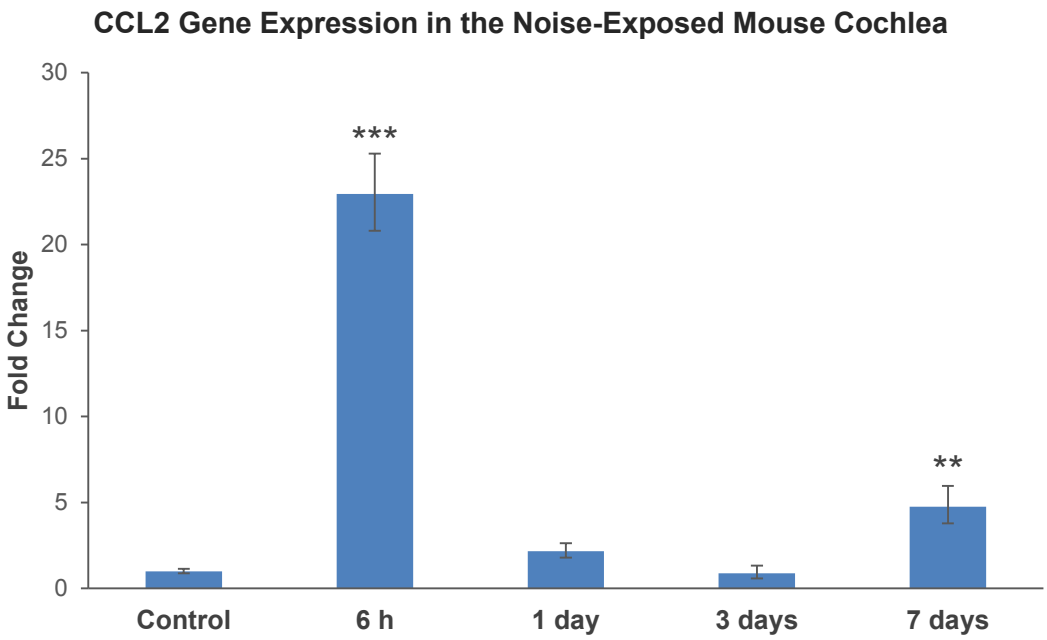

Figure 4.5: Quantitative real-time RT-PCR analysis of CCL2 gene expression in the C57BL/6 mouse cochlea following acute noise exposure. The graph illustrates the fold change in gene expression of CCL2 at 6 h, 1 day, 3 days and 7 days following acute exposure to traumatic noise (100 dB SPL, 8-16 kHz for 24 h) relative to non-noise exposed controls. Two peaks in CCL2 expression were observed; an early upregulation at 6 h (22.9-fold increase) and a later peak at 7 days post-exposure (4.7-fold increase). Data presented as mean ± SEM (n = 8 per group). **$p < 0.01$, ***$p < 0.001$; relative to the control group (one-way ANOVA followed by Tukey's post-hoc test).

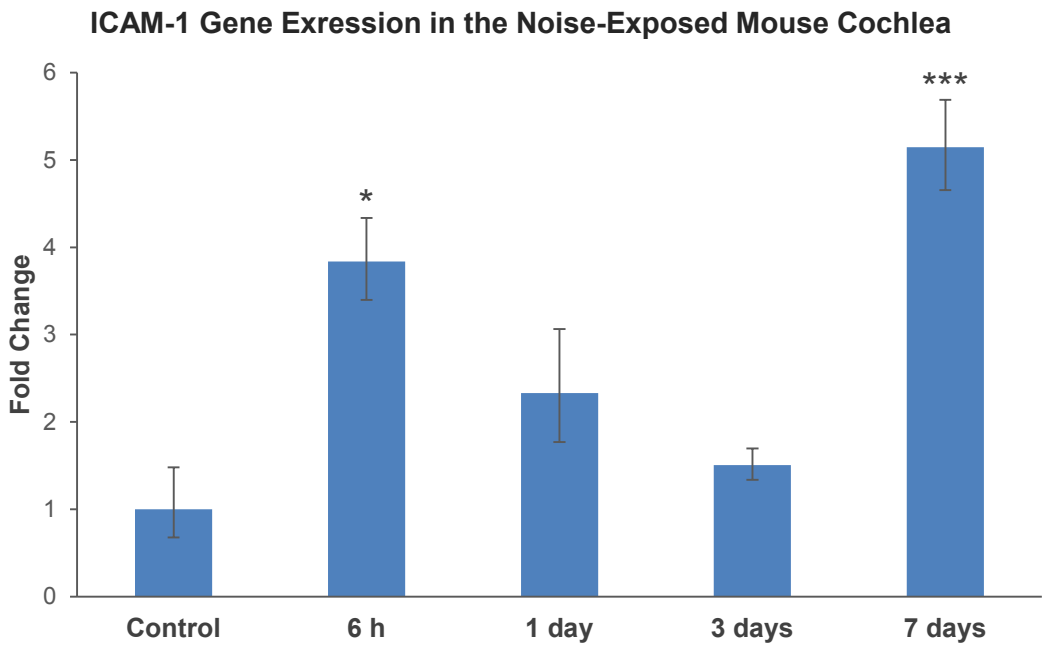

Figure 4.6: Quantitative real-time RT-PCR analysis of ICAM-1 gene expression in the C57BL/6 mouse cochlea following acute noise exposure. The graph illustrates the fold change in gene expression of ICAM-1 at 6 h, 1 day, 3 days and 7 days following acute exposure to traumatic noise (100 dB SPL, 8-16 kHz for 24 h) relative to non-noise exposed controls. Two peaks in ICAM-1 expression were observed; an early upregulation at 6 h (3.8-fold increase) and a later peak at 7 days post-exposure (5.1-fold increase). Data presented as mean ± SEM (n = 8 per group). *$p < 0.05$, ***$p < 0.001$; relative to the control group (one-way ANOVA followed by Tukey's post-hoc test).

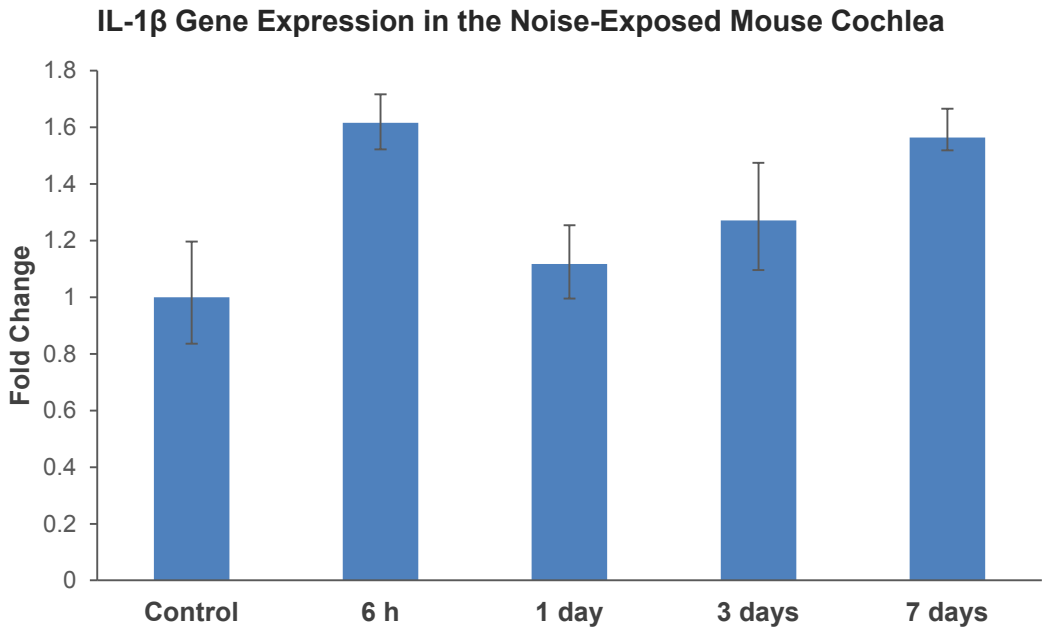

Figure 4.7: Quantitative real-time RT-PCR analysis of IL-1β gene expression in the C57BL/6 mouse cochlea following acute noise exposure. The graph illustrates the fold change in gene expression of IL-1β at 6 h, 1 day, 3 days and 7 days following acute exposure to traumatic noise (100 dB SPL, 8-16 kHz for 24 h) relative to non-noise exposed controls. Two peaks in IL-1β expression were observed; an early upregulation at 6 h (1.6-fold increase) and a later peak at 7 days post-exposure (1.6-fold increase), however these showed no statistically significant difference from the control group ($p > 0.05$, one-way ANOVA followed by Tukey's post-hoc test). Data presented as mean ± SEM (n = 8 per group).

4.2.3. NF-κB Activation in the Noise-Exposed Cochlea

The gene expression levels of these cytokines, chemokines and cell adhesion molecules are regulated by the nuclear transcription factor NF-κB. In this section of the study, the noise-induced cochlear activation of p65 and p50, the two main subunits of NF-κB, were examined. These NF-κB subunits normally exist together as heterodimers in the cytoplasm of quiescent cells, and when activated, translocate to the nucleus, where they bind to their target promoters, inducing the expression of numerous inflammatory mediators.

Immunofluorescence was carried out to localise the protein expression of NF-κB p65 and p50 in the normal and noise-exposed mouse cochlea ($n = 2$). In the non-exposed cochlea, p65 immunoreactivity was localised primarily in the spiral ligament, stria vascularis (marginal

cells), spiral limbus and organ of Corti (**Figure 4.8a** and **Figure 4.9a**), whereas p50 expression was observed in the spiral ligament and spiral ganglion (**Figure 4.10a**, **b**). As expected, the immunofluorescence in these cells was confined to the cytoplasm in the non-noise exposed cochlea, which indicates the latent form of NF-κB. No remarkable differences in the immunostaining pattern of p65 and p50 were found among the turns of the cochlea. However, it was surprising that p65 and p50 differ in their immunolocalisation in the cochlea (apart from the spiral ligament) because the two subunits are normally located together as heterodimers.

At 6 h following exposure to traumatic noise (100 dB SPL, 8-16 kHz for 24 h), the cytoplasmic immunofluorescence of p65 (**Figure 4.8b**, **d**) and p50 decreased substantially in intensity compared with the non-exposed cochlea. However, the expected nuclear translocation (i.e. the shift in immunostaining from the cytoplasm to the nucleus) of p65 and p50, indicating their activation, was not observed. It was suspected that NF-κB might have been activated earlier during the 24 h noise exposure, so the noise exposure was shortened to 2 h and NF-κB activation was tested immediately, 2 h or 6 h after exposure (n = 2 per time point). These experiments produced similar results to the initial findings (**Figure 4.9b**, **d** and **Figure 4.10c**, **d)**. Even after exposing mice to higher noise levels (110 dB SPL for 2 h), no nuclear staining of the NF-κB subunits was detected (data not shown) either immediately or 2 h after noise exposure (n = 2 per time point).

Immunoperoxidase staining was carried out before immunofluorescence staining was attempted. However, it was found that the p65 and p50 immunolabelling in the cochlea was best resolved with immunofluorescence. As a negative control while carrying out immunoperoxidase histochemistry, a peptide blocking experiment was performed in which the primary antibodies for p65 and p50 (the same antibodies used for immunofluorescence) were pre-absorbed with the corresponding immunising peptides. This abolished the immunostaining for both p65 (see **Appendix A1**: **Figure A.1**) and p50 (see **Appendix A2**: **Figure A.2**), confirming the specificity of the respective antibodies. In addition, negative controls using cochlear sections without the primary antibodies for p65 and p50 were also carried out (no primary antibody controls). As shown in the images below, sections were completely devoid of immunofluorescence staining in the absence of the p65 (**Figure 4.8e** and **Figure 4.9e**) and p50 (**Figure 4.10e**, **f**) antibodies.

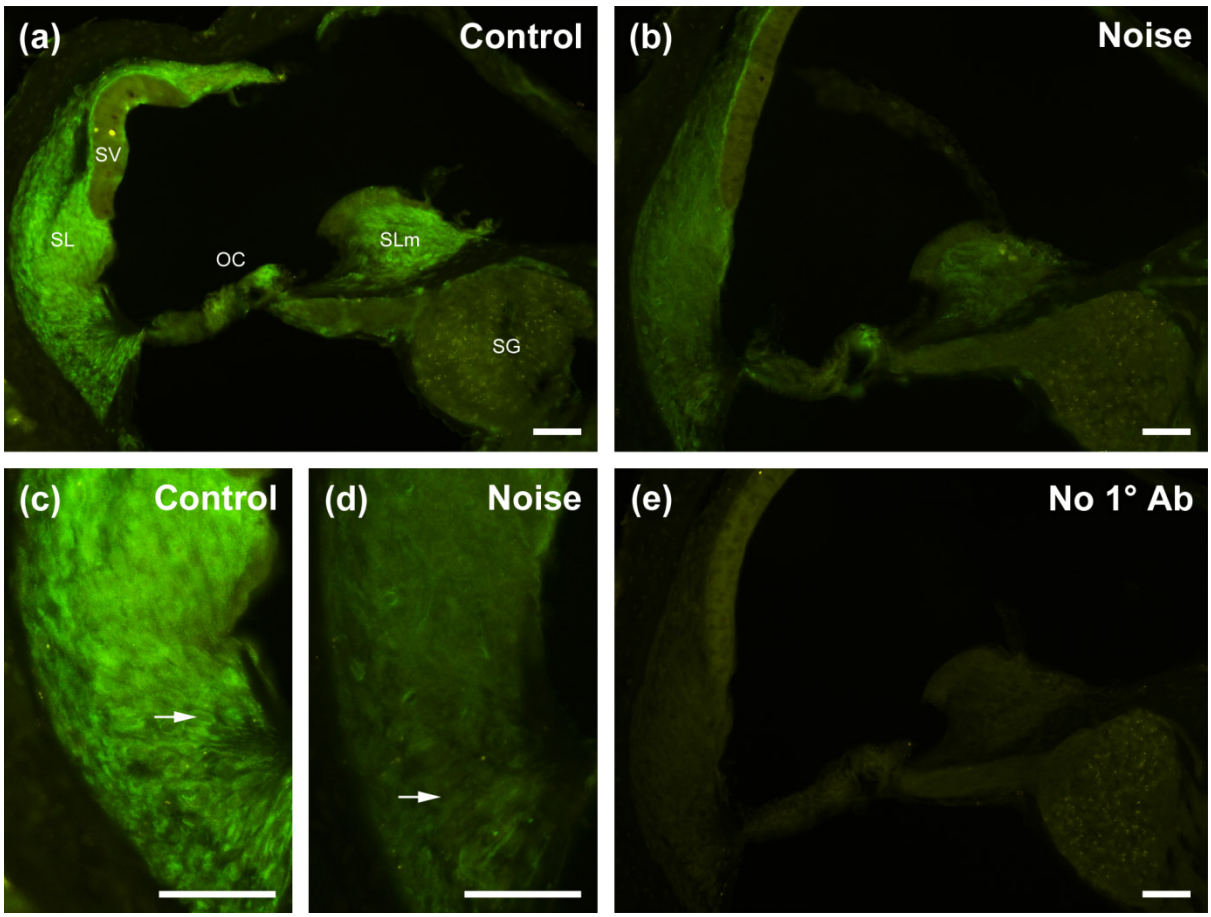

Figure 4.8: NF-κB p65 immunofluorescence in the C57BL/6 mouse cochlea before and 6 h after acute (24 h) noise exposure. (**a**) In the non-noise exposed cochlea, strong NF-κB p65 immunofluorescence was observed in the spiral ligament, marginal cells of the stria vascularis, organ of Corti and spiral limbus. Immunolabelling in these cell types was confined to the cytoplasm (**c**), indicative of the latent form of p65. (**b**) At 6 h following acute exposure to traumatic noise (100 dB SPL, 8-16 kHz for 24 h), cytoplasmic immunofluorescence intensity decreased substantially in all cochlear regions. Nuclear staining of p65 was not detected in either the non-exposed control (**c**) or noise-exposed (**d**) cochlea (arrows point to the clear nuclei of the cells). Image (c) and (d) are 40x magnifications of the spiral ligament in (a) and (b) respectively. (**e**) No immunostaining was detected when the primary antibody for p65 was omitted. *Abbreviations*: SL, spiral ligament; SV, stria vascularis; OC, organ of Corti; SLm, spiral limbus; SG, spiral ganglion. Scale bars = 50 µm.

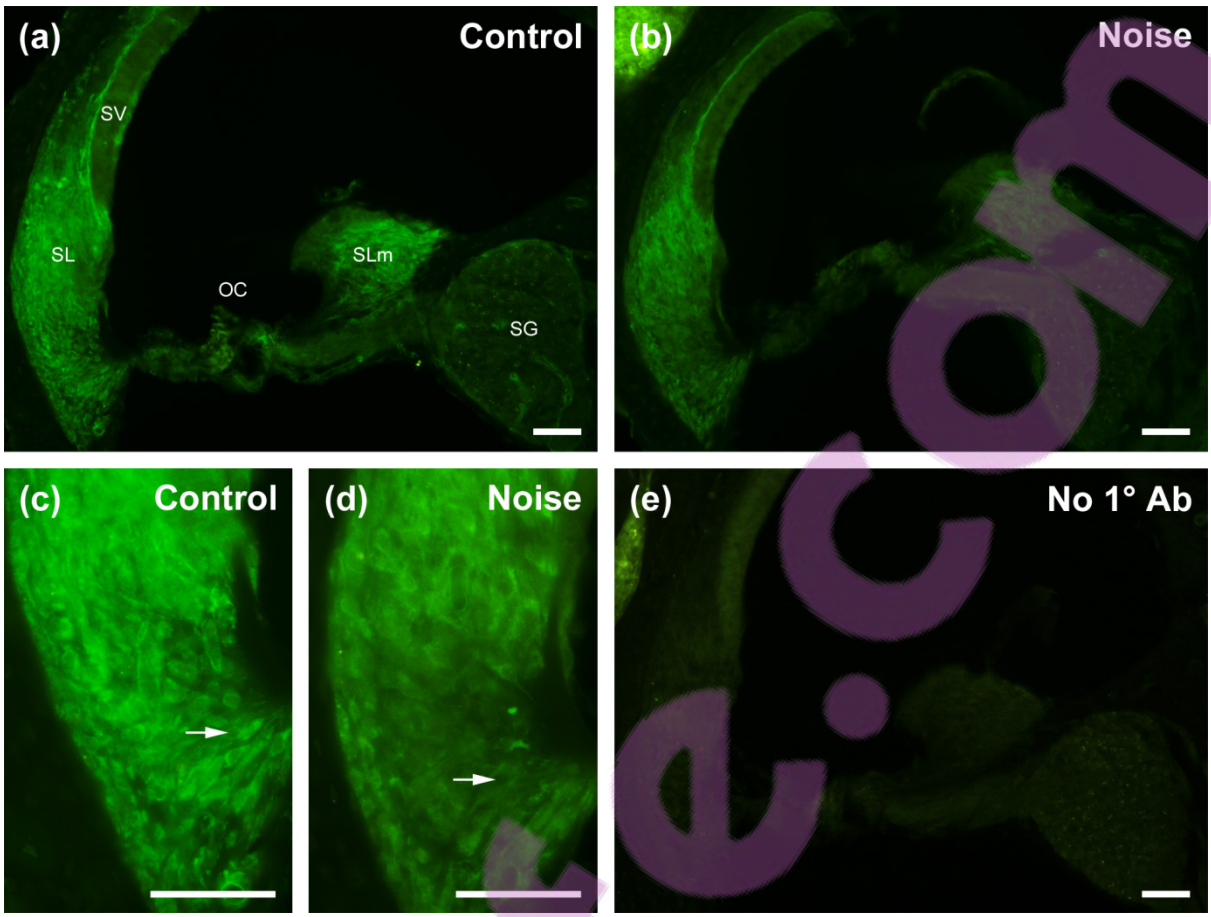

Figure 4.9: NF-κB p65 immunofluorescence in the C57BL/6 mouse cochlea before and 6 h after acute (2 h) noise exposure. (**a**) In the non-noise exposed cochlea, strong NF-κB p65 immunofluorescence was observed in the spiral ligament, marginal cells of the stria vascularis, organ of Corti and spiral limbus. Immunolabelling in these cell types was confined to the cytoplasm (**c**), indicative of the latent form of p65. (**b**) At 6 h following acute exposure to traumatic noise (100 dB SPL, 8-16 kHz for 2 h), cytoplasmic immunofluorescence intensity decreased in all cochlear regions. Nuclear staining of p65 was not detected in either the non-exposed control (**c**) or noise-exposed (**d**) cochlea (arrows point to the clear nuclei of the cells). Image (c) and (d) are 40x magnifications of the spiral ligament in (a) and (b) respectively. (**e**) No immunostaining was detected when the primary antibody for p65 was omitted. *Abbreviations*: SL, spiral ligament; SV, stria vascularis; OC, organ of Corti; SLm, spiral limbus; SG, spiral ganglion. Scale bars = 50 µm.

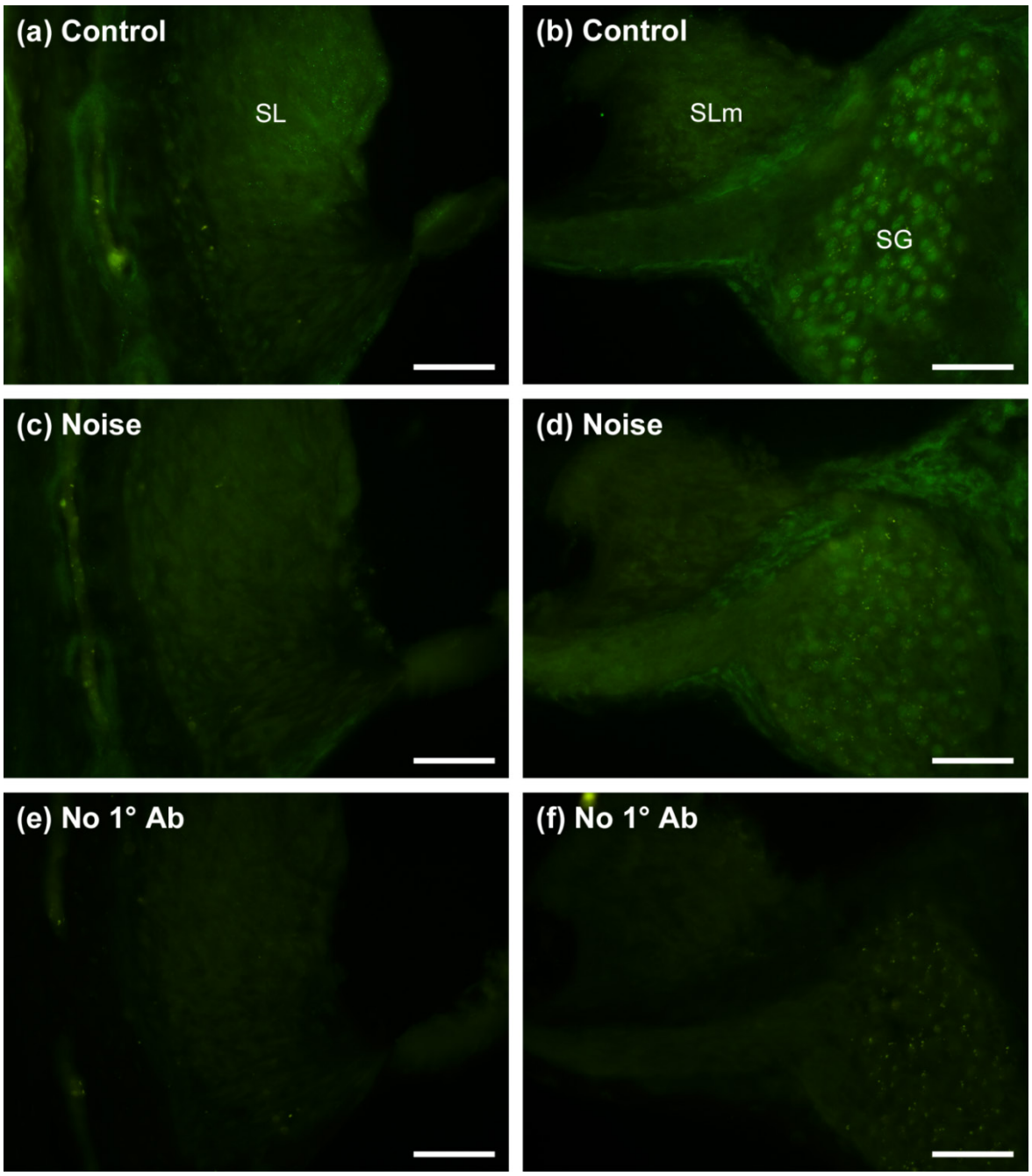

Figure 4.10: NF-κB p50 immunofluorescence in the C57BL/6 mouse cochlea at 6 h after acute (2 h) noise exposure. In the non-noise exposed cochlea, weak NF-κB p50 immunofluorescence was observed in the spiral ligament (**a**) and moderate immunofluorescence in the spiral ganglion (**b**). As with p65, immunolabelling was confined to the cytoplasm, indicative of the latent form of p50. At 6 h following acute exposure to traumatic noise (100 dB SPL, 8-16 kHz for 2 h), cytoplasmic immunofluorescence intensity decreased in both cochlear regions (**c**, **d**). Nuclear staining of p50 was not detected in either the non-exposed control or noise-exposed cochleae. No immunostaining was detected when the primary antibody for p50 was omitted (**e**, **f**). *Abbreviations*: SL, spiral ligament; SLm, spiral limbus; SG, spiral ganglion. Scale bars = 50 µm.

4.2.4. ICAM-1 Immunoexpression in the Noise-Exposed Cochlea

Using immunoperoxidase staining, the tissue expression and distribution of two key vascular cell adhesion molecules, ICAM-1 and PECAM-1, was characterised in the noise-exposed mouse cochlea. To assess the time-dependent changes in their protein expression following noise exposure, cochleae were harvested from mice at four different time intervals after noise exposure (6 h, 1 day, 3 days and 7 days) (n = 8 per time point).

ICAM-1 has a critical role in mediating the temporary immobilisation of leukocytes to the luminal surface of vascular endothelial cells in preparation for their extravasation. The overall distribution of ICAM-1 expression in the normal non-exposed mouse cochlea is shown in **Figure 4.11a**. ICAM-1 immunoreactivity was localised primarily in the inferior region of the spiral ligament, specifically in the type IV fibrocytes and vascular endothelial cells of blood vessels (see **Figure 4.12a** and **Figure 4.13a** for higher magnification images of ICAM-1 immunostaining in the basal and middle turn spiral ligament respectively). Other blood vessels in the spiral ligament, stria vascularis, spiral limbus, and spiral ganglion also showed ICAM-1 immunolabelling. In addition, the endothelium of collecting venules below the lateral wall (see **Figure 4.12e**) and endosteal cells lining the scala tympani were also labelled. Following acute exposure to traumatic noise, expression of ICAM-1 increased markedly, reaching maximum expression one day (24 h) after acoustic injury (**Figure 4.12c** and **Figure 4.13c**). The ICAM-1 immunopositive area in the spiral ligament became more intense and expanded to cover a considerably greater area of the inferior region. The immunoexpression of ICAM-1 therefore corroborates the gene expression data (**Figure 4.6**), with maximum protein expression occurring shortly following peak levels of gene expression (6 h post-exposure).

The immunohistochemical staining pattern of ICAM-1 was similar along the entire length of the cochlea. However, the immunostaining area in the spiral ligament of the basal turn of the cochlea (**Figure 4.12**) was considerably larger in size due to the lateral wall of the basal turn being much thicker in comparison to the other turns (**Figure 4.13**). In contrast to the basal and middle turn, relatively weaker ICAM-1 immunolabelling was observed in the spiral ligament of the apical turn. All non-exposed and noise-exposed cochleae examined showed a comparable distribution of ICAM-1 immunostaining.

Negative controls were included with each immunohistochemistry experiment in which the primary antibody for ICAM-1 was either omitted (no primary antibody control) or replaced with the corresponding IgG isotype control. As shown in the images below, cochlear sections were completely devoid of immunostaining in the absence of the ICAM-1 primary antibody (**Figure 4.11b**) or when incubated with hamster IgG1, κ chain (**Figure 4.11c**), confirming the specificity of antibody binding. The small dark coloured spots present in the stria vascularis are melanin pigment granules located in the intermediate cells.

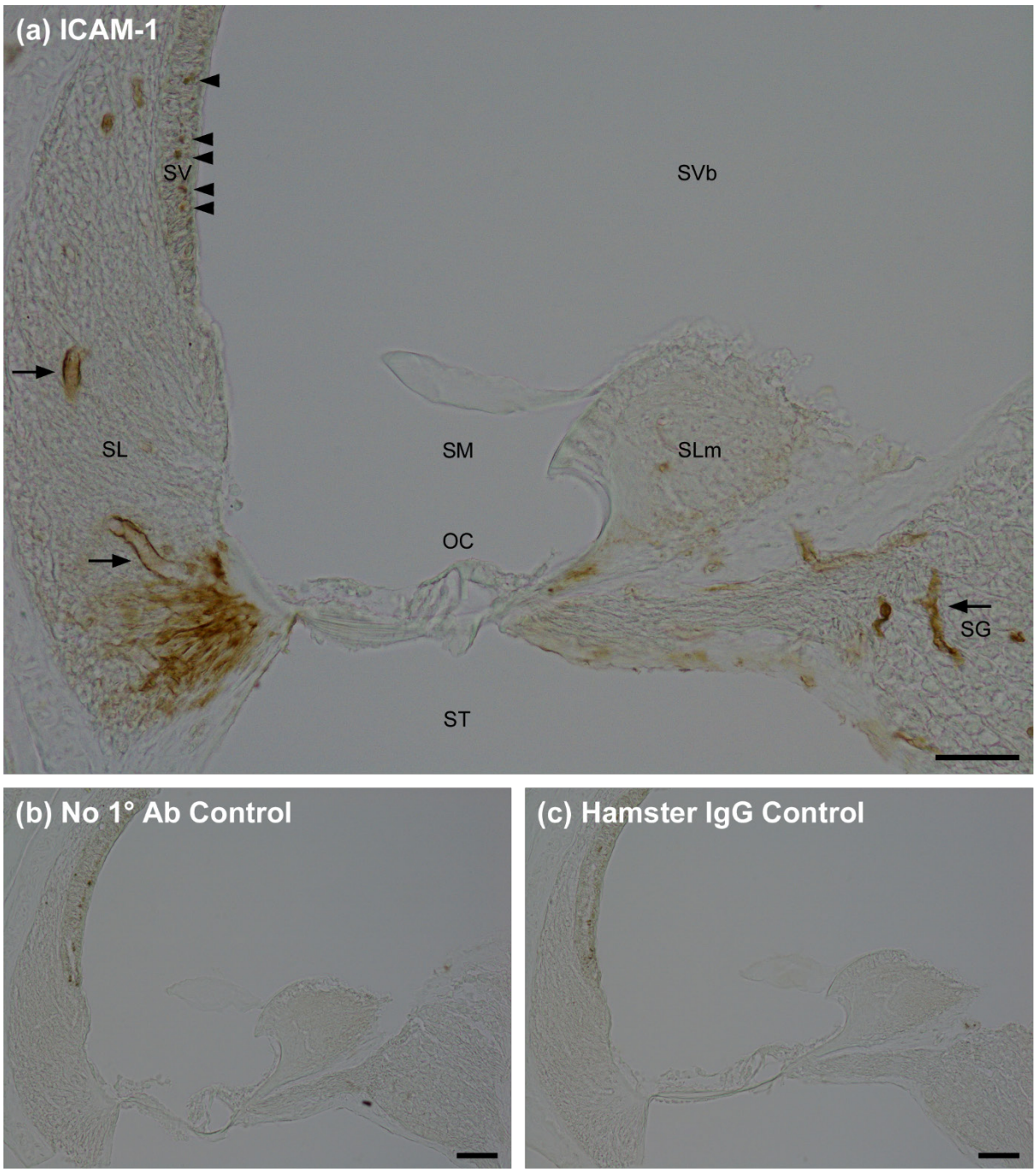

Figure 4.11: Distribution of ICAM-1 in the non-noise exposed C57BL/6 mouse cochlea. ICAM-1 in the cochlea exposed to ambient noise was localised predominantly in the inferior region of the spiral ligament among type IV fibrocytes and vascular endothelial cells (arrow) (**a**). ICAM-1 immunolabelling was also observed in blood vessels elsewhere in the spiral ligament (arrow) as well as in the spiral limbus and spiral ganglion (arrow). In addition, endosteal cells lining the scala tympani and the endothelium of collecting venules below the lateral wall (not seen here) were labelled. No immunostaining was detected when the primary antibody for ICAM-1 was either omitted (**b**) or replaced with the corresponding IgG isotype control (hamster IgG1, κ chain) (**c**). The small dark coloured spots present in the stria

vascularis (arrowheads) are melanin pigment granules in the intermediate cells. *Abbreviations*: SL, spiral ligament; SV, stria vascularis; OC, organ of Corti; SLm, spiral limbus; SG, spiral ganglion; SM, scala media; ST, scala tympani; SVb, scala vestibuli. Scale bars = 50 µm.

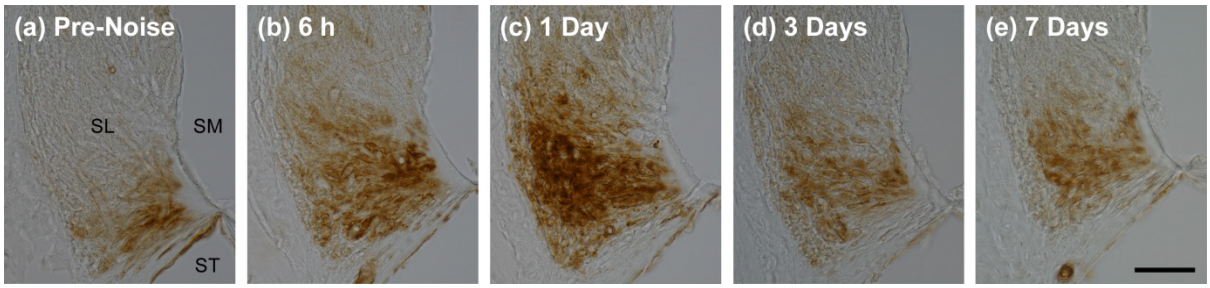

Figure 4.12: Time course of ICAM-1 expression in the basal turn spiral ligament of the C57BL/6 mouse cochlea following acute noise exposure. Above are photomicrographs of ICAM-1 immunostaining in the inferior region of the spiral ligament of the cochlear basal turn before (**a**) and 6 h (**b**), 1 day (**c**), 3 days (**d**) and 7 days (**e**) following acute exposure to traumatic noise (100 dB SPL, 8-16 kHz for 24 h). In the normal non-noise exposed cochlea, relatively weak ICAM-1 immunostaining was detected in the inferior region of the spiral ligament among type IV fibrocytes and vascular endothelial cells (**a**). Following noise exposure, ICAM-1 immunoexpression increased, peaking one day post-exposure (**c**). The immunostaining became more intense and expanded to cover a much greater area of the inferior region of the spiral ligament. Thereafter, ICAM-1 immunoexpression decreased in intensity and size. *Abbreviations*: SL, spiral ligament; SM, scala media; ST, scala tympani. Scale bar = 50 µm (applies to a-e).

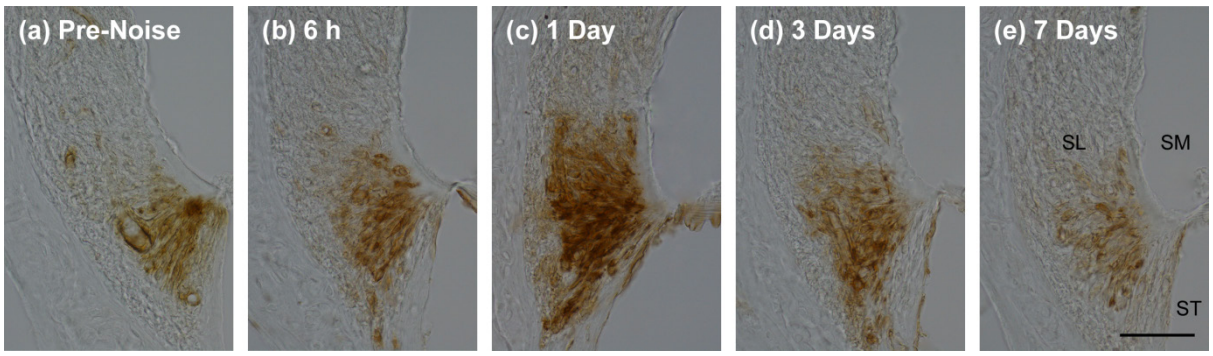

Figure 4.13: Time course of ICAM-1 expression in the middle turn spiral ligament of the C57BL/6 mouse cochlea following acute noise exposure. Above are photomicrographs of ICAM-1 immunostaining in the inferior region of the spiral ligament of the cochlear middle turn before (**a**) and 6 h (**b**), 1 day (**c**), 3 days (**d**) and 7 days (**e**) following acute exposure to traumatic noise (100 dB SPL, 8-16 kHz for 24 h). In the non-noise exposed cochlea, relatively weak ICAM-1 immunostaining was detected in the inferior region of the spiral ligament among type IV fibrocytes and vascular endothelial cells (**a**). Following noise exposure, ICAM-1 immunoexpression increased, peaking one day post-exposure (**c**). The immunostaining became more intense and expanded to cover a much greater area of the inferior region of the spiral ligament. Thereafter, ICAM-1 immunoexpression decreased in intensity and size. *Abbreviations*: SL, spiral ligament; SM, scala media; ST, scala tympani. Scale bar = 50 µm (applies to a-e).

To provide a more accurate assessment of the protein expression level of ICAM-1 in the spiral ligament of the noise-exposed cochlea, semi-quantitative image analysis was carried out. The immunoperoxidase staining in the inferior region of the spiral ligament in the upper basal and middle cochlear turn were selected as the regions of interest (ROI) as these were consistently stained areas of the cochlea with strong ICAM-1 immunolabelling. For each cochlea, three to five mid-modiolar sections were quantitatively analysed, and for each noise exposure group, one cochlea was examined from five different mice (n = 5). The mean gray values (pixel intensities) and areas (in calibrated units of μm^2) of the ICAM-1 immunostaining in both cochlear turns were averaged per experimental group (**Table 4.1** and **Table 4.2**) and relative ratios (compared to non-exposed controls) were calculated and plotted (**Figure 4.14** and **Figure 4.15**).

Image analysis revealed that the change in the intensity and area of ICAM-1 immunostaining in both the cochlear basal and middle turn after noise exposure followed a similar pattern. As shown in **Figure 4.14a** and **Figure 4.15a**, the intensity of ICAM-1 immunolabelling with

noise exposure increased to a maximum at one day (24 h) after noise exposure and thereafter returned to the level seen in the non-exposed cochlea. The average staining intensity in the basal and middle turn one day post-exposure was significantly 15% (82.4 ± 1.9 versus 94.8 ± 1.2) and 24% (75.4 ± 2.7 versus 93.7 ± 1.8) higher than in the non-exposed cochlea respectively ($p < 0.001$, one-way ANOVA).

The average area of the ICAM-1 immunolabelling in the spiral ligament also increased to a maximum one day post-exposure (**Figure 4.14b** and **Figure 4.15b**). In the basal turn, the immunolabelled area one day post-exposure (11,599 ± 704 μm^2) was double that of the non-exposed cochlea (5800 ± 289 μm^2) ($p < 0.001$, one-way ANOVA), whereas in the middle turn, the area was significantly ($p < 0.001$, one-way ANOVA) 1.5 times larger (6113 ± 454 μm^2 versus 4077 ± 244 μm^2). Thereafter, the area of immunolabelling declined in size in both cochlear turns, but still remained significantly larger than in the non-exposed cochlea ($p < 0.001$, one-way ANOVA) apart from the immunolabelling in the middle turn at seven days post-exposure. The area of immunolabelling was similar at 6 h, 1 day and 3 days for both turns ($p > 0.05$, one-way ANOVA).

Table 4.1: Average intensity (mean gray value) and area of ICAM-1 immunostaining in the spiral ligament of the cochlear basal turn before and after acute noise exposure. Data presented as mean ± SEM ($n = 5$ per group). Note that the lower the mean gray value, the higher the pixel intensity.

Group	Average Mean Gray Value	Average Area (μm^2)
Control	94.8 ± 1.2	5,800 ± 289
6 h	92.3 ± 3.0	10,144 ± 604
1 day	82.4 ± 1.9	11,599 ± 704
3 days	95.3 ± 2.1	10,404 ± 612
7 days	98.2 ± 2.3	8,141.48 ± 263

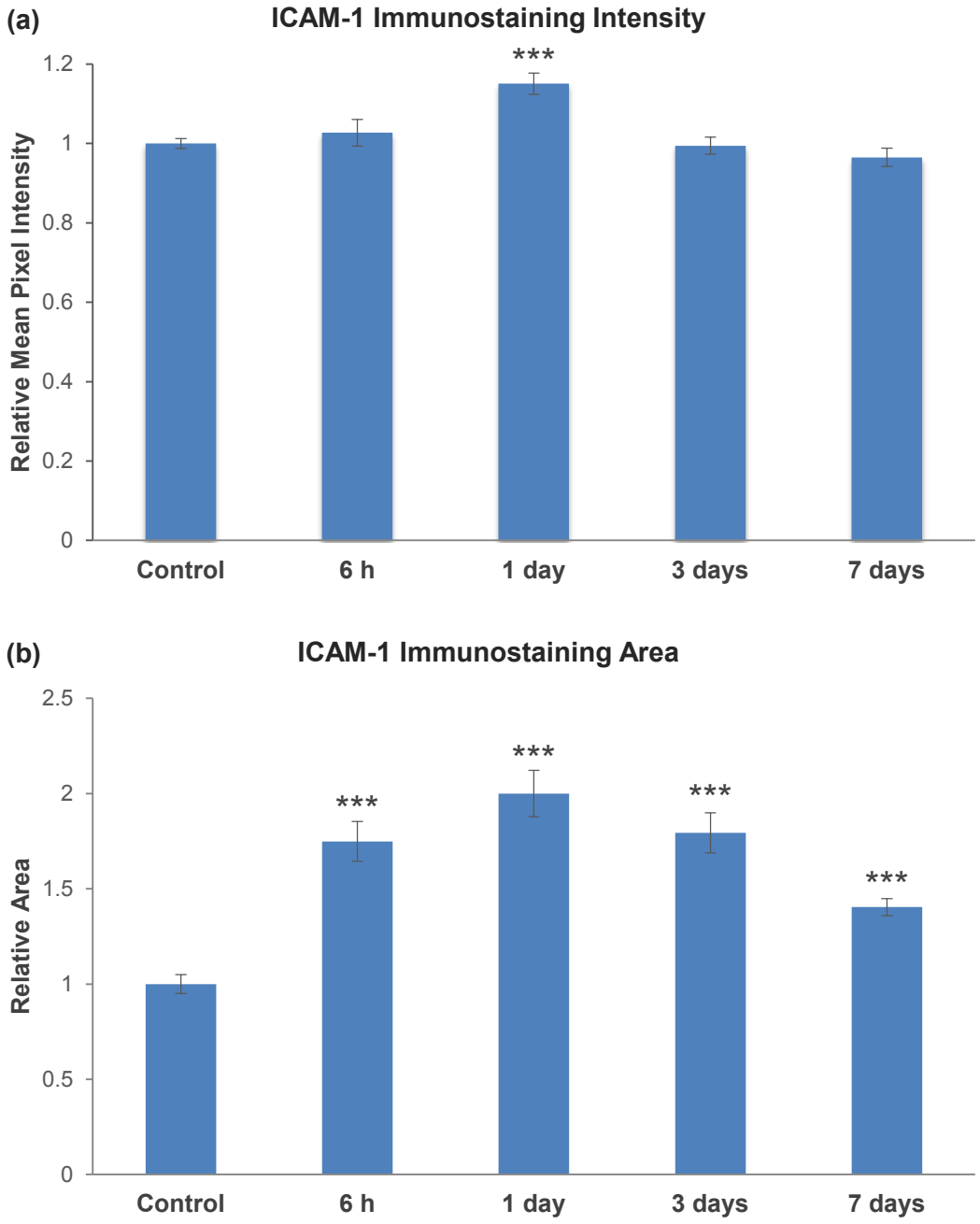

Figure 4.14: Semi-quantitative analysis of ICAM-1 immunostaining in the basal turn spiral ligament of the C57BL/6 mouse cochlea following acute noise exposure. The graphs illustrate the ratio of the intensity (**a**) and area (**b**) of ICAM-1 immunostaining in the inferior region of the spiral ligament in the cochlear basal turn at 6 h, 1 day, 3 days and 7 days following acute exposure to traumatic noise (100 dB SPL, 8-16 kHz for 24 h) relative to non-noise exposed controls. Both ICAM-1 immunostaining intensity and area increased to a maximum one day post-exposure by 15% and 200% respectively relative to non-exposed controls. Data presented as mean ± SEM (n = 5 per group). ***$p < 0.001$, relative to the control group (one-way ANOVA followed by Tukey's post-hoc test).

Table 4.2: Average intensity (mean gray value) and area of ICAM-1 immunostaining in the spiral ligament of the cochlear middle turn before and after acute noise exposure. Data presented as mean ± SEM (n = 5 per group).

Group	Average Mean Gray Value	Average Area (µm^2)
Control	93.7 ± 1.8	4,077 ± 244
6 h	89.3 ± 4.4	4,916 ± 531
1 day	75.4 ± 2.7	6,113 ± 454
3 days	89.9 ± 2.5	5,872 ± 204
7 days	102.4 ± 2.0	4,592 ± 276

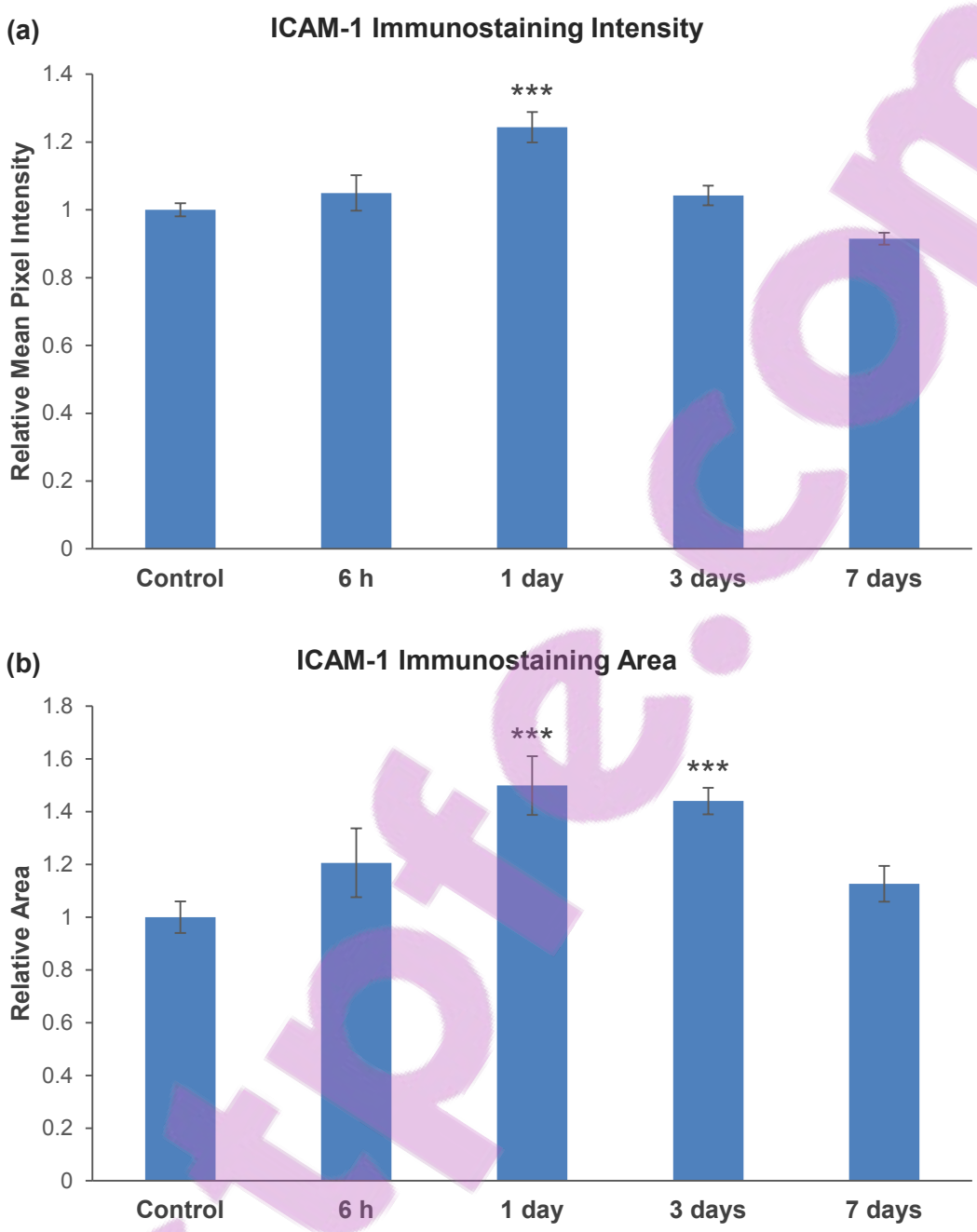

Figure 4.15: Semi-quantitative analysis of ICAM-1 immunostaining in the middle turn spiral ligament of the C57BL/6 mouse cochlea following acute noise exposure. The graphs illustrate the ratio of the intensity (**a**) and area (**b**) of ICAM-1 immunostaining in the spiral ligament of the cochlear middle turn at 6 h, 1 day, 3 days and 7 days following acute exposure to traumatic noise (100 dB SPL, 8-16 kHz for 24 h) relative to non-noise exposed controls. Both ICAM-1 immunostaining intensity and area increased to a maximum one day post-exposure by 24% and 150% respectively relative to non-exposed controls. Data presented as mean ± SEM (n = 5 per group). ***$p < 0.001$, relative to the control group (one-way ANOVA followed by Tukey's post-hoc test).

4.2.5. PECAM-1 Immunoexpression in the Noise-Exposed Cochlea

PECAM-1, a cell adhesion molecule expressed at the intercellular junctions of vascular endothelial cells, has an important role in mediating the transendothelial migration of leukocytes during an inflammatory response. Immunoperoxidase histochemistry revealed a widespread distribution of PECAM-1 in the mouse cochlea. Expression was confined to the vascular endothelial cells in the spiral ligament, stria vascularis, spiral limbus, and spiral ganglion (**Figure 4.16a**). This expression pattern is therefore similar to that of ICAM-1, however the PECAM-1 expression in the strial capillaries was more intense and more blood vessels throughout the spiral ligament showed positive PECAM-1 immunostaining. In contrast to ICAM-1, no PECAM-1 immunoreactivity was observed in the type IV fibrocytes in the inferior region of the spiral ligament. Following acute exposure to traumatic noise, the immunostaining of the cochlear blood vessels became more intense, peaking one to three days post-exposure (**Figure 4.16c, d)** and returning to basal level of expression by seven days (**Figure 4.16e**). No qualitative differences in PECAM-1 immunostaining were noted along the entire length of the cochlea. Aside from non-specific staining of the bony capsule, PECAM-1 immunostaining was absent when the primary antibody for PECAM-1 was either omitted (**Figure 4.16f**) or replaced with the corresponding IgG isotype control (rat IgG2a, κ chain) (**Figure 4.16g**). Because only the cochlear vasculature was immunolabelled, changes in the intensity of the immunoperoxidase staining following noise exposure were not assessed quantitatively.

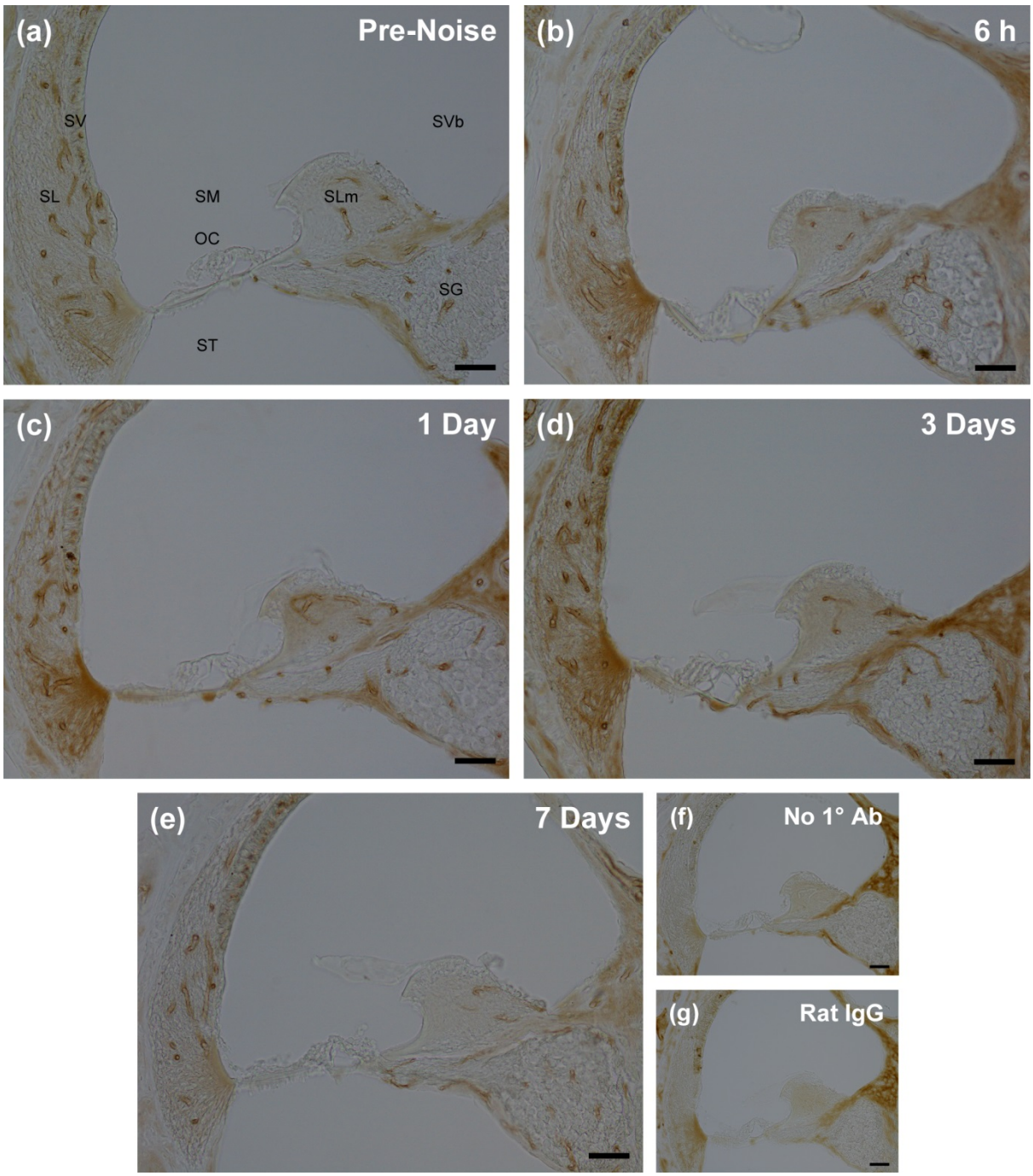

Figure 4.16: Time course of PECAM-1 expression in the C57BL/6 mouse cochlea following acute noise exposure. Above are photomicrographs of PECAM-1 immunostaining in the cochlea before (**a**) and 6 h (**b**), 1 day (**c**), 3 days (**d**) and 7 days (**e**) following acute exposure to traumatic noise (100 dB SPL, 8-16 kHz for 24 h). PECAM-1 immunostaining was detected in the blood vessels of the spiral ligament, stria vascularis, spiral limbus, and spiral ganglion (**a**). Following noise exposure, PECAM-1 immunostaining became stronger, peaking one (**c**) to three days (**d**) post-exposure, and returning to the basal level by seven days (**e**). No immunostaining was detected in blood vessels when the primary antibody for PECAM-1 was either omitted (**f**) or replaced with the corresponding IgG isotype control (rat

IgG2a, κ chain) (**g**). However, non-specific staining was observed in the bony capsule of the cochlea. *Abbreviations*: SL, spiral ligament; SV, stria vascularis; OC, organ of Corti; SLm, spiral limbus; SG, spiral ganglion; SM, scala media; ST, scala tympani; SVb, scala vestibuli. Scale bars = 50 µm.

In addition to ICAM-1 and PECAM-1, the expression of P-selectin, another important cell adhesion molecule involved in the extravasation of inflammatory cells, was also examined immunohistochemically. Unfortunately, the P-selectin antibody (Santa Cruz Biotechnology, Inc., Santa Cruz, CA, U.S.A.) that was used in this study produced non-specific immunolabelling in cochlear sections.

4.2.6. Proinflammatory Cytokine and F4/80 Immunoexpression in the Noise-Exposed Cochlea

The tissue distribution of key proinflammatory cytokines (TNF-α, IL-6 and IL-1β) and the presence of F4/80-positive inflammatory cells (macrophages and monocytes) in the noise-exposed cochlea was also examined using immunoperoxidase histochemistry. However, antibodies to these inflammatory markers either produced non-specific staining or no staining in both non-exposed control and noise-exposed cochleae (data not shown).

In summary, this study has demonstrated a substantial inflammatory response induced in the mouse cochlea following acute noise exposure. This involved an early (6 h post-exposure) upregulation in the gene expression levels of the proinflammatory cytokines TNF-α and IL-1β, the chemokine CCL2, and the cell adhesion molecule ICAM-1, followed by a subsequent peak in gene expression at 7 days post-exposure. Accompanying this upregulation of inflammatory mediators was an increased immunoexpression of the cell adhesion molecules, ICAM-1 and PECAM-1. ICAM-1 immunostaining in the inferior region of the spiral ligament among vascular endothelial cells and type IV fibrocytes increased in intensity and area, peaking 24 h post-exposure, while PECAM-1 immunostaining in the cochlear blood vessels became more intense, peaking 1-3 days post-exposure.

4.3. STUDY 2: Cochlear Inflammatory Response Associated with Chronic Noise Exposure

Previous research on noise-induced cochlear inflammation has used acute exposures such as that in Study 1. There has not been any focus on the possible inflammatory response in animals with chronic, low-level exposures that cause limited permanent threshold shift and probably relate more to the type of environmental noise exposure in the workplace. The possibility that chronic environmental noise exposure which leads to slowly developing permanent hearing loss in humans is related to the development of an inflammatory response has not been explored. This study thus investigated the cochlear inflammatory response induced by chronic exposure to moderate level noise. Mice were exposed to moderate noise (90 dB SPL, 8-16 kHz) on a daily basis (2 h per day) over an extended length of time (one to four weeks). This sound level is known to produce a temporary threshold shift in mice, but was not confirmed with ABR measurements in the present study. Similar to the initial study examining the cochlear inflammatory response following acute noise exposure, quantitative real-time RT-PCR and immunohistochemistry were carried out to analyse the gene expression levels of key inflammatory markers (TNF-α, CCL2, ICAM-1 and IL-1β) and the protein expression and distribution of cell adhesion molecules (ICAM-1 and PECAM-1) respectively.

4.3.1. Gene Expression Levels of TNF-α, CCL2, ICAM-1 and IL-1β in the Noise-Exposed Cochlea

Similar to the acute noise exposure study (**Section 4.2.2**), markedly elevated transcript levels of TNF-α, CCL2, ICAM-1 and IL-1β were detected by quantitative real-time RT-PCR in the cochleae of mice exposed chronically to moderate noise (n = 8 per group). The data showed that all four inflammatory genes displayed a similar pattern of expression following chronic noise exposure (**Figure 4.17** to **Figure 4.20**). Increased mRNA expression of these inflammatory mediators relative to non-noise exposed controls was first observed after one week of noise exposure and reached a maximum after two weeks of exposure. The respective fold changes in gene expression of TNF-α, CCL2, ICAM-1 and IL-1β after exposure for two weeks were 2.2, 3.6, 2.1 and 1.9, with all changes determined to be statistically significant ($p < 0.001$ for TNF-α, CCL2 and ICAM-1, $p < 0.05$ for IL-1β; one-way ANOVA). CCL2

again showed the largest upregulation relative to controls. There were no statistically significant differences in the fold changes between the one week and two week exposure groups ($p > 0.05$, one-way ANOVA). Transcript levels of the four genes returned to basal pre-noise levels after the second week post-exposure.

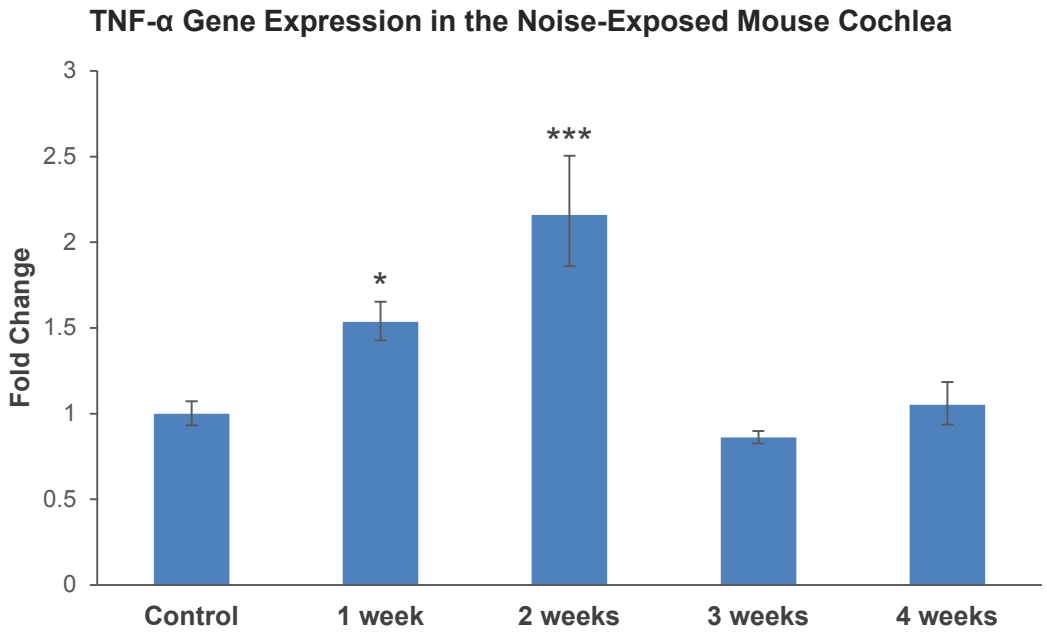

Figure 4.17: Quantitative real-time RT-PCR analysis of TNF-α gene expression in the C57BL/6 mouse cochlea following chronic noise exposure. The graph illustrates the fold change in gene expression of TNF-α following one, two, three and four weeks of exposure to moderate noise (90 dB SPL, 8-16 kHz, 2 h/day) relative to non-noise exposed controls. Peak expression of TNF-α was observed after two weeks of noise exposure (2.2-fold increase). Data presented as mean ± SEM ($n = 8$ per group). *$p < 0.05$, ***$p < 0.001$; relative to the control group (one-way ANOVA followed by Tukey's post-hoc test).

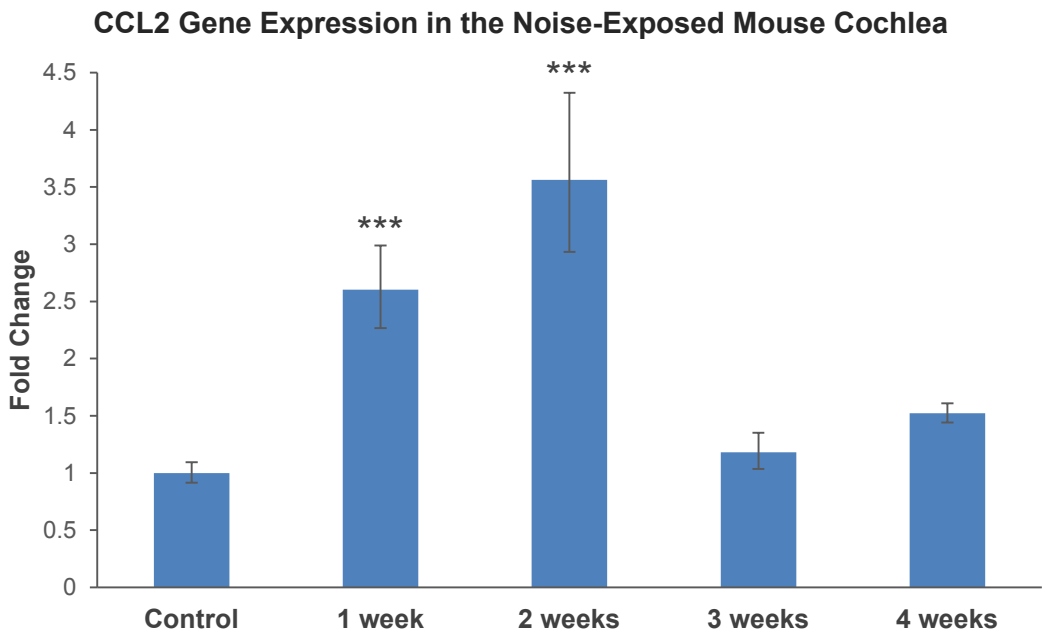

Figure 4.18: Quantitative real-time RT-PCR analysis of CCL2 gene expression in the C57BL/6 mouse cochlea following chronic noise exposure. The graph illustrates the fold change in gene expression of CCL2 following one, two, three and four weeks of exposure to moderate noise (90 dB SPL, 8-16 kHz, 2 h/day) relative to non-noise exposed controls. Peak expression of CCL2 was observed after two weeks of noise exposure (3.6-fold increase). Data presented as mean ± SEM (n = 8 per group). ***$p < 0.001$; relative to the control group (one-way ANOVA followed by Tukey's post-hoc test).

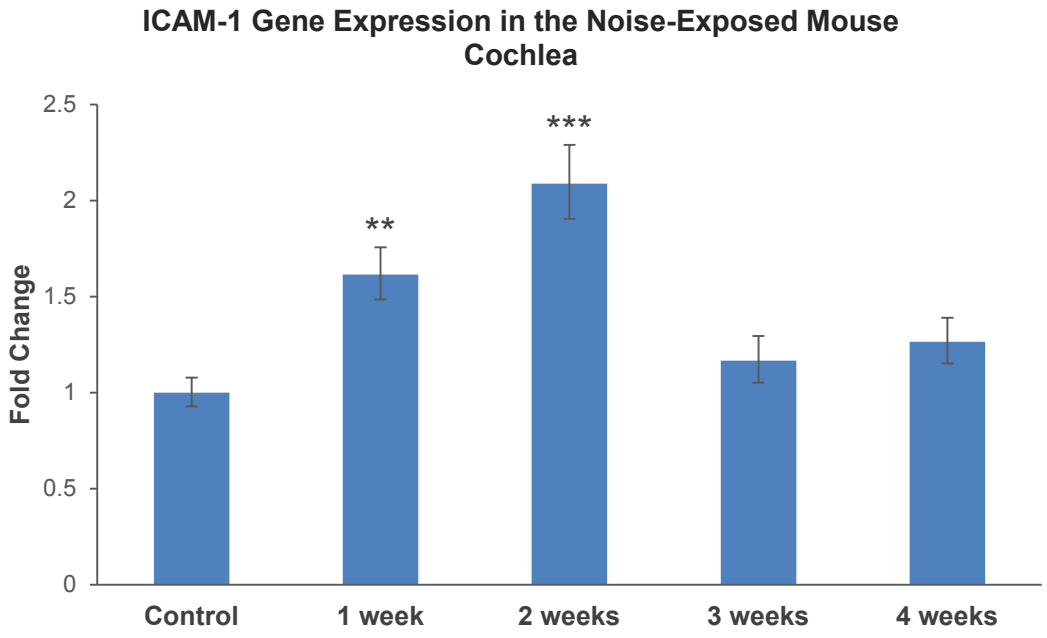

Figure 4.19: Quantitative real-time RT-PCR analysis of ICAM-1 gene expression in the C57BL/6 mouse cochlea following chronic noise exposure. The graph illustrates the fold change in gene expression of ICAM-1 following one, two, three and four weeks of exposure to moderate noise (90 dB SPL, 8-16 kHz, 2 h/day) relative to non-noise exposed controls. Peak expression of ICAM-1 was observed after two weeks of noise exposure (2.1-fold increase). Data presented as mean ± SEM (n = 8 per group). $^{**}p < 0.01$, $^{***}p < 0.001$; relative to the control group (one-way ANOVA followed by Tukey's post-hoc test).

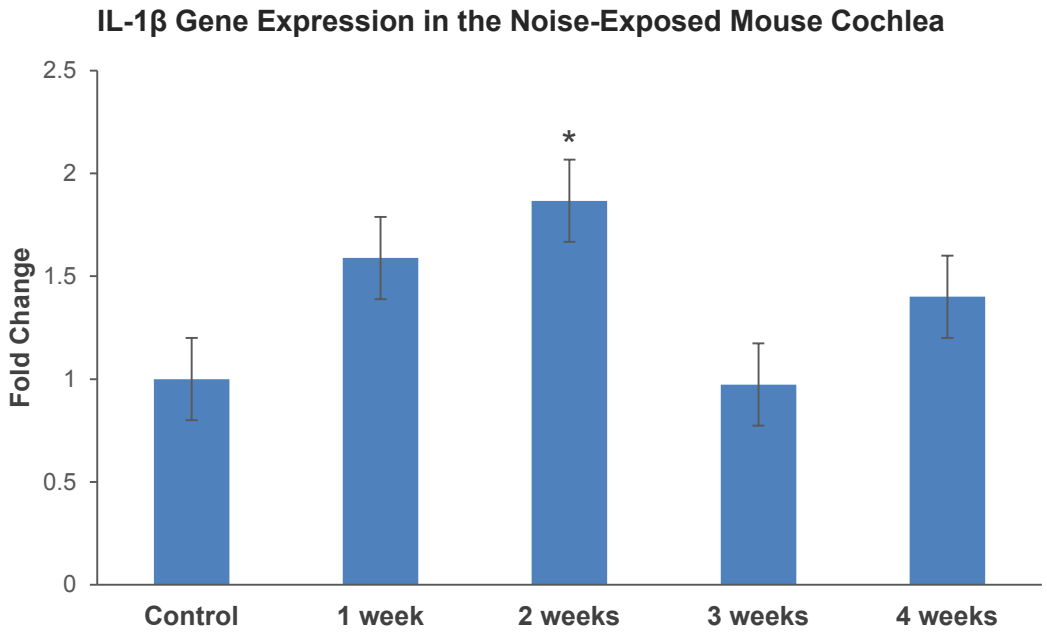

Figure 4.20: Quantitative real-time RT-PCR analysis of IL-1β gene expression in the C57BL/6 mouse cochlea following chronic noise exposure. The graph illustrates the fold change in gene expression of IL-1β following one, two, three and four weeks of exposure to moderate noise (90 dB SPL, 8-16 kHz, 2 h/day) relative to non-noise exposed controls. Peak expression of IL-1β was observed after two weeks of noise exposure (1.9-fold increase). Data presented as mean ± SEM (n = 8 per group). *$p < 0.05$; relative to the control group (one-way ANOVA followed by Tukey's post-hoc test).

4.3.2. ICAM-1 Immunoexpression in the Noise-Exposed Cochlea

Figure 4.21a shows the distribution of ICAM-1 immunolabelling in the cochlea following chronic noise exposure, which is similar to that observed following acute noise exposure. Prominent immunolabelling was observed within the inferior region of the spiral ligament in addition to positive immunostaining of blood vessels throughout the cochlea, including the collecting venules. The intensity and area of the ICAM-1 immunostaining in the spiral ligament of both the upper basal and middle cochlear turn was semi-quantitatively analysed using ImageJ to assess the protein expression level of ICAM-1. The average measured mean gray value and area of ICAM-1 immunostaining for each noise exposure group (n = 5 per group) is shown in **Table 4.3** (basal turn) and **Table 4.4** (middle turn).

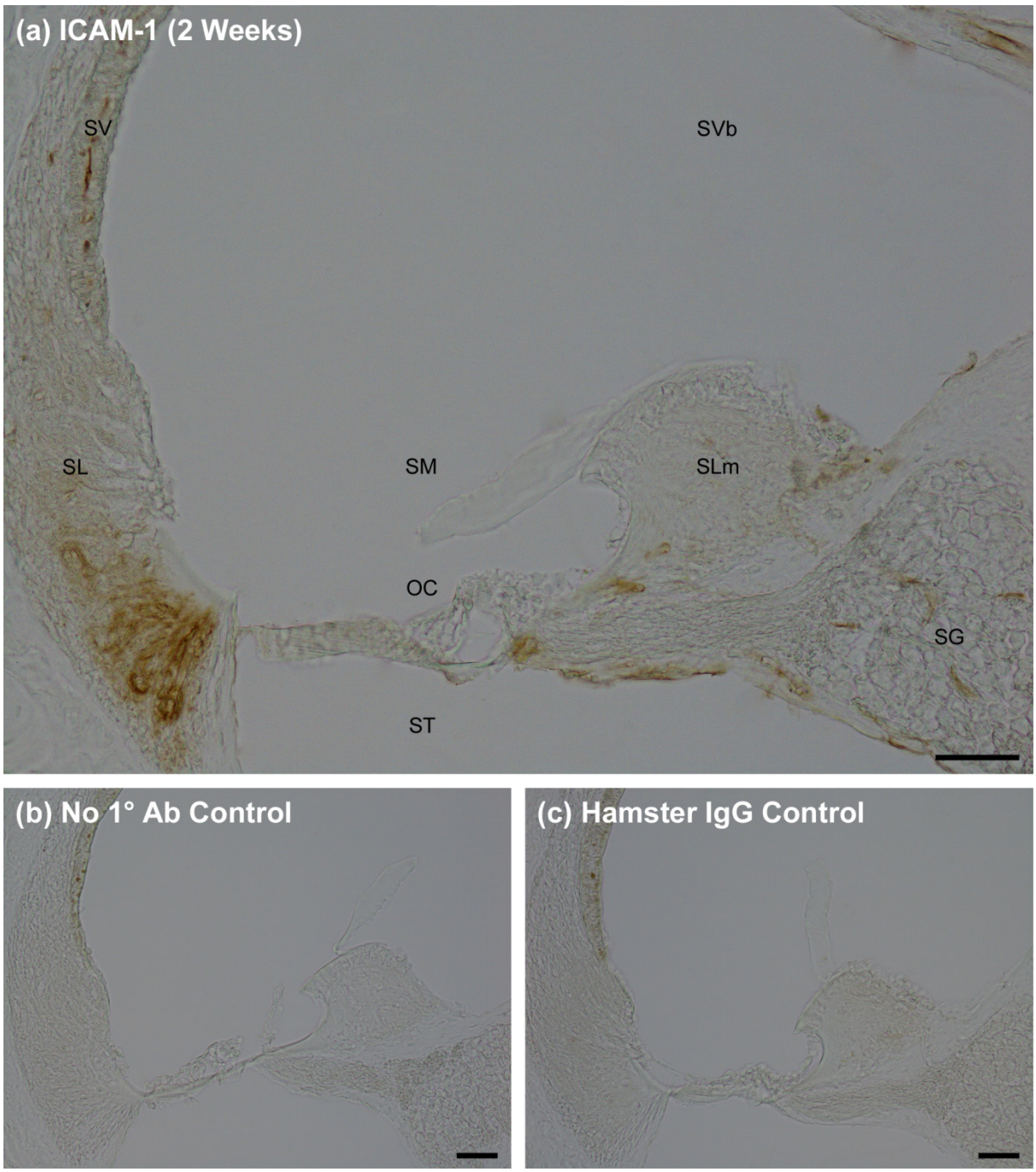

Figure 4.21: Distribution of ICAM-1 in the C57BL/6 mouse cochlea following chronic noise exposure. The distribution of ICAM-1 in the cochlea following chronic noise exposure (90 dB SPL, 8-16 kHz, 2 h/day for 2 weeks) was similar to that observed following acute noise exposure. Prominent immunolabelling was observed within the inferior region of the spiral ligament and in blood vessels throughout the cochlea. No immunostaining was detected when the primary antibody for ICAM-1 was either omitted (**b**) or replaced with the corresponding IgG isotype control (hamster IgG1, κ chain) (**c**). *Abbreviations*: SL, spiral ligament; SV, stria vascularis; OC, organ of Corti; SLm, spiral limbus; SG, spiral ganglion; SM, scala media; ST, scala tympani; SVb, scala vestibuli. Scale bars = 50 µm.

Maximum intensity of ICAM-1 immunostaining in the basal turn spiral ligament occurred after one week of exposure to moderate noise (**Figure 4.22b** and **Figure 4.23a**). The average mean gray value decreased significantly ($p < 0.001$, one-way ANOVA) from 94.8 ± 1.2 in non-exposed controls to 79.4 ± 1.7 after one week of noise exposure, representing a 20% increase in staining intensity, slightly higher than the peak intensity seen following acute noise exposure (15% increase). Thenceforth, ICAM-1 immunostaining intensity decreased to levels comparable with the non-exposed control cochlea. The area of ICAM-1 immunostaining in the basal turn doubled in size after exposure for one week (**Figure 4.22b** and **Figure 4.23b**), from 5,800 ± 289 μm^2 to 11,574 ± 558 μm^2 ($p < 0.001$, one-way ANOVA), almost the same size observed 24 h after acute noise exposure (11,599 μm^2). The ROI remained a similar size after two (11,964 ± 843 μm^2) and three weeks (10,238 ± 421 μm^2) ($p > 0.05$, one-way ANOVA). However, after four weeks, the ROI returned to the pre-noise size.

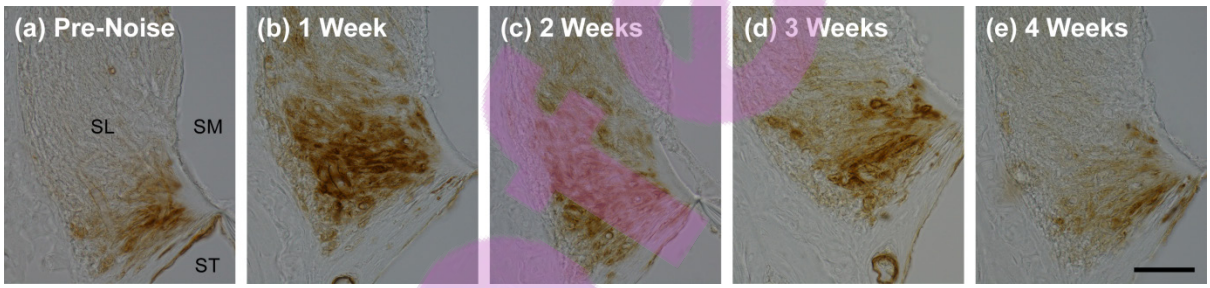

Figure 4.22: Time course of ICAM-1 expression in the basal turn spiral ligament of the C57BL/6 mouse cochlea following chronic noise exposure. Above are photomicrographs of ICAM-1 immunostaining in the spiral ligament of the cochlear basal turn before (**a**) and after one (**b**), two (**c**), three (**d**) and four (**e**) weeks of exposure to moderate noise (90 dB SPL, 8-16 kHz, 2 h/day). In the non-noise exposed cochlea, relatively weak ICAM-1 immunostaining was detected in the inferior region of the spiral ligament among type IV fibrocytes and vascular endothelial cells (**a**). Following noise exposure, expression of ICAM-1 increased substantially, peaking after one week of exposure (**b**). The immunolabelling became more intense and expanded to cover a much greater area of the spiral ligament. *Abbreviations*: SL, spiral ligament; SM, scala media; ST, scala tympani. Scale bar = 50 µm (applies to a-e).

Table 4.3: Average intensity (mean gray value) and area of ICAM-1 immunostaining in the spiral ligament of the cochlear basal turn before and after chronic noise exposure. Data presented as mean ± SEM (n = 5 per group).

Group	Average Mean Gray Value	Average Area (µm^2)
Control	94.8 ± 1.2	5,800 ± 289
1 week	79.4 ± 1.7	11,574 ± 558
2 weeks	89.5 ± 3.2	11,964 ± 843
3 weeks	98.2 ± 2.4	10,238 ± 421
4 weeks	100.3 ± 2.1	6,633 ± 411

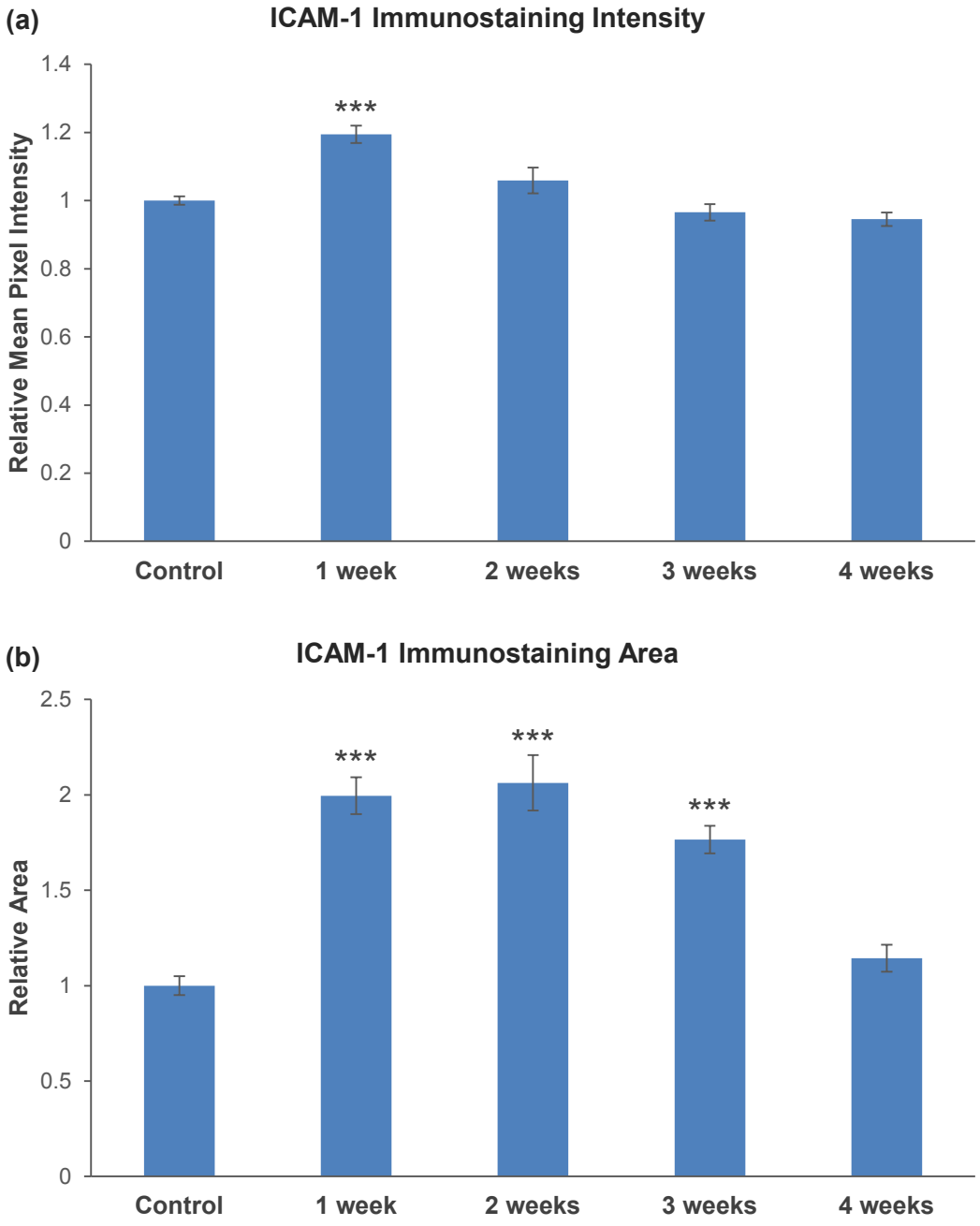

Figure 4.23: Semi-quantitative analysis of ICAM-1 immunostaining in the basal turn spiral ligament of the C57BL/6 mouse cochlea following chronic noise exposure. The graphs illustrate the ratio of the intensity (**a**) and area (**b**) of ICAM-1 immunostaining in the inferior region of the spiral ligament of the cochlear basal turn after one, two, three and four weeks of exposure to moderate noise (90 dB SPL, 8-16 kHz, 2 h/day) relative to non-noise exposed controls. A significant increase in the staining intensity occurred after one week of noise exposure. Area of staining doubled after one week, maintained a similar size after two weeks, and gradually declined to pre-noise size after four weeks. Data presented as mean ± SEM (n = 5 per group). ***$p < 0.001$, relative to the control group (one-way ANOVA followed by Tukey's post-hoc test).

Comparable findings were observed in the middle turn of the cochlea (**Figure 4.24** and **Figure 4.25**). The intensity of the staining was again highest in the one week exposure group (**Figure 4.24b** and **Figure 4.25a**), with the mean gray value decreasing significantly ($p < 0.001$, one-way ANOVA) from 93.7 ± 1.8 in the controls to 76.8 ± 2.9 after one week of exposure, a 22% increase in intensity. Mean pixel intensity returned to the control level thereafter. The staining area increased about 1.6-fold after one week (**Figure 4.24b** and **Figure 4.25b**), from 4,077 ± 244 μm^2 to 6,634 ± 241 μm^2 ($p < 0.001$, one-way ANOVA), and remained approximately the same size after two weeks (6,329 ± 279 μm^2). The immunolabelled area then declined with increasing duration of exposure.

As demonstrated earlier, gene expression levels of ICAM-1 were highest after two weeks of noise exposure (**Figure 4.19**), consistent with strong protein expression of ICAM-1. However, the peak of immunoexpression was observed after one week (**Figure 4.24**). After that, the average size of the ICAM-1 immunopositive region in the spiral ligament remained large, but with reduced average staining intensity.

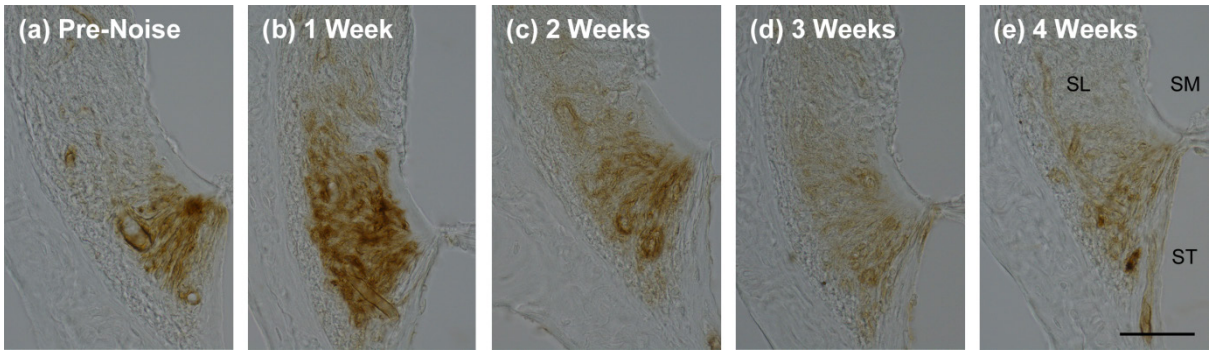

Figure 4.24: Time course of ICAM-1 expression in the middle turn spiral ligament of the C57BL/6 mouse cochlea following chronic noise exposure. Above are photomicrographs of ICAM-1 immunostaining in the spiral ligament of the cochlear middle turn before (**a**) and after one (**b**), two (**c**), three (**d**) and four (**e**) weeks of exposure to moderate noise (90 dB SPL, 8-16 kHz, 2 h/day). In the non-noise exposed cochlea, relatively weak ICAM-1 immunostaining was detected in the inferior region of the spiral ligament among type IV fibrocytes and vascular endothelial cells (**a**). Following noise exposure, expression of ICAM-1 increased substantially, peaking after one week of exposure (**b**). The immunolabelling became more intense and expanded to cover a much greater area of the spiral ligament. *Abbreviations*: SL, spiral ligament; SM, scala media; ST, scala tympani. Scale bar = 50 µm (applies to a-e).

Table 4.4: Average intensity (mean gray value) and area of ICAM-1 immunostaining in the spiral ligament of the cochlear middle turn before and after chronic noise exposure. Data presented as mean ± SEM (n = 5 per group).

Group	Average Mean Gray Value	Average Area (µm^2)
Control	93.7 ± 1.8	4,077 ± 244
1 week	76.8 ± 2.9	6,634 ± 241
2 weeks	91.9 ± 1.4	6,329 ± 279
3 weeks	100.6 ± 3.3	5,090 ± 427
4 weeks	102.1 ± 2.0	4,520 ± 469

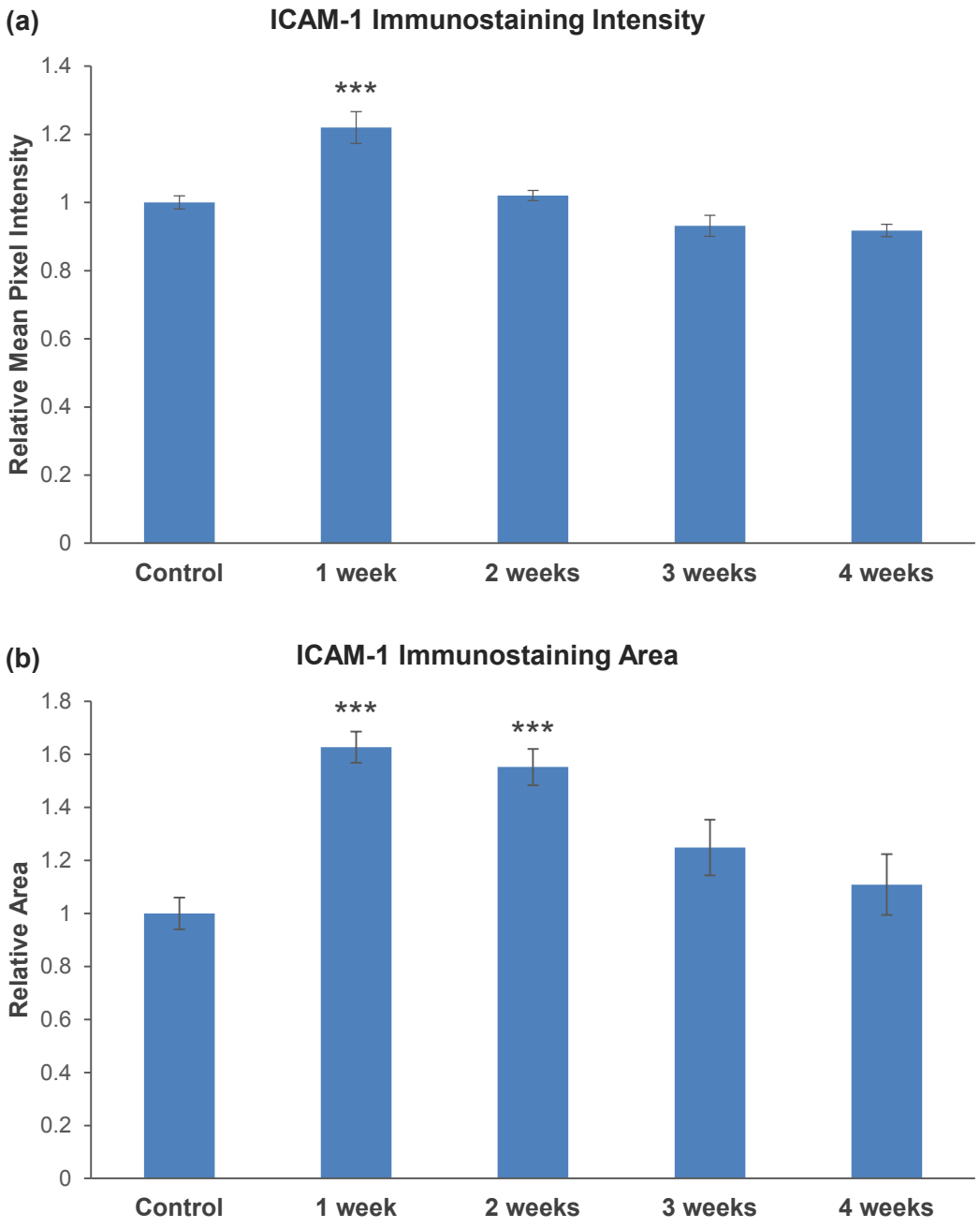

Figure 4.25: Semi-quantitative analysis of ICAM-1 immunostaining in the middle turn spiral ligament of the C57BL/6 mouse cochlea following chronic noise exposure. The graphs illustrate the ratio of the intensity (**a**) and area (**b**) of ICAM-1 immunostaining in the inferior region of the spiral ligament of the cochlear middle turn after one, two, three and four weeks of exposure to moderate noise (90 dB SPL, 8-16 kHz, 2 h/day) relative to non-noise exposed controls. A significant increase in the immunostaining intensity occurred after one week of noise exposure. Area of staining increased by about 60% after one week, maintained a similar size after two weeks, and gradually declined to pre-noise size after four weeks. Data presented as mean ± SEM (n = 5 per group). ***$p < 0.001$; relative to the control group (one-way ANOVA followed by Tukey's post-hoc test).

4.3.3. PECAM-1 Immunoexpression in the Noise-Exposed Cochlea

Expression of PECAM-1 in the cochlea was also assessed following chronic exposure to moderate noise (**Figure 4.26**). As indicated in the previous study (**Section 4.2.5**), PECAM-1 is expressed by the vascular endothelial cells in the spiral ligament, stria vascularis, spiral limbus, and spiral ganglion. However, unlike ICAM-1, no noticeable increase in the intensity of PECAM-1 immunolabelling was detected after chronic noise exposure. The distribution of PECAM-1 immunostaining was comparable in all cochlear turns.

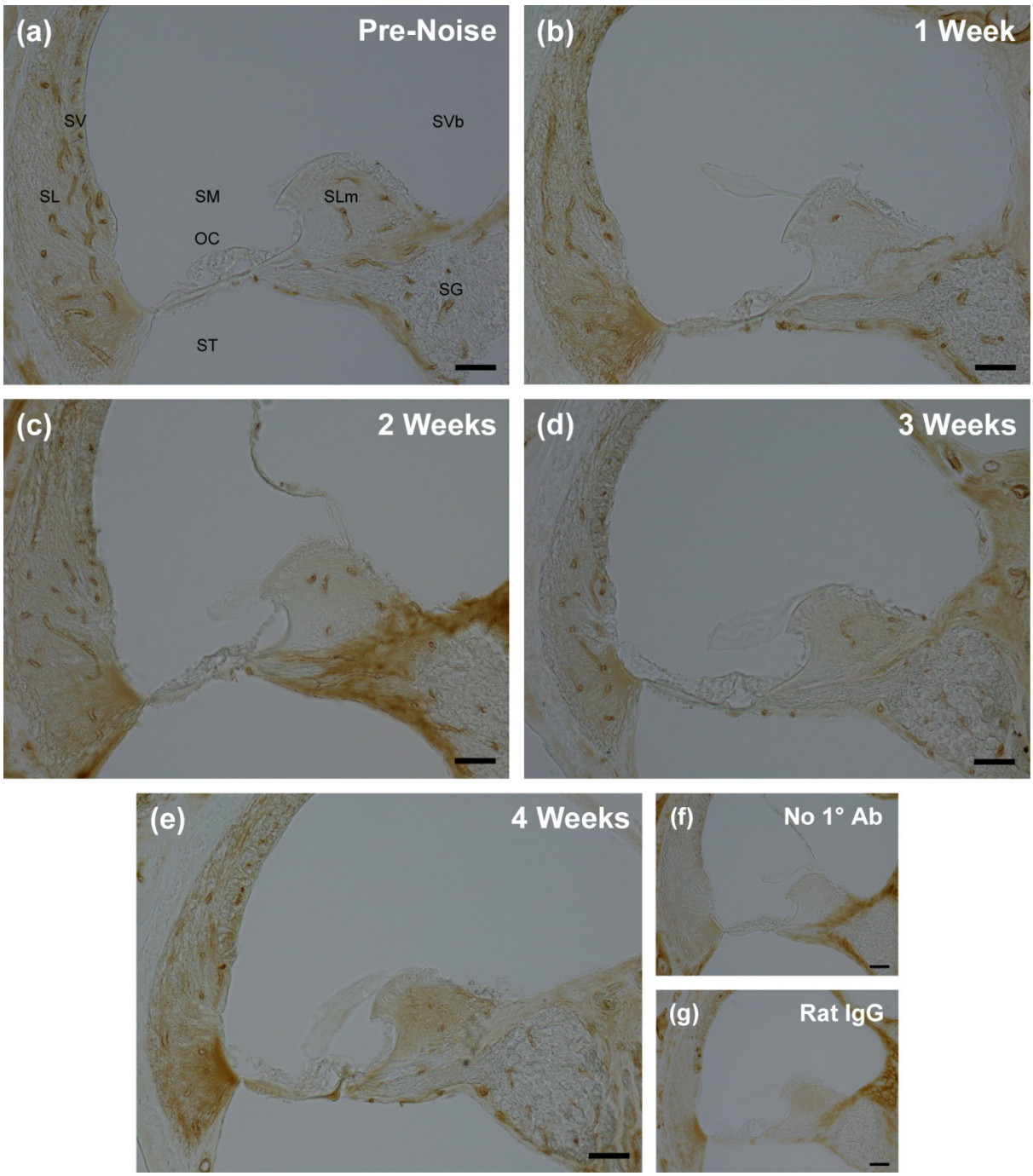

Figure 4.26: Time course of PECAM-1 expression in the C57BL/6 mouse cochlea following chronic noise exposure. Above are photomicrographs of PECAM-1 immunostaining in the spiral ligament of the cochlear basal turn before (**a**) and after one (**b**), two (**c**), three (**d**) and four (**e**) weeks of exposure to moderate noise (90 dB SPL, 8-16 kHz, 2 h/day). PECAM-1 immunostaining was detected in the blood vessels of the spiral ligament, stria vascularis, spiral limbus, and spiral ganglion (**a**). No noticeable difference in the intensity of PECAM-1 immunostaining was detected after chronic noise exposure (**b-e**). No immunostaining was detected (apart from non-specific staining of the bony capsule of the cochlea) when the primary antibody for PECAM-1 was either omitted (**f**) or replaced with the

corresponding IgG isotype control (rat IgG2a, κ chain) (**g**). *Abbreviations*: SL, spiral ligament; SV, stria vascularis; OC, organ of Corti; SLm, spiral limbus; SG, spiral ganglion; SM, scala media; ST, scala tympani; SVb, scala vestibuli. Scale bars = 50 µm.

In summary, this study has demonstrated that chronic exposure to moderate noise levels also induces an inflammatory response in the mouse cochlea. Gene expression levels of TNF-α, CCL2, ICAM-1 and IL-1β peaked after two weeks of noise exposure, and subsided thereafter. Maximum ICAM-1 immunoexpression in the spiral ligament was observed after one week of noise exposure; however the area of the immunostaining remained the same size after two weeks, but with reduced immunostaining intensity. In contrast to ICAM-1, PECAM-1 showed no noticeable increase in expression following chronic noise exposure.

4.4. STUDY 3: Role of Adenosine A_{2A} Receptor Signalling in Noise-Induced Cochlear Inflammation

The adenosine A_{2A} receptor plays a crucial role in the regulation of inflammatory and immune responses (Sullivan & Linden, 1998; Haskó & Cronstein, 2004; Bours *et al.*, 2006; Linden, 2006; Blackburn *et al.*, 2009; Haskó *et al.*, 2013). The selective activation of the adenosine A_{2A} receptor produces strong anti-inflammatory effects in a wide range of tissues in the body (Jacobson & Gao, 2006; Blackburn *et al.*, 2009). Adenosine A_{2A} receptor distribution has been demonstrated in the rat cochlea (Vlajkovic *et al.*, 2007) and also preliminary evidence from our group (unpublished data) shows their distribution in the vasculature in the mouse cochlea. Based on this expression and the role of adenosine A_{2A} receptors in mediating inflammation in tissues, this final study was undertaken to ascertain the role of adenosine A_{2A} receptors in the regulation of noise-induced cochlear inflammation, based on the observations of the previous studies showing inflammatory changes in the cochlea after noise exposure.

4.4.1. Adenosine A_{2A} Receptor Expression in the Noise-Exposed Cochlea

Firstly, using immunofluorescence, the distribution of adenosine A_{2A} receptors was characterised in the normal non-exposed mouse cochlea (**Figure 4.27a**) and in the cochlea exposed to acute traumatic noise (100 dB SPL, 8-16 kHz for 24 h) (**Figure 4.27b**). The adenosine A_{2A} receptor was mainly confined to the vasculature of the cochlea. Specific immunofluorescence was detected in blood vessels of the spiral ligament, stria vascularis, spiral ganglion, and modiolus. Within the spiral ligament, immunoreactivity was observed in the inferior region among type IV fibrocytes and also on the lateral side adjacent to the otic capsule among type III fibrocytes. The adenosine A_{2A} receptor immunolabelling in the inferior region of the spiral ligament resembled ICAM-1 immunolabelling. As all immune cells are known to express adenosine receptors, it is unsurprising that the haematopoietic stem cells in the bone marrow regions of the otic capsule and in the modiolus (**Figure 4.27e**) also showed adenosine A_{2A} receptor immunoreactivity. Following noise exposure, there was increased immunolabelling in the inferior region of the spiral ligament (**Figure 4.27b**, **c**). In addition, the endothelium of collecting venules below the lateral wall showed strong immunofluorescence (**Figure 4.27d**), which was generally not detectable in the non-exposed control cochlea. No immunolabelling was detected in cochlear sections when the adenosine A_{2A} receptor primary antibody was omitted (**Figure 4.27f**).

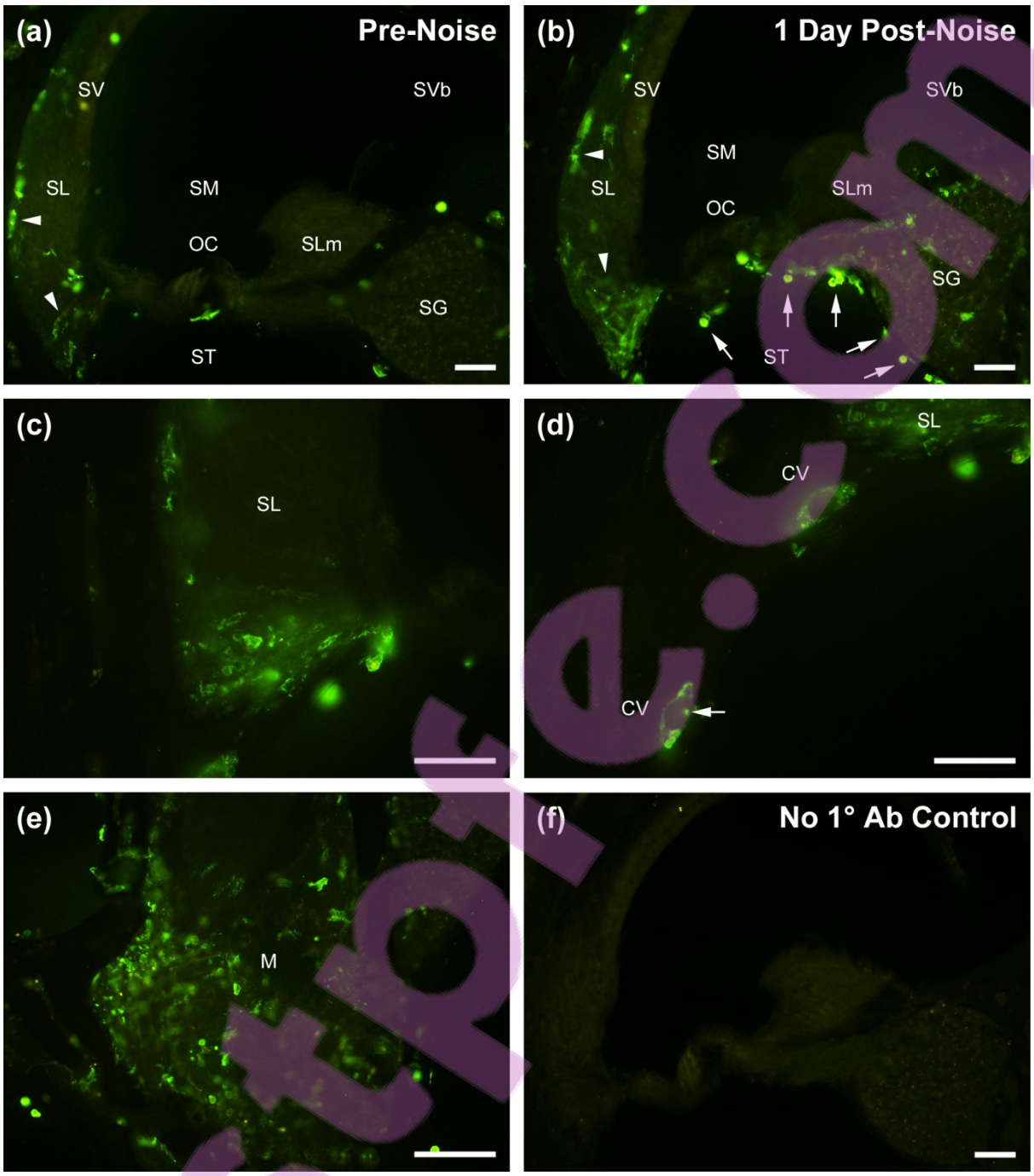

Figure 4.27: Distribution of adenosine A_{2A} receptor in the normal and noise-exposed C57BL/6 mouse cochlea. Figures (**a**) and (**b**) show the overall distribution of adenosine A_{2A} receptor in the non-noise exposed and noise-exposed cochlea respectively. Adenosine A_{2A} receptor expression was mainly confined to blood vessels located in the inferior region and lateral side of the spiral ligament (arrowheads), stria vascularis, spiral ganglion, and modiolus (**e**). Following noise exposure, there was increased immunolabelling in the inferior region of the spiral ligament (**b**, **c**) and the collecting venules below the lateral wall showed strong immunofluorescence (**d**), which was generally not detectable in the non-exposed cochlea. In addition, numerous infiltrating cells (arrows) were observed in the cochlea following noise

exposure (peaking one day post-exposure), mainly lining the wall of the scala tympani (**b**) (see **Figure 4.28** for higher magnification). Some cells appeared to be extravasating from the collecting venules (**d**; arrow). No immunostaining was detected when the primary antibody was omitted (**f**). Image (a), (b), (d) and (f) are taken from the middle turn and image (c) from the basal turn. *Abbreviations*: SL, spiral ligament; SV, stria vascularis; OC, organ of Corti; SLm, spiral limbus; SG, spiral ganglion; CV, collecting venule; M, modiolus; SM, scala media; ST, scala tympani; SVb, scala vestibuli. Scale bars = 50 µm.

In addition to immunofluorescence labelling of the cochlear vasculature, numerous adenosine A_{2A} receptor-positive infiltrating cells were observed within the cochlea following noise exposure (**Figure 4.27b** and **Figure 4.28**). Cells involved in immune and inflammatory responses are known to express adenosine A_{2A} receptors as well as the other three adenosine receptor subtypes (A_1, A_{2B}, and A_3) (Sullivan & Linden, 1998; Bours *et al.*, 2006; Fredholm, 2007; Blackburn *et al.*, 2009; Haskó *et al.*, 2013). These infiltrating cells were predominantly found within the scala tympani, adhering to the wall of the perilymphatic space. Positively labelled cells were also present in the spiral ligament (**Figure 4.28e**), scala vestibuli, spiral limbus (**Figure 4.28d**), spiral ganglion (**Figure 4.28d**), and in the modiolus (**Figure 4.27e**). Some cells appeared to be extravasating from the collecting venules below the lateral wall (i.e. they were observed within and in the perivascular space of the venules) at 6 h and 1 day after noise exposure (**Figure 4.27d**). Infiltrating cells were notably absent in the endolymph-filled space of the scala media and in the organ of Corti. The vast majority of infiltrating cells were located in the middle and basal turn of the cochlea. Morphologically, most of the labelled cells appeared round in shape without any processes, while some of the cells lining the fluid-filled spaces of the scala tympani and scala vestibuli were slightly flattened against the wall (**Figure 4.28b**). In contrast to the noise-exposed cochlea, these cells were absent or few in number in the normal non-exposed cochlea.

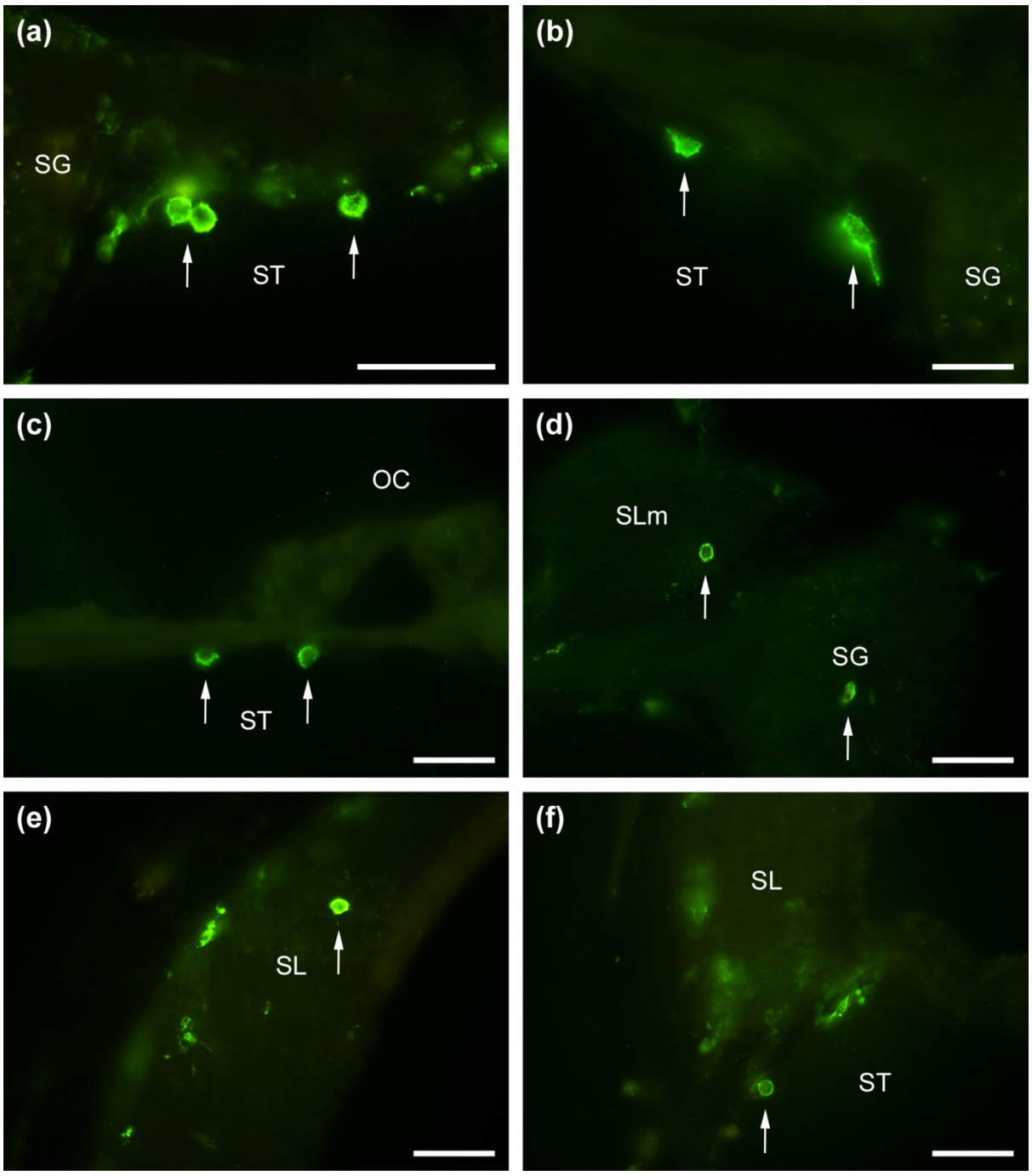

Figure 4.28: A_{2A}R-positive infiltrating cells in the noise-exposed C57BL/6 mouse cochlea. Following acute exposure to traumatic noise (100 dB SPL, 8-16 kHz for 24 h), numerous adenosine A_{2A} receptor-positive infiltrating cells (arrows) were observed within the cochlea, peaking one day post-exposure. These labelled cells were predominantly found attached to the wall of the scala tympani and basilar membrane (**a**, **b**, **c**, **f**). A few cells were also seen in the spiral ligament (**e**), spiral limbus (**d**), and spiral ganglion (**d**). Morphologically, these cells appeared round in shape or flat if positioned against the wall of scala tympani. *Abbreviations*: SL, spiral ligament; OC, organ of Corti; SLm, spiral limbus; SG, spiral ganglion; ST, scala tympani. Scale bars = 50 µm.

A quantitative analysis was carried out to assess the average number of adenosine A_{2A} receptor-positive infiltrating cells present in the cochlea prior to and 6 h, 1 day, 3 days and 7 days following acute exposure to traumatic noise (n = 4 per time point) (**Table 4.5** and **Figure 4.29**). The total number of labelled cells was counted in all cochlear turns (apical, middle and basal) of every second mid-modiolar cross-section from each cochlea (about five sections per cochlea). The average number of cells per cochlear section for each experimental group was determined from a total of four cochleae. Cells were counted under the fluorescent microscope (Nikon Eclipse 80i) at 40x magnification. To ensure all cells throughout the depth of the cochlear sections were identified, the entire thickness (30 µm) of the sections was examined. Only those cells that were round in shape or flat against the wall of the scala tympani (as shown in **Figure 4.28**) were included in the total cell count, whereas irregular-shaped cells observed in the lower portion of the spiral ligament were excluded. In the non-exposed cochlea, very few cells were found (2.4 ± 0.5 labelled cells/section). However, following noise exposure, the average number of infiltrating cells increased significantly to 8.7 ± 0.6 cells/section at 6 h post-exposure ($p < 0.001$, one-way ANOVA) and reached a maximum of 13.1 ± 1.8 cells/section at 24 h post-exposure, reflecting an increase of approximately 5.5-fold ($p < 0.001$, one-way ANOVA). Thereafter, the total number of labelled cells gradually declined, and by seven days after noise exposure there were 5.8 ± 0.4 cells/section.

Table 4.5: Quantitative analysis of A_{2A}R-positive infiltrating cells in the noise-exposed C57BL/6 mouse cochlea. The table below shows the average number of A_{2A}R-positive infiltrating cells per cochlear section before and 6 h, 1 day, 3 days and 7 days following acute exposure to traumatic noise (100 dB SPL, 8-16 kHz for 24 h). The maximum number of infiltrating cells was observed at 24 h post-exposure (13.1 cells/section), an approximate 5.5-fold increase relative to the non-exposed cochlea (2.4 cells/section). Data presented as mean ± SEM (n = 4 per group).

Time point	Average number of $A_{2A}R^+$ infiltrating cells/section
Pre-noise	2.4 ± 0.5
6 h	8.7 ± 0.6
1 day	13.1 ± 1.8
3 days	7.7 ± 0.4
7 days	5.8 ± 0.4

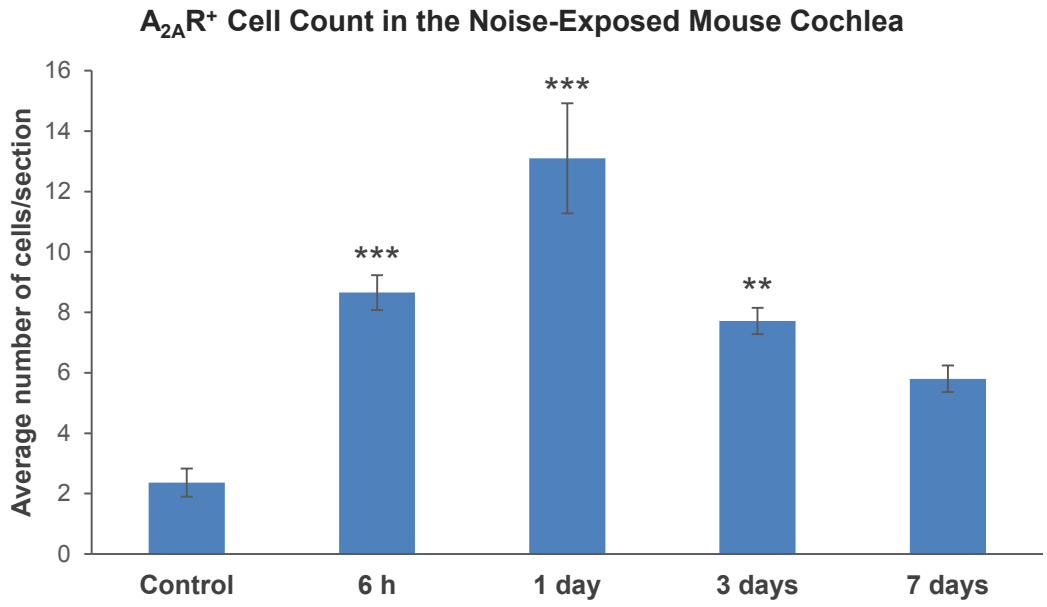

Figure 4.29: Quantitative analysis of A_{2A}R-positive infiltrating cells in the noise-exposed C57BL/6 mouse cochlea. The graph illustrates the average number of A_{2A}R-positive infiltrating cells per cochlear section before and at 6 h, 1 day, 3 days and 7 days following acute exposure to traumatic noise (100 dB SPL, 8-16 kHz for 24 h). The average number of infiltrating cells/section increased from 2.4 ± 0.5 prior to noise exposure to a maximum of 13.1 ± 1.8 at 24 h post-exposure, reflecting an approximate 5.5-fold increase. Data presented as mean ± SEM (n = 4 per group). $^{**}p < 0.01$, $^{***}p < 0.001$; relative to the control group (one-way ANOVA followed by Tukey's post-hoc test).

4.4.2. Noise-Induced Cochlear Inflammatory Response in Adenosine A_{2A} Receptor Knockout Mice

To gain further insight into the role of adenosine A_{2A} receptor signalling in noise-induced cochlear inflammation, the protein expression of ICAM-1 and the gene expression levels of TNF-α, ICAM-1, CCL2 and IL-1β were assessed in the cochleae of noise-exposed C57BL/6 mice with deleted adenosine A_{2A} receptor gene ($A_{2A}RKO^{-/-}$). These homozygous recessive knockout mice were exposed to acute traumatic noise (100 dB SPL, 8-16 kHz for 24 h) and their cochleae examined at 6 and 24 h post-exposure. The selection of these two time points was based on the time of the initial peak in transcriptional expression of the inflammation-related genes and the time of maximum ICAM-1 expression and cellular infiltration respectively, as was demonstrated previously.

4.4.2.1. ICAM-1 Immunoexpression in the Noise-Exposed $A_{2A}RKO^{-/-}$ Mouse Cochlea

ICAM-1 expression in the noise-exposed $A_{2A}RKO^{-/-}$ mouse cochlea was examined 24 h post-exposure using immunoperoxidase staining. Similar to the previous studies, the intensity and area of the ICAM-1 immunostaining in the spiral ligament was semi-quantitatively analysed. Four different groups of mice were assessed and compared in this study (n = 5 per group): 1) non-exposed wild-type; 2) non-exposed $A_{2A}RKO^{-/-}$; 3) noise-exposed wild-type; and 4) noise-exposed $A_{2A}RKO^{-/-}$. **Table 4.6** and **Table 4.7** show the average measured pixel intensity (mean gray value) and area of the ROI (inferior region of the spiral ligament) in both the cochlear basal and middle turns for the non-exposed and noise-exposed groups respectively. The data for the wild-type mice (non-exposed and noise-exposed) were obtained from study one (**Section 4.2.4**).

The results revealed no significant difference in the ICAM-1 immunostaining intensity in both cochlear turns between wild-type and $A_{2A}RKO^{-/-}$ mice exposed to ambient noise ($p > 0.05$, unpaired t-test) (**Figure 4.30** and **Figure 4.31a**). In regards to the area of the ICAM-1 immunostaining, there was again no significant difference between the non-exposed wild-type and $A_{2A}RKO^{-/-}$ cochlea for the middle turn ($p > 0.05$, unpaired t-test) (**Figure 4.30c,d** and **Figure 4.31b**), however the size of the ROI in the basal turn of the $A_{2A}RKO^{-/-}$ cochlea (3,966 ± 236 μm^2) was significantly smaller (by 32%) than that in the wild-type cochlea (5,800 ± 289 μm^2) ($p < 0.001$, unpaired t-test) (**Figure 4.30a,b** and **Figure 4.31b**).

Following acute exposure to traumatic noise, ICAM-1 immunostaining intensity was similar in the wild-type and $A_{2A}RKO^{-/-}$ mouse cochlea for both the basal and middle turn ($p > 0.05$, unpaired t-test) (**Figure 4.32** and **Figure 4.33a**). Similarly, the ICAM-1 immunostaining area was similar in the wild-type and $A_{2A}RKO^{-/-}$ cochlea for both turns ($p > 0.05$, unpaired t-test) (**Figure 4.32** and **Figure 4.33b**).

An additional analysis was carried out to compare the ICAM-1 immunostaining area in the basal turn spiral ligament before and after noise exposure for both wild-type and $A_{2A}KRO^{-/-}$ mice (**Figure 4.34**). As was demonstrated in study one for wild-type mice, the area of ICAM-1 immunolabelling doubled in size 24 h after noise exposure. In comparison, the staining area increased by 3-fold after noise exposure in the KO mice. Deletion of the $A_{2A}R$ gene therefore results in a larger increase in ICAM-1 immunoexpression following noise exposure.

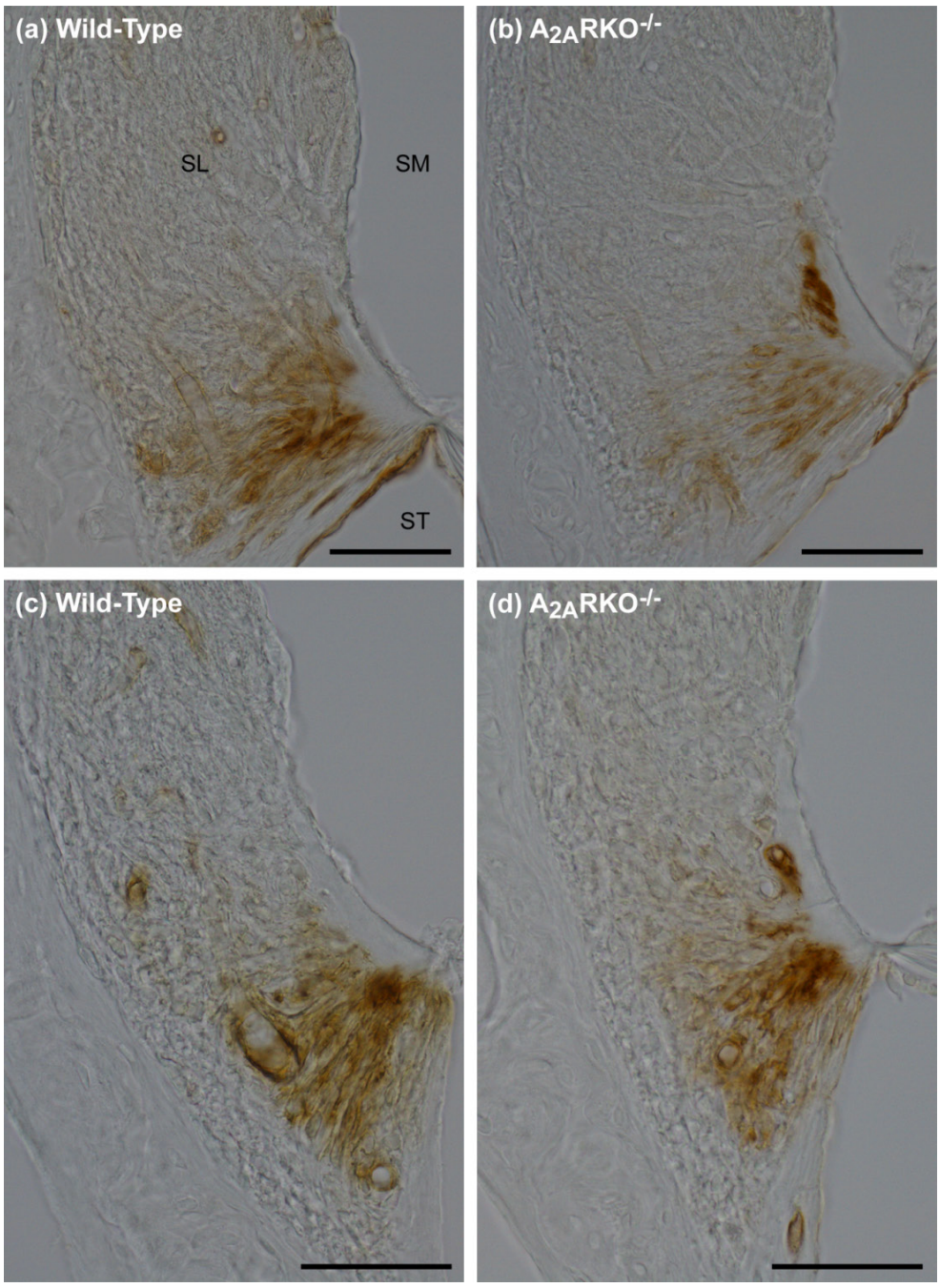

Figure 4.30: ICAM-1 immunostaining in the spiral ligament of the cochlear basal and middle turn in non-noise exposed wild-type and $A_{2A}RKO^{-/-}$ C57BL/6 mice. Above are photomicrographs of ICAM-1 immunostaining in the inferior region of the spiral ligament of the cochlear basal and middle turn in wild-type and $A_{2A}RKO^{-/-}$ mice exposed to ambient noise. (**a**, **b**) In the basal turn, the overall intensity of the ICAM-1 immunostaining in the spiral ligament was similar in both the wild-type and $A_{2A}RKO^{-/-}$ mouse cochlea, however the size of the immunopositive area was smaller in the $A_{2A}RKO^{-/-}$ cochlea. (**c**, **d**) In the middle turn, no noticeable difference in both the intensity and area of the ICAM-1 immunostaining in the spiral ligament was observed between the wild-type and $A_{2A}RKO^{-/-}$ cochlea. *Abbreviations*: SL, spiral ligament; SM, scala media; ST, scala tympani. Scale bars = 50 μm.

Table 4.6: Average intensity (mean gray value) and area of ICAM-1 immunostaining in the spiral ligament of the cochlear basal and middle turns in non-noise exposed wild-type and $A_{2A}RKO^{-/-}$ C57BL/6 mice. Data presented as mean ± SEM (*n* = 5 per group).

	Average Mean Gray Value		Average Area (µm^2)	
Group	**Basal**	**Middle**	**Basal**	**Middle**
Wild-Type	94.8 ± 1.2	93.7 ± 1.8	5,800 ± 289	4,077 ± 244
$A_{2A}RKO^{-/-}$	94.5 ± 1.7	92.1 ± 2.1	3,966 ± 236	3,826 ± 144

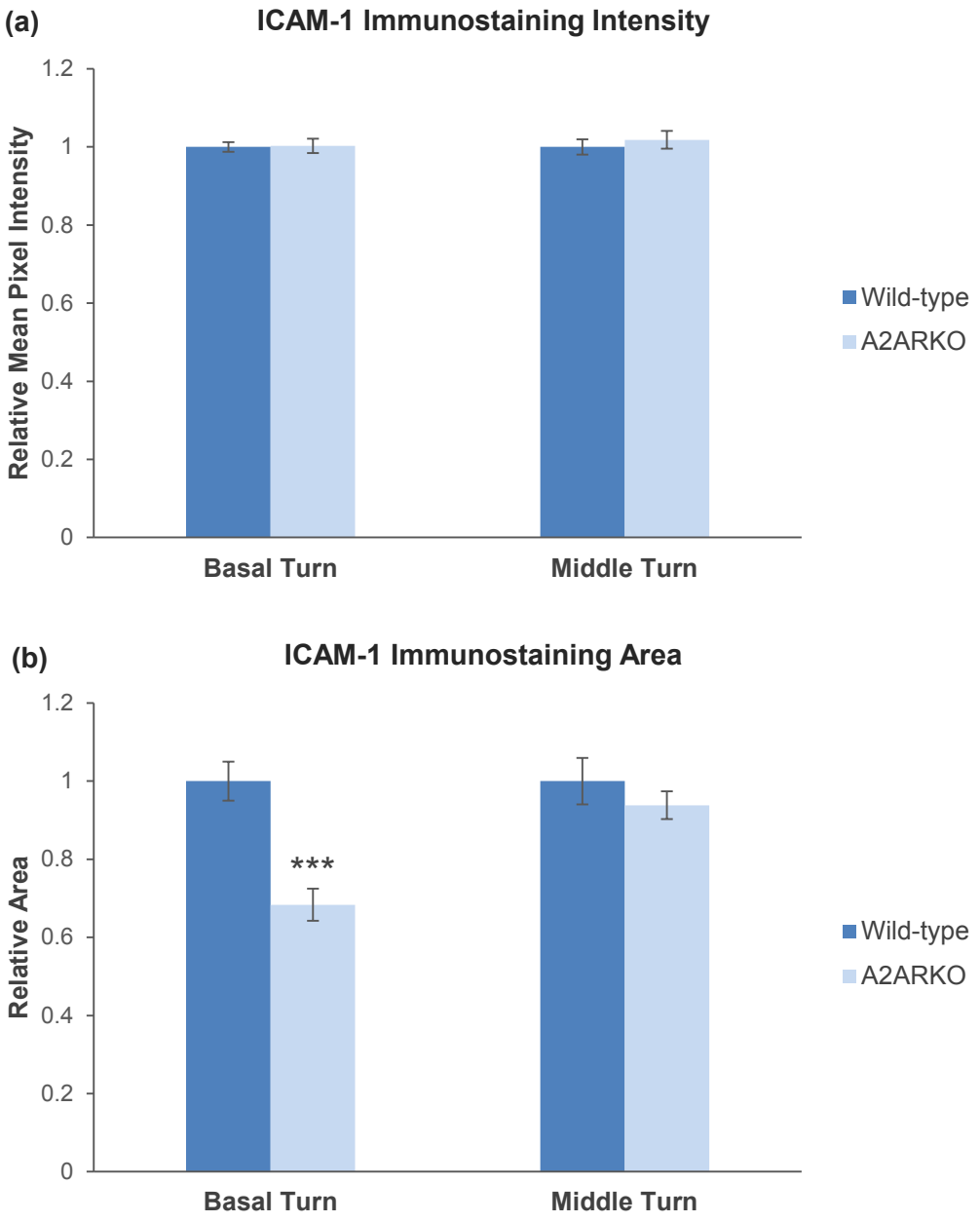

Figure 4.31: Semi-quantitative analysis of ICAM-1 immunostaining in the spiral ligament of the cochlear basal and middle turn in non-noise exposed wild-type and $A_{2A}RKO^{-/-}$ C57BL/6 mice. The graphs illustrate the ratio of the intensity (**a**) and area (**b**) of ICAM-1 immunostaining in the inferior region of the spiral ligament of the cochlear basal and middle turn in non-exposed $A_{2A}RKO^{-/-}$ mice relative to non-exposed wild-type mice. There was no significant difference in the immunostaining intensity between the wild-type and $A_{2A}RKO^{-/-}$ cochlea in both cochlear turns ($p > 0.05$, unpaired *t*-test). Regarding the immunostaining area, there was no significant difference in the middle turn ($p > 0.05$, unpaired *t*-test), however the ROI in the basal turn of the $A_{2A}RKO^{-/-}$ cochlea was 32% smaller than in the wild-type cochlea (***$p < 0.001$, unpaired *t*-test). Data presented as mean ± SEM ($n = 5$ per group).

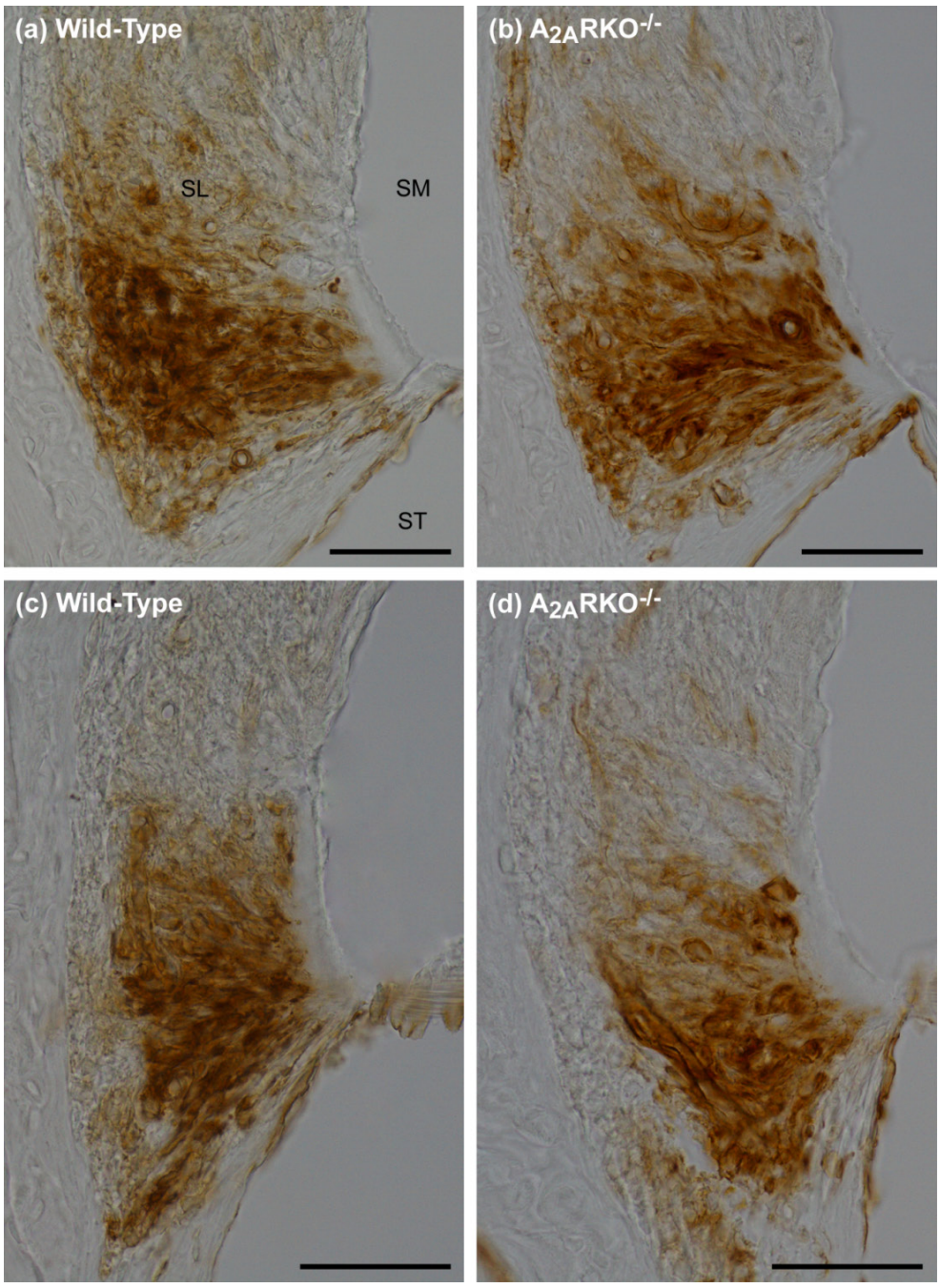

Figure 4.32: ICAM-1 immunostaining in the spiral ligament of the cochlear basal and middle turn in noise-exposed wild-type and $A_{2A}RKO^{-/-}$ C57BL/6 mice. Above are photomicrographs of ICAM-1 immunostaining in the inferior region of the spiral ligament in the cochlear basal and middle turn in wild-type and $A_{2A}RKO^{-/-}$ mice 24 h following acute exposure to traumatic noise (100 dB SPL, 8-16 kHz for 24 h). (**a**, **b**) In the basal turn, no noticeable difference in both the intensity and area of the ICAM-1 immunostaining in the spiral ligament was observed between the wild-type and $A_{2A}RKO^{-/-}$ cochlea. (**c**, **d**) Similarly, no apparent difference in both the intensity and area of ICAM-1 immunostaining was observed in the middle turn. *Abbreviations*: SL, spiral ligament; SM, scala media; ST, scala tympani. Scale bars = 50 μm.

Table 4.7: Average intensity (mean gray value) and area of ICAM-1 immunostaining in the spiral ligament of the cochlear basal and middle turn in noise-exposed wild-type and $A_{2A}RKO^{-/-}$ C57BL/6 mice. Data presented as mean ± SEM (n = 5 per group).

	Average Mean Gray Value		Average Area (µm^2)	
Group	**Basal**	**Middle**	**Basal**	**Middle**
Wild-Type	82.4 ± 1.9	75.4 ± 2.7	11,599 ± 704	6,113 ± 454
$A_{2A}RKO^{-/-}$	83.5 ± 1.3	80.7 ± 1.4	12,083 ± 776	6,429 ± 366

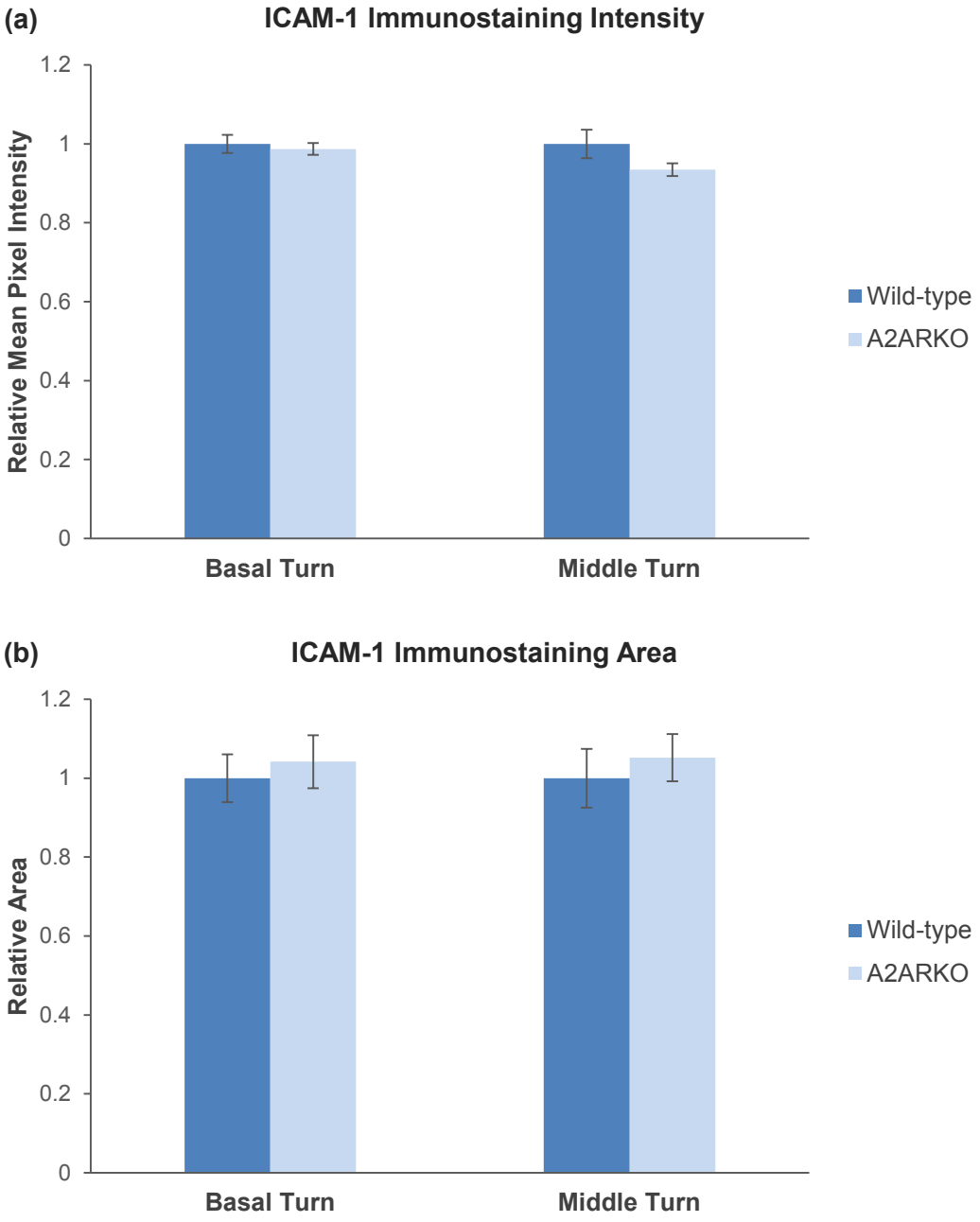

Figure 4.33: Semi-quantitative analysis of ICAM-1 immunostaining in the spiral ligament of the cochlear basal and middle turns in noise-exposed wild-type and $A_{2A}RKO^{-/-}$ C57BL/6 mice. The graphs illustrate the ratio of the intensity (**a**) and area (**b**) of ICAM-1 immunostaining in the inferior region of the spiral ligament of the cochlear basal and middle turns in $A_{2A}RKO^{-/-}$ mice relative to wild-type mice 24 h following acute exposure to traumatic noise (100 dB, 8-16 kHz for 24 h). There was no significant difference in the immunostaining intensity and area between the noise-exposed wild-type and $A_{2A}RKO^{-/-}$ cochlea in both cochlear turns ($p > 0.05$, unpaired *t*-test). Data presented as mean ± SEM ($n = 5$ per group).

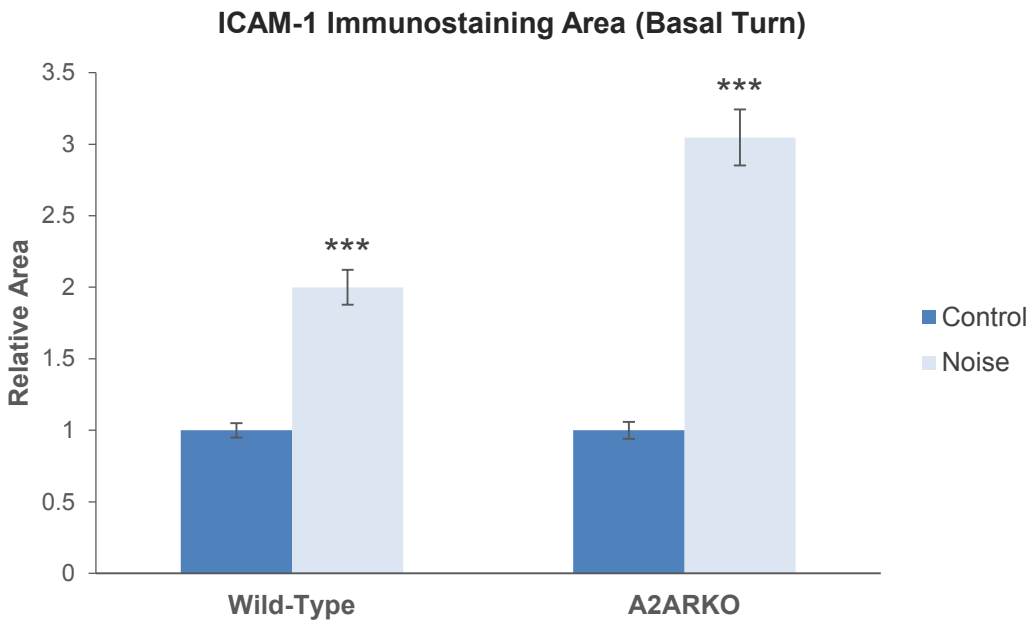

Figure 4.34: Semi-quantitative analysis of ICAM-1 immunostaining area in the basal turn spiral ligament before and after noise exposure in wild-type and $A_{2A}RKO^{-/-}$ C57BL/6 mice. The graph illustrates the ratio of the area of ICAM-1 immunostaining in the cochlear basal turn in noise-exposed wild-type and $A_{2A}RKO^{-/-}$ mice relative to non-exposed wild-type and $A_{2A}RKO^{-/-}$ mice. The immunostaining area in the wild-type mouse cochlea increased by 2-fold following noise exposure, whereas in the $A_{2A}RKO^{-/-}$ mouse cochlea, the immunostaining area increased by 3-fold following noise exposure. Data presented as mean ± SEM (n = 5 per group). ***$p < 0.001$, relative to the non-exposed control group (unpaired t-test).

4.4.2.2. Gene Expression Levels of TNF-α, CCL2, ICAM-1 and IL-1β in the Noise-Exposed $A_{2A}RKO^{-/-}$ Mouse Cochlea

Quantitative real-time RT-PCR was performed to assess the difference in the cochlear gene expression levels of TNF-α, ICAM-1, CCL2 and IL-1β between wild-type and $A_{2A}RKO^{-/-}$ mice prior to and 6 and 24 h following acute exposure to traumatic noise (n = 5 per time point). As **Figure 4.35** shows, the deletion of the adenosine A_{2A} receptor gene ($A_{2A}RKO^{-/-}$) had no significant effect on the transcriptional expression of TNF-α, ICAM-1, CCL2 and IL-1β in the non-exposed mouse cochlea ($p > 0.05$ for all four genes, unpaired t-test). At 6 h following acute exposure to traumatic noise, the expression of CCL2 and IL-1β was significantly downregulated by three- and two-fold respectively in the $A_{2A}RKO^{-/-}$ mouse cochlea relative to the wild-type cochlea ($p < 0.01$ for CCL2, $p < 0.001$ for IL-1β; unpaired t-test), whereas no significant difference was observed for TNF-α and ICAM-1 ($p > 0.05$,

unpaired *t*-test) (**Figure 4.36**). Because the data for the non-noise and noise-exposed groups were derived from different real-time PCR runs, pre- and post-exposure expression levels could not be compared. Nevertheless, the results seem to show that deletion of the $A_{2A}R$ gene leads to much lower gene expression levels of CCL2 and IL-1β following noise exposure relative to wild-type mice, while having no effect on TNF-α and ICAM-1 gene expression. At 24 h after noise exposure, all four inflammatory genes showed no significant difference in cochlear expression levels between wild-type and $A_{2A}RKO^{-/-}$ mice ($p > 0.05$, unpaired *t*-test) (**Figure 4.37**).

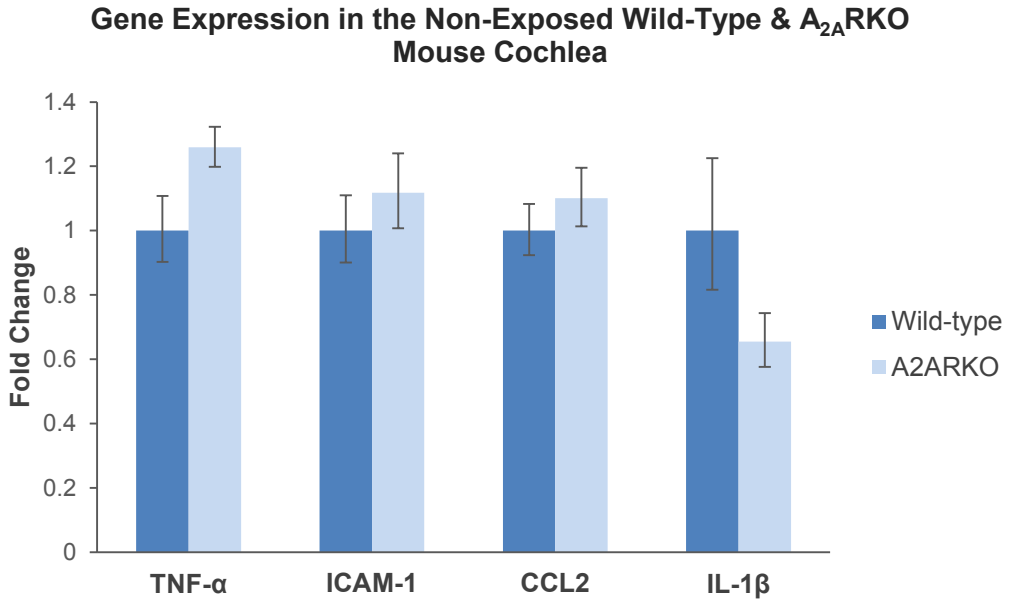

Figure 4.35: Quantitative real-time RT-PCR analysis of TNF-α, ICAM-1, CCL2 and IL-1β gene expression in the cochleae of $A_{2A}RKO^{-/-}$ C57BL/6 mice exposed to ambient noise. The graph illustrates the fold change in gene expression of TNF-α, ICAM-1, CCL2 and IL-1β in the cochleae of non-exposed $A_{2A}RKO^{-/-}$ mice relative to non-exposed wild-type mice. There was no significant difference in the cochlear mRNA expression levels of all four inflammatory genes between wild-type and $A_{2A}RKO^{-/-}$ mice ($p > 0.05$, unpaired *t*-test). Data presented as mean ± SEM ($n = 5$ per group).

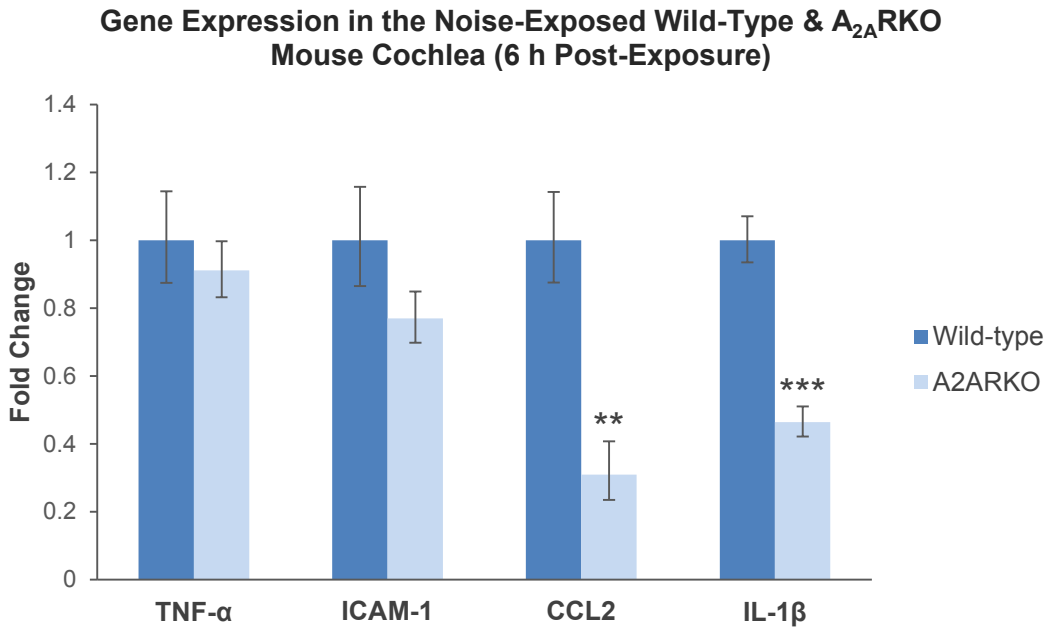

Figure 4.36: Quantitative real-time RT-PCR analysis of TNF-α, ICAM-1, CCL2 and IL-1β gene expression in the cochleae of $A_{2A}RKO^{-/-}$ C57BL/6 mice 6 h following acute noise exposure. The graph illustrates the fold change in gene expression of TNF-α, ICAM-1, CCL2 and IL-1β in the cochlea of $A_{2A}RKO^{-/-}$ mice relative to wild-type mice 6 h following acute exposure to traumatic noise (100 dB SPL, 8-16 kHz for 24 h). There was no significant difference in the cochlear mRNA expression levels of TNF-α and ICAM-1 between wild-type and $A_{2A}RKO^{-/-}$ mice ($p > 0.05$, unpaired *t*-test). However, CCL2 and IL-1β expression was significantly downregulated by three- and two-fold respectively in the $A_{2A}RKO^{-/-}$ mouse cochlea relative to the wild-type cochlea (**$p < 0.01$, ***$p < 0.001$; unpaired *t*-test). Data presented as mean ± SEM ($n = 5$ per group).

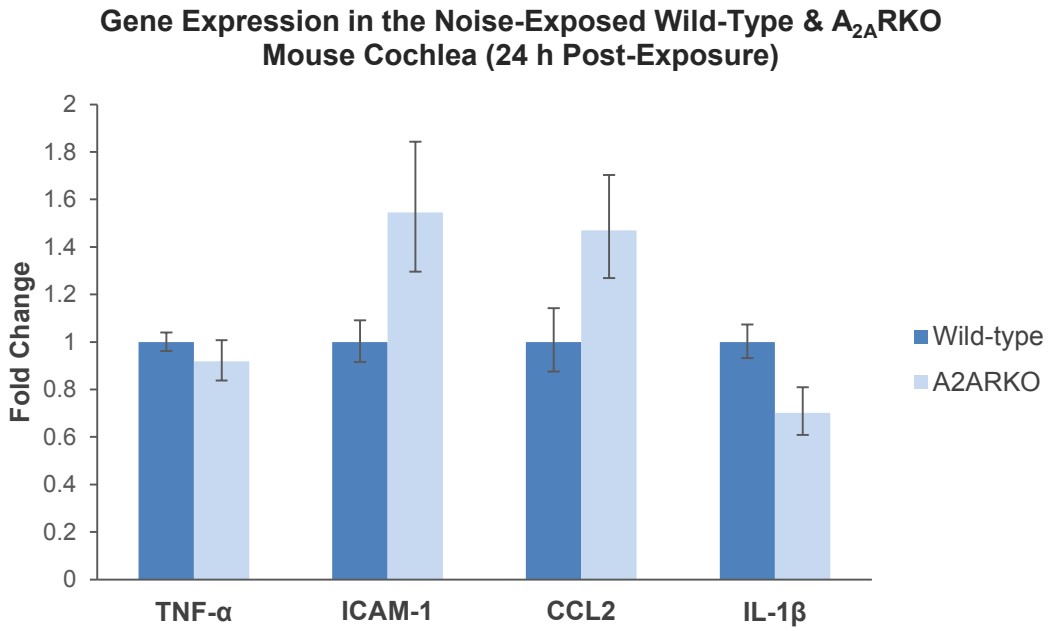

Figure 4.37: Quantitative real-time RT-PCR analysis of TNF-α, ICAM-1, CCL2 and IL-1β gene expression in the cochleae of $A_{2A}RKO^{-/-}$ C57BL/6 mice 24 h following acute noise exposure. The graph illustrates the fold change in gene expression of TNF-α, ICAM-1, CCL2 and IL-1β in the cochlea of $A_{2A}RKO^{-/-}$ mice relative to wild-type mice 24 h following acute exposure to traumatic noise (100 dB SPL, 8-16 kHz for 24 h). There was no significant difference in the cochlear mRNA expression levels of all four inflammatory genes between wild-type and $A_{2A}RKO^{-/-}$ mice ($p > 0.05$, unpaired *t*-test). Data presented as mean ± SEM ($n = 5$ per group).

4.4.3. Anti-Inflammatory Effect of Regadenoson, a Selective Adenosine A_{2A} Receptor Agonist, in the Noise-Exposed Cochlea

The objective of this study was to investigate whether activation of adenosine A_{2A} receptors in the cochlea would mitigate noise-induced inflammatory response. This intervention was carried out using the selective adenosine A_{2A} receptor agonist, regadenoson (Lexiscan®). As described in the methodology, mice were treated with regadenoson (50 µg/kg) via an intracardiac injection (while under anaesthesia) immediately following exposure to acute traumatic noise (100 dB SPL, 8-16 kHz for 24 h). Tail vein injections were initially attempted, but the dark colour of the C57BL/6 mouse tail made it difficult to visualise and insert the needle through the vein. The outcome of this treatment was determined by assessing the expression of inflammatory markers in the noise-exposed cochlea and

comparing those to the noise-exposed vehicle-treated cochlea. The effect of regadenoson on the cochlear inflammatory response was examined at 6 and 24 h after the cessation of noise exposure.

4.4.3.1. Effect of Adenosine A_{2A} Receptor Activation on Cellular Infiltration in the Noise-Exposed Cochlea

Firstly, the effect of regadenoson on noise-induced cellular infiltration was examined. The average number of infiltrating cells per cochlear section was determined 24 h post-exposure/treatment (n = 6 per group). Adenosine A_{2A} receptor was used as the marker for infiltrating cells. The results showed that post-exposure regadenoson treatment significantly reduced the number of infiltrating cells in the cochlea as compared to vehicle-treated controls (**Figure 4.38**). The average number of cells/section decreased from 10.7 ± 0.7 in drug vehicle-treated mice to 4.0 ± 0.3 in regadenoson-treated mice, reflecting an approximate 2.7-fold decrease ($p < 0.001$, unpaired t-test).

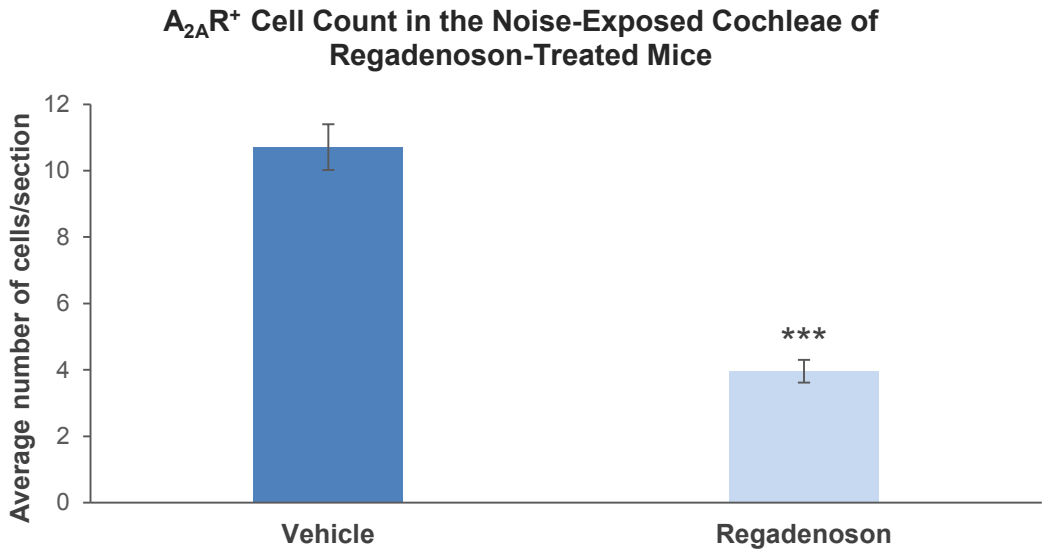

Figure 4.38: Quantitative analysis of A_{2A}R-positive infiltrating cells in the noise-exposed cochleae of drug vehicle and regadenoson-treated C57BL/6 mice. The graph illustrates the average number of A_{2A}R-positive infiltrating cells per cochlear section 24 h following acute exposure to traumatic noise (100 dB SPL, 8-16 kHz for 24 h). Post-exposure regadenoson treatment significantly reduced the number of infiltrating cells in the cochlea by approximately 2.7-fold relative to vehicle-treated controls (***$p < 0.001$, unpaired t-test). Data presented as mean ± SEM (n = 6 per group).

4.4.3.2. Effect of Adenosine A_{2A} Receptor Activation on the Immunoexpression of ICAM-1 in the Noise-Exposed Cochlea

Secondly, the protein expression level of ICAM-1 in the spiral ligament was analysed in vehicle and regadenoson-treated mice 24 h following noise exposure using semi-quantitative immunoperoxidase histochemistry (n = 6 per group) (**Table 4.8**). The overall immunostaining intensity of ICAM-1 was reduced in both the cochlear basal (**Figure 4.39b**) and middle turn (**Figure 4.40b**) following post-exposure treatment with regadenoson. Semi-quantitative image analysis revealed that the average mean gray value increased (which represents a decrease in pixel intensity) from 78.6 ± 1.4 to 82.9 ± 1.2 in the basal turn (a 5.1% decrease in intensity), and from 69.7 ± 1.0 to 74.5 ± 1.5 in the middle turn (a 6.5% decrease in intensity), with both changes determined to be statistically significant ($p < 0.05$, unpaired t-test) (**Figure 4.41a**). Similarly, the area of ICAM-1 immunostaining was also reduced in size in both cochlear turns after regadenoson treatment (**Figure 4.39b** and **Figure 4.40b**). The staining area decreased significantly ($p < 0.05$, unpaired t-test) from 11,607 ± 699 μm^2 to 10,050 ± 424 μm^2 in the basal turn (a 13.4% decrease), and from 6,902 ± 311 μm^2 to 6,116 ± 211 μm^2 in the middle turn (an 11.4% decrease) (**Figure 4.41b**). The findings thus demonstrate that regadenoson treatment reduces noise-induced immunoexpression of ICAM-1 in the spiral ligament.

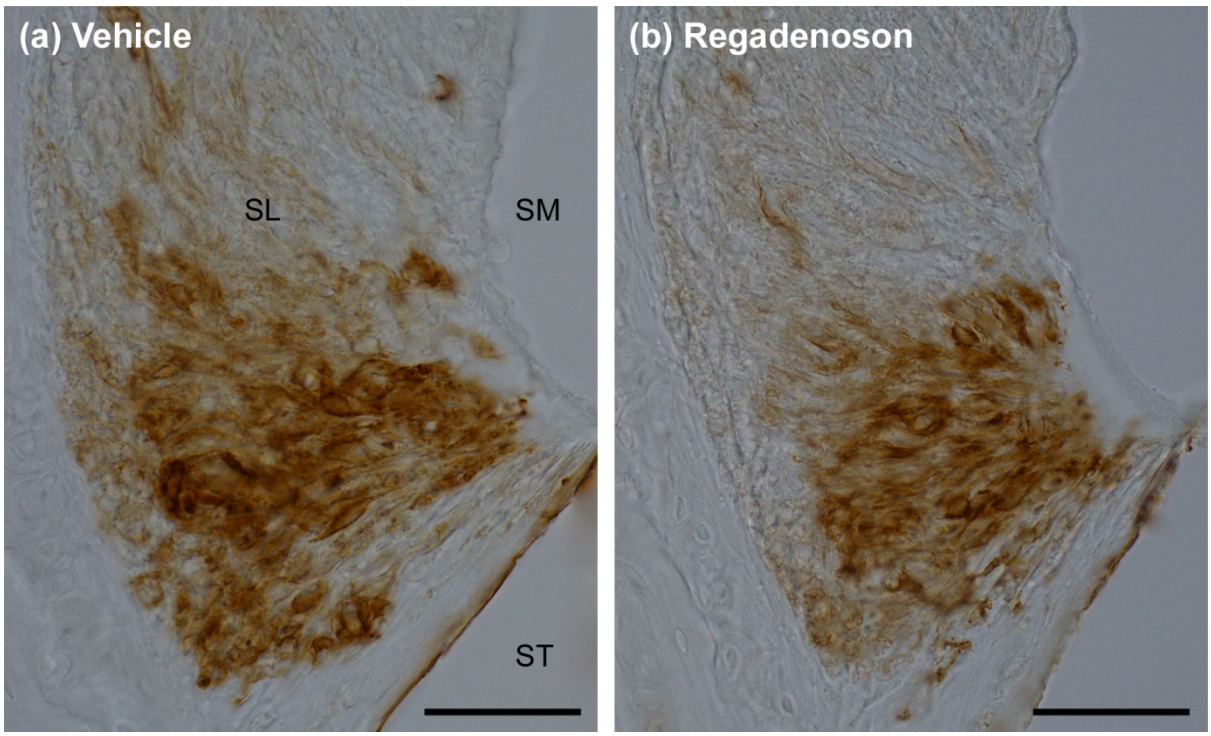

Figure 4.39: ICAM-1 immunostaining in the spiral ligament of the cochlear basal turn in C57BL/6 mice treated with drug vehicle or regadenoson following acute noise exposure. (**a**) ICAM-1 expression in the inferior region of the spiral ligament of the cochlear basal turn in a vehicle-treated mouse 24 h following acute exposure to traumatic noise (100 dB SPL, 8-16 kHz for 24 h). (**b**) Post-exposure regadenoson treatment reduced both the intensity and size of the ICAM-1 immunostaining in the spiral ligament. *Abbreviations*: SL, spiral ligament; SM, scala media; ST, scala tympani. Scale bars = 50 µm.

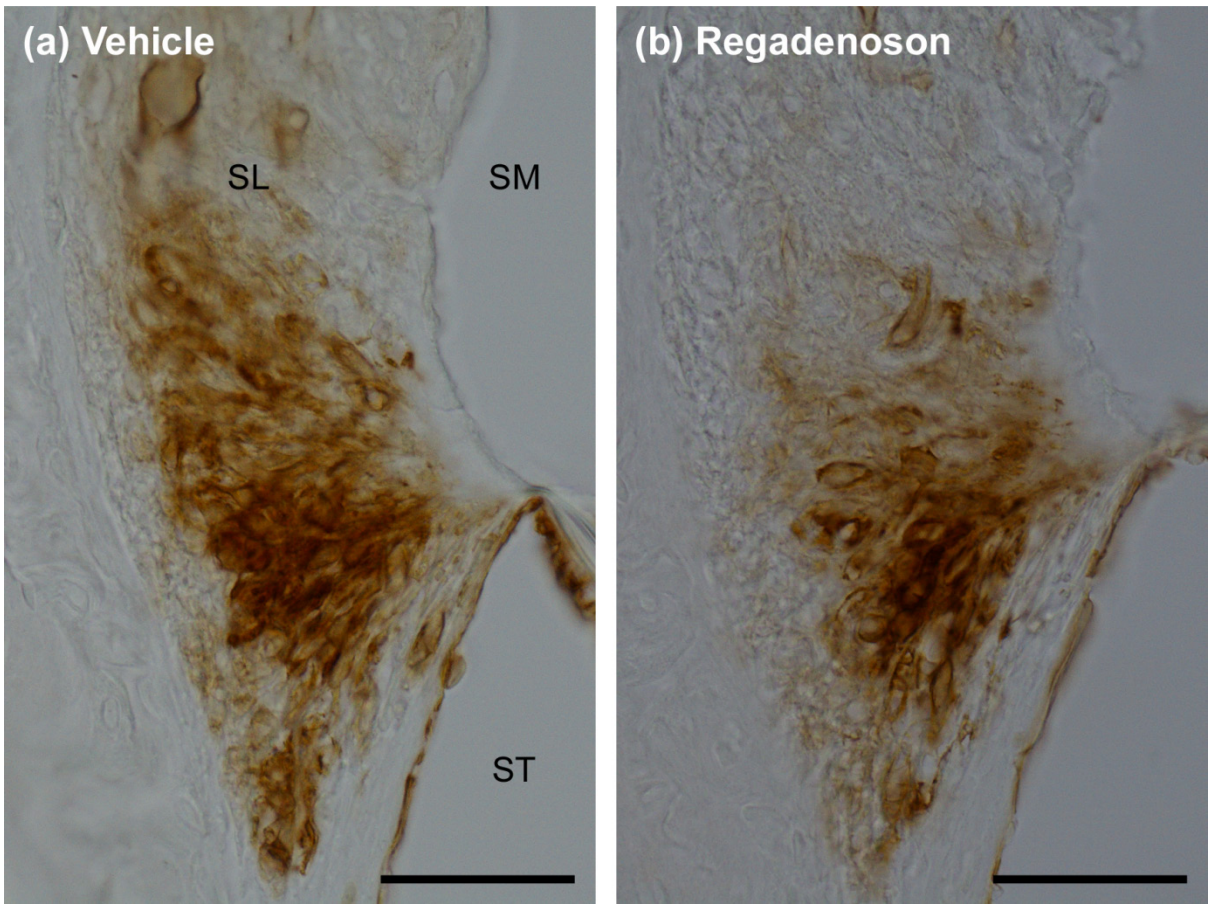

Figure 4.40: ICAM-1 immunostaining in the spiral ligament of the cochlear middle turn in C57BL/6 mice treated with drug vehicle or regadenoson following acute noise exposure. (**a**) ICAM-1 expression in the inferior region of the spiral ligament of the cochlear middle turn in a vehicle-treated mouse 24 h following acute exposure to traumatic noise (100 dB SPL, 8-16 kHz for 24 h). (**b**) Post-exposure regadenoson treatment reduced both the intensity and size of the ICAM-1 immunostaining in the spiral ligament. *Abbreviations*: SL, spiral ligament; SM, scala media; ST, scala tympani. Scale bars = 50 µm.

Table 4.8: Average intensity (mean gray value) and area of ICAM-1 immunostaining in the spiral ligament of the cochlear basal and middle turns in drug vehicle and regadenoson-treated C57BL/6 mice. Data presented as mean ± SEM (n = 6 per group).

	Average Mean Gray Value		Average Area (µm^2)	
Treatment Group	**Basal**	**Middle**	**Basal**	**Middle**
Vehicle	78.6 ± 1.4	69.7 ± 1.0	11,607 ± 699	6,902 ± 311
Regadenoson	82.9 ± 1.2	74.5 ± 1.5	10,050 ± 424	6,116 ± 211

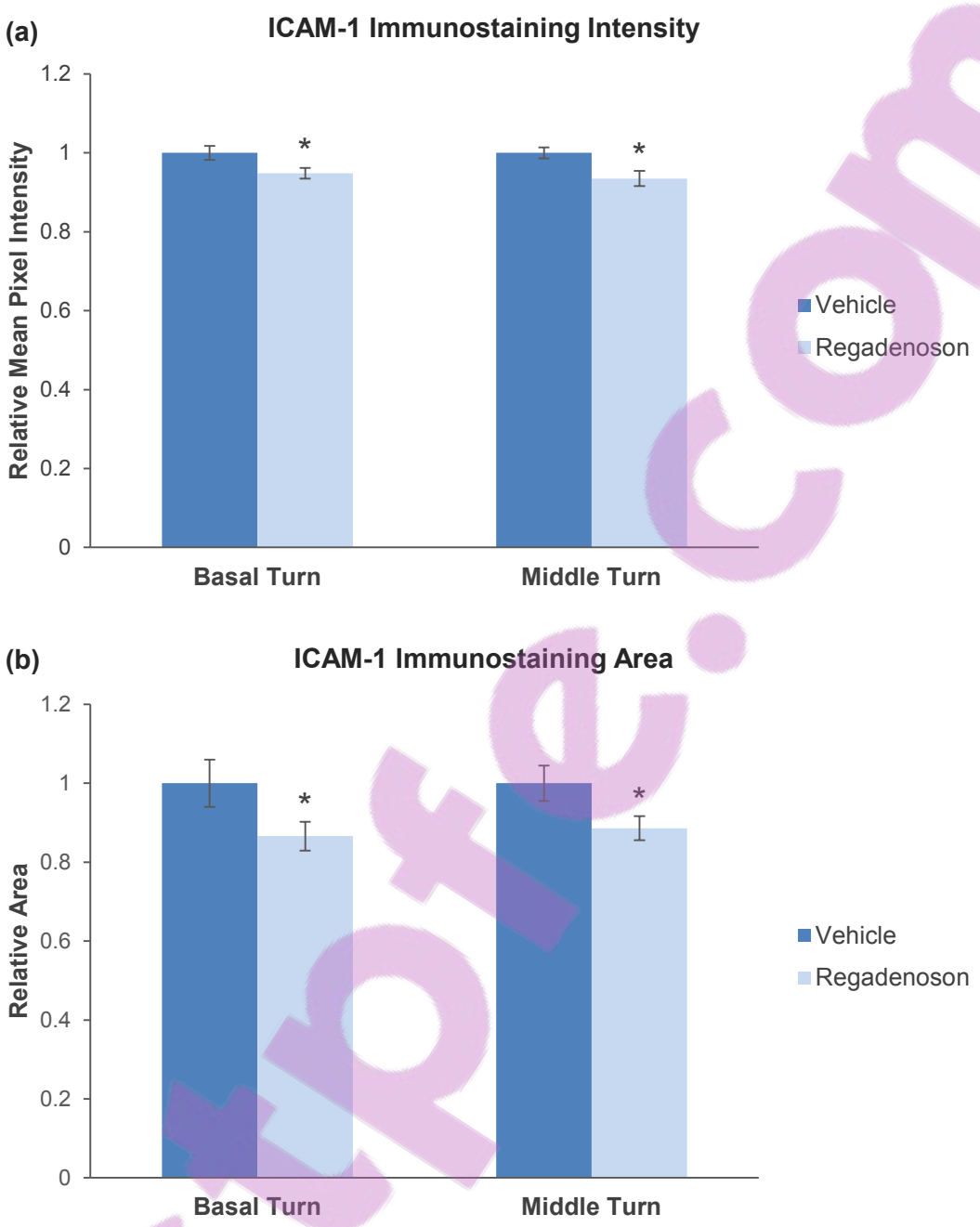

Figure 4.41: Semi-quantitative analysis of ICAM-1 immunostaining in the spiral ligament of the cochlear basal and middle turn in C57BL/6 mice treated with drug vehicle or regadenoson following acute noise exposure. The graphs illustrate the ratio of the intensity (**a**) and area (**b**) of ICAM-1 immunostaining in the inferior region of the spiral ligament of the cochlear basal and middle turns in regadenoson-treated mice relative to vehicle-treated mice 24 h following acute exposure to traumatic noise (100 dB SPL, 8-16 kHz for 24 h). Post-exposure regadenoson treatment significantly reduced the intensity and area of ICAM-1 immunostaining in both the cochlear basal and middle turns (*$p < 0.05$, unpaired *t*-test). Data presented as mean ± SEM ($n = 6$ per group).

4.4.3.3. Effect of Adenosine A_{2A} Receptor Activation on the Gene Expression Levels of TNF-α, CCL2, ICAM-1 and IL-1β in the Noise-Exposed Cochlea

The effect of regadenoson treatment on the gene expression levels of inflammatory cytokines/chemokines (TNF-α, IL-1β, CCL2) and cell adhesion molecules (ICAM-1) in the noise-exposed cochlea was assessed at 6 and 24 h post-exposure using quantitative real-time RT-PCR (n = 8 per time point). As expected, there was no significant difference in the cochlear transcript levels of all four inflammatory-related genes between vehicle controls and regadenoson-treated mice at 24 h following noise exposure ($p > 0.05$, unpaired t-test) (**Figure 4.43**). As demonstrated earlier (**Section 4.2.2**), mRNA levels of all inflammatory markers returned to pre-noise (baseline) levels at 24 h after noise exposure following the initial peak in expression at 6 h post-exposure. However, regadenoson treatment also did not alter gene expression levels at 6 h after noise exposure ($p > 0.05$, unpaired t-test) (**Figure 4.42**) despite the observed decrease in the protein expression of ICAM-1. Therefore, the results showed no change in the cochlear gene expression levels of TNF-α, ICAM-1, CCL2 and IL-1β following post-exposure regadenoson treatment in mice.

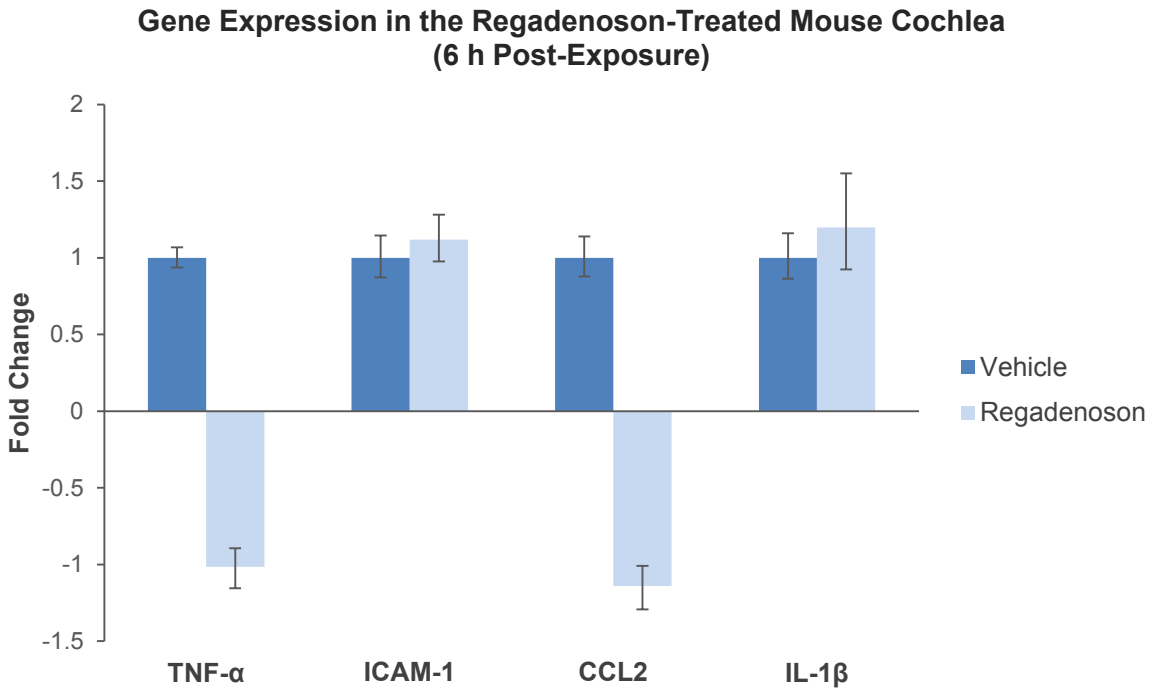

Figure 4.42: Quantitative real-time RT-PCR analysis of TNF-α, ICAM-1, CCL2 and IL-1β gene expression in the cochleae of regadenoson-treated C57BL/6 mice 6 h following acute noise exposure. The graph illustrates the fold change in gene expression of TNF-α, ICAM-1, CCL2 and IL-1β in the cochleae of regadenoson-treated mice relative to vehicle-treated mice 6 h following acute exposure to traumatic noise (100 dB SPL, 8-16 kHz for 24 h). There was no significant difference in the cochlear mRNA expression levels of all four proinflammatory genes between vehicle and regadenoson-treated mice ($p > 0.05$, unpaired *t*-test). Data presented as mean ± SEM ($n = 8$ per group).

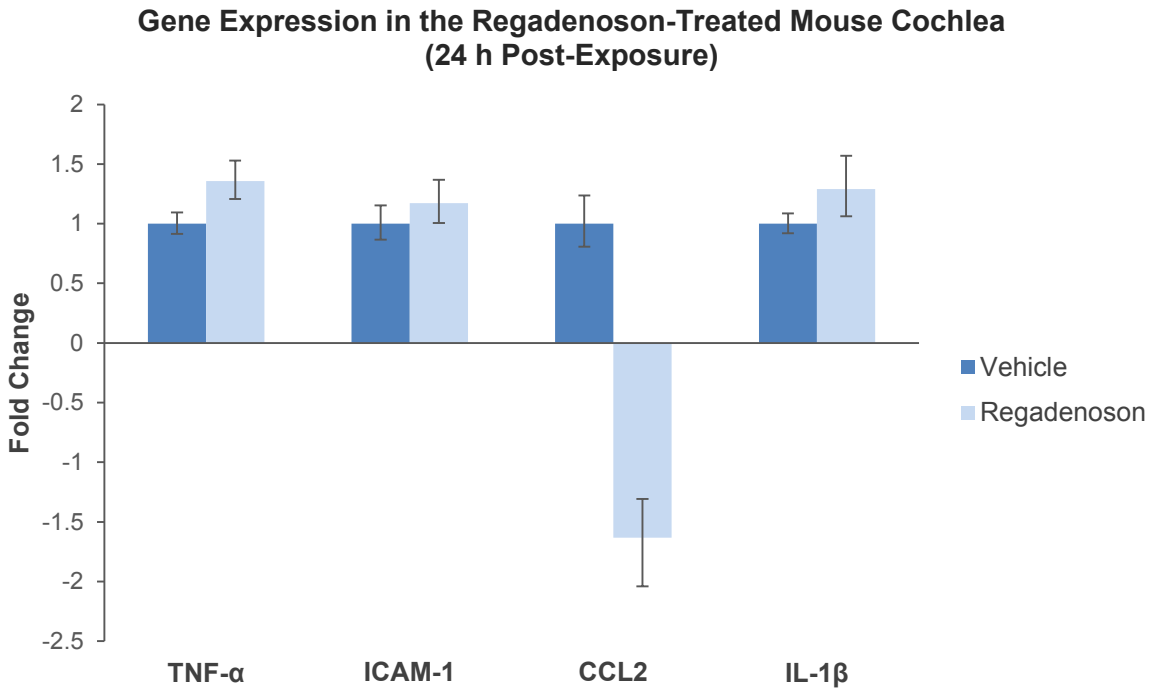

Figure 4.43: Quantitative real-time RT-PCR analysis of TNF-α, ICAM-1, CCL2 and IL-1β gene expression in the cochleae of regadenoson-treated C57BL/6 mice 24 h following acute noise exposure. The graph illustrates the fold change in gene expression of TNF-α, ICAM-1, CCL2 and IL-1β in the cochleae of regadenoson-treated mice relative to vehicle-treated mice 24 h following acute exposure to traumatic noise (100 dB SPL, 8-16 kHz for 24 h). There was no significant difference in the cochlear mRNA expression levels of all four proinflammatory genes between vehicle and regadenoson-treated mice ($p > 0.05$, unpaired *t*-test). Data presented as mean ± SEM ($n = 8$ per group).

In summary, this final study has demonstrated expression of adenosine A_{2A} receptors mainly in the blood vessels of the cochlea, and that immunoexpression of the receptor increased in the inferior region of the spiral ligament following noise exposure. In addition, numerous adenosine A_{2A} receptor-positive infiltrating cells were observed in the cochlea following noise exposure, peaking 24 h post-exposure. These cells were mainly located in the scala tympani, attached to the wall of the perilymph-filled compartment. Using $A_{2A}RKO^{-/-}$ mice, it was shown that deletion of the adenosine A_{2A} receptor gene resulted in a larger increase in ICAM-1 immunoexpression in the basal turn and lower gene expression levels of CCL2 and IL-1β following noise exposure. Furthermore, it was demonstrated that activation of adenosine A_{2A} receptors in the cochlea after noise exposure using the selective adenosine A_{2A} receptor agonist, regadenoson, reduced ICAM-1 immunoexpression and cellular infiltration.

CHAPTER 5: DISCUSSION

5.1. Introduction

Hearing loss is the most common sensory disability and has considerable social and economic implications. According to 2012 estimates by the World Health Organisation, 360 million people worldwide suffer from moderate to profound hearing loss (over 5% of the world's population). Exposure to excessive noise is one of the major causes of sensorineural hearing loss, secondary only to age-related hearing loss (presbyacusis). Acoustic overstimulation inflicts injury to the cochlea, affecting almost all cell types, particularly the sensory hair cells. Since sensory cells in the mammalian cochlea are incapable of regeneration, unlike those in the avian cochlea, this damage is irreversible, leading to cochlear dysfunction and permanent hearing loss. A significant proportion (16%) of the disabling hearing loss in the adult population worldwide is attributed to occupational noise exposure (WHO, 2002), ranging from 7% in the most developed countries to 21% in developing regions (Nelson *et al.*, 2005). Hence, substantial efforts have been made over the years to understand the pathophysiological mechanisms underlying noise-induced cochlear injury in order to develop pharmacological interventions to reduce or prevent noise-induced hearing loss.

There is a growing body of evidence that oxidative stress in the cochlea induced by the acoustic overstimulation is a key mechanism of the noise-induced injury (Ohlemiller *et al.*, 1999; Henderson *et al.*, 2006; Talaska & Schacht, 2007; Poirrier *et al.*, 2010; Wong *et al.*, 2013; Hu & Henderson, 2014). This involves the excessive production of ROS and free radicals in cochlear tissues, which can lead to substantial sensory hair cell loss via both the apoptotic and necrotic cell death pathways. Oxidative stress is also implicated in age-related and drug-induced cochlear injury (ototoxicity) and the resultant hearing loss (Poirrier *et al.*, 2010; Hu & Henderson, 2014). In addition, ischemia/reperfusion injury, glutamate excitotoxicity (at inner hair cell – type I spiral ganglion neuron synapses), and calcium overload (in outer hair cells) are also thought to have important roles in the pathogenesis of noise-induced hearing loss (Fridberger *et al.*, 1998; Puel *et al.*, 1998; Pujol & Puel, 1999; Le Prell *et al.*, 2007; Henderson *et al.*, 2008).

Emerging evidence suggests that inflammation may also be a major contributor to noise-induced cochlear injury and hearing loss. Early ultrastructural studies in the noise-exposed mammalian cochlea using electron microscopy identified a population of macrophage-like cells in the damaged organ of Corti (Fredelius, 1988; Fredelius & Rask-Andersen, 1990). Subsequent studies demonstrated the presence of a robust inflammatory response in the cochlea following acoustic overstimulation characterised by the production of proinflammatory mediators followed by a large influx of inflammatory cells into the cochlea from the vasculature (Hirose *et al.*, 2005; Fujioka *et al.*, 2006; Tornabene *et al.*, 2006; Shi & Nuttall, 2007; Sato *et al.*, 2008; Tan *et al.*, 2008; Yamamoto *et al.*, 2009; Jo *et al.*, 2010; Wakabayashi *et al.*, 2010; Nakamoto *et al.*, 2012). Interestingly, the cochlea was originally considered an immunologically privileged organ because of its separation from the systemic circulation by the blood-labyrinth barrier. However, later studies refuted this evidence by demonstrating that the cochlea was capable of generating an inflammatory/immune response (labyrinthitis) in the presence of bacterial or viral pathogens or antigens (Harris, 1983; Harris, 1984; Harris *et al.*, 1990; Fukuda *et al.*, 1992). Cochlear inflammation is also implicated as a causative factor in a range of other conditions that cause hearing loss including otitis media, meningitis, ototoxicity, and autoimmune inner ear disease (Kawauchi *et al.*, 1988; Gloddek *et al.*, 1999; Trinidad *et al.*, 2005; So *et al.*, 2007; So *et al.*, 2008; Cayé-Thomasen *et al.*, 2009). Cochlear surgery and the insertion of cochlear implants can also evoke an inflammatory reaction due to the local exogenous stress on the cochlea (Backhouse *et al.*, 2008; Okano *et al.*, 2008; Kel *et al.*, 2013).

It is recognised that noise-induced cochlear inflammation involves complex signalling pathways. To date, various inflammation-related genes and proteins (transcription factors, cytokines, chemokines and cell adhesion molecules) have been implicated in the inflammatory response (Hirose & Keasler, 2004; Fujioka *et al.*, 2006; Kirkegaard *et al.*, 2006; Tornabene *et al.*, 2006; Shi & Nuttall, 2007; Yamamoto *et al.*, 2009; Jo *et al.*, 2010; Wakabayashi *et al.*, 2010; Nakamoto *et al.*, 2012), yet the precise molecular mechanisms underlying the response and its role in the development of cochlear injury remain to be elucidated. Therefore, the present study was designed to achieve a better understanding of the underlying cellular and molecular mechanisms that comprise the inflammatory response in the mammalian cochlea induced by noise exposure (acute and chronic). In addition, as a potential treatment strategy for mitigating noise-induced cochlear inflammation and the concomitant hearing loss, the anti-inflammatory effect of adenosine A_{2A} receptor activation

in the noise-exposed cochlea was explored using the selective adenosine A_{2A} receptor agonist, regadenoson.

5.2. Summary of Findings

In order to address these important research questions, an experimental mouse model of noise-induced hearing loss was firstly established. A main advantage for using animal models in studies of noise-induced hearing loss is that noise can be presented at a defined intensity, frequency and duration. Furthermore, researchers can harvest cochlear tissues at various time points following noise exposure for histological and molecular analysis. In contrast to this, human cochlear tissues can only be accessed for examination at autopsy. By then, a lengthy time will have elapsed since the noise exposure and hence the pathological changes observed in the cochlea may in fact reflect the cumulative impact of noise exposure over many years as well as the effects of other environmental/external factors and aging. All studies in this research project were carried out on C57BL/6 mice, which is the most widely used inbred strain of laboratory mice. An advantage of inbred strains of mice for noise studies is the low variability in outcome measures between different mice (inter-animal variability) due to their genetic homogeneity (Wang *et al.*, 2002).

Here, two models of noise exposure were utilised, an acute exposure that leads to a permanent threshold shift, and a chronic exposure at a level that induces a temporary loss of function. For the experimental model of permanent noise-induced hearing loss, mice were exposed to 100 dB SPL octave band (8-16 kHz) noise for 24 h. Permanent threshold shift was corroborated by measuring auditory thresholds prior to and one month after noise exposure using ABRs, a standard method of assessing auditory function in small rodents. Acute exposure to traumatic noise produced significant hearing loss, with all mice sustaining comparable permanent threshold shifts to both tone pips and acoustic clicks.

The present study clearly demonstrated that the C57BL/6 mouse cochlea mounts a substantial inflammatory response following exposure to traumatic noise. A number of inflammatory genes and proteins were increased following noise exposure as demonstrated by quantitative real-time RT-PCR and immunohistochemistry. The results revealed significant upregulation in the transcriptional expression of the proinflammatory cytokines TNF-α and IL-1β, the

chemokine CCL2 and the cell adhesion molecule ICAM-1, and also an elevated protein expression of ICAM-1 and PECAM-1 in the noise-exposed cochlea. Concomitant with the upregulation of proinflammatory mediators and cell adhesion molecules was an increased number of adenosine A_{2A} receptor-expressing cells in the cochlea, which were most likely infiltrating inflammatory cells recruited from the systemic circulation. Interestingly, chronic exposure to moderate noise levels, which is thought to produce only a temporary threshold shift, also induced an inflammatory reaction within the cochlea, with increased expression of the aforementioned inflammatory mediators and cell adhesion molecules. Furthermore, the study also successfully demonstrated for the first time that stimulation of adenosine A_{2A} receptors in the noise-exposed cochlea with the selective adenosine A_{2A} receptor agonist, regadenoson, mitigates some aspects of the noise-induced cochlear inflammatory response, reducing ICAM-1 immunoexpression and cellular infiltration.

5.3. Gene Expression Levels of Inflammatory Mediators in the Noise-Exposed Cochlea

The presence of a biphasic inflammatory response in the noise-damaged cochlea, as shown by the increased expression of TNF-α, CCL2, ICAM-1 and IL-1β at 6 h and 7 days post-exposure, was rather unexpected as previous studies have reported the local upregulation of these inflammatory mediators only in the early phase of noise-induced cochlea trauma (Hirose & Keasler, 2004; Fujioka *et al.*, 2006; Tornabene *et al.*, 2006; Jo *et al.*, 2010; Wakabayashi *et al.*, 2010; Nakamoto *et al.*, 2012). It is speculated that the initial rise in expression levels of these cytokines, chemokines and cell adhesion molecules in the noise-exposed cochlea mediates the recruitment and extravasation of inflammatory cells, which could exacerbate the noise-induced cochlear damage by causing bystander injury (a source of secondary damage). The occurrence of the latter peak in expression at seven days after acoustic trauma is not clear, but it is postulated that it may be associated with reparative processes, i.e. a wound healing response (this will be further discussed in **Section 5.7**).

Expression of TNF-α, considered one of the primary mediators of inflammation, was substantially upregulated following acoustic overstimulation. Studies on organ of Corti explants have shown that TNF-α alone, in the absence of antigens or pathogens, has the ability to induce the recruitment of inflammatory cells from the systemic circulation into the

cochlea (Keithley *et al.*, 2008). Furthermore, blocking TNF-α using Etanercept, a soluble TNF-α-receptor-FC fusion protein, significantly attenuates the cochlear inflammatory response in animal models of labyrinthitis induced by the inoculation of KLH into the inner ear (Satoh *et al.*, 2002; Wang *et al.*, 2003b). Taken together, these data therefore strongly suggest that TNF-α plays a pivotal role in the development of cochlear inflammation.

In addition to TNF-α and IL-1β, transcript levels of IL-6, another cytokine traditionally associated with inflammation, was also analysed in the noise-exposed cochlea. Unfortunately, no quantitative real-time RT-PCR data for IL-6 was obtained due to potential problems with the IL-6 primer/probe set used in the experiment. However, previous studies have documented that IL-6 is also significantly induced in the cochlea following noise exposure (Fujioka *et al.*, 2006; Wakabayashi *et al.*, 2010). This upregulation of IL-6 likely contributes to noise-induced cochlear injury, as post-exposure inhibition of IL-6 using IL-6 receptor neutralising antibody (MR16-1) effectively suppresses the cochlear inflammatory response (macrophage infiltration) and mitigates hearing loss (Wakabayashi *et al.*, 2010).

Of the four proinflammatory genes examined in this study, CCL2 (also known as MCP-1), which is an inflammatory chemokine with potent monocyte/macrophage chemotactic activity, showed the largest upregulation in the cochlea following noise exposure, with an approximate 23-fold increase relative to controls at 6 h post-exposure. This is similar to previous studies (Sautter *et al.*, 2006; Tornabene *et al.*, 2006), suggesting that CCL2 may play a key role in the recruitment of inflammatory cells into the noise-damaged cochlea. However, the study conducted by Sautter *et al.* (2006) showed that neither CCL2 nor its receptor CCR2 is necessary for inflammatory cell migration into the cochlea after acoustic injury. No suppression of monocyte migration was observed in the cochleae of $CCL2^{-/-}$ or $CCR2^{-/-}$ knockout mice after acoustic trauma (Sautter *et al.*, 2006). It appears that other chemokines/chemokine receptors are capable of replacing the roles of CCL2/CCR2 in the noise-exposed cochlea. Consistent with these findings, another study showed that deficiency of CCL2 or CCR2 did not inhibit otitis media-induced migration of monocytes into the cochlea due to unspecified compensatory mechanisms (Woo *et al.*, 2010).

It is likely that these proinflammatory mediators are expressed and secreted by various resident cells in the cochlea, particularly the fibrocytes in the spiral ligament. *In vitro* studies using cultured murine spiral ligament fibrocytes have shown that upon stimulation with

proinflammatory cytokines (TNF-α, IL-1β), fibrocytes secrete various inflammatory mediators such as TNF-α, IL-1β, IL-6, monocyte chemoattractant protein-1 (MCP-1), macrophage inflammatory protein-2 (MIP-2), keratinocyte-derived chemokine (KC), soluble intercellular adhesion molecule-1 (sICAM-1) and vascular endothelial growth factor (VEGF) (Yoshida *et al.*, 1999; Ichimiya *et al.*, 2000; Maeda *et al.*, 2005; Moon *et al.*, 2006). It is likely that endothelial cells within the spiral ligament also secrete inflammatory mediators. Once released, cytokines and chemokines appear to act in an autocrine and paracrine manner, promoting further release. It has been speculated that chemokines produced by the fibrocytes are presented onto the luminal surface of vascular endothelial cells via transcytosis (Yoshida *et al.*, 1999). The chemokines then bind to glycosaminoglycans (GAGs) on the endothelial cell surface, facilitating their retention at the inflammatory site, and enabling a localised high concentration of chemokines, which in turn provides a directional cue for inflammatory cells (Proudfoot *et al.*, 2003; Allen *et al.*, 2007). Engagement of chemokines with their corresponding receptors on leukocytes would consequently activate these leukocytes.

Due to the lack of specificity of antibodies used in the immunolabelling experiments, the cellular source of each of the upregulated proinflammatory cytokines (TNF-α, IL-6 and IL-1β) in the noise-exposed cochlea was not able to be determined. However, the localisation and expression profiles of these cytokines in the cochlea have been reported by previous studies in various models of cochlear inflammation. The study by Fujioka *et al.* (2006) demonstrated the induction of IL-6 expression in type IV and type III fibrocytes in the lower and lateral part of the spiral ligament respectively as well as in the stria vascularis and spiral ganglion neurons in the noise-exposed rat cochlea. IL-1β has also been shown to be expressed in the fibrocytes of the spiral ligament following acoustic trauma (Hashimoto *et al.*, 2004). In addition, in a mouse model of cochlear inflammation induced by the inoculation of KLH into the inner ear, expression of IL-6 was localised in type II fibrocytes in the spiral ligament while IL-1β was expressed by type I fibrocytes in the spiral ligament and fibrocytes in the spiral limbus (Satoh *et al.*, 2002). Cytokines are also produced in the cochlea following cisplatin injection, and have been suggested to play a central role in cisplatin-induced ototoxicity (So *et al.*, 2007). TNF-α expression was observed mainly in the spiral ligament, stria vascularis, spiral limbus, spiral modiolar veins and hair cells in the organ of Corti. IL-1β was expressed in the spiral ligament and spiral modiolar veins, while IL-6 was localised exclusively in the spiral modiolar veins.

Resident tissue macrophages can produce and secrete cytokines (Gordon & Taylor, 2005), and resident cochlear macrophages likely have a similar role. In addition, infiltrating inflammatory cells also express their own cytokines (Allan & Rothwell, 2001; Satoh *et al.*, 2002), which may further amplify the recruitment of inflammatory cells. This positive feedback loop possibly continues to recruit inflammatory cells until the levels of cytokines start to decrease. Because previous reports show expression of cytokines and chemokines within a few hours post-exposure prior to the influx of inflammatory cells, it is most likely that the resident cochlear cells are responsible for their initial upregulation rather than infiltrating inflammatory cells. The earliest endpoint examined in the present study was 6 h post-exposure, but it is possible that the induction of gene expression occurred earlier. The latter upregulation in gene expression observed at seven days post-exposure, on the other hand, is likely the contribution of both resident cells in the cochlea (e.g. fibrocytes and resident macrophages) and non-resident inflammatory cells recruited from the circulation.

The cochlear activation of p65 and p50, the two predominant subunits of the transcription factor NF-κB, which regulates the expression of various proinflammatory mediators and cell adhesion molecules, was examined in the noise-exposed cochlea. p65 immunoreactivity was localised primarily in the spiral ligament, marginal cells of the stria vascularis, spiral limbus and organ of Corti, whereas p50 was observed in the spiral ligament and spiral ganglion. Aside from the spiral ligament, it is surprising that the immunolocalisation of p65 and p50 in the cochlea differ as they are normally found together as a heterodimeric complex. Expectedly, NF-κB immunofluorescence in the quiescent cells of the non-exposed cochlea was confined to the cytoplasm, indicative of their inactive form. At 6 h following noise exposure, the cytoplasmic immunofluorescence staining became considerably weaker compared to the non-exposed controls, but the expected shift of p65 or p50 immunostaining from the cytoplasm into the nucleus was not observed. Even after shortening the noise exposure to 2 h and examining NF-κB activation immediately, 2 h or 6 h after exposure, no nuclear translocation of NF-κB was detected despite the decrease in cytoplasmic immunofluorescence intensity. The study by Masuda *et al.* (2006) demonstrated nuclear activation of both subunits of NF-κB in fibrocytes in the lateral wall of the C57BL/6 mouse cochlea 2 h following exposure to an intense noise (124 dB SPL, 4 kHz for 2 h). However, no nuclear staining was detected again even after using higher noise levels (110 dB SPL for 2 h). It is not clear why the expected shift in NF-κB immunostaining to the nucleus was not observed despite the consistent decrease in the cytoplasmic expression of NF-κB in the noise-

exposed cochlea. A possible explanation is that nuclear translocation and activation of NF-κB did occur in these cells, but the antibodies for p65 and p50 could not reach cell nuclei, thereby resulting in the absence of nuclear staining. Alternatively, noise exposure parameters used in the present study were insufficient to trigger NF-κB translocation to the nucleus.

NF-κB can be activated by TNF-α and IL-1β through TNF-receptor associated factors (TRAFs), a family of intracellular adaptor proteins that bind directly or indirectly to members of the TNF receptor and the IL-1/Toll-like receptor (IL-1R/TLR) superfamily (Dempsey *et al.*, 2003). TRAFs induce the activation of mitogen-activated protein kinases (MAPKs), which phosphorylate and activate IκB kinases, which in turn phosphorylate and ubiquitinate the inhibitors of κB (IκBs), leading to their degradation. This releases NF-κB, allowing it to translocate into the nucleus and activate the transcription of target genes. TRAFs also mediate the activation of other signalling pathways such as the JNK, ERK, p38 and PI3K pathways (Dempsey *et al.*, 2003).

The exact mechanisms of how proinflammatory mediators are generated by cochlear fibrocytes following noise exposure have not been identified. It is speculated that there is an early immediate release of pre-existing stores of TNF-α and IL-1β following noise exposure by noise-damaged cochlear cells and/or resident macrophages, which then bind to their corresponding receptors on fibrocytes, activating the NF-κB signalling pathway and ultimately the expression of the various proinflammatory mediators. This is consistent with the findings from the *in vitro* studies mentioned earlier in which cultured spiral ligament fibrocytes produced various inflammatory mediators after stimulation with TNF-α and IL-1β. In addition, ROS produced during oxidative stress can also induce the generation of proinflammatory mediators. Kaur *et al.* (2011) showed that the increased expression of inflammatory mediators such as TNF-α, iNOS and COX-2 following cisplatin treatment was due to the activation of the transcription factor STAT1, whose activation was dependent on ROS generation.

5.4. Immunoexpression of Cell Adhesion Molecules in the Noise-Exposed Cochlea

This study demonstrated expression and distribution of ICAM-1 in both the normal and noise-exposed mouse cochlea largely in the type IV fibrocytes and vascular endothelial cells in the lowermost region of spiral ligament. Other blood vessels in the spiral ligament, stria vascularis, spiral limbus and spiral ganglion, as well as the endothelium of collecting venules and the endosteal cells lining the scala tympani also showed ICAM-1 immunolabelling. The significant increase in ICAM-1 expression in the spiral ligament of both the cochlear middle and basal turns 24 h after noise exposure is consistent with the early upregulation (6 h post-exposure) in the cochlear gene expression of ICAM-1, suggesting that ICAM-1 protein is newly produced by translation between 6 and 24 h after noise exposure. These findings are consistent with previous studies by Tornabene *et al.* (2006), Miyao *et al.* (2008) and Yamamoto *et al.* (2009), showing that ICAM-1 likely plays a crucial role in the extravasation of inflammatory cells in the cochlea during the noise-induced inflammatory response. A previous study (Seidman *et al.*, 2009) demonstrated that treatment of rats with anti-ICAM-1 antibody significantly attenuated noise-induced temporary threshold shifts, suggesting the pivotal role of ICAM-1 in inflammation-induced cochlear damage.

Increased expression of ICAM-1 in various cells has been attributed to stimulation by proinflammatory cytokines (TNF-α). An *in vitro* study by Ichimiya *et al.* (2003) demonstrated that cultured murine spiral ligament fibrocytes expressed the cell adhesion molecules ICAM-1 and VCAM-1 at both the mRNA and protein level upon stimulation with TNF-α. This is presumably mediated by cytokine-induced activation of NF-κB activity, as described earlier. In addition to proinflammatory cytokines, ROS can also promote ICAM-1 expression in endothelial cells (Lo *et al.*, 1993; Linas *et al.*, 1995). Thus, Lo *et al.* (1993) reported that cultured human umbilical vein endothelial cells treated with hydrogen peroxide (H_2O_2) showed an increase in both mRNA and protein expression of ICAM-1 within 0.5 to 2 h of stimulation. Similar increase in ICAM-1 expression can be postulated for the noise-exposed cochlea due to excessive ROS production.

Data in this study show that in addition to vascular endothelial cells, type IV fibrocytes of the spiral ligament have the potential to express ICAM-1. Other studies have also documented the expression of cell adhesion molecules on certain connective tissue cells. For example,

lung fibroblasts, upon stimulation by TNF-α and IL-1β, increase their expression of ICAM-1 and VCAM-1 (Spoelstra *et al.*, 1999). This is thought to be important for the migration of inflammatory cells through the submucosa to the lumen of the airway during the asthmatic inflammatory response. In the cochlea, the expression of ICAM-1 by fibrocytes in the lateral wall suggest that they may serve some role in regulating and directing the infiltration and migration of inflammatory cells among the spiral ligament fibrocytes following noise exposure. The inflammatory cells may persist in the spiral ligament via binding to the cell adhesion molecules on the fibrocytes.

During steady-state conditions, integrins on the surface of leukocytes cannot bind to the cell adhesion molecules on endothelial cells, as they first need to be activated by intracellular signals transmitted via stimulation with various chemokines (Hynes, 1992). It has been speculated that chemokines such as CCL2 produced by fibrocytes in the spiral ligament are presented onto the luminal surface of vascular endothelial cells via the process of transcytosis, which would consequently activate inflammatory cells and allow them to extravasate (Yoshida *et al.*, 1999).

The observed expression pattern of ICAM-1 in the cochlea following noise exposure resembles that seen following antigen challenge into the inner ear of sensitised (pre-immunised) animals (condition known as immune-mediated labyrinthitis) (Suzuki & Harris, 1995; Pawankar *et al.*, 1998) and in response to cochlear electrode implantation (Kel *et al.*, 2013). Suzuki and Harris (1995) demonstrated strong expression of ICAM-1 in the spiral ligament and the spiral modiolar vein and its collecting venules in the early phase of labyrinthitis (6 h to 2 days post-challenge) induced by the inoculation of KLH into the scala tympani of sensitised animals. Furthermore, a recent study which examined the early response of the cochlea to implantation of a cochlear electrode into the scala tympani reported an increased expression of ICAM-1 in the spiral ligament (type II and IV fibrocytes), peaking 24 h post-implantation, a time course similar to that observed in the present study (Kel *et al.*, 2013).

Consistent with ICAM-1 expression, PECAM-1 was constitutively expressed in the blood vessels of the cochlea and showed increased expression one to three days following noise exposure. PECAM-1 is therefore also likely to play an important role in the extravasation of inflammatory cells during the noise-induced cochlear inflammatory response. While ICAM-1

is expressed on the luminal surface of vascular endothelial cells and mediates the temporary adherence of leukocytes to the vasculature, PECAM-1 is localised in the intercellular junctions of endothelial cells and mediates the transmigration of leukocytes across the endothelium (Muller *et al.*, 1993). Furthermore, in contrast to ICAM-1, PECAM-1 was not expressed by type IV fibrocytes, suggesting it does not have a potential role like ICAM-1 in directing and regulating the migration of inflammatory cells among the fibrocytes of the spiral ligament.

Other cell adhesion molecules that have shown elevated protein expression following noise exposure include P-selectin and VCAM-1 (Shi & Nuttall, 2007; Yamamoto *et al.*, 2009). P-selectin is involved in the initial step in the extravasation process, mediating the deceleration and rolling of leukocytes along the luminal surface of activated endothelial cells by forming loose connections with the circulating leukocytes. VCAM-1, another member of the immunoglobulin superfamily, plays a similar role to ICAM-1, facilitating the temporary immobilisation of leukocytes to the endothelium. The entire extravasation process thus consists of three successive stages: 1) rolling, mediated by P-selectin (and E-selectin); 2) firm adhesion, mediated by ICAM-1 and VCAM-1; and 3) transendothelial migration, mediated by PECAM-1.

It has been previously demonstrated by Shi and Nuttall (2007) that the expression of cell adhesion molecules such as ICAM-1, PECAM-1 and P-selectin is modulated by a DNA repair enzyme called PARP-1. They showed that in contrast to wild-type mice, no upregulation of cell adhesion molecules was observed in the blood vessels of the cochlear lateral wall in PARP-$1^{-/-}$ knockout mice following noise exposure. Consistent with the relative lack of cell adhesion molecules, increased numbers of leukocytes were also not detected in these noise-exposed mutant mice. The authors suggested that noise-induced cellular damage activates PARP-1 in endothelial cells lining capillaries of the spiral ligament and stria vascularis, which may act via NF-κB to regulate the expression of cell adhesion molecules in the lateral wall.

5.5. Adenosine A_{2A} Receptor Expression in the Noise-Exposed Cochlea

The distribution of adenosine A_{2A} receptor in the C57BL/6 mouse cochlea was characterised using immunofluorescence staining. The results showed adenosine A_{2A} receptor expression mainly confined to the cochlear vasculature. Positive immunolabelling was detected in blood vessels located in the spiral ligament, stria vascularis, spiral limbus, spiral ganglion, and modiolus. Within the spiral ligament, immunoreactivity was observed specifically in the inferior region and on the lateral side adjacent to the otic capsule. In addition, it is likely that some of the type IV fibrocytes in the inferior region of the spiral ligament also expressed adenosine A_{2A} receptors. A previously published study by our group (Vlajkovic *et al.*, 2007) showed that in the rat cochlea, adenosine A_{2A} receptors are also expressed in blood vessels but only those within the modiolus. Furthermore, in contrast to the mouse cochlea, adenosine A_{2A} receptors in the rat cochlea are also immunolocalised in the inner hair cells and supporting Deiters' cells of the organ of Corti, spiral ganglion neurons, and type II fibrocytes in the root region of the spiral ligament. This discrepancy in the immunostaining pattern between the mouse and rat cochlea implies a species-specific difference in the cochlear distribution of adenosine A_{2A} receptors.

The abundant expression of adenosine A_{2A} receptors in the vasculature of the cochlea implicates a role of adenosine signalling in the regulation of cochlear blood flow. Indeed, adenosine has been demonstrated to induce a dose-dependent increase in cochlear blood flow (Muñoz *et al.*, 1999). Adenosine A_{2A} receptor expression in the cochlear vasculature is consistent with the expression of the receptor in the brain. It is thought that during systemic hypoxia, adenosine is released from the endothelium and acts on adenosine A_{2A} receptors on endothelial cells, and thus having a major role in the hypoxia-induced cortical vasodilation (Coney & Marshall, 1998).

Interestingly, the immunolocalisation of the adenosine A_{2A} receptor coincides with that of ICAM-1 in the vascular endothelial cells in the inferior region of the spiral ligament. Furthermore, both adenosine A_{2A} receptor and ICAM-1 showed increased immunolabelling in this region following noise exposure, suggesting an important association between the two. Noise-induced changes in the cochlear expression of adenosine A_{2A} receptor at the mRNA level was not assessed in the present study. However, a previous study carried out by our

group showed that the transcript level of adenosine A_{2A} receptor was not altered in the rat cochlea following prolonged exposure (24 h) to noise levels that induce either temporary (90 and 100 dB SPL) or permanent (110 dB SPL) hearing loss (Wong *et al.*, 2010). A similar finding in mice would suggest that there is only an increased translation (protein synthesis) of the receptor following noise exposure.

Because of the potent anti-inflammatory effects of adenosine via the adenosine A_{2A} receptor (Cronstein, 1994; Sullivan & Linden, 1998; Bours *et al.*, 2006; Cronstein, 2007) and the fact that extracellular levels of adenosine are elevated during acoustic overstimulation (Vlajkovic *et al.*, 2009), it is postulated that the increased expression of adenosine A_{2A} receptors in the cochlea following noise exposure may represent an important endogenous protective mechanism to limit inflammation. To gain further insight into the potential role of adenosine A_{2A} receptor-mediated signalling in noise-induced cochlear inflammation, genetically modified C57BL/6 mice lacking the gene encoding the adenosine A_{2A} receptor ($A_{2A}RKO^{-/-}$) were studied. This "loss of function" approach showed that the absence of adenosine A_{2A} receptors differentially affected specific aspects of the noise-induced cochlear inflammatory response. $A_{2A}RKO^{-/-}$ mice had a larger increase in ICAM-1 immunoexpression in the basal cochlear turn but lower gene expression levels of CCL2 and IL-1β after noise exposure. The much larger response to noise exposure in $A_{2A}RKO^{-/-}$ mice in regards to ICAM-1 protein expression is in line with the hypothesis that deletion of the adenosine A_{2A} receptor gene leads to a stronger cochlear inflammatory response. However, it is interesting that gene expression levels of CCL2 and IL-1β were downregulated after noise exposure while TNF-α and ICAM-1 expression levels remained unaltered. To further evaluate the effect of adenosine A_{2A} receptor gene deletion, it would be of interest in future studies to compare the number of inflammatory cells in the cochlea between noise-exposed wild-type and $A_{2A}RKO^{-/-}$ mice.

5.6. Adenosine A_{2A} Receptor-Positive Infiltrating Cells in the Noise-Exposed Cochlea

In addition to the immunofluorescence labelling in the cochlear vasculature, numerous adenosine A_{2A} receptor-expressing cells were observed in the noise-exposed cochlea, which were assumed to be infiltrating inflammatory cells recruited from the systemic circulation. This assumption was based on the similarity of their morphology and location to the cochlear inflammatory cells reported by previous studies (Hirose *et al.*, 2005; Tornabene *et al.*, 2006; Sato *et al.*, 2008; Tan *et al.*, 2008). The vast majority of the adenosine A_{2A} receptor-positive cells were found adherent to the wall of the scala tympani. Similarly, the previous studies also observed a large accumulation of infiltrating cells attached to the perilymphatic compartment wall. These cells were described as having a rounded shape or slightly flattened against the wall, which is consistent with the present study. Labelled round-shaped cells, which were similar in appearance to those in the scala tympani, were also present in the scala vestibuli, spiral ligament, spiral limbus, spiral ganglion and modiolus, but were notably absent in the organ of Corti and scala media. Most studies have also reported rare sightings of inflammatory cells in the organ of Corti, however early ultrastructural studies using electron microscopy identified phagocytic cells located in the noise-damaged organ of Corti, mainly in the tunnel of Corti and outer hair cell region (Fredelius, 1988; Fredelius & Rask-Andersen, 1990).

Because adenosine A_{2A} receptors are expressed by every type of immune cell, including those involved in both innate (monocytes, macrophages, neutrophils, dendritic cells, mast cells, natural killer cells) and adaptive (B and T lymphocytes) immunity (Sullivan & Linden, 1998; Bours *et al.*, 2006; Fredholm, 2007; Blackburn *et al.*, 2009; Haskó *et al.*, 2013), the nature of these infiltrating cells observed in the present study is unknown. However, others have characterised the population of inflammatory cells in the noise-exposed cochlea using immunohistochemistry with various leukocyte markers, and found that the vast majority are derived from the monocyte/macrophage lineage ($F4/80^+$, $CD68^+$, Iba-1^+, $CX3CR1^+$), with a small number representing other types of leukocytes such as polymorphonuclear leukocytes (e.g. neutrophils) and lymphocytes (Hirose *et al.*, 2005; Tornabene *et al.*, 2006; Okano *et al.*, 2008; Tan *et al.*, 2008). Hirose *et al.* (2005) proposed the term “cochlear macrophage” for these inflammatory cells, to indicate an inducible exchanging population of phagocytic cells that respond to acoustic injury.

In addition to the scala tympani, another location in the cochlea where inflammatory cells have been consistently observed is the spiral ligament, particularly in the inferior region where type IV fibrocytes are located. Morphologically, the cochlear macrophages observed in the spiral ligament, as well as in other cochlear structures such as the spiral limbus and spiral ganglion, have been characterised as possessing a spindle shape with several ramified processes, resembling tissue macrophages (Hirose *et al.*, 2005; Tornabene *et al.*, 2006; Okano *et al.*, 2008; Sato *et al.*, 2008; Tan *et al.*, 2008). It is possible that some of the adenosine A_{2A} receptor-positive cells observed in the inferior region of the spiral ligament could in fact be macrophages due to their ramified morphology; however this could not be verified.

Previous reports have suggested the vasculature of the lateral wall as the primary route of entry of inflammatory cells due to the large cellular infiltration observed in the spiral ligament following acoustic trauma and the highly vascularised nature of this cochlear region (Hirose *et al.*, 2005; Tan *et al.*, 2008). In addition, infiltrating cells within the fluid-filled spaces of the scala tympani and scala vestibuli are also likely to have migrated from the spiral modiolar vein and its collecting venules, which were traditionally thought to be the main vascular source of inflammatory cells (Harris *et al.*, 1990). In the early phase of acoustic injury (mainly at 6 h post-exposure), a few infiltrating cells appeared to be extravasating from the collecting venules below the lateral wall.

Cellular infiltration in the cochlea was short-lived, with the maximum number of infiltrating cells observed 24 h following the cessation of noise exposure (13.1 ± 1.8 $A_{2A}R^{+}$ cells/section), after which time the number of cells declined over the next six days. This time course is in contrast to previous reports in which peak cellular infiltration was observed between three and seven days after noise exposure (Discolo *et al.*, 2004; Hirose *et al.*, 2005; Tornabene *et al.*, 2006; Sato *et al.*, 2008; Tan *et al.*, 2008; Wakabayashi *et al.*, 2010). The cell densities reported in these prior studies were also much higher than that observed in the present study. In the current study, only round-shaped cells or those flat against the perilymphatic wall were included in the total cell count, whereas irregular-shaped cells, such as those observed in the lower portion of the spiral ligament, were excluded as their identity was not entirely clear. In addition, these previous studies utilised much higher noise levels (e.g. 118 dB to 124 dB SPL), which may have contributed to the larger cellular infiltration due to more extensive noise-induced injury to cochlear tissues.

The present study also revealed the presence of a few resident inflammatory cells (2.4 ± 0.5 $A_{2A}R^{+}$ cells/section) within the cochleae of non-exposed mice, which is consistent with previous studies (Hirose *et al.*, 2005; Lang *et al.*, 2006; Tornabene *et al.*, 2006; Okano *et al.*, 2008; Sato *et al.*, 2008). Data from radiation chimeras have shown that these resident cells form an exchanging and migratory population, supplied continuously from haematopoietic precursors in the bone marrow, and exhibiting slow turnover during steady-state conditions (Okano *et al.*, 2008; Sato *et al.*, 2008; Shi, 2010). These cochlear haematopoietic bone marrow-derived cells have been characterised to be derived from the monocyte/macrophage lineage, and morphologically resemble microglia, the resident tissue macrophage of the central nervous system (Okano *et al.*, 2008). Moreover, it has been demonstrated by bromodeoxyuridine (BrdU) labelling (a method of detecting proliferating cells) that the marked increase in cochlear macrophages following noise exposure arises from the migration of macrophages from the systemic circulation rather than the proliferation of these resident macrophages in the cochlea (Hirose *et al.*, 2005).

This recruitment of inflammatory cells from the systemic circulation to the noise-damaged cochlea is presumably mediated by the early upregulation (6 h post-exposure) of chemoattractant molecules such as proinflammatory cytokines (TNF-α, IL-1β) and chemokines (CCL2). The subsequent transendothelial migration (extravasation) of the recruited inflammatory cells is likely mediated by cell adhesion molecules such as ICAM-1 and PECAM-1, whose expression were shown to peak at the time of maximum cellular infiltration (24 h post-exposure). There is therefore a positive correlation between the upregulation of cell adhesion molecules and leukocyte infiltration. Furthermore, leukocyte recruitment also parallels cytokine and chemokine upregulation, with the peak in inflammatory cell infiltration (24 h post-exposure) occurring shortly following the initial peak in cytokine and chemokine expression (6 h post-exposure).

5.7. Role of Noise-Induced Cochlear Inflammation

The exact role infiltrating inflammatory cells play in the noise-damaged cochlea remains unclear. It is most likely that inflammatory cells (macrophages) are recruited to the cochlea to serve a purely phagocytic role, helping to clear cellular debris caused by acoustic trauma. This hypothesis is based on the fact that infiltrating cells are largely observed in the region of the spiral ligament (inferior region) where noise-induced fibrocyte loss is most evident (Wang *et al.*, 2002; Hirose *et al.*, 2005; Tornabene *et al.*, 2006; Ohlemiller, 2008; Sato *et al.*, 2008). In further support of this interpretation, inflammatory cells are present in the spiral limbus only in regions of the cochlea (lower apical turn) where there is pronounced fibrocyte loss after noise exposure, but not in other cochlear turns where no fibrocyte loss is observed (Hirose *et al.*, 2005). In addition to clearing cellular debris, macrophages may also contribute to the repair process by altering the local environment via the secretion of cytokines and growth factors, such as TNF-α, IL-6, IL-1, transforming growth factor-α/β, platelet-derived growth factor, and insulin-like growth factor-1 that regulate angiogenesis, fibroplasia, and matrix synthesis (a wound healing response) (Park & Barbul, 2004). Furthermore, a study by Abrashkin *et al.* (2006) has revealed a macrophage role for supporting cells in the organ of Corti, particularly the Deiters' cells, in the removal (phagocytosis) of injured/dead outer hair cells and/or their debris. Prestin, a protein unique to outer hair cells, was detected inside the cytoplasm of supporting cells in the organ of Corti damaged by acoustic overstimulation or ototoxic drugs.

Conversely, it is also possible that the damage to the fibrocytes in the spiral ligament and spiral limbus is caused directly by macrophages as a result of bystander injury as they infiltrate these regions from the vasculature and migrate among the fibrocytes on their way to clear debris of noise-damaged sensory cells. Macrophages can cause death of cells via the release of cytotoxic products such as quinolinate, ROS and nitric oxide (Park & Barbul, 2004; Ladrech *et al.*, 2007). Infiltration of inflammatory cells may therefore be another pathophysiological source of secondary damage in the cochlea. In addition to recruiting inflammatory cells, proinflammatory cytokines may be directly involved in the apoptotic death of hair cells. The JNK and p38 signalling pathways, which are associated with apoptosis among a variety of other cellular functions, are activated by proinflammatory cytokines such as TNF-α and IL-1β in various types of cochlear injury (Tabuchi & Hara, 2012). Several studies have indicated that the JNK signalling pathway is involved in both

ototoxicity and noise-induced hair cell death leading to permanent hearing loss (Wang *et al.*, 2003a; Murai *et al.*, 2008). The involvement of inflammation in the development of noise-induced cochlear injury is unclear, as it is difficult to separate its contribution from other putative mechanisms such as oxidative stress.

In support of the detrimental role of inflammation in the cochlea, glucocorticoids such as dexamethasone and methylprednisolone, which suppress cochlear inflammation, have been reported to exhibit protective effects against noise-induced cochlear injury and hearing loss (Takemura *et al.*, 2004; Sendowski *et al.*, 2006; Tabuchi *et al.*, 2006; Hirose *et al.*, 2007). In addition, post-exposure treatment of C57BL/6 mice with an IL-6 inhibitor (MR16-1) attenuated the inflammatory response (cellular infiltration) in the cochlea and significantly improved hearing (Wakabayashi *et al.*, 2010). A very recent study demonstrated that TNF-α inhibition improves cochlear blood flow and prevents permanent threshold shift after noise overexposure (Arpornchayanon *et al.*, 2013). Although this study did not examine the effects on the cochlear inflammatory response, earlier studies showed that TNF-α inhibition supressed the infiltration of inflammatory cells into the cochlea and reduced hearing loss in an experimental model of labyrinthitis induced with KLH (Satoh *et al.*, 2002; Wang *et al.*, 2003b).

The results presented here and in prior studies provide evidence that fibrocytes of the spiral ligament contribute to the inflammatory response in the cochlea. They release various proinflammatory mediators and cell adhesion molecules that are involved in the recruitment of inflammatory cells from the circulation. Following acoustic injury, significant leukocyte infiltration occurs in the spiral ligament, particularly in the inferior region among the type IV fibrocytes, an area highly susceptible to noise. In the present study, cells that resemble macrophages were also identified in this region but their true identity was not verified. Based on these data, it has been suggested that the type IV fibrocytes are likely the initiator of the local inflammatory response in the cochlea (Fujioka *et al.*, 2006; Tan *et al.*, 2008). Since cochlear fibrocytes express similar inflammatory mediators as leukocytes, and also respond to signals used by leukocytes for cell-cell signalling, they can perhaps be considered facultative resident macrophages, serving some functions normally performed by resident tissue macrophages. Hence, inflammatory leukocytes could function along with resident fibrocytes of the spiral ligament to regulate repair of the noise-damaged cochlear structures.

Based on the findings of the present study, the following scenario in the noise-induced cochlear inflammatory response is postulated. Damage to sensory and non-sensory cells of the cochlea by noise overexposure causes an early and excessive release of proinflammatory mediators (cytokines, chemokines and cell adhesion molecules) that recruit inflammatory cells from the circulation to phagocytose the cellular debris in the cochlea. However, as the macrophages migrate among the cells in the cochlea to clear debris, they cause significant bystander tissue injury, exacerbating the noise-induced cochlear damage. In direct response to this, a wound healing response is initiated via the secretion of various cytokines and growth factors. According to the results of the current study, this recovery phase of cochlear inflammation occurs by the end of the first week post-exposure, and presumably with the contribution of both resident cochlear cells (fibrocytes and resident macrophages) and non-resident infiltrating cells recruited from the circulation.

5.8. Cochlear Inflammatory Response Associated with Chronic Noise Exposure

This study demonstrated that an inflammatory response was induced in the mouse cochlea following repeated exposure to moderate noise levels. The inflammatory response, characterised by an increased expression of proinflammatory cytokines, chemokines and cell adhesion molecules, continued until after the second week of noise exposure and then subsided thereafter. To my knowledge, this is the first study demonstrating the presence of a cochlear inflammatory response in animals exposed to chronic moderate level noise, which is the type of environmental noise exposure that can be found in the workplace.

The findings from this study therefore show that even moderate noise, which is thought to produce only a temporary threshold shift, can induce an inflammatory response in the cochlea. Consistent with this, Tornabene *et al.* (2006) showed that even cochleae that were protected (by about 30 dB) by surgical disruption to the tympanic membrane and ossicular chain prior to exposure to 118 dB SPL noise, which caused a temporary threshold shift, had some infiltration of inflammatory cells in the spiral ligament and scala tympani. Hence, it appears that damage to the sensory hair cells, which does not occur substantially with temporary threshold shift, is not necessary to induce an inflammatory response. Although once thought to be harmless and recoverable, it is now known that noise levels that cause

temporary threshold shifts can in fact cause cochlear injury that eventuate to permanent hearing loss (Wong *et al.*, 2013). Kujawa and Liberman (2009) showed that there is an acute (within 24 h post-exposure) and extensive loss of afferent nerve terminals and a delayed and progressive degeneration of cochlear neurons over weeks to months post-exposure, with no loss of sensory hair cells. It is yet to be established, however, whether the inflammatory response contributes to neuronal degeneration.

The purpose of this inflammatory reaction in the cochlea following chronic noise exposure is not entirely clear. Although a single exposure to noise at 90 dB SPL causes temporary threshold shift in mice, it is possible that repeated exposure of mice to this noise level on a daily basis for an extended length of time may cause cochlear injury (e.g. degeneration of spiral ganglion neurons, the loss of spiral ligament fibrocytes and sensory hair cells), which may lead to permanent threshold shift, much like that observed following acute exposure to traumatic noise. As the cochlear function of these mice was not assessed to determine the degree of threshold shift following chronic noise exposure, it is speculated that chronic exposure to moderate noise levels initiates an inflammatory response, which peaks after two weeks, to aid in the clearance of debris from the damaged cells, but may itself contribute to cochlear injury. The data also show that the inflammation resolves thereafter, indicating a limited duration of the inflammatory response with chronic noise exposure. Hence, this study suggests that chronic environmental noise exposure, such as workplace noise, which leads to a slowly developing permanent hearing loss in humans, may be related to the development of an inflammatory response in the cochlea.

5.9. Anti-Inflammatory Effect of Regadenoson, a Selective Adenosine A_{2A} Receptor Agonist, in the Noise-Exposed Mouse Cochlea

It was shown herein that post-exposure treatment with regadenoson, a selective adenosine A_{2A} receptor agonist, suppressed the noise-induced cochlear inflammatory response, by significantly reducing the immunoexpression of ICAM-1 in the spiral ligament and the number of infiltrating cells in the cochlea relative to vehicle-treated controls. This is the first study to demonstrate the mitigation of cochlear inflammation by the selective activation of adenosine A_{2A} receptors in the cochlea. The findings thus support the therapeutic potential of adenosine A_{2A} receptor agonists in noise-induced cochlear inflammation. Consistent with this study, it has been shown that adenosine A_{2A} receptor activation using the selective adenosine A_{2A} receptor agonist, DWH-146e, attenuates the expression of ICAM-1 as well as P-selectin after ischemia-reperfusion injury (Okusa *et al.*, 2000).

Regadenoson, the first adenosine receptor agent to be approved by the FDA (10 April 2008), is used clinically as a coronary vasodilator (pharmacological stress agent) for radionuclide myocardial perfusion imaging in adult patients who are unable to exercise adequately (Astellas Pharma, 2008; Al Jaroudi & Iskandrian, 2009; Garnock-Jones & Curran, 2010; Chen *et al.*, 2013; Ghimire *et al.*, 2013). For almost two decades prior to the FDA approval of regadenoson, adenosine and dipyridamole were the main pharmacological stress agents of choice for myocardial perfusion imaging (Buhr *et al.*, 2008; Al Jaroudi & Iskandrian, 2009; Garnock-Jones & Curran, 2010). Because coronary vasodilation (myocardial hyperaemia) requires the selective stimulation of adenosine A_{2A} receptors on the vascular smooth muscle cells of coronary arteries, these agents are not ideal as they also cause activation of other adenosine receptor subtypes (A_1, A_{2B} and A_3 receptors) not involved in coronary vasodilation, leading to many undesirable side effects such as chest pain, dyspnea, decreased atrioventricular conduction, and bronchiolar constriction (Cerqueira *et al.*, 1994; Rakesh N. Patel *et al.*, 2007). In addition to producing considerably less serious side effects, regadenoson also has a longer half-life and lower affinity for the adenosine A_{2A} receptor. The longer half-life of regadenoson allows it to be administered as a bolus injection rather than by a constant intravenous infusion, while the low affinity of regadenoson in a large adenosine A_{2A} receptor reserve in the coronary arterial bed allows maximal coronary vasodilation and rapid termination of action (Buhr *et al.*, 2008; Al Jaroudi & Iskandrian, 2009).

A recent study demonstrated that regadenoson increased the permeability of the blood-brain barrier and facilitated the entry of macromolecules such as dextrans into the brains of C57BL/6 mice and Sprague Dawley rats (Carman *et al.*, 2011). These results suggest that adenosine receptor signalling can be used to modulate the permeability of the blood-brain barrier to facilitate the entry of therapeutic drugs into the central nervous system. Based on the similarity between blood-brain and blood-labyrinth barriers, it was assumed that regadenoson could cross the blood-labyrinth barrier and thus reach cochlear tissues. The results of this study therefore confirm the delivery of systemically injected regadenoson into the inner ear. The dose of regadenoson (0.05 mg/kg) given to the mice in the current study was based on the same study by Carman *et al.* (2011).

In the present study, regadenoson was dissolved in DMSO, an amphipathic solvent that has been used by many studies to dissolve otoprotective compounds given systemically or applied locally into the middle ear or onto the round window membrane. It has been demonstrated that DMSO administered intratympanically into the middle ear does not produce any morphological or functional changes in the inner ear (Roldán-Fidalgo *et al.*, 2014). However, it has yet to be evaluated whether DMSO has any anti-inflammatory effects in the cochlea given its known anti-inflammatory properties. The results from the current study suggest that DMSO had no impact on the noise-induced cochlear inflammatory response as cochlear expression levels of inflammatory markers were comparable in noise-exposed vehicle-treated mice and noise-exposed non-treated mice. This is most likely due to the very low concentration of DMSO that actually reached the cochlear tissues after systemic administration.

The underlying cellular/molecular mechanism(s) by which regadenoson mediates its anti-inflammatory effect in the noise-exposed cochlea is not entirely clear. As demonstrated in the study, adenosine A_{2A} receptors are predominantly immunolocalised in the blood vessels in the spiral ligament (mainly in the inferior region), which points to the site of action of regadenoson. The adenosine A_{2A} receptor immunolabelling in this region was shown to increase following noise exposure, which would serve to increase the efficacy of regadenoson. Based on the findings of this study, it is speculated that after crossing the blood-labyrinth barrier of the cochlea, regadenoson selectively binds to and activates adenosine A_{2A} receptors on vascular endothelial cells in the spiral ligament. The stimulation of the adenosine A_{2A} receptors results in the suppression of ICAM-1 expression on the

surface of the endothelial cells, which in turn reduces the extravasation of inflammatory cells from the systemic circulation. Interestingly, the results showed a decrease in the protein expression of ICAM-1 following post-exposure regadenoson treatment despite no change in the transcriptional expression of ICAM-1. It is postulated that regadenoson-mediated activation of adenosine A_{2A} receptors initiates an intracellular signalling cascade, which causes a decrease in the translation (protein synthesis) of ICAM-1, without affecting its transcription levels.

In addition to activating adenosine A_{2A} receptors on vascular endothelial cells, regadenoson likely stimulates adenosine A_{2A} receptors on the surface of infiltrating leukocytes and resident cochlear macrophages. In other tissues, this reduces the production of proinflammatory mediators such as TNF-α, decreases the production of ROS and reactive nitrogen species (RNS), and also augments the production of anti-inflammatory cytokines such as IL-10 from the inflammatory cells (Sullivan & Linden, 1998; Bours *et al.*, 2006; Haskó *et al.*, 2013), which in turn reduces further recruitment of circulating leukocytes.

The major signalling pathway linking adenosine A_{2A} receptor activation with downregulation of inflammation is the cAMP-PKA-NF-κB pathway (Sullivan & Linden, 1998; Okusa, 2002; Morello *et al.*, 2009). Stimulation of the adenosine A_{2A} receptor increases the intracellular levels of cAMP by adenylyl cyclase, which signals through protein kinase A (PKA; also known as cAMP-dependent protein kinase) that activates cAMP response element-binding protein (CREB), which in turn inhibits the transcriptional activity NF-κB, suppressing the expression of proinflammatory mediators and cell adhesion molecules. As downregulation in the gene expression levels of TNF-α, IL-1β, CCL2, and ICAM-1 was not observed, despite a decrease in both ICAM-1 immunoexpression and cellular infiltration, suppression of cochlear inflammation by regadenoson likely involves alternative signalling pathways.

Because of the widespread distribution of adenosine receptors, adenosine receptor agonists can have effects in many organs of the body, causing a variety of responses. However, no observable signs of major systemic side effects, such as significant loss of body weight or difficulty breathing, were detected in mice treated with regadenoson. Regadenoson has been reported to have a good safety and tolerability profile. In the phase III clinical trials, regadenoson was reasonably well tolerated by patients, and there were no serious side effects such as acute myocardial infarction, congestive heart failure, or stroke (Iskandrian *et al.*,

2007; Astellas Pharma, 2008; Cerqueira *et al.*, 2008). The majority of the adverse effects were reported to be of mild severity, and included shortness of breath (dyspnea), headache, flushing, chest discomfort or chest pain, dizziness, angina pectoris, nausea, and abdominal discomfort. Most of these effects were transient in nature, beginning soon after administration of the drug and generally resolving within approximately 15 minutes. These side effects of regadenoson can be readily reversed by an antagonist if needed (Al Jaroudi & Iskandrian, 2009).

At present, there is no cure for noise-induced hearing loss, or any other type of sensorineural hearing loss. Therapeutic management of hearing loss includes the use of hearing devices such as hearing aids that amplify sound or cochlear implants, which boost the residual hearing functionality. A cochlear implant is a neural prosthesis that functions by electrically stimulating residual spiral ganglion neurons, the primary auditory neurons of the cochlea (Loizou, 1999).

Corticosteroids (glucocorticoids) are widely used in the treatment of numerous acute and chronic inflammatory diseases, and have also long been used in the management of sensorineural hearing loss of various causes, including noise-induced hearing loss (Abi-Hachem *et al.*, 2010; Tabuchi & Hara, 2012). Corticosteroids are typically administered systemically, either intravenously or orally. Appropriate doses of steroids supress excessive inflammation, but are unable to completely recover the associated hearing loss. Higher doses, on the other hand, can be deleterious to cochlear function in the long term and are often accompanied by a wide range of adverse side effects (Abi-Hachem *et al.*, 2010). Glucocorticoids exert their actions by binding to and activating soluble cytoplasmic glucocorticoid receptors, which translocate to the nucleus and bind to specific DNA sites, culminating in the downregulation of proinflammatory cytokines and cell adhesion molecules (Vandevyver *et al.*, 2013). Previous studies have demonstrated that dexamethasone, a widely used synthetic glucocorticoid, suppresses TNF-α-induced inflammatory mediator release from cultured spiral ligament fibrocytes (Maeda *et al.*, 2005). The otoprotective effects of steroids may be mediated through the actions of NF-κB, as glucocorticoids are shown to be potent inhibitors of NF-κB activation via the induction of the IκBα inhibitory protein (Auphan *et al.*, 1995). Local routes of steroid delivery have also been developed without the unfavourable side effects. Direct infusion of dexamethasone into the perilymphatic space using osmotic mini-pumps has been reported to show protective effects against noise-induced

injury in the guinea pig cochlea (Takemura *et al.*, 2004). Intratympanic administration of steroids have also shown good therapeutic efficacy (Zhou *et al.*, 2009).

There is a need to develop more effective pharmacological therapies for cochlear inflammation that prevent (or rescue) cochlear tissue from injury and mitigate hearing loss. The findings from this study reveal an important role of adenosine A_{2A} receptor signalling in controlling noise-induced cochlear inflammation, and pinpoint regadenoson as a potential therapeutic option. An advantage of regadenoson is that it can be administered systemically as a rapid intravenous injection (a single 10 second bolus) avoiding the inconvenience of intratympanic injections or surgical procedures required for direct drug delivery into the cochlea.

5.10. Potential Therapeutic Interventions for Noise-Induced Cochlear Inflammation

Based on our existing understanding of the underlying mechanisms and pathways of the cochlear inflammatory response, rational therapeutic approaches can be devised to supress the inflammation and reduce cochlear injury. It is has been postulated that there are networks in the cochlea comprising cochlear fibrocytes, vascular endothelial cells, and inflammatory cells, which are interconnected by various proinflammatory mediators (cytokines, chemokines and cell adhesion molecules) (Yoshida *et al.*, 1999). Appropriate control of these networks could potentially attenuate the inflammatory reaction in the cochlea. Because of their early expression in the inflammatory response and their role in recruiting inflammatory cells into the cochlea, targeting chemokines/cytokines through direct inhibition may represent an effective therapeutic strategy.

Satoh *et al.* (2002) and Wang *et al.* (2003b) examined the therapeutic potential of anti-TNF-α therapy and showed that blocking the activity of TNF-α using Etanercept, a soluble TNF-α receptor-FC fusion protein, significantly attenuated the cochlear inflammatory response (reduced inflammatory cell infiltration and cochlear fibrosis) in an animal model of immune-mediated labyrinthitis induced by immunisation with KLH. A further study showed that neutralisation of TNF-α using Etanercept markedly decreased the expression and secretion of proinflammatory cytokines (TNF-α, IL-1β and IL-6) in the cochlea after cisplatin injection

(So *et al.*, 2007). In addition, a very recent study demonstrated that TNF-α inhibition using Etanercept also improves cochlear blood flow and prevents permanent threshold shift after noise overexposure (Arpornchayanon *et al.*, 2013).

Another potential treatment strategy would be to block IL-6 signalling in the cochlea. It is interesting in this regard that specific humanised neutralising antibodies against IL-6 have been used clinically with promising effects in patients with rheumatoid arthritis and inflammatory bowel disease. A recent study by Wakabayashi *et al.* (2010) showed that inhibition of IL-6 with IL-6 receptor neutralising antibody (MR16-1) resulted in a dramatic suppression of the cochlear inflammatory response (reduced infiltration of inflammatory cells) and significantly improved hearing function in noise-exposed mice.

Nakamoto *et al.* (2012) showed that administration of geranylgeranylacetone (GGA), an anti-ulcer drug, suppressed the expression of proinflammatory cytokines (IL-6 and IL-1β) in the noise-exposed cochlea and also improved auditory function. GGA activates heat shock transcription factor 1 (HSF1), which induces the expression of heat shock proteins (HSPs). HSF1 is also known to directly or indirectly regulate cytokine expression, such as inhibiting the expression of IL-6 and IL-1β. GGA can also reduce inflammation in other organs (e.g. liver) without apparent side effects even at large doses. GGA may therefore provide a novel beneficial strategy for the prevention of noise-induced hearing loss.

The role of antioxidants in noise-induced hearing loss has been the subject of extensive research. Antioxidants have been demonstrated to provide a protective effect in the cochlea by restoring the redox balance. A recent study examined the effects of antioxidant treatment on the inflammatory response in the cochlea following noise exposure (Du *et al.*, 2011). This study reported that antioxidant treatment not only reduced markers of oxidative stress, but also significantly reduced the infiltration of inflammatory cells into the cochlea. This finding suggests an anti-inflammatory role of antioxidants in the cochlea.

Combination therapy involving more than one therapeutic agent could be a more effective approach at suppressing cochlear inflammation. Administering regadenoson in combination with one of the above mentioned agents such as the TNF-α inhibitor Etanercept or dexamethasone may potentially provide a stronger anti-inflammatory effect in the cochlea than either drug alone. Previous studies by our group have demonstrated that adenosine

amine congener (ADAC), a selective adenosine A_1 receptor agonist, can ameliorate noise- and cisplatin-induced cochlear injury (Vlajkovic *et al.*, 2010a; Gunewardene *et al.*, 2013; Vlajkovic *et al.*, 2014). ADAC can also be administered systemically with no cardiovascular side effects at the therapeutic dose. Coupling regadenoson with ADAC could therefore provide better otoprotection against noise-induced cochlear injury and hearing loss.

CHAPTER 6: LIMITATIONS & FUTURE DIRECTIONS

As is the case with any research, the present study had limitations that need to be addressed, and to overcome these shortcomings, further research needs to be carried out. In addition, directions for future research to further evaluate and extend the findings of the current study and to address other relevant ideas are proposed.

All studies in this project were conducted on only male C57BL/6 mice to remove potential gender-related variability and ensure consistency of results. Future studies could examine the presence of any gender-specific differences in the noise-induced cochlear inflammatory response.

Sound-evoked ABR responses were the only measure of cochlear function used to verify that the noise parameters used for the acute noise exposures produced permanent threshold shifts in the mice. This could be complemented with distortion product otoacoustic emissions (DPOAEs), which measure the performance of the outer hair cells in tuning sound transduction, and/or compound action potentials (CAPs), which is a measure of the neural afferent output. This would enable correlation of gene expression and immunohistochemical studies with the functional outcomes.

The present study examined noise-induced changes in the gene expression of several key proinflammatory mediators including TNF-α, IL-1β, CCL2 and ICAM-1. To gain further insight into the molecular changes associated with noise-induced cochlear inflammation, the expression of additional inflammatory cytokines and chemokines should be examined. A genome-wide DNA microarray analysis could be carried out to identify further inflammation-related genes expressed in the noise-exposed cochlea. In addition, it would be worthwhile to assess any turn-related differences in gene expression of inflammatory mediators in the noise-exposed cochlea, e.g. apical lateral wall/sensory epithelium versus basal lateral wall/sensory epithelium.

Due to the lack of specificity of the antibodies used in the immunohistochemistry experiments, the cellular source of proinflammatory cytokines in the cochlea could not be determined. Antibodies sourced from other manufacturers could be tested in future studies. In addition, protein expression levels of inflammatory mediators in the noise-exposed cochlea could be assessed by Western blotting and enzyme-linked immunosorbent assay (ELISA) to corroborate the gene expression results.

To quantitatively analyse the protein expression level of ICAM-1, the pixel intensity (mean gray value) and area were measured by selecting the ROI (inferior region of the spiral ligament) manually using the freehand selection tool, which is not a highly accurate procedure. A more accurate method of measuring intensity and area is thresholding (also known as segmentation), which works by separating pixels which fall within a desired range of pixel intensity values from those that don't. Moreover, these measurements should always be carried out blindly, i.e. measurements undertaken without knowing whether the sections are from non-exposed or noise-exposed cochleae.

The adenosine A_{2A} receptor-positive cells largely observed within the scala tympani of the cochlea following traumatic noise exposure were assumed to be infiltrating inflammatory cells as they appeared similar to those reported by previous studies. Although they may indeed be inflammatory cells recruited from the circulation, further evidence is needed to prove this as the adenosine A_{2A} receptor is not a specific marker of inflammatory cells, and can be expressed by a variety of cell types. To verify that these labelled cells in the noise-exposed cochlea are truly inflammatory cells, they should be characterised further using specific leukocyte cell surface markers such as CD45, F4/80, CD68, CX3CR1, and Iba-1, however, staining with F4/80 markers yielded inconclusive results in the current study. Furthermore, double labelling should be carried out to fully characterise the adenosine A_{2A} receptor-positive cells in the cochlear structures, particularly in the spiral ligament – whether they are vascular endothelial cells, fibrocytes or inflammatory cells.

For the acute noise exposure study, four time points following noise exposure (6 h, 1 day, 3 days and 7 days) were selected to examine the time course (dynamics) of the inflammatory response. Future experiments should include additional time points in order to accurately examine the temporal sequence of events comprising the cochlear inflammatory response. Because of the long intervals between these selected time points, important events may have

gone undetected. Previous studies demonstrated the expression of inflammatory mediators within a few hours after acoustic trauma, so it would be worthwhile examining whether the initial peak in gene expression observed in the present study occurs earlier than 6 h. In addition, later time points after seven days post-exposure should also be examined to explore what happens after the second peak in gene expression.

The degree of noise-induced threshold shift in mice following chronic exposure to moderate noise levels was not assessed to determine whether a temporary or permanent threshold shift was induced. In addition, future experiments should examine the presence of infiltrating inflammatory cells in the cochlea as was done in the acute noise exposure study.

Increased immunoexpression of adenosine A_{2A} receptors in the spiral ligament of the cochlea following noise exposure was only assessed qualitatively due to receptor distribution in blood vessels. A semi-quantitative analysis based on Western blotting/ELISA should be carried out in order to obtain a more accurate assessment of the protein expression levels.

It was assumed that regadenoson was capable of reaching the cochlea by crossing the blood-labyrinth barrier. How much regadenoson actually reaches the cochlear tissues after systemic administration (bioavailability) and how long it remains in the cochlea until it is metabolised needs to be determined in future experiments. In the present study, only a single dose, delivery route and post-exposure injection time was assessed. In order to translate these findings to clinical research, further studies are needed to assess the optimal dose and route of drug administration (local vs. systemic) to provide the most effective treatment outcome with the least side effects. There is also the need to consider the optimal time of regadenoson treatment and also whether pre-exposure drug administration (i.e. prophylactic treatment) or post-exposure administration is most effective. Other measurements such as body temperature and blood pressure/heart rate should be taken after regadenoson treatment to control for possible side effects of the drug.

It would be of interest in future studies to assess the impact of regadenoson treatment on cochlear tissue injury and function. Noise-induced cochlear injury can be assessed by quantifying the loss of sensory hair cells and spiral ganglion neurons, as well as assessing markers of apoptosis and necrosis. Functional auditory measurements should also be performed prior to noise exposure (baseline) and after drug treatment to determine whether

regadenoson improves noise-induced threshold shifts in mice. Reduction in cochlear injury together with an improvement to auditory thresholds following regadenoson treatment would support the hypothesis that inflammation is involved in the development of noise-induced cochlear injury and hearing loss. The therapeutic efficacy of regadenoson in suppressing noise-induced cochlear inflammation should also be evaluated in other animal models. Additionally, the potential efficacy of combining regadenoson with selective adenosine A_1 receptor agonists, such as ADAC, should also be explored as an otoprotective treatment strategy in noise-induced hearing loss.

CHAPTER 7: CONCLUSIONS

The present study was undertaken to elucidate the underlying molecular and cellular mechanisms and time course of the inflammatory response in the mammalian cochlea following acute and chronic noise exposure. In addition, the anti-inflammatory effect of regadenoson, a selective adenosine A_{2A} receptor agonist, in the noise-exposed cochlea was investigated. The main findings of this thesis are summarised below.

Cochlear Inflammatory Response Associated with Acute Noise Exposure

- Acute exposure to traumatic noise induces an inflammatory response in the mouse cochlea characterised by:
  - An early (6 h post-exposure) upregulation in the gene expression of proinflammatory cytokines (TNF-α and IL-1β), chemokines (CCL2) and cell adhesion molecules (ICAM-1), presumably via the activation of the transcription factor NF-κB, followed by a second peak of expression of these inflammatory mediators 7 days post-exposure.
  - Increased ICAM-1 immunoexpression in the inferior region of the spiral ligament, peaking 24 h post-exposure.
  - Increased PECAM-1 immunoexpression in the cochlear vasculature, peaking 1-3 days post-exposure.
  - Recruitment of adenosine A_{2A} receptor-positive infiltrating cells, peaking 24 h post-exposure. These cells were found predominantly within the scala tympani, free-floating or attached to the wall of this perilymph-filled compartment.
- It is speculated that inflammatory cells are recruited to the noise-damaged cochlea following the early upregulation of proinflammatory mediators and cell adhesion molecules. The main role of these cells is to clear cellular debris, but they may also cause significant bystander tissue injury, thus exacerbating the noise-induced injury. The occurrence of the latter peak in gene expression at 7 days post-exposure is not entirely clear, but it is postulated that it may be associated with reparative processes (i.e. a wound healing response) initiated in response to the cochlear damage.

Cochlear Inflammatory Response Associated with Chronic Noise Exposure

- Chronic exposure to moderate noise also induces an inflammatory response in the mouse cochlea. This response is characterised by an increased expression of TNF-α, IL-1β, CCL2 and ICAM-1, peaking after two weeks of noise exposure, and subsiding thereafter.
- Repeated exposure over an extended period of time may also result in cochlear injury leading to permanent hearing loss. An inflammatory response is likely initiated to clear cellular debris from the noise-damaged cochlea, but may also contribute to cochlear injury.

Adenosine A_{2A} Receptor Expression in the Noise-Exposed Cochlea

- Adenosine A_{2A} receptor is mainly immunlocalised in the cochlear vasculature, thus resembling ICAM-1 and PECAM-1 immunoexpression.
- Adenosine A_{2A} receptor immunoexpression increases in the inferior region of the spiral ligament following acute exposure to traumatic noise, which may suggest an endogenous protective mechanism of cochlear tissues to limit the inflammatory response.

Noise-Induced Cochlear Inflammatory Response in $A_{2A}RKO^{-/-}$ Mice

- Deletion of the adenosine A_{2A} receptor gene ($A_{2A}RKO^{-/-}$ mice) differentially affects specific aspects of the noise-induced inflammatory response in the cochlea.

Anti-Inflammatory Effect of Regadenoson in the Noise-Exposed Cochlea

- Post-exposure treatment of mice with regadenoson, a selective adenosine A_{2A} receptor agonist, mitigates some aspects of the noise-induced cochlear inflammatory response.
- Regadenoson reduces the infiltration/extravasation of inflammatory cells into the cochlea, most likely by downregulating the expression of ICAM-1 on the vascular endothelium.

In conclusion, the present study provides fundamental novel insights into the mechanisms and dynamics of the cochlear inflammatory response induced by exposure to acute and chronic noise. Noise-induced cochlear inflammation is a complex physiological process characterised by the coordinated activation of various signalling pathways that regulate the expression of various proinflammatory mediators, which in turn orchestrate the directed migration of inflammatory cells to the noise-damaged cochlea. However, the exact mechanisms by which noise elicits this inflammatory response in the cochlea still remains unclear. This study also reveals an important role of adenosine A_{2A} receptor signalling in controlling noise-induced cochlear inflammation, and suggests that regadenoson, a FDA approved selective adenosine A_{2A} receptor agonist, is a feasible therapeutic option for suppression of cochlear inflammation caused by noise, but also with implications for other inflammatory conditions affecting the inner ear. With improved understanding of the cochlear inflammatory response, novel therapeutic interventions can be explored and developed to protect, and perhaps rescue, cochlear tissues from inflammation-induced injury, leading to prevention of noise-induced hearing loss.

APPENDICES

Appendix A: Supplementary Figures

Appendix A1: NF-κB p65 Blocking Peptide Control

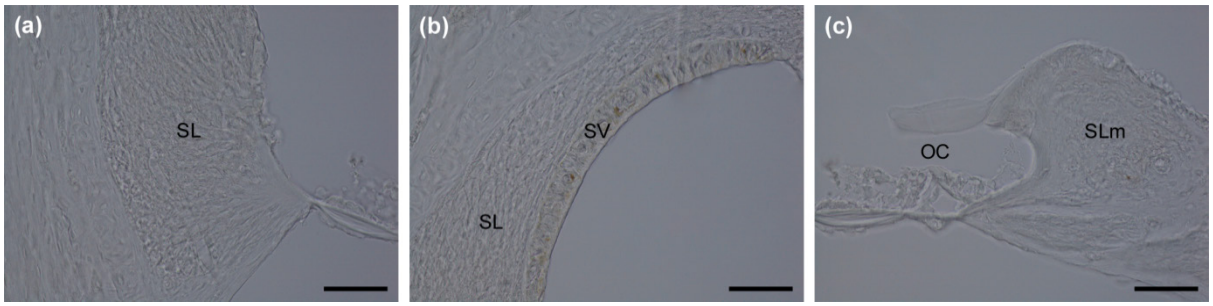

Figure A.1: NF-κB p65 blocking peptide control. Pre-absorbing the antibody for p65 with the corresponding immunising peptide abolished the p65 immunostaining in the spiral ligament (**a**, **b**), stria vascularis (**b**), organ of Corti (**c**) and spiral limbus (**c**), confirming the specificity of the antibody. *Abbreviations*: SL, spiral ligament; SV, stria vascularis; OC, organ of Corti; SLm, spiral limbus. Scale bars = 50 µm.

Appendix A2: NF-κB p50 Blocking Peptide Control

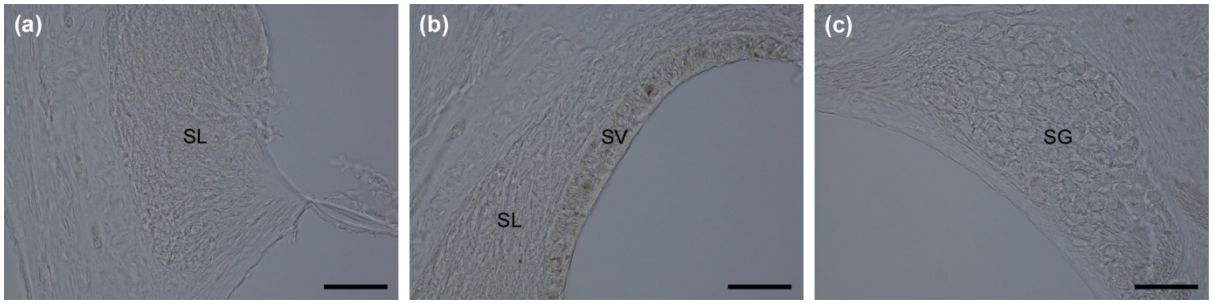

Figure A.2: NF-κB p50 blocking peptide control. Pre-absorbing the antibody for p50 with the corresponding immunising peptide abolished the p50 immunostaining in the spiral ligament (**a**, **b**) and spiral ganglion (**c**), confirming the specificity of the antibody. *Abbreviations*: SL, spiral ligament; SV, stria vascularis; SG, spiral ganglion. Scale bars = 50 µm.

Appendix B: Tukey's Post-Hoc Multiple Comparisons Tables

Appendix B1: Gene Expression (Acute Noise)

Table A.1: Tukey's post-hoc test | TNF-α gene expression (acute noise)

(I) Endpoint	(J) Endpoint	Mean Difference (I-J)	Std. Error	Sig.	95% Confidence Interval	
					Lower Bound	Upper Bound
Control	6 h	2.187716*	.502050	.001	.72139	3.65405
	1 d	.101903	.546432	1.000	-1.49405	1.69786
	3 d	.999536	.487353	.270	-.42387	2.42294
	7 d	2.502553*	.521002	.000	.98087	4.02424
6 h	Control	-2.187716*	.502050	.001	-3.65405	-.72139
	1 d	-2.085813*	.528393	.004	-3.62908	-.54255
	3 d	-1.188180	.467038	.110	-2.55225	.17589
	7 d	.314837	.502050	.969	-1.15149	1.78117
1 d	Control	-.101903	.546432	1.000	-1.69786	1.49405
	6 h	2.085813*	.528393	.004	.54255	3.62908
	3 d	.897633	.514448	.425	-.60491	2.40017
	7 d	2.400650*	.546432	.001	.80470	3.99660
3 d	Control	-.999536	.487353	.270	-2.42294	.42387
	6 h	1.188180	.467038	.110	-.17589	2.55225
	1 d	-.897633	.514448	.425	-2.40017	.60491
	7 d	1.503017*	.487353	.035	.07961	2.92642
7 d	Control	-2.502553*	.521002	.000	-4.02424	-.98087
	6 h	-.314837	.502050	.969	-1.78117	1.15149
	1 d	-2.400650*	.546432	.001	-3.99660	-.80470
	3 d	-1.503017*	.487353	.035	-2.92642	-.07961

Table A.2: Tukey's post-hoc test | CCL2 gene expression (acute noise)

(I) Endpoint	(J) Endpoint	Mean Difference (I-J)	Std. Error	Sig.	95% Confidence Interval	
					Lower Bound	Upper Bound
Control	6 h	4.519749*	.495813	.000	3.03609	6.00341
	1 d	1.118076	.495813	.201	-.36558	2.60173
	3 d	-.195923	.515264	.995	-1.73779	1.34594
	7 d	2.247655*	.543136	.004	.62239	3.87292
6 h	Control	-4.519749*	.495813	.000	-6.00341	-3.03609
	1 d	-3.401672*	.443469	.000	-4.72870	-2.07465
	3 d	-4.715672*	.465114	.000	-6.10747	-3.32388
	7 d	-2.272093*	.495813	.002	-3.75575	-.78843
1 d	Control	-1.118076	.495813	.201	-2.60173	.36558
	6 h	3.401672*	.443469	.000	2.07465	4.72870
	3 d	-1.313999	.465114	.070	-2.70579	.07780
	7 d	1.129579	.495813	.193	-.35408	2.61324
3 d	Control	.195923	.515264	.995	-1.34594	1.73779
	6 h	4.715672*	.465114	.000	3.32388	6.10747
	1 d	1.313999	.465114	.070	-.07780	2.70579
	7 d	2.443578*	.515264	.001	.90172	3.98544
7 d	Control	-2.247655*	.543136	.004	-3.87292	-.62239
	6 h	2.272093*	.495813	.002	.78843	3.75575
	1 d	-1.129579	.495813	.193	-2.61324	.35408
	3 d	-2.443578*	.515264	.001	-3.98544	-.90172

Table A.3: Tukey's post-hoc test | ICAM-1 gene expression (acute noise)

(I) Endpoint	(J) Endpoint	Mean Difference (I-J)	Std. Error	Sig.	95% Confidence Interval	
					Lower Bound	Upper Bound
Control	6 h	.886771*	.293499	.042	.02211	1.75143
	1 d	.165634	.330656	.986	-.80849	1.13976
	3 d	-.462972	.293499	.525	-1.32763	.40168
	7 d	1.309681*	.293499	.001	.44502	2.17434
6 h	Control	-.886771*	.293499	.042	-1.75143	-.02211
	1 d	-.721137	.340529	.245	-1.72434	.28207
	3 d	-1.349743*	.304578	.002	-2.24704	-.45245
	7 d	.422910	.304578	.641	-.47439	1.32021
1 d	Control	-.165634	.330656	.986	-1.13976	.80849
	6 h	.721137	.340529	.245	-.28207	1.72434
	3 d	-.628606	.340529	.372	-1.63181	.37460
	7 d	1.144047*	.340529	.020	.14084	2.14725
3 d	Control	.462972	.293499	.525	-.40168	1.32763
	6 h	1.349743*	.304578	.002	.45245	2.24704
	1 d	.628606	.340529	.372	-.37460	1.63181
	7 d	1.772653*	.304578	.000	.87536	2.66995
7 d	Control	-1.309681*	.293499	.001	-2.17434	-.44502
	6 h	-.422910	.304578	.641	-1.32021	.47439
	1 d	-1.144047*	.340529	.020	-2.14725	-.14084
	3 d	-1.772653*	.304578	.000	-2.66995	-.87536

Table A.4: Tukey's post-hoc test | IL-1β gene expression (acute noise)

(I) Endpoint	(J) Endpoint	Mean Difference (I-J)	Std. Error	Sig.	95% Confidence Interval	
					Lower Bound	Upper Bound
Control	6 h	.692648	.262448	.087	-.06567	1.45096
	1 d	.159835	.262448	.973	-.59848	.91815
	3 d	.346348	.253549	.653	-.38626	1.07895
	7 d	.645128	.262448	.126	-.11319	1.40344
6 h	Control	-.692648	.262448	.087	-1.45096	.06567
	1 d	-.532812	.271055	.305	-1.31600	.25037
	3 d	-.346299	.262448	.681	-1.10462	.41202
	7 d	-.047519	.271055	1.000	-.83071	.73567
1 d	Control	-.159835	.262448	.973	-.91815	.59848
	6 h	.532812	.271055	.305	-.25037	1.31600
	3 d	.186513	.262448	.953	-.57180	.94483
	7 d	.485293	.271055	.396	-.29789	1.26848
3 d	Control	-.346348	.253549	.653	-1.07895	.38626
	6 h	.346299	.262448	.681	-.41202	1.10462
	1 d	-.186513	.262448	.953	-.94483	.57180
	7 d	.298780	.262448	.785	-.45954	1.05710
7 d	Control	-.645128	.262448	.126	-1.40344	.11319
	6 h	.047519	.271055	1.000	-.73567	.83071
	1 d	-.485293	.271055	.396	-1.26848	.29789
	3 d	-.298780	.262448	.785	-1.05710	.45954

Appendix B2: ICAM-1 Immunoexpression (Acute Noise)

Table A.5: Tukey's post-hoc test | ICAM-1 immunostaining intensity in the spiral ligament of the cochlear basal turn (acute noise)

(I) Endpoint	(J) Endpoint	Mean Difference (I-J)	Std. Error	Sig.	95% Confidence Interval	
					Lower Bound	Upper Bound
Control	6 h	2.524480	3.228466	.935	-6.50912	11.55808
	1 d	12.425880*	2.465782	.000	5.52635	19.32541
	3 d	-.519751	2.581609	1.000	-7.74337	6.70387
	7 d	-3.423402	2.373397	.603	-10.06443	3.21762
6 h	Control	-2.524480	3.228466	.935	-11.55808	6.50912
	1 d	9.901400*	3.455867	.042	.23151	19.57129
	3 d	-3.044231	3.539440	.910	-12.94797	6.85951
	7 d	-5.947882	3.390568	.408	-15.43506	3.53929
1 d	Control	-12.425880*	2.465782	.000	-19.32541	-5.52635
	6 h	-9.901400*	3.455867	.042	-19.57129	-.23151
	3 d	-12.945631*	2.860895	.000	-20.95073	-4.94053
	7 d	-15.849282*	2.674516	.000	-23.33287	-8.36570
3 d	Control	.519751	2.581609	1.000	-6.70387	7.74337
	6 h	3.044231	3.539440	.910	-6.85951	12.94797
	1 d	12.945631*	2.860895	.000	4.94053	20.95073
	7 d	-2.903652	2.781665	.834	-10.68705	4.87975
7 d	Control	3.423402	2.373397	.603	-3.21762	10.06443
	6 h	5.947882	3.390568	.408	-3.53929	15.43506
	1 d	15.849282*	2.674516	.000	8.36570	23.33287
	3 d	2.903652	2.781665	.834	-4.87975	10.68705

Table A.6: Tukey's post-hoc test | ICAM-1 immunostaining area in the spiral ligament of the cochlear basal turn (acute noise)

(I) Endpoint	(J) Endpoint	Mean Difference (I-J)	Std. Error	Sig.	95% Confidence Interval	
					Lower Bound	Upper Bound
Control	6 h	-4343.674562*	791.644152	.000	-6558.78097	-2128.56815
	1 d	-5798.182920*	604.628208	.000	-7489.99839	-4106.36745
	3 d	-4604.046305*	633.029808	.000	-6375.33254	-2832.76007
	7 d	-2341.047391*	581.974858	.001	-3969.47632	-712.61846
6 h	Control	4343.674562*	791.644152	.000	2128.56815	6558.78097
	1 d	-1454.508358	847.404437	.431	-3825.63811	916.62140
	3 d	-260.371742	867.897315	.998	-2688.84279	2168.09931
	7 d	2002.627172	831.392654	.125	-323.69987	4328.95422
1 d	Control	5798.182920*	604.628208	.000	4106.36745	7489.99839
	6 h	1454.508358	847.404437	.431	-916.62140	3825.63811
	3 d	1194.136615	701.513048	.439	-768.77317	3157.04640
	7 d	3457.135529*	655.811370	.000	1622.10401	5292.16705
3 d	Control	4604.046305*	633.029808	.000	2832.76007	6375.33254
	6 h	260.371742	867.897315	.998	-2168.09931	2688.84279
	1 d	-1194.136615	701.513048	.439	-3157.04640	768.77317
	7 d	2262.998914*	682.085054	.012	354.45077	4171.54706
7 d	Control	2341.047391*	581.974858	.001	712.61846	3969.47632
	6 h	-2002.627172	831.392654	.125	-4328.95422	323.69987
	1 d	-3457.135529*	655.811370	.000	-5292.16705	-1622.10401
	3 d	-2262.998914*	682.085054	.012	-4171.54706	-354.45077

Table A.7: Tukey's post-hoc test | ICAM-1 immunostaining intensity in the spiral ligament of the cochlear middle turn (acute noise)

(I) Endpoint	(J) Endpoint	Mean Difference (I-J)	Std. Error	Sig.	95% Confidence Interval	
					Lower Bound	Upper Bound
Control	6 h	4.431835	4.077913	.812	-7.12565	15.98932
	1 d	18.331872*	3.101661	.000	9.54125	27.12249
	3 d	3.790963	3.101661	.739	-4.99966	12.58158
	7 d	-8.721542	3.304282	.079	-18.08643	.64334
6 h	Control	-4.431835	4.077913	.812	-15.98932	7.12565
	1 d	13.900036*	4.323294	.019	1.64710	26.15297
	3 d	-.640873	4.323294	1.000	-12.89381	11.61206
	7 d	-13.153378*	4.470889	.038	-25.82462	-.48214
1 d	Control	-18.331872*	3.101661	.000	-27.12249	-9.54125
	6 h	-13.900036*	4.323294	.019	-26.15297	-1.64710
	3 d	-14.540909*	3.417864	.001	-24.22770	-4.85412
	7 d	-27.053414*	3.602745	.000	-37.26419	-16.84264
3 d	Control	-3.790963	3.101661	.739	-12.58158	4.99966
	6 h	.640873	4.323294	1.000	-11.61206	12.89381
	1 d	14.540909*	3.417864	.001	4.85412	24.22770
	7 d	-12.512505*	3.602745	.009	-22.72328	-2.30173
7 d	Control	8.721542	3.304282	.079	-.64334	18.08643
	6 h	13.153378*	4.470889	.038	.48214	25.82462
	1 d	27.053414*	3.602745	.000	16.84264	37.26419
	3 d	12.512505*	3.602745	.009	2.30173	22.72328

Table A.8: Tukey's post-hoc test | ICAM-1 immunostaining area in the spiral ligament of the cochlear middle turn (acute noise)

(I) Endpoint	(J) Endpoint	Mean Difference (I-J)	Std. Error	Sig.	95% Confidence Interval	
					Lower Bound	Upper Bound
Control	6 h	-839.251459	542.599413	.538	-2377.06824	698.56532
	1 d	-2035.777802*	412.701127	.000	-3205.44128	-866.11432
	3 d	-1794.999166*	412.701127	.001	-2964.66265	-625.33568
	7 d	-515.478752	439.661463	.767	-1761.55230	730.59480
6 h	Control	839.251459	542.599413	.538	-698.56532	2377.06824
	1 d	-1196.526343	575.249286	.245	-2826.87829	433.82560
	3 d	-955.747707	575.249286	.467	-2586.09965	674.60424
	7 d	323.772707	594.887992	.982	-1362.23859	2009.78400
1 d	Control	2035.777802*	412.701127	.000	866.11432	3205.44128
	6 h	1196.526343	575.249286	.245	-433.82560	2826.87829
	3 d	240.778636	454.774492	.984	-1048.12775	1529.68502
	7 d	1520.299051*	479.374405	.021	161.67243	2878.92567
3 d	Control	1794.999166*	412.701127	.001	625.33568	2964.66265
	6 h	955.747707	575.249286	.467	-674.60424	2586.09965
	1 d	-240.778636	454.774492	.984	-1529.68502	1048.12775
	7 d	1279.520414	479.374405	.074	-79.10621	2638.14703
7 d	Control	515.478752	439.661463	.767	-730.59480	1761.55230
	6 h	-323.772707	594.887992	.982	-2009.78400	1362.23859
	1 d	-1520.299051*	479.374405	.021	-2878.92567	-161.67243
	3 d	-1279.520414	479.374405	.074	-2638.14703	79.10621

Appendix B3: Gene Expression (Chronic Noise)

Table A.9: Tukey's post-hoc test | TNF-α gene expression (chronic noise)

(I) Endpoint	(J) Endpoint	Mean Difference (I-J)	Std. Error	Sig.	95% Confidence Interval	
					Lower Bound	Upper Bound
Control	1 wk	.618971*	.200050	.030	.04382	1.19413
	2 wks	1.110359*	.200050	.000	.53520	1.68551
	3 wks	-.216189	.200050	.815	-.79134	.35897
	4 wks	.073439	.200050	.996	-.50172	.64859
1 wk	Control	-.618971*	.200050	.030	-1.19413	-.04382
	2 wks	.491388	.200050	.124	-.08377	1.06654
	3 wks	-.835160*	.200050	.002	-1.41031	-.26001
	4 wks	-.545532	.200050	.070	-1.12069	.02962
2 wks	Control	-1.110359*	.200050	.000	-1.68551	-.53520
	1 wk	-.491388	.200050	.124	-1.06654	.08377
	3 wks	-1.326548*	.200050	.000	-1.90170	-.75139
	4 wks	-1.036919*	.200050	.000	-1.61207	-.46176
3 wks	Control	.216189	.200050	.815	-.35897	.79134
	1 wk	.835160*	.200050	.002	.26001	1.41031
	2 wks	1.326548*	.200050	.000	.75139	1.90170
	4 wks	.289629	.200050	.602	-.28553	.86478
4 wks	Control	-.073439	.200050	.996	-.64859	.50172
	1 wk	.545532	.200050	.070	-.02962	1.12069
	2 wks	1.036919*	.200050	.000	.46176	1.61207
	3 wks	-.289629	.200050	.602	-.86478	.28553

Table A.10: Tukey's post-hoc test | CCL2 gene expression (chronic noise)

(I) Endpoint	(J) Endpoint	Mean Difference (I-J)	Std. Error	Sig.	95% Confidence Interval	
					Lower Bound	Upper Bound
Control	1 wk	1.380008*	.254461	.000	.64477	2.11525
	2 wks	1.832469*	.263392	.000	1.07142	2.59351
	3 wks	.241101	.263392	.889	-.51994	1.00215
	4 wks	.607022	.263392	.170	-.15402	1.36807
1 wk	Control	-1.380008*	.254461	.000	-2.11525	-.64477
	2 wks	.452461	.263392	.438	-.30858	1.21351
	3 wks	-1.138906*	.263392	.001	-1.89995	-.37786
	4 wks	-.772985*	.263392	.045	-1.53403	-.01194
2 wks	Control	-1.832469*	.263392	.000	-2.59351	-1.07142
	1 wk	-.452461	.263392	.438	-1.21351	.30858
	3 wks	-1.591368*	.272030	.000	-2.37737	-.80536
	4 wks	-1.225447*	.272030	.001	-2.01145	-.43944
3 wks	Control	-.241101	.263392	.889	-1.00215	.51994
	1 wk	1.138906*	.263392	.001	.37786	1.89995
	2 wks	1.591368*	.272030	.000	.80536	2.37737
	4 wks	.365921	.272030	.666	-.42008	1.15192
4 wks	Control	-.607022	.263392	.170	-1.36807	.15402
	1 wk	.772985*	.263392	.045	.01194	1.53403
	2 wks	1.225447*	.272030	.001	.43944	2.01145
	3 wks	-.365921	.272030	.666	-1.15192	.42008

Table A.11: Tukey's post-hoc test | ICAM-1 gene expression (chronic noise)

(I) Endpoint	(J) Endpoint	Mean Difference (I-J)	Std. Error	Sig.	95% Confidence Interval	
					Lower Bound	Upper Bound
Control	1 wk	.691053*	.184823	.006	.15968	1.22243
	2 wks	1.062139*	.184823	.000	.53076	1.59352
	3 wks	.222039	.184823	.751	-.30934	.75341
	4 wks	.338225	.184823	.373	-.19315	.86960
1 wk	Control	-.691053*	.184823	.006	-1.22243	-.15968
	2 wks	.371086	.184823	.283	-.16029	.90246
	3 wks	-.469014	.184823	.105	-1.00039	.06236
	4 wks	-.352828	.184823	.332	-.88420	.17855
2 wks	Control	-1.062139*	.184823	.000	-1.59352	-.53076
	1 wk	-.371086	.184823	.283	-.90246	.16029
	3 wks	-.840100*	.184823	.001	-1.37148	-.30872
	4 wks	-.723914*	.184823	.003	-1.25529	-.19254
3 wks	Control	-.222039	.184823	.751	-.75341	.30934
	1 wk	.469014	.184823	.105	-.06236	1.00039
	2 wks	.840100*	.184823	.001	.30872	1.37148
	4 wks	.116186	.184823	.969	-.41519	.64756
4 wks	Control	-.338225	.184823	.373	-.86960	.19315
	1 wk	.352828	.184823	.332	-.17855	.88420
	2 wks	.723914*	.184823	.003	.19254	1.25529
	3 wks	-.116186	.184823	.969	-.64756	.41519

Table A.12: Tukey's post-hoc test | IL-1β gene expression (chronic noise)

(I) Endpoint	(J) Endpoint	Mean Difference (I-J)	Std. Error	Sig.	95% Confidence Interval	
					Lower Bound	Upper Bound
Control	1 wk	.667760	.278809	.141	-.13508	1.47060
	2 wks	.900371*	.288594	.028	.06935	1.73139
	3 wks	-.039459	.278809	1.000	-.84230	.76338
	4 wks	.485639	.278809	.423	-.31720	1.28848
1 wk	Control	-.667760	.278809	.141	-1.47060	.13508
	2 wks	.232611	.288594	.927	-.59841	1.06363
	3 wks	-.707219	.278809	.106	-1.51006	.09562
	4 wks	-.182121	.278809	.965	-.98496	.62072
2 wks	Control	-.900371*	.288594	.028	-1.73139	-.06935
	1 wk	-.232611	.288594	.927	-1.06363	.59841
	3 wks	-.939830*	.288594	.020	-1.77085	-.10881
	4 wks	-.414732	.288594	.609	-1.24575	.41629
3 wks	Control	.039459	.278809	1.000	-.76338	.84230
	1 wk	.707219	.278809	.106	-.09562	1.51006
	2 wks	.939830*	.288594	.020	.10881	1.77085
	4 wks	.525098	.278809	.345	-.27775	1.32794
4 wks	Control	-.485639	.278809	.423	-1.28848	.31720
	1 wk	.182121	.278809	.965	-.62072	.98496
	2 wks	.414732	.288594	.609	-.41629	1.24575
	3 wks	-.525098	.278809	.345	-1.32794	.27775

Appendix B4: ICAM-1 Immunostaining (Chronic Noise)

Table A.13: Tukey's post-hoc test | ICAM-1 immunostaining intensity in the spiral ligament of the cochlear basal turn (chronic noise)

(I) Endpoint	(J) Endpoint	Mean Difference (I-J)	Std. Error	Sig.	95% Confidence Interval	
					Lower Bound	Upper Bound
Control	1 wk	16.435730*	2.602730	.000	9.14769	23.72377
	2 wks	5.058063	2.855008	.398	-2.93640	13.05252
	3 wks	-3.399520	2.779824	.738	-11.18345	4.38441
	4 wks	-5.500964	3.160206	.416	-14.35002	3.34809
1 wk	Control	-16.435730*	2.602730	.000	-23.72377	-9.14769
	2 wks	-11.377667*	3.104528	.004	-20.07082	-2.68451
	3 wks	-19.835250*	3.035530	.000	-28.33520	-11.33530
	4 wks	-21.936694*	3.387318	.000	-31.42170	-12.45169
2 wks	Control	-5.058063	2.855008	.398	-13.05252	2.93640
	1 wk	11.377667*	3.104528	.004	2.68451	20.07082
	3 wks	-8.457583	3.254429	.082	-17.57048	.65532
	4 wks	-10.559028*	3.584800	.034	-20.59702	-.52104
3 wks	Control	3.399520	2.779824	.738	-4.38441	11.18345
	1 wk	19.835250*	3.035530	.000	11.33530	28.33520
	2 wks	8.457583	3.254429	.082	-.65532	17.57048
	4 wks	-2.101444	3.525215	.975	-11.97258	7.76970
4 wks	Control	5.500964	3.160206	.416	-3.34809	14.35002
	1 wk	21.936694*	3.387318	.000	12.45169	31.42170
	2 wks	10.559028*	3.584800	.034	.52104	20.59702
	3 wks	2.101444	3.525215	.975	-7.76970	11.97258

Table A.14: Tukey's post-hoc test | ICAM-1 immunostaining area in the spiral ligament of the cochlear basal turn (chronic noise)

(I) Endpoint	(J) Endpoint	Mean Difference (I-J)	Std. Error	Sig.	95% Confidence Interval	
					Lower Bound	Upper Bound
Control	1 wk	-5816.545295*	628.742474	.000	-7577.12040	-4055.97019
	2 wks	-6495.791087*	689.685510	.000	-8427.01601	-4564.56616
	3 wks	-4437.544458*	671.523143	.000	-6317.91198	-2557.17694
	4 wks	-832.878698	763.412148	.811	-2970.54948	1304.79209
1 wk	Control	5816.545295*	628.742474	.000	4055.97019	7577.12040
	2 wks	-679.245792	749.962016	.894	-2779.25415	1420.76257
	3 wks	1379.000837	733.294113	.337	-674.33485	3432.33652
	4 wks	4983.666597*	818.275645	.000	2692.36963	7274.96357
2 wks	Control	6495.791087*	689.685510	.000	4564.56616	8427.01601
	1 wk	679.245792	749.962016	.894	-1420.76257	2779.25415
	3 wks	2058.246628	786.173810	.078	-143.16029	4259.65355
	4 wks	5662.912389*	865.981544	.000	3238.03160	8087.79317
3 wks	Control	4437.544458*	671.523143	.000	2557.17694	6317.91198
	1 wk	-1379.000837	733.294113	.337	-3432.33652	674.33485
	2 wks	-2058.246628	786.173810	.078	-4259.65355	143.16029
	4 wks	3604.665761*	851.587497	.001	1220.09051	5989.24101
4 wks	Control	832.878698	763.412148	.811	-1304.79209	2970.54948
	1 wk	-4983.666597*	818.275645	.000	-7274.96357	-2692.36963
	2 wks	-5662.912389*	865.981544	.000	-8087.79317	-3238.03160
	3 wks	-3604.665761*	851.587497	.001	-5989.24101	-1220.09051

Table A.15: Tukey's post-hoc test | ICAM-1 immunostaining intensity in the spiral ligament of the cochlear middle turn (chronic noise)

(I) Endpoint	(J) Endpoint	Mean Difference (I-J)	Std. Error	Sig.	95% Confidence Interval	
					Lower Bound	Upper Bound
Control	1 wk	16.893307*	3.254784	.000	7.68956	26.09705
	2 wks	1.854235	4.050065	.991	-9.59837	13.30684
	3 wks	-6.769401	3.489700	.310	-16.63743	3.09863
	4 wks	-8.387765	4.050065	.248	-19.84037	3.06484
1 wk	Control	-16.893307*	3.254784	.000	-26.09705	-7.68956
	2 wks	-15.039071*	4.174711	.006	-26.84415	-3.23399
	3 wks	-23.662708*	3.633620	.000	-33.93771	-13.38771
	4 wks	-25.281071*	4.174711	.000	-37.08615	-13.47599
2 wks	Control	-1.854235	4.050065	.991	-13.30684	9.59837
	1 wk	15.039071*	4.174711	.006	3.23399	26.84415
	3 wks	-8.623636	4.360344	.291	-20.95364	3.70637
	4 wks	-10.242000	4.820541	.226	-23.87333	3.38933
3 wks	Control	6.769401	3.489700	.310	-3.09863	16.63743
	1 wk	23.662708*	3.633620	.000	13.38771	33.93771
	2 wks	8.623636	4.360344	.291	-3.70637	20.95364
	4 wks	-1.618364	4.360344	.996	-13.94837	10.71164
4 wks	Control	8.387765	4.050065	.248	-3.06484	19.84037
	1 wk	25.281071*	4.174711	.000	13.47599	37.08615
	2 wks	10.242000	4.820541	.226	-3.38933	23.87333
	3 wks	1.618364	4.360344	.996	-10.71164	13.94837

Table A.16: Tukey's post-hoc test | ICAM-1 immunostaining area in the spiral ligament of the cochlear middle turn (chronic noise)

(I) Endpoint	(J) Endpoint	Mean Difference (I-J)	Std. Error	Sig.	95% Confidence Interval	
					Lower Bound	Upper Bound
Control	1 wk	-2557.013029*	400.952053	.000	-3690.80884	-1423.21722
	2 wks	-2252.338101*	498.921494	.000	-3663.16788	-841.50832
	3 wks	-958.191984	429.890934	.186	-2173.81997	257.43600
	4 wks	-442.967529	498.921494	.900	-1853.79731	967.86225
1 wk	Control	2557.013029*	400.952053	.000	1423.21722	3690.80884
	2 wks	304.674929	514.276504	.976	-1149.57512	1758.92498
	3 wks	1598.821045*	447.620242	.007	333.05885	2864.58324
	4 wks	2114.045500*	514.276504	.001	659.79545	3568.29555
2 wks	Control	2252.338101*	498.921494	.000	841.50832	3663.16788
	1 wk	-304.674929	514.276504	.976	-1758.92498	1149.57512
	3 wks	1294.146117	537.144290	.129	-224.76852	2813.06076
	4 wks	1809.370571*	593.835356	.029	130.14726	3488.59389
3 wks	Control	958.191984	429.890934	.186	-257.43600	2173.81997
	1 wk	-1598.821045*	447.620242	.007	-2864.58324	-333.05885
	2 wks	-1294.146117	537.144290	.129	-2813.06076	224.76852
	4 wks	515.224455	537.144290	.872	-1003.69018	2034.13909
4 wks	Control	442.967529	498.921494	.900	-967.86225	1853.79731
	1 wk	-2114.045500*	514.276504	.001	-3568.29555	-659.79545
	2 wks	-1809.370571*	593.835356	.029	-3488.59389	-130.14726
	3 wks	-515.224455	537.144290	.872	-2034.13909	1003.69018

Appendix B5: Adenosine A_{2A} Receptor-Positive Infiltrating Cell Count

Table A.17: Tukey's post-hoc test | $A_{2A}R^{+}$ infiltrating cell count

(I) Endpoint	(J) Endpoint	Mean Difference (I-J)	Std. Error	Sig.	95% Confidence Interval	
					Lower Bound	Upper Bound
Control	6 h	-6.289*	1.267	.000	-9.82	-2.76
	1 d	-10.736*	1.312	.000	-14.39	-7.08
	3 d	-5.351*	1.452	.004	-9.39	-1.31
	7 d	-3.436	1.422	.120	-7.40	.52
6 h	Control	6.289*	1.267	.000	2.76	9.82
	1 d	-4.448*	1.299	.008	-8.06	-.83
	3 d	.938	1.440	.966	-3.07	4.95
	7 d	2.852	1.410	.263	-1.07	6.78
1 d	Control	10.736*	1.312	.000	7.08	14.39
	6 h	4.448*	1.299	.008	.83	8.06
	3 d	5.386*	1.480	.004	1.26	9.51
	7 d	7.300*	1.451	.000	3.26	11.34
3 d	Control	5.351*	1.452	.004	1.31	9.39
	6 h	-.938	1.440	.966	-4.95	3.07
	1 d	-5.386*	1.480	.004	-9.51	-1.26
	7 d	1.914	1.578	.744	-2.48	6.31
7 d	Control	3.436	1.422	.120	-.52	7.40
	6 h	-2.852	1.410	.263	-6.78	1.07
	1 d	-7.300*	1.451	.000	-11.34	-3.26
	3 d	-1.914	1.578	.744	-6.31	2.48

REFERENCES

Abi-Hachem, R. N., Zine, A., & Van De Water, T. R. (2010). The injured cochlea as a target for inflammatory processes, initiation of cell death pathways and application of related otoprotective strategies. *Recent Patents CNS Drug Discov., 5*, 147-163.

Abrashkin, K. A., Izumikawa, M., Miyazawa, T., Wang, C.-H., Crumling, M. A., Swiderski, D. L., et al. (2006). The fate of outer hair cells after acoustic or ototoxic insults. *Hear. Res., 218*(1–2), 20-29.

Adams, J. C. (2002). Clinical implications of inflammatory cytokines in the cochlea: a technical note. *Otol. Neurotol., 23*(3), 316-322.

Adams, J. C., Seed, B., Lu, N., Landry, A., & Xavier, R. J. (2009). Selective activation of nuclear factor kappa B in the cochlea by sensory and inflammatory stress. *Neuroscience, 160*(2), 530-539.

Al Jaroudi, W., & Iskandrian, A. E. (2009). Regadenoson: a new myocardial stress agent. *J. Am. Coll. Cardiol., 54*(13), 1123-1130.

Allan, S. M., & Rothwell, N. J. (2001). Cytokines and acute neurodegeneration. *Nat. Rev. Neurosci., 2*(10), 734-744.

Allen, S. J., Crown, S. E., & Handel, T. M. (2007). Chemokine: receptor structure, interactions, and antagonism. *Annu. Rev. Immunol., 25*(1), 787-820.

Arpornchayanon, W., Canis, M., Ihler, F., Settevendemie, C., & Strieth, S. (2013). TNF-α inhibition using etanercept prevents noise-induced hearing loss by improvement of cochlear blood flow in vivo. *Int. J. Audiol., 52*(8), 545-552.

Astellas Pharma (2008). Lexiscan (regadenoson): full prescribing information. *Revised July 2014*. Retrieved from http://www.astellas.us/docs/lexiscan.pdf

Auphan, N., DiDonato, J. A., Rosette, C., Helmberg, A., & Karin, M. (1995). Immunosuppression by glucocorticoids: inhibition of NF-κB activity through induction of IκB synthesis. *Science, 270*(5234), 286-290.

Axelsson, A., & Dengerink, H. (1987). The effects of noise on histological measures of the cochlear vasculature and red blood cells: A review. *Hear. Res., 31*(2), 183-191.

Axelsson, A. (1988). Comparative anatomy of cochlear blood vessels. *Am. J. Otolaryngol., 9*(6), 278-290.

Backhouse, S., Coleman, B., & Shepherd, R. (2008). Surgical access to the mammalian cochlea for cell-based therapies. *Exp. Neurol., 214*(2), 193-200.

Baldwin, S., Beal, P., Yao, S. M., King, A., Cass, C., & Young, J. (2004). The equilibrative nucleoside transporter family, SLC29. *Pflügers Archiv European Journal of Physiology, 447*(5), 735-743.

Baldwin, S. A., Mackey, J. R., Cass, C. E., & Young, J. D. (1999). Nucleoside transporters: molecular biology and implications for therapeutic development. *Mol. Med. Today, 5*(5), 216-224.

Bánfi, B., Malgrange, B., Knisz, J., Steger, K., Dubois-Dauphin, M., & Krause, K.-H. (2004). NOX3, a superoxide-generating NADPH oxidase of the inner ear. *J. Biol. Chem., 279*(44), 46065-46072.

Barkdull, G. C., Vu, C., Keithley, E. M., & Harris, J. P. (2005). Cochlear microperfusion: experimental evaluation of a potential new therapy for severe hearing loss caused by inflammation. *Otol. Neurotol., 26*(1), 19-26.

Baud, V., & Karin, M. (2001). Signal transduction by tumor necrosis factor and its relatives. *Trends Cell Biol., 11*(9), 372-377.

Bear, M. F., Connors, B. W., & Paradiso, M. A. (2007). *Neuroscience: exploring the brain* (Third ed.). Baltimore, MD, U.S.A: Lippincott Williams & Wilkins.

Benarroch, E. E. (2008). Adenosine and its receptors: multiple modulatory functions and potential therapeutic targets for neurologic disease. *Neurology, 70*(3), 231-236.

Blackburn, M. R., Vance, C. O., Morschl, E., & Wilson, C. N. (2009). Adenosine receptors and inflammation. In C. N. Wilson & S. J. Mustafa (Eds.), *Adenosine Receptors in Health and Disease* (Vol. 193, pp. 215-269): Springer-Verlag Berlin Heidelberg.

Boison, D. (2006). Adenosine kinase, epilepsy and stroke: mechanisms and therapies. *Trends Pharmacol. Sci., 27*(12), 652-658.

Bours, M. J. L., Swennen, E. L. R., Di Virgilio, F., Cronstein, B. N., & Dagnelie, P. C. (2006). Adenosine 5'-triphosphate and adenosine as endogenous signaling molecules in immunity and inflammation. *Pharmacol. Ther., 112*(2), 358-404.

Boyle, D. L., Kowaluk, E. A., Jarvis, M. F., Lee, C.-H., Bhagwat, S. S., Williams, M., et al. (2001). Anti-inflammatory effects of ABT-702, a novel non-nucleoside adenosine kinase inhibitor, in rat adjuvant arthritis. *J. Pharmacol. Exp. Ther., 296*(2), 495-500.

Buhr, C., Gössl, M., Erbel, R., & Eggebrecht, H. (2008). Regadenoson in the detection of coronary artery disease. *Vascular Health and Risk Management, 4*(2), 337-340.

Bustin, S. A., Benes, V., Nolan, T., & Pfaffl, M. W. (2005). Quantitative real-time RT-PCR – a perspective. *J. Mol. Endocrinol., 34*(3), 597-601.

Carcia-Berrocal, J. R., Trinidad, A., De La Funente, R., Ramirez-Camacho, R., Zurita, M., & Lobo, D. (2004). Controversies and criticisms on designs for experimental autoimmune labyrinthitis. *Ann. Otol. Rhinol. Laryngol., 113*, 404-410.

Carman, A. J., Mills, J. H., Krenz, A., Kim, D.-G., & Bynoe, M. S. (2011). Adenosine receptor signaling modulates permeability of the blood–brain barrier. *J. Neurosci., 31*(37), 13272-13280.

Cayé-Thomasen, P., Worsøe, L., Brandt, C. T., Miyazaki, H., Østergaard, C., Frimodt-Møller, N., et al. (2009). Routes, dynamics, and correlates of cochlear inflammation in terminal and recovering experimental meningitis. *Laryngoscope, 119*(8), 1560-1570.

Cerqueira, M. D., Verani, M. S., Schwaiger, M., Heo, J., & Iskandrian, A. S. (1994). Safety profile of adenosine stress perfusion imaging: results from the adenoscan multicenter trial registry. *J. Am. Coll. Cardiol., 23*(2), 384-389.

Cerqueira, M. D., Nguyen, P., Staehr, P., Underwood, S. R., & Iskandrian, A. E. (2008). Effects of age, gender, obesity, and diabetes on the efficacy and safety of the selective A2a agonist regadenoson versus adenosine in myocardial perfusion imaging: Integrated ADVANCE-MPI TRIAL RESULTS. *JACC: Cardiovascular Imaging, 1*(3), 307-316.

Chen, J. F., Eltzschig, H. K., & Fredholm, B. B. (2013). Adenosine receptors as drug targets - what are the challenges? *Nat. Rev. Drug Discov., 12*(4), 265-286.

Coney, A. M., & Marshall, J. M. (1998). Role of adenosine and its receptors in the vasodilatation induced in the cerebral cortex of the rat by systemic hypoxia. *J. Physiol., 509*(2), 507-518.

Crawford, J. M., & Watanabe, K. (1994). Cell adhesion molecules in inflammation and immunity: relevance to periodontal diseases. *Crit. Rev. Oral Biol. Med., 5*(2), 91-123.

Cronstein, B. N. (1994). Adenosine, an endogenous anti-inflammatory agent. *J. Appl. Physiol., 76*(1), 5-13.

Cronstein, B. N. (2007). Adenosine and inflammation. *Immunology, Endocrine & Metabolic Agents in Medicinal Chemistry 7*, 280-285.

Cunha, R. (2005). Neuroprotection by adenosine in the brain: From A1 receptor activation to A2A receptor blockade. *Purinergic Signalling, 1*(2), 111-134.

Cunha, R. A. (2001). Adenosine as a neuromodulator and as a homeostatic regulator in the nervous system: different roles, different sources and different receptors. *Neurochem. Int., 38*(2), 107-125.

Cureoglu, S., Schachern, P., A. , Rinaldo, A., Tsuprun, V., Ferlito, A., & Paparella, M., M. (2005). Round window membrane and labyrinthine pathological changes: an overview. *Acta Otolaryngol, 125*(1), 9-15.

Dai, M., Yang, Y., Omelchenko, I., Nuttall, A. L., Kachelmeier, A., Xiu, R., et al. (2010). Bone marrow cell recruitment mediated by inducible nitric oxide synthase/stromal cell-derived factor-1α signaling repairs the acoustically damaged cochlear blood-labyrinth barrier. *Am. J. Pathol., 177*(6), 3089-3099.

Dallos, P. (1992). The active cochlea. *J. Neurosci., 12*(12), 4575-4585.

Dallos, P., Popper, A. N., & Fay, R. R. (1996). *The cochlea* (Vol. 8). New York, NY, USA: Springer New York.

Daniel, E. (2007). Noise and hearing loss: a review. *J. Sch. Health, 77*(5), 225-231.

Davis, H. (1953). Acoustic trauma in the guinea pig. *J. Acoust. Soc. Am., 25*(6), 1180-1189.

Dempsey, P. W., Doyle, S. E., He, J. Q., & Cheng, G. (2003). The signaling adaptors and pathways activated by TNF superfamily. *Cytokine Growth Factor Rev., 14*(3–4), 193-209.

Denk, A., Wirth, T., & Baumann, B. (2000). NF-κB transcription factors: critical regulators of hematopoiesis and neuronal survival. *Cytokine Growth Factor Rev., 11*(4), 303-320.

Dinarello, C. A. (2000). Proinflammatory cytokines. *CHEST Journal, 118*(2), 503-508.

Dinarello, C. A. (2002). The IL-1 family and inflammatory diseases. *Clin. Exp. Rheumatol., 20*(5 Suppl 27), S1-13.

Dinarello, C. A. (2009). Immunological and inflammatory functions of the interleukin-1 family. *Annu. Rev. Immunol., 27*(1), 519-550.

Discolo, C. M., Keasler, J. R., & Hirose, K. (2004). *Inflammatory cells in the mouse cochlea after acoustic trauma.* Proceedings of the 27th Association for Research in Otolaryngology (ARO) MidWinter Meeting, Daytona Beach, Florida, USA.

Drury, A. N., & Szent-Gyorgyi, A. (1929). The physiological activity of adenine compounds with especial reference to their action upon the mammalian heart. *J Physiol, 68*(3), 213-237.

Du, X., Choi, C.-H., Chen, K., Cheng, W., Floyd, R. A., & Kopke, R. D. (2011). Reduced formation of oxidative stress biomarkers and migration of mononuclear phagocytes in the cochleae of chinchilla after antioxidant treatment in acute acoustic trauma. *Int J Otolaryngol, 2011*, 1-13.

Engel, F., Blatz, R., Kellner, J., Palmer, M., Weller, U., & Bhadki, S. (1995). Breakdown of the round window membrane permeability barrier evoked by streptolysin O: possible etiologic role in development of sensorineural hearing loss in acute otitis media. *Infect. Immun., 63*(4), 1305-1310.

Fettiplace, R., & Hackney, C. M. (2006). The sensory and motor roles of auditory hair cells. *Nat. Rev. Neurosci., 7*(1), 19-29.

Fogal, B., & Hewett, S., J. . (2008). Interleukin-1β: a bridge between inflammation and excitotoxicity? *J. Neurochem., 106*(1), 1-23.

Forge, A., Becker, D., Casalotti, S., Edwards, J., Evans, W. H., Lench, N., et al. (2007). Gap junctions and connexin expression in the inner ear. In *Novartis Foundation Symposium 219 - Gap Junction-Mediated Intercellular Signalling in Health and Disease* (pp. 134-156): John Wiley & Sons, Ltd.

Fortin, A., Harbour, D., Fernandes, M., Borgeat, P., & Bourgoin, S. (2006). Differential expression of adenosine receptors in human neutrophils: up-regulation by specific Th1 cytokines and lipopolysaccharide. *J. Leukoc. Biol., 79*(3), 574-585.

Fredelius, L. (1988). Time sequence of degeneration pattern of the organ of Corti after acoustic overstimulation: a transmission electron microscopy study. *Acta Otolaryngol, 106*(5-6), 373-385.

Fredelius, L., & Rask-Andersen, H. (1990). The role of macrophages in the disposal of degeneration products within the organ of Corti after acoustic overstimulation. *Acta Otolaryngol, 109*(1-2), 76-82.

Fredholm, B. B., Arslan, G., Halldner, L., Kull, B., Schulte, G., & Wasserman, W. (2000). Structure and function of adenosine receptors and their genes. *Naunyn. Schmiedebergs Arch. Pharmacol., 362*(4), 364-374.

Fredholm, B. B., Ijzerman, A. P., Jacobson, K. A., Klotz, K.-N., & Linden, J. (2001). International union of pharmacology. XXV. Nomenclature and classification of adenosine receptors. *Pharmacol. Rev., 53*(4), 527-552.

Fredholm, B. B., Chen, J.-F., Cunha, R. A., Svenningsson, P., Vaugeois, J.-M., & Ronald J. Bradley, R. A. H. a. P. J. (2005a). Adenosine and brain function. In *Int. Rev. Neurobiol.* (Vol. Volume 63, pp. 191-270): Academic Press.

Fredholm, B. B., Chen, J.-F., Masino, S. A., & Vaugeois, J.-M. (2005b). Actions of adenosine at its receptors in the CNS: insights from knockouts and drugs. *Annu. Rev. Pharmacol. Toxicol., 45*(1), 385-412.

Fredholm, B. B. (2007). Adenosine, an endogenous distress signal, modulates tissue damage and repair. *Cell Death Differ., 14*(7), 1315-1323.

Fridberger, A., Flock, Å., Ulfendahl, M., & Flock, B. (1998). Acoustic overstimulation increases outer hair cell Ca2+ concentrations and causes dynamic contractions of the hearing organ. *Proc. Natl. Acad. Sci. U. S. A., 95*(12), 7127-7132.

Fujioka, M., Kanzaki, S., Okano, H. J., Masuda, M., Ogawa, K., & Okano, H. (2006). Proinflammatory cytokines expression in noise-induced damaged cochlea. *J. Neurosci. Res., 83*(4), 575-583.

Fukuda, S., Harris, J. P., Keithley, E. M., Ishikawa, K., Kucuk, B., & Inuyama, Y. (1992). Spiral modiolar vein: its importance in viral load of the inner ear. *Ann. Otol. Rhinol. Laryngol. Suppl., 157*, 67-71.

Furness, D. N., & Hackney, C. M. (1985). Cross-links between stereocilia in the guinea pig cochlea. *Hear. Res., 18*(2), 177-188.

Garnock-Jones, K., & Curran, M. (2010). Regadenoson. *Am. J. Cardiovasc. Drugs, 10*(1), 65-71.

Ghaheri, B. A., Kempton, J. B., Pillers, D. A. M., & Trune, D. R. (2007). Cochlear cytokine gene expression in murine acute otitis media. *Laryngoscope, 117*(1), 22-29.

Ghimire, G., Hage, F., Heo, J., & Iskandrian, A. (2013). Regadenoson: a focused update. *J. Nucl. Cardiol., 20*(2), 284-288.

Ghosh, S., May, M. J., & Kopp, E. B. (1998). NF-κB and rel proteins: evolutionarily conserved mediators of immune responses. *Annu. Rev. Immunol., 16*(1), 225-260.

Gloddek, B., Lassmann, S., Gloddek, J., & Arnold, W. (1999). Role of S-100β as potential autoantigen in an autoimmune disease of the inner ear. *J. Neuroimmunol., 101*(1), 39-46.

Gong, T.-W., & Lomax, M. (2012). Genes that influence susceptibility to noise-induced hearing loss. In C. G. Le Prell, D. Henderson, R. R. Fay & A. N. Popper (Eds.), *Noise-Induced Hearing Loss* (Vol. 40, pp. 179-203). New York, USA: Springer.

Gopen, Q., & Harris, J. P. (2008). Autoimmune inner ear disease. In J. Schacht, A. N. Popper & R. R. Fay (Eds.), *Auditory Trauma, Protection, and Repair* (Vol. 31, pp. 131-144): Springer US.

Gordon, S., & Taylor, P. R. (2005). Monocyte and macrophage heterogeneity. *Nat. Rev. Immunol., 5*(12), 953-964.

Gray, J., Owen, R., & Giacomini, K. (2004). The concentrative nucleoside transporter family, SLC28. *Pflügers Archiv European Journal of Physiology, 447*(5), 728-734.

Griffith, D. A., & Jarvis, S. M. (1996). Nucleoside and nucleobase transport systems of mammalian cells. *Biochimica et Biophysica Acta (BBA) - Reviews on Biomembranes, 1286*(3), 153-181.

Griffith, J. W., Sokol, C. L., & Luster, A. D. (2014). Chemokines and chemokine receptors: positioning cells for host defense and immunity. *Annu. Rev. Immunol., 32*(1), 659-702.

Gunewardene, N., Guo, C. X., Wong, A. C., Thorne, P. R., & Vlajkovic, S. M. (2013). Adenosine amine congener ameliorates cisplatin-induced hearing loss. *World J Otorhinolaryngol, 3*(3), 100-107.

Hamernik, R., Turrentine, G., & Roberto, M. (1986). Mechanically-induced morphological changes in the organ of Corti. In R. Salvi, D. Henderson, R. P. Hamernik & V. Colletti (Eds.), *Basic and Applied Aspects of Noise-Induced Hearing Loss* (Vol. 111, pp. 69-83): Springer US.

Han, J., & Ulevitch, R. J. (2005). Limiting inflammatory responses during activation of innate immunity. *Nat. Immunol., 6*(12), 1198-1205.

Harris, J. P. (1983). Immunology of the inner ear: Response of the inner ear to antigen challenge. *Otolaryngol. Head Neck Surg., 91*(1), 18-23.

Harris, J. P. (1984). Immunology of the inner ear: evidence of local antibody production. *Ann. Otol. Rhinol. Laryngol., 93*(2 Pt 1), 157-162.

Harris, J. P., Fukuda, S., & Keithley, E. M. (1990). Spiral modiolar vein: its importance in inner ear inflammation. *Acta Otolaryngol, 110*(3-4), 357-364.

Harris, J. P., & Ryan, A. F. (1995). Fundamental immune mechanisms of the brain and inner ear. *Otolaryngol. Head Neck Surg., 112*(6), 639-653.

Hashimoto, S., Moradzadeh, A., Billings, P., Firestein, G. S., Harris, J. P., & Keithley, E. M. (2004). *Contribution of acoustic trauma to cochlear inflammation.* Proceedings of the 27th Association for Research in Otolaryngology (ARO) MidWinter Meeting, Daytona Beach, Florida, USA.

Hashimoto, S., Billings, P., Harris, J. P., Firestein, G. S., & Keithley, E. M. (2005). Innate immunity contributes to cochlear adaptive immune responses. *Audiology and Neurotology, 10*(1), 35-43.

Haskó, G., & Cronstein, B. N. (2004). Adenosine: an endogenous regulator of innate immunity. *Trends Immunol., 25*(1), 33-39.

Haskó, G., Koscsó, B., & Csóka, B. (2013). Adenosine in the immune system. In S. Masino & D. Boison (Eds.), *Adenosine* (pp. 233-251): Springer New York.

Hawkins, J. E. (2004). Sketches of otohistory part 1: otoprehistory: how it all began. *Audiol. Neurootol., 9*(2), 66-71.

Hawkins, J. E., & Schacht, J. (2005). Sketches of otohistory part 10: noise-induced hearing loss. *Audiol. Neurootol., 10*(6), 305-309.

Hawkins, J. E., Jr. (1976). Microcirculation in the labyrinth. *Arch. Otorhinolaryngol., 212*(4), 241-251.

Henderson, D., & Hamernik, R. P. (1986). Impulse noise: critical review. *J. Acoust. Soc. Am., 80*(2), 569-584.

Henderson, D., Bielefeld, E. C., Harris, K. C., & Hu, B. H. (2006). The role of oxidative stress in noise-induced hearing loss. *Ear Hear., 27*(1), 1-19.

Henderson, D., Hu, B., & Bielefeld, E. (2008). Patterns and mechanisms of noise-induced cochlear pathology. In J. Schacht, A. Popper & R. Fay (Eds.), *Auditory Trauma, Protection, and Repair* (Vol. 31, pp. 195-217). New York, USA: Springer.

Hess, A., Bloch, W., Huverstuhl, J., Su, J., Stennert, E., Addicks, K., et al. (1999). Expression of inducible nitric oxide synthase (iNOS/NOS II) in the cochlea of guinea pigs after intratympanical endotoxin-treatment. *Brain Res., 830*(1), 113-122.

Hilding, D. A., & Ginzberg, R. D. (1977). Pigmentation of the Stria Vascularis The Contribution of Neural Crest Melanocytes. *Acta Otolaryngol. (Stockh.), 84*(1-6), 24-37.

Hirose, K., & Liberman, M. C. (2003). Lateral wall histopathology and endocochlear potential in the noise-damaged mouse cochlea. *J. Assoc. Res. Otolaryngol., 4*(3), 339-352.

Hirose, K., & Keasler, J. R. (2004). *Proinflammatory cytokine and chemokine expression in the noise-exposed murine cochlea.* Proceedings of the 27th Association for Research in Otolaryngology (ARO) MidWinter Meeting, Daytona Beach, Florida, USA.

Hirose, K., Discolo, C. M., Keasler, J. R., & Ransohoff, R. (2005). Mononuclear phagocytes migrate into the murine cochlea after acoustic trauma. *J. Comp. Neurol., 489*(2), 180-194.

Hirose, K., Li, S.-Z., Ohlemiller, K., & Ransohoff, R. (2014). Systemic lipopolysaccharide induces cochlear inflammation and exacerbates the synergistic ototoxicity of kanamycin and furosemide. *J. Assoc. Res. Otolaryngol.*, 1-16.

Hirose, Y., Tabuchi, K., Oikawa, K., Murashita, H., Sakai, S., & Hara, A. (2007). The effects of the glucocorticoid receptor antagonist RU486 and phospholipase A2 inhibitor quinacrine on acoustic injury of the mouse cochlea. *Neurosci. Lett., 413*(1), 63-67.

Housley, G. D., Marcotti, W., Navaratnam, D., & Yamoah, E. N. (2006). Hair cells – beyond the transducer. *J. Membr. Biol., 209*(2), 89-118.

Hu, B. (2012). Noise-induced structural damage to the cochlea. In C. G. Le Prell, D. Henderson, R. R. Fay & A. N. Popper (Eds.), *Noise-Induced Hearing Loss* (Vol. 40, pp. 57-86). New York, USA: Springer.

Hu, B., & Henderson, D. (2014). Oxidative stress and cochlear damage. In I. Laher (Ed.), *Systems Biology of Free Radicals and Antioxidants* (pp. 3561-3580): Springer Berlin Heidelberg.

Hu, B. H., Henderson, D., & Nicotera, T. M. (2002). Involvement of apoptosis in progression of cochlear lesion following exposure to intense noise. *Hear. Res., 166*(1-2), 62-71.

Hubbard, A. K., & Rothlein, R. (2000). Intercellular adhesion molecule-1 (ICAM-1) expression and cell signaling cascades. *Free Radic. Biol. Med., 28*(9), 1379-1386.

Hynes, R. O. (1992). Integrins: Versatility, modulation, and signaling in cell adhesion. *Cell, 69*(1), 11-25.

Ichimiya, I., Kurono, Y., Hirano, T., & Mogi, G. (1998). Changes in immunostaining of inner ears after antigen challenge into the scala tympani. *Laryngoscope, 108*(4), 585-591.

Ichimiya, I., Suzuki, M., Hirano, T., & Mogi, G. (1999). The influence of pneumococcal otitis media on the cochlear lateral wall. *Hear. Res., 131*(1–2), 128-134.

Ichimiya, I., Yoshida, K., Hirano, T., Suzuki, M., & Mogi, G. (2000). Significance of spiral ligament fibrocytes with cochlear inflammation. *Int. J. Pediatr. Otorhinolaryngol., 56*(1), 45-51.

Ichimiya, I., Yoshida, K., Suzuki, M., & Mogi, G. (2003). Expression of adhesion molecules by cultured spiral ligament fibrocytes stimulated with proinflammatory cytokines. *Ann. Otol. Rhinol. Laryngol., 112*(8), 722-728.

Ichimiya, I., Yoshida, K., Hirano, T., Suzuki, M., & Mogi, G. (2004). Aspects of cochlear lateral wall inflammation. *Audiological Medicine, 2*, 179-181.

Iskandrian, A. E., Bateman, T. M., Belardinelli, L., Blackburn, B., Cerqueira, M. D., Hendel, R. C., et al. (2007). Adenosine versus regadenoson comparative evaluation in myocardial perfusion imaging: results of the ADVANCE phase 3 multicenter international trial. *J. Nucl. Cardiol., 14*(5), 645-658.

Jacobson, K. A., & Gao, Z.-G. (2006). Adenosine receptors as therapeutic targets. *Nat. Rev. Drug Discov., 5*(3), 247-264.

Jacobson, K. A. (2009). Introduction to adenosine receptors as therapeutic targets. In *Adenosine Receptors in Health and Disease* (pp. 1-24).

Jagger, D. J., & Forge, A. (2013). The enigmatic root cell – emerging roles contributing to fluid homeostasis within the cochlear outer sulcus. *Hear. Res., 303*(0), 1-11.

Jarvis, M. F., Yu, H., Kohlhaas, K., Alexander, K., Lee, C.-H., Jiang, M., et al. (2000). ABT-702 (4-amino-5-(3-bromophenyl)-7-(6-morpholinopyridin-3-yl)pyrido[2,3-d]pyrimidine), a novel orally effective adenosine kinase inhibitor with analgesic and anti-inflammatory properties: I. in vitro characterization and acute antinociceptive effects in the mouse. *J. Pharmacol. Exp. Ther., 295*(3), 1156-1164.

Jo, M. H., Kim, C. J., Koh, S. H., Nam, G. S., Jeong, H. M., Lee, J. H., et al. (2010). Expression and distribution of tumor necrosis factor-alpha in mice cochlea exposed to noise. *Korean J Otorhinolaryngol-Head Neck Surg, 53*(9), 527-533.

Juhn, S. K., Hunter, B. A., & Odland, R. M. (2001). Blood-labyrinth barrier and fluid dynamics of the inner ear. *Int. Tinnitus. J., 7*(2), 72-83.

Kastenbauer, S., Klein, M., Koedel, U., & Pfister, H. W. (2001). Reactive nitrogen species contribute to blood–labyrinth barrier disruption in suppurative labyrinthitis complicating experimental pneumococcal meningitis in the rat. *Brain Res., 904*(2), 208-217.

Kaur, T., Mukherjea, D., Sheehan, K., Jajoo, S., Rybak, L. P., & Ramkumar, V. (2011). Short interfering RNA against STAT1 attenuates cisplatin-induced ototoxicity in the rat by suppressing inflammation. *Cell Death and Dis, 2*, e180.

Kawauchi, H., Demaria, T. F., & Lim, D. J. (1988). Endotoxin permeability through the round window. *Acta Otolaryngol, 105*(s457), 100-115.

Keithley, E. M., Woolf, N. K., & Harris, J. P. (1989). Development of morphological and physiological changes in the cochlea induced by cytomegalovirus. *Laryngoscope, 99*(4), 409-414.

Keithley, E. M., Chen, M.-C., & Linthicum, F. (1998). Clinical diagnoses associated with histologic findings of fibrotic tissue and new bone in the inner ear. *Laryngoscope, 108*(1), 87-91.

Keithley, E. M., Wang, X., & Barkdull, G. C. (2008). Tumor necrosis factor α can induce recruitment of inflammatory cells to the cochlea. *Otol. Neurotol., 29*(6), 854-859.

Kel, G. E., Tan, J., Eastwood, H. T., Wongprasartsuk, S., & O'Leary, S. J. (2013). Early cochlear response and ICAM-1 expression to cochlear implantation. *Otol. Neurotol., 7*, 7.

Kesser, B. W., Hashisaki, G. T., Spindel, J. H., Ruth, R. A., & Scheld, W. M. (1999). Time course of hearing loss in an animal model of pneumococcal meningitis. *Otolaryngol. Head Neck Surg., 120*(5), 628-637.

Khan, A. F., Thorne, P. R., Munoz, D. J., Wang, C. J., Housley, G. D., & Vlajkovic, S. M. (2007). Nucleoside transporter expression and adenosine uptake in the rat cochlea. *Neuroreport, 18*(3), 235-239.

Khan, M., Szczepek, A. J., Haupt, H., Olze, H., & Mazurek, B. (2010). Expression of the proinflammatory cytokines in cochlear explant cultures: influence of normoxia and hypoxia. *Neurosci. Lett., 479*(3), 249-252.

Kikuchi, T., Adams, J. C., Miyabe, Y., So, E., & Kobayashi, T. (2000). Potassium ion recycling pathway via gap junction systems in the mammalian cochlea and its interruption in hereditary nonsyndromic deafness. *Med Electron Microsc, 33*(2), 51-56.

Kimura, R. S., Nye, C. L., & Southard, R. E. (1990). Normal and pathologic features of the limbus spiralis and its functional significance. *Am. J. Otolaryngol., 11*(2), 99-111.

King, E. B., Salt, A. N., Kel, G. E., Eastwood, H. T., & O'Leary, S. J. (2014). The oval window, not the round window, is the primary route into the inner ear following intratympanic administration of gentamicin in guinea pigs. *Hear. Res. (in press)*.

Kirkegaard, M., Murai, N., Risling, M., Suneson, A., Jarlebark, L., & Ulfendahl, M. (2006). Differential gene expression in the rat cochlea after exposure to impulse noise. *Neuroscience, 142*(2), 425-435.

Kirkpatrick, P. (2002). G-protein-coupled receptors: putting the brake on inflammation. *Nature Reviews Drug Discovery, 1*(2), 99.

Klein, M., Koedel, U., Kastenbauer, S., & Pfister, H. W. (2008). Nitrogen and oxygen molecules in meningitis-associated labyrinthitis and hearing impairment. *Infection, 36*(1), 2-14.

Kong, W., Engel, K., & Wang, J. (2004). Mammalian nucleoside transporters. *Curr. Drug Metab., 5*, 63-84.

Kopke, R. D. (2007). Pharmacological approaches to the prevention and treatment of cochlear injury due to noise. *Audiological Medicine, 5*(1), 66-80.

Kowaluk, E. A., Mikusa, J., Wismer, C. T., Zhu, C. Z., Schweitzer, E., Lynch, J. J., et al. (2000). ABT-702 (4-amino-5-(3-bromophenyl)-7-(6-morpholino-pyridin- 3-yl)pyrido[2,3-d]pyrimidine), a novel orally effective adenosine kinase inhibitor with analgesic and anti-inflammatory properties. II. in vivo characterization in the rat. *J. Pharmacol. Exp. Ther., 295*(3), 1165-1174.

Kujawa, S. G., & Liberman, M. C. (2009). Adding insult to injury: cochlear nerve degeneration after "temporary" noise-induced hearing loss. *J. Neurosci., 29*(45), 14077-14085.

Ladrech, S., Wang, J., Simonneau, L., Puel, J.-L., & Lenoir, M. (2007). Macrophage contribution to the response of the rat organ of Corti to amikacin. *J. Neurosci. Res., 85*(9), 1970-1979.

Lang, H., Ebihara, Y., Schmiedt, R. A., Minamiguchi, H., Zhou, D., Smythe, N., et al. (2006). Contribution of bone marrow hematopoietic stem cells to adult mouse inner ear: mesenchymal cells and fibrocytes. *J. Comp. Neurol., 496*(2), 187-201.

Lawson, C., & Wolf, S. (2009). ICAM-1 signaling in endothelial cells. *Pharmacol. Rep., 61*(1), 22-32.

Le Floc'h, J., Tan, W., Telang, R. S., Vlajkovic, S. M., Nuttall, A., Rooney, W. D., et al. (2013). Markers of cochlear inflammation using MRI. *J. Magn. Reson. Imaging*.

Le Prell, C. G., Yamashita, D., Minami, S. B., Yamasoba, T., & Miller, J. M. (2007). Mechanisms of noise-induced hearing loss indicate multiple methods of prevention. *Hear. Res., 226*(1-2), 22-43.

Le, Y., Zhou, Y., Iribarren, P., & Wang, J. (2004). Chemokines and chemokine receptors: their manifold roles in homeostasis and disease. *Cell. Mol. Immunol., 1*(2), 95-104.

Liberman, M. C. (1987). Chronic ultrastructural changes in acoustic trauma: serial-section reconstruction of stereocilia and cuticular plates. *Hear. Res., 26*(1), 65-88.

Linas, S. L., Whittenburg, D., Parsons, P. E., & Repine, J. E. (1995). Ischemia increases neutrophil retention and worsens acute renal failure: role of oxygen metabolites and ICAM-1. *Kidney Int., 48*(5), 1584-1591.

Linden, J. (2005). Adenosine in tissue protection and tissue regeneration. *Mol. Pharmacol., 67*(5), 1385-1387.

Linden, J. (2006). New insights into the regulation of inflammation by adenosine. *J. Clin. Invest., 116*(7), 1835-1837.

Livak, K. J., & Schmittgen, T. D. (2001). Analysis of relative gene expression data using real-time quantitative PCR and the 2-[Delta][Delta]CT method. *Methods, 25*(4), 402-408.

Lo, S. K., Janakidevi, K., Lai, L., & Malik, A. B. (1993). Hydrogen peroxide-induced increase in endothelial adhesiveness is dependent on ICAM-1 activation. *American Journal of Physiology - Lung Cellular and Molecular Physiology, 264*(4), L406-L412.

Loizou, P. C. (1999). Introduction to cochlear implants. *Engineering in Medicine and Biology Magazine, IEEE, 18*(1), 32-42.

Luster, A. D., Alon, R., & von Andrian, U. H. (2005). Immune cell migration in inflammation: present and future therapeutic targets. *Nat. Immunol., 6*(12), 1182-1190.

Ma, C., Billings, P., Harris, J. P., & Keithley, E. M. (2000). Characterization of an experimentally induced inner ear immune response. *Laryngoscope, 110*(3), 451-456.

MacArthur, C. J., Hefeneider, S. H., Kempton, J. B., & Trune, D. R. (2006). C3H/HeJ mouse model for spontaneous chronic otitis media. *Laryngoscope, 116*(7), 1071-1079.

MacArthur, C. J., & Trune, D. R. (2006). Mouse models of otitis media. *Curr Opin Otolaryngol Head Neck Surg, 14*(5), 341-346.

Maeda, K., Yoshida, K., Ichimiya, I., & Suzuki, M. (2005). Dexamethasone inhibits tumor necrosis factor-α-induced cytokine secretion from spiral ligament fibrocytes. *Hear. Res., 202*(1-2), 154-160.

Malakoff, D. (2000). The rise of the mouse, biomedicine's model mammal. *Science, 288*(5464), 248-253.

Masuda, M., Nagashima, R., Kanzaki, S., Fujioka, M., Ogita, K., & Ogawa, K. (2006). Nuclear factor-kappa B nuclear translocation in the cochlea of mice following acoustic overstimulation. *Brain Res., 1068*(1), 237-247.

Mathews, I. I., Erion, M. D., & Ealick, S. E. (1998). Structure of Human Adenosine Kinase at 1.5 Å Resolution. *Biochemistry, 37*(45), 15607-15620.

McCabe, B. F. (1979). Autoimmune sensorineural hearing loss. *Ann. Otol. Rhinol. Laryngol., 88*(5 Pt 1), 585-589.

McGaraughty, S., Cowart, M., Jarvis, M. F., & Berman, R. F. (2005). Anticonvulsant and antinociceptive actions of novel adenosine kinase inhibitors. *Curr. Top. Med. Chem., 5*, 43-58.

Medzhitov, R. (2008). Origin and physiological roles of inflammation. *Nature, 454*(7203), 428-435.

Mélik-Parsadaniantz, S., & Rostène, W. (2008). Chemokines and neuromodulation. *J. Neuroimmunol., 198*(1–2), 62-68.

Mendes-Jorge, L., Ramos, D., Luppo, M., Llombart, C., Alexandre-Pires, G., Nacher, V., et al. (2009). Scavenger function of resident autofluorescent perivascular macrophages and their contribution to the maintenance of the blood–retinal barrier. *Invest. Ophthalmol. Vis. Sci., 50*(12), 5997-6005.

Merchant, S. N., & Gopen, Q. (1996). A human temporal bone study of acute bacterial meningogenic labyrinthitis. *Am. J. Otol., 17*(3), 375-385.

Miyao, M., Firestein, G. S., & Keithley, E. M. (2008). Acoustic trauma augments the cochlear immune response to antigen. *Laryngoscope, 118*(10), 1801-1808.

Mom, T., Chazal, J., Gabrillargues, J., Gilain, L., & Avan, P. (2005). Cochlear blood supply: an update on anatomy and function. *Fr ORL*(88), 81-88.

Moon, S.-K., Park, R., Lee, H.-Y., Nam, G.-J., Cha, K., Andalibi, A., et al. (2006). Spiral ligament fibrocytes release chemokines in response to otitis media pathogens. *Acta Otolaryngol, 126*(6), 564 - 569.

Morello, S., Sorrentino, R., & Pinto, A. (2009). Adenosine A2a receptor agonists as regulators of inflammation: pharmacology and therapeutic opportunities. *Journal of Receptor, Ligand and Channel Research, 2*, 11-17.

Mukherjea, D., Jajoo, S., Kaur, T., Sheehan, K. E., Ramkumar, V., & Rybak, L. P. (2010). Transtympanic administration of short interfering (si)RNA for the NOX3 isoform of NADPH oxidase protects against cisplatin-induced hearing loss in the rat. *Antioxid. Redox. Signal., 13*(5), 589-598.

Muller, W. A., Weigl, S. A., Deng, X., & Phillips, D. M. (1993). PECAM-1 is required for transendothelial migration of leukocytes. *J. Exp. Med., 178*(2), 449-460.

Muñoz, D. J. B., McFie, C., & Thorne, P. R. (1999). Modulation of cochlear blood flow by extracellular purines. *Hear. Res., 127*(1–2), 55-61.

Murai, N., Kirkegaard, M., Järlebark, L., Risling, M., Suneson, A., & Ulfendahl, M. (2008). Activation of JNK in the inner ear following impulse noise exposure. *J. Neurotrauma, 25*(1), 72-77.

Nakamoto, T., Mikuriya, T., Sugahara, K., Hirose, Y., Hashimoto, T., Shimogori, H., et al. (2012). Geranylgeranylacetone suppresses noise-induced expression of proinflammatory cytokines in the cochlea. *Auris. Nasus. Larynx, 39*(3), 270-274.

Nelson, D. I., Nelson, R. Y., Concha-Barrientos, M., & Fingerhut, M. (2005). The global burden of occupational noise-induced hearing loss. *Am. J. Ind. Med., 48*(6), 446-458.

Neng, L., Zhang, F., Kachelmeier, A., & Shi, X. (2013). Endothelial cell, pericyte, and perivascular resident macrophage-type melanocyte interactions regulate cochlear intrastrial fluid–blood barrier permeability. *J. Assoc. Res. Otolaryngol., 14*(2), 175-185.

Newby, A. C., Worku, Y., Meghji, P., Nakazawa, M., & Skladanowski, A. C. (1990). Adenosine: A Retaliatory Metabolite or Not? *News Physiol Sci, 5*(2), 67-70.

Nishimoto, N., & Kishimoto, T. (2006). Interleukin 6: from bench to bedside. *Nat Clin Pract Rheum, 2*(11), 619-626.

Nishimoto, N. (2010). Interleukin-6 as a therapeutic target in candidate inflammatory diseases. *Clin. Pharmacol. Ther., 87*(4), 483-487.

Ohlemiller, K. K., Wright, J. S., & Dugan, L. L. (1999). Early elevation of cochlear reactive oxygen species following noise exposure. *Audiol. Neurootol., 4*(5), 229-236.

Ohlemiller, K. K. (2008). Recent findings and emerging questions in cochlear noise injury. *Hear. Res., 245*(1-2), 5-17.

Ohta, A., & Sitkovsky, M. (2001). Role of G-protein-coupled adenosine receptors in downregulation of inflammation and protection from tissue damage. *Nature, 414*(6866), 916-920.

Okano, T., Nakagawa, T., Kita, T., Kada, S., Yoshimoto, M., Nakahata, T., et al. (2008). Bone marrow-derived cells expressing Iba1 are constitutively present as resident tissue macrophages in the mouse cochlea. *J. Neurosci. Res., 86*(8), 1758-1767.

Okusa, M. D., Linden, J., Huang, L., Rieger, J. M., Macdonald, T. L., & Huynh, L. P. (2000). A2A adenosine receptor-mediated inhibition of renal injury and neutrophil adhesion. *American Journal of Physiology - Renal Physiology, 279*(5), F809-F818.

Okusa, M. D. (2002). A2A adenosine receptor: a novel therapeutic target in renal disease. *American Journal of Physiology - Renal Physiology, 282*(1), F10-F18.

Park, J., & Gupta, R. (2008). Adenosine kinase and ribokinase – the RK family of proteins. *Cell. Mol. Life Sci., 65*(18), 2875-2896.

Park, J., & Gupta, R. (2013). Adenosine metabolism, adenosine kinase, and evolution. In S. Masino & D. Boison (Eds.), *Adenosine* (pp. 23-54): Springer New York.

Park, J. E., & Barbul, A. (2004). Understanding the role of immune regulation in wound healing. *Am. J. Surg., 187*(5, Supplement 1), S11-S16.

Park, K. M., & Bowers, W. J. (2010). Tumor necrosis factor-alpha mediated signaling in neuronal homeostasis and dysfunction. *Cell. Signal., 22*(7), 977-983.

Pawankar, R., Tomiyama, S., Jinnouchi, K., Ikezono, T., Nonaka, M., & Yagi, T. (1998). Intercellular adhesion molecule-1 expression in the inner ear of rats following secondary immune reaction in the endolymphatic sac. *Acta Otolaryngol. (Stockh.), 118*(539), 5-14.

Pickles, J. O., Comis, S. D., & Osborne, M. P. (1984). Cross-links between stereocilia in the guinea pig organ of Corti, and their possible relation to sensory transduction. *Hear. Res., 15*(2), 103-112.

Pickles, J. O., Osborne, M. P., & Comis, S. D. (1987). Vulnerability of tip links between stereocilia to acoustic trauma in the guinea pig. *Hear. Res., 25*(2–3), 173-183.

Poirrier, A. L., Pincemail, J., Van Den Ackerveken, P., Lefebvre, P. P., & Malgrange, B. (2010). Oxidative stress in the cochlea: an update. *Curr. Med. Chem., 17*, 3591-3604.

Proudfoot, A. E. I., Handel, T. M., Johnson, Z., Lau, E. K., LiWang, P., Clark-Lewis, I., et al. (2003). Glycosaminoglycan binding and oligomerization are essential for the in vivo activity of certain chemokines. *Proc. Natl. Acad. Sci. U. S. A., 100*(4), 1885-1890.

Puel, J.-L., Ruel, J., d'Aldin, C. G., & Pujol, R. (1998). Excitotoxicity and repair of cochlear synapses after noise-trauma induced hearing loss. *Neuroreport, 9*(9), 2109-2114.

Pujol, R., & Puel, J.-L. (1999). Excitotoxicity, synaptic repair, and functional recovery in the mammalian cochlea: a review of recent findings. *Ann. N. Y. Acad. Sci., 884*(1), 249-254.

Rabinowitz, P. M. (2000). Noise-induced hearing loss. *Am. Fam. Physician, 61*(9), 2759-2760.

Rakesh N. Patel, M., Roque B. Arteaga, M. D., Mahendra K. Mandawat, M. D., John W. Thornton, M. D., & Vincent J. B. Robinson, M. F. F. (2007). Pharmacologic stress myocardial perfusion imaging. *South. Med. J., 100*(10), 1006-1014.

Ramkumar, V., Whitworth, C. A., Pingle, S. C., Hughes, L. F., & Rybak, L. P. (2004). Noise induces A1 adenosine receptor expression in the chinchilla cochlea. *Hear. Res., 188*(1–2), 47-56.

Raphael, Y., & Altschuler, R. A. (2003). Structure and innervation of the cochlea. *Brain Res. Bull., 60*(5-6), 397-422.

Ribeiro, J. A., Sebastiao, A. M., & de Mendonca, A. (2002). Adenosine receptors in the nervous system: pathophysiological implications. *Prog. Neurobiol., 68*(6), 377-392.

Roldán-Fidalgo, A., Trinidad, A., Rodríguez-Valiente, A., García-Berrocal, J. R., Millán, I., Coronado, M. J., et al. (2014). Effect of intratympanic dimethyl sulphoxide (DMSO) in an in vivo model of cisplatin-related ototoxicity. *Eur. Arch. Otorhinolaryngol., 271*(12), 3121-3126.

Rosenbluth, J. (1962). The fine structure of the acoustic ganglia in the rat. *J. Cell Biol., 12*(2), 329-359.

Rosengren, S., Bong, G. W., & Firestein, G. S. (1995). Anti-inflammatory effects of an adenosine kinase inhibitor. Decreased neutrophil accumulation and vascular leakage. *J Immunol, 154*(10), 5444-5451.

Rutar, M., Provis, J. M., & Valter, K. (2010). Brief exposure to damaging light causes focal recruitment of macrophages, and long-term destabilization of photoreceptors in the albino rat retina. *Curr. Eye Res., 35*(7), 631-643.

Ryan, A. F., Harris, J. P., & Keithley, E. M. (2002). Immune-mediated hearing loss: basic mechanisms and options for therapy. *Acta Otolaryngol, 122*(5), 38-43.

Sato, E., Shick, H. E., Ransohoff, R. M., & Hirose, K. (2008). Repopulation of cochlear macrophages in murine hematopoietic progenitor cell chimeras: the role of CX3CR1. *J. Comp. Neurol., 506*(6), 930-942.

Sato, E., Shick, H., Ransohoff, R., & Hirose, K. (2010). Expression of fractalkine receptor CX3CR1 on cochlear macrophages influences survival of hair cells following ototoxic injury. *J. Assoc. Res. Otolaryngol., 11*(2), 223-234.

Satoh, H., Firestein, G. S., Billings, P. B., Harris, J. P., & Keithley, E. M. (2002). Tumor necrosis factor-α, an initiator, and etanercept, an inhibitor of cochlear inflammation. *Laryngoscope, 112*(9), 1627-1634.

Sautter, N., Shick, E., Ransohoff, R., Charo, I., & Hirose, K. (2006). CC chemokine receptor 2 is protective against noise-induced hair cell death: Studies in CX3CR1(+/GFP) mice. *J. Assoc. Res. Otolaryngol., 7*(4), 361-372.

Schramm, H. M. (2010). The role of the osteoimmune axis in the inflammation of the inner auditory ear and with regard to the putative anticarcinogenetic principle: part 2. *Inflamm. Allergy Drug Targets, 9*, 120-129.

Sebastião, A. M., & Ribeiro, J. A. (2009). Adenosine Receptors and the Central Nervous System. In *Adenosine Receptors in Health and Disease* (pp. 471-534).

Seidman, M. D., Tang, W., Shirwany, N., Bai, U., Rubin, C. J., Henig, J. P., et al. (2009). Anti-intercellular adhesion molecule-1 antibody's effect on noise damage. *Laryngoscope, 119*(4), 707-712.

Sendowski, I., Abaamrane, L., Raffin, F., Cros, A., & Clarençon, D. (2006). Therapeutic efficacy of intra-cochlear administration of methylprednisolone after acoustic trauma caused by gunshot noise in guinea pigs. *Hear. Res., 221*(1–2), 119-127.

Serhan, C. N., & Savill, J. (2005). Resolution of inflammation: the beginning programs the end. *Nat. Immunol., 6*(12), 1191-1197.

Sha, S.-H., Taylor, R., Forge, A., & Schacht, J. (2001). Differential vulnerability of basal and apical hair cells is based on intrinsic susceptibility to free radicals. *Hear. Res., 155*(1–2), 1-8.

Sheth, S., Brito, R., Mukherjea, D., Rybak, L., & Ramkumar, V. (2014). Adenosine Receptors: Expression, Function and Regulation. *Int. J. Mol. Sci., 15*(2), 2024-2052.

Shi, X., & Nuttall, A. L. (2003). Upregulated iNOS and oxidative damage to the cochlear stria vascularis due to noise stress. *Brain Res., 967*(1-2), 1-10.

Shi, X., & Nuttall, A. L. (2007). Expression of adhesion molecular proteins in the cochlear lateral wall of normal and PARP-1 mutant mice. *Hear. Res., 224*(1-2), 1-14.

Shi, X. (2010). Resident macrophages in the cochlear blood-labyrinth barrier and their renewal via migration of bone-marrow-derived cells. *Cell Tissue Res., 342*(1), 21-30.

So, H., Kim, H., Lee, J.-H., Park, C., Kim, Y., Kim, E., et al. (2007). Cisplatin cytotoxicity of auditory cells requires secretions of proinflammatory cytokines via activation of ERK and NF-κB. *J. Assoc. Res. Otolaryngol., 8*(3), 338-355.

So, H., Kim, H., Kim, Y., Kim, E., Pae, H.-O., Chung, H.-T., et al. (2008). Evidence that cisplatin-induced auditory damage is attenuated by downregulation of pro-inflammatory cytokines via Nrf2/HO-1. *J. Assoc. Res. Otolaryngol., 9*(3), 290-306.

Spandow, O., Hellstrom, S., & Anniko, M. (1990). Structural Changes in the Round Window Membrane Following Exposure to Escherichia coli Lipopolysaccharide and Hydrocortisone. *Laryngoscope, 100*(9), 995-1000.

Spicer, S. S., & Schulte, B. A. (1996). The fine structure of spiral ligament cells relates to ion return to the stria and varies with place-frequency. *Hear. Res., 100*(1–2), 80-100.

Spoelstra, F., Postma, D., Hovenga, H., Noordhoek, J., & Kauffman, H. (1999). Interferon-gamma and interleukin-4 differentially regulate ICAM-1 and VCAM-1 expression on human lung fibroblasts. *Eur. Respir. J., 14*(4), 759-766.

Spoendlin, H. (1971). Primary Structural Changes in the Organ of Corti After Acoustic Overstimulation. *Acta Otolaryngol. (Stockh.), 71*(1-6), 166-176.

Steel, K. P., & Barkway, C. (1989). Another role for melanocytes: their importance for normal stria vascularis development in the mammalian inner ear. *Development, 107*(3), 453-463.

Sullivan, G. W., & Linden, J. (1998). Role of A2A adenosine receptors in inflammation. *Drug Development Research, 45*(3-4), 103-112.

Suzuki, M., & Harris, J. P. (1995). Expression of intercellular adhesion molecule-1 during inner ear inflammation. *Ann. Otol. Rhinol. Laryngol., 104*(1), 69-75.

Tabuchi, K., Murashita, H., Sakai, S., Hoshino, T., Uemaetomari, I., & Hara, A. (2006). Therapeutic time window of methylprednisolone in acoustic injury. *Otol. Neurotol., 27*(8), 1176-1179.

Tabuchi, K., & Hara, A. (2012). Implications of cytokines in cochlear pathophysiology. In A. Kamkin & I. Kiseleva (Eds.), *Mechanosensitivity in Cells and Tissues* (Vol. 5, pp. 189-199): Springer Netherlands.

Takemura, K., Komeda, M., Yagi, M., Himeno, C., Izumikawa, M., Doi, T., et al. (2004). Direct inner ear infusion of dexamethasone attenuates noise-induced trauma in guinea pig. *Hear. Res., 196*(1–2), 58-68.

Talaska, A. E., & Schacht, J. (2007). Mechanisms of noise damage to the cochlea. *Audiological Medicine, 5*(1), 3-9.

Tan, B. T. G., Lee, M. M. G., & Ruan, R. (2008). Bone marrow-derived cells that home to acoustic deafened cochlea preserved their hematopoietic identity. *J. Comp. Neurol., 509*(2), 167-179.

Thomsen, E. (1967). The ultrastructuhe of the spiral ganglion in the guinea pig. *Acta Otolaryngol. (Stockh.), 63*(s224), 442-448.

Thorne, P. R., Duncan, C. E., & Gavin, J. B. (1986). The pathogenesis of stereocilia abnormalities in acoustic trauma. *Hear. Res., 21*(1), 41-49.

Thorne, P. R., & Nuttall, A. L. (1987). Laser doppler measurements of cochlear blood flow during loud sound exposure in the guinea pig. *Hear. Res., 27*(1), 1-10.

Thorne, P. R., Ameratunga, S. N., Stewart, J., Reid, N., Williams, W., Purdy, S. C., et al. (2008). Epidemiology of noise-induced hearing loss in New Zealand. *N. Z. Med. J., 121*(1280), 33-44.

Tornabene, S. V., Sato, K., Pham, L., Billings, P., & Keithley, E. M. (2006). Immune cell recruitment following acoustic trauma. *Hear. Res., 222*(1-2), 115-124.

Tracey, K. J., & Cerami, A. (1993). Tumor necrosis factor, other cytokines and disease. *Annu. Rev. Cell Biol., 9*(1), 317-343.

Trinidad, A., Ramírez-Camacho, R., García-Berrocal, J. R., Verdaguer, J. M., & Daza, R. (2005). Labyrinthitis secondary to experimental otitis media. *Am. J. Otolaryngol., 26*(4), 226-229.

Trivedi, M., & Pingle, S. (2013). Noise-induced hearing loss (NIHL): risk factors, genes and associated proteins. *Asiatic J Biotechnology Resources, 4*(1), 1-6.

Van De Water, T. R., & Staecker, H. (2011). *Otolaryngology: basic science and clinical review*. New York, NY, U.S.A.: Thieme.

Vandevyver, S., Dejager, L., Tuckermann, J., & Libert, C. (2013). New insights into the anti-inflammatory mechanisms of glucocorticoids: an emerging role for glucocorticoid-receptor-mediated transactivation. *Endocrinology, 154*(3), 993-1007.

Verbeek, J. H., Kateman, E., Morata, T. C., Dreschler, W. A., & Mischke, C. (2012). Interventions to prevent occupational noise-induced hearing loss. *Cochrane Database Syst. Rev., 10*, CD006396.

Vlajkovic, S., Lee, K.-H., Wong, A., Guo, C., Gupta, R., Housley, G., et al. (2010a). Adenosine amine congener mitigates noise-induced cochlear injury. *Purinergic Signal., 6*(2), 273-281.

Vlajkovic, S. M., Thorne, P. R., Munoz, D. J. B., & Housley, G. D. (1996). Ectonucleotidase activity in the perilymphatic compartment of the guinea pig cochlea. *Hear. Res., 99*(1-2), 31-37.

Vlajkovic, S. M., Housley, G. D., Greenwood, D., & Thorne, P. R. (1999). Evidence for alternative splicing of ecto-ATPase associated with termination of purinergic transmission. *Molecular Brain Research, 73*(1–2), 85-92.

Vlajkovic, S. M., Thorne, P. R., Sévigny, J., Robson, S. C., & Housley, G. D. (2002a). NTPDase1 and NTPDase2 immunolocalization in mouse cochlea: implications for regulation of P2 Receptor signaling. *J. Histochem. Cytochem., 50*(11), 1435-1441.

Vlajkovic, S. M., Thorne, P. R., Sévigny, J., Robson, S. C., & Housley, G. D. (2002b). Distribution of ectonucleoside triphosphate diphosphohydrolases 1 and 2 in rat cochlea. *Hear. Res., 170*(1–2), 127-138.

Vlajkovic, S. M., Abi, S., Wang, C. J., Housley, G. D., & Thorne, P. R. (2007). Differential distribution of adenosine receptors in rat cochlea. *Cell Tissue Res., 328*(3), 461-471.

Vlajkovic, S. M., Housley, G. D., & Thorne, P. R. (2009). Adenosine and the auditory system. *Current Neuropharmacology, 7*(3), 246-256.

Vlajkovic, S. M., Guo, C. X., Dharmawardana, N., Wong, A. C. Y., Boison, D., Housley, G. D., et al. (2010b). Role of adenosine kinase in cochlear development and response to noise. *J. Neurosci. Res., 88*(12), 2598-2609.

Vlajkovic, S. M., Guo, C. X., Telang, R., Wong, A. C. Y., Paramananthasivam, V., Boison, D., et al. (2011). Adenosine kinase inhibition in the cochlea delays the onset of age-related hearing loss. *Exp. Gerontol., 46*(11), 905-914.

Vlajkovic, S. M., Lin, S. C.-y., Wong, A. C. Y., Wackrow, B., & Thorne, P. R. (2013). Noise-induced changes in expression levels of NADPH oxidases in the cochlea. *Hear. Res., 304*(0), 145-152.

Vlajkovic, S. M., Chang, H., Paek, S. Y., Chi, H. H., Sreebhavan, S., Telang, R. S., et al. (2014). Adenosine amine congener as a cochlear rescue agent. *BioMed Research International (in press)*.

Wakabayashi, K., Fujioka, M., Kanzaki, S., Okano, H. J., Shibata, S., Yamashita, D., et al. (2010). Blockade of interleukin-6 signaling suppressed cochlear inflammatory response and improved hearing impairment in noise-damaged mice cochlea. *Neurosci. Res., 66*(4), 345-352.

Wang, J., Van De Water, T. R., Bonny, C., de Ribaupierre, F., Puel, J. L., & Zine, A. (2003a). A peptide Inhibitor of c-jun N-terminal kinase protects against both aminoglycoside and acoustic trauma-induced auditory hair cell death and hearing loss. *J. Neurosci., 23*(24), 8596-8607.

Wang, X., Truong, T., Billings, P. B., Harris, J. P., & Keithley, E. M. (2003b). Blockage of immune-mediated inner ear damage by etanercept. *Otol. Neurotol., 24*(1), 52-57.

Wang, Y., Hirose, K., & Liberman, M. C. (2002). Dynamics of noise-induced cellular injury and repair in the mouse cochlea. *J. Assoc. Res. Otolaryngol., 3*(3), 248-268.

Wangemann, P. (2006). Supporting sensory transduction: cochlear fluid homeostasis and the endocochlear potential. *J. Physiol., 576*(1), 11-21.

Warchol, M. E. (1997). Macrophage activity in organ cultures of the avian cochlea: demonstration of a resident population and recruitment to sites of hair cell lesions. *J. Neurobiol., 33*(6), 724-734.

Watanabe, K., Jinnouchi, K., Pawankar, R., & Yagi, T. (2001). Expression of myeloperoxidase and cochlear dysfunction in the lipopolysaccharide-treated guinea pig. *Eur. Arch. Otorhinolaryngol., 258*(4), 164-167.

Willott, J. F. (2001). Measurement of the auditory brainstem response (ABR) to study auditory sensitivity in mice. In *Current Protocols in Neuroscience*: John Wiley & Sons, Inc.

Wong, A. C. Y., Guo, C. X., Gupta, R., Housley, G. D., Thorne, P. R., & Vlajkovic, S. M. (2010). Post exposure administration of A1 adenosine receptor agonists attenuates noise-induced hearing loss. *Hear. Res., 260*(1-2), 81-88.

Wong, A. C. Y., Froud, K. E., & Hsieh, Y. S.-Y. (2013). Noise-induced hearing loss in the 21st century: A research and translational update. *World J Otorhinolaryngol, 3*(3), 58-70.

Woo, J.-I., Pan, H., Oh, S., Lim, D., & Moon, S. (2010). Spiral ligament fibrocyte-derived MCP-1/CCL2 contributes to inner ear inflammation secondary to nontypeable H. influenzae-induced otitis media. *BMC Infect. Dis., 10*(1), 314.

Woodfin, A., Voisin, M.-B., & Nourshargh, S. (2007). PECAM-1: a multi-functional molecule in inflammation and vascular biology. *Arterioscler. Thromb. Vasc. Biol., 27*(12), 2514-2523.

Xu, H. X., Joglekar, S. S., & Paparella, M. M. (2009). Labyrinthitis ossificans. *Otol. Neurotol., 30*(4), 579-580.

Yamamoto, H., Omelchenko, I., Shi, X., & Nuttall, A. L. (2009). The influence of NF-κB signal-transduction pathways on the murine inner ear by acoustic overstimulation. *J. Neurosci. Res., 87*(8), 1832-1840.

Yamane, H., Nakai, Y., Takayama, M., Iguchi, H., Nakagawa, T., & Kojima, A. (1995). Appearance of free radicals in the guinea pig inner ear after noise-induced acoustic trauma. *Eur. Arch. Otorhinolaryngol., 252*(8), 504-508.

Yimtae, K., Song, H., Billings, P., Harris, J. P., & Keithley, E. M. (2001). Connection between the inner ear and the lymphatic system. *Laryngoscope, 111*(9), 1631-1635.

Yoo, T. J., Tomoda, K., Stuart, J. M., Cremer, M. A., Townes, A. S., & Kang, A. H. (1983). Type II collagen-induced autoimmune sensorineural hearing loss and vestibular dysfunction in rats. *Ann. Otol. Rhinol. Laryngol., 92*(3 Pt 1), 267-271.

Yoshida, K., Ichimiya, I., Suzuki, M., & Mogi, G. (1999). Effect of proinflammatory cytokines on cultured spiral ligament fibrocytes. *Hear. Res., 137*(1-2), 155-159.

Zhang, C. (2000). Expression of vascular cell adhesion molecule-1, a4-integrin and L-selectin during inner ear immunity reaction. *Acta Otolaryngol. (Stockh.), 120*(5), 607-614.

Zhang, F., Dai, M., Neng, L., Zhang, J. H., Zhi, Z., Fridberger, A., et al. (2013). Perivascular macrophage-like melanocyte responsiveness to acoustic trauma - a salient feature of strial barrier associated hearing loss. *FASEB J, 27*(9), 3730-3740.

Zhang, W., Dai, M., Fridberger, A., Hassan, A., DeGagne, J., Neng, L., et al. (2012). Perivascular-resident macrophage-like melanocytes in the inner ear are essential for the integrity of the intrastrial fluid–blood barrier. *Proc. Natl. Acad. Sci. U. S. A., 109*(26), 10388-10393.

Zhou, Y., Zheng, H., Shen, X., Zhang, Q., & Yang, M. (2009). Intratympanic administration of methylprednisolone reduces impact of experimental intensive impulse noise trauma on hearing. *Acta Otolaryngol, 129*(6), 602 - 607.